ODEP

Operative Dentistry, Endodontology and Periodontology

THE JAPANESE SOCIETY OF CONSERVATIVE DENTISTRY
1955

歯科用根管充填シーラ

CANALISTA キャナリスタ

管理医療機器 | 医療機器認証番号：301AFBZX00037000 ／ 一般名称：歯科用根管充填シーラ
【包装】散：15g　液：10mL　【参考医院価格（税別）】散：¥4,700　液：¥4,700

根管清掃剤

保険適用
医療用医薬品

キャナルクリーナー
歯科用液10％

次亜塩素酸ナトリウム製剤

有効成分	包装
1mL中　次亜塩素酸ナトリウム　100mg	30mL

作成日：2020.3

効能・効果、用法・用量、禁忌を含む使用上の注意等については、製品添付文書をご参照ください。

JIZAI ー自在ー

a master of endo.

NiTiロータリーファイル

MANI®

Concept

SMOOTH　急な引き込まれを大幅軽減

FLEXIBLE　本来の根管から逸脱しづらい
刃部構造と柔軟性

SIMPLE　Ⅰ・Ⅱ・Ⅲの3本で終了
簡単な手順、使用方法を採用

035 04 Ⅲ
025 06 Ⅱ
025 04 Ⅰ

JIZAI 拡大 使用ファイル【Ⅰ：025/.04】 MANI.

ホームページより
動画をご覧頂けます

OPERATIVE DENTISTRY, ENDODONTOLOGY AND PERIODONTOLOGY

CONTENTS

Case Report

PREFACE

Launch of the ODEP

Tᴀɴɪ-Iꜱʜɪɪ Nobuyuki
President
The Japanese Society of Conservative Dentistry

The Japanese Society of Conservative Dentistry is pleased to announce that it will start publishing its English journal, Operative Dentistry, Endodontology and Periodontology (ODEP), from December 2021.

Since the first edition of our journal was published in Japanese in 1958, it has been issued six times a year since 1986, and 280 volumes have been published to date. The circulation of each copy is about 4,500, and these have been mailed to academic society members, but since 2020, it has been published online and can be distributed to researchers overseas via the Web.

By publishing an English journal, the members of the Japanese Society of Conservative Dentistry will be able to disseminate their scientific research, clinical research, and education in the field of conservative dentistry to researchers all over the world. It will be a great honor and pleasure for us to contribute to the development of research.

Publication of this ODEP journal will help establish close cooperation with related academic societies in Japan and overseas ; we will strive to conduct research, clinical practice, education and training that will be disseminated to the world as well as contribute to Japanese dentistry.

I hope that the journal will provide a platform for the further development of conservative dentistry based on the long-held philosophy of our Society.

Original Article

Influence of Etching Mode on the Dentin Bond Effectiveness of a Universal Adhesive

Jennifer A. Hasslen[1], Akimasa Tsujimoto[2], Mark D. Markham[1],
Mone Shoji[3], Toshiki Takamizawa[3], Mark A. Latta[1],
Masashi Miyazaki[3], Atsushi Kamimoto[4] and Wayne W. Barkmeier[1]

[1]Department of General Dentistry, Creighton University School of Dentistry
[2]Department of Operative Dentistry, Iowa University School of Dentistry
[3]Department of Operative Dentistry, Nihon University School of Dentistry
[4]Department of Comprehensive Dentistry and Clinical Education, Nihon University School of Dentistry

Abstract

Purpose: This laboratory study aimed to assess the dentin bond fatigue resistance and interfacial characteristics of a universal adhesive in etch-and-rinse and self-etch modes.

Methods: The universal adhesive used was Clearfil Universal Bond Quick (Kuraray Noritake Dental, Tokyo, Japan). The dentin surfaces were treated with the universal adhesive in either etch-and-rinse or self-etch mode. Initial bond strength was measured by loading 15 specimens per test group to failure using an all-electric dynamic instrument with a chisel-shaped metal load at a crosshead speed of 1.0 mm/min. The fatigue load was applied to the specimens using a sine wave at a frequency of 20 Hz for 50,000 cycles or until failure occurred. The surface free energy characteristics of adhesive-treated dentin were determined. Scanning electron microscopy (SEM) observations of the resin-dentin interface of the adhesive were also conducted for each etching mode.

Results: For the universal adhesive tested, etching mode did not affect the bond fatigue resistance. The surface free energy characteristics of the baseline showed that the γ_s, γ_s^d, γ_s^p, and γ_s^h values for dentin in etch-and-rinse mode were significantly lower than in self-etch mode. The surface free energy values of adhesive-treated dentin in etch-and-rinse mode were not significantly decreased by adhesive application, while both γ_s and γ_s^h values were decreased after adhesive application in self-etch mode. In SEM observations of adhesive interfaces, deeper penetration of adhesives into the dentinal tubules was observed in etch-and-rinse mode due to removal of the smear layer and opening of the dentinal tubules.

Conclusion: The results suggest that the dentin bonding performance of the universal adhesive was not affected by etching mode.

Key words: universal adhesive, dentin bonding performance, etching mode

Introduction

Recently, universal adhesives have become popular in dentistry because they can be used in a variety of modes: etch-and-rinse, self-etch, or selective-etch[1]. With the expiration of the patent for 10-methacryloyloxydecyl dihydrogen phosphate (10-MDP) in 2003, manufacturers began exploring the usage of 10-MDP in combination with other components in novel adhesive formulations. Universal adhesives that can be used with resin cements on different substrates[2], with shortened application times[3], or with different surface moisture conditions on enamel and dentin substrates[4] have been brought to market. On the contrary, the bond durability of universal adhesives has been reported to be inferior to that of two-step self-etch adhesives[5]. Nevertheless, the flexibility of universal adhesives has ensured their increasing popularity in clinics[6], creating a need to further investigate better ways to utilize universal adhesives.

Over the past decade, a method of assessing bond fatigue resistance in adhesives has been developed in a collaborative effort between the Creighton University School of Dentistry (CU, Omaha, NE, USA) and the Nihon University School of Dentistry (NU, Tokyo, Japan). Development began with Erickson et al.[7] and has been refined by researchers from CU and NU[8-10]. The appropriate frequency[9], number of cycles[10], and method of analysis[11] have been established. However, the universal adhesive made by the manufacturer that developed 10-MDP has not been investigated with this established testing method, although such an investigation could provide novel insights for the further development of universal adhesives.

Yoshida et al.[12] reported that the chemical interaction of 10-MDP with dentin is essential in obtaining durable bonds, while Inoue et al.[13] showed that chemical interactions between 10-MDP and dentin can be explained through changes in dentin surface characteristics. Although it has been shown that the bonding strategy employed does not significantly affect the bonding performance of a given universal adhesive, it remains possible that the chemical bonding interactions of a universal adhesive with ground dentin and with etched dentin differ. Moreover, further assessment of changes in the energy characteristics of dentin surfaces

treated with universal adhesive in the two different modes may provide an explanation for the discrepancy between bond strength and chemical bonding effectiveness, as long as such an assessment is accompanied by a bond fatigue resistance analysis.

The purpose of this laboratory study was to assess the dentin bond fatigue resistance and energy characteristics of a universal adhesive in each of two modes: etch-and-rinse and self-etch. The two null hypotheses tested were as follows: (i) etching mode would make no difference to the dentin bond fatigue resistance, and (ii) etching mode would make no difference to the energy characteristics of universal adhesive-treated dentin.

Materials and Methods

1．Study materials

The universal adhesive used in this study was Clearfil Universal Bond Quick (CU, Kuraray Noritake Dental, Tokyo, Japan). A phosphoric acid-etching agent (Ultra-Etch; Ultradent Products, South Jordan, UT, USA) and a composite resin (Z100 Universal Restorative; 3M Oral Care, St. Paul, MN, USA) were employed to construct the specimens (Table 1).

2．Specimen preparation

De-identified extracted human molar teeth were used in this study. The experimental protocol for using de-identified human molar teeth was reviewed and approved by the Biomedical Institutional Review Board at the CU (No. 760765-1) and the Ethics Committee for Human Studies of the NU (No. 2015-06).

Sectioned buccal and lingual halves of the teeth with the apical portions removed were mounted in 25 mm brass rings using an acrylic resin (Bosworth Fastray; Keystone Industries, Myerstown, PA, USA). Flat dentin surfaces were prepared on the mounted buccal and lingual surfaces by wet-grinding using a sequence of silicon carbide (SiC) papers (Struers, Cleveland, OH, USA) of gradually increasing fineness (#180-, #320-, #600-, #1,200-, #2,000-, and #4,000-grit) in a grinder-polisher (Ecomet 4; Buehler, Lake Bluff, IL, USA). As the directionality of surface scratches created by the abrasives might substantially influence the bond strength testing results, the surfaces were polished up to #4,000-grit to minimize this influence. These surfaces were then washed with water and dried using a dental three-way syringe at a distance of 5 cm above the surface at an

Table 1　Materials used in this study

Material (lot no.)	Type of material (code)	Main component (pH)	Manufacturer
Clearfil Universal Bond Quick (1L0003)	Universal adhesive (CU)	bis-GMA, HEMA, 10-MDP, hydrophilic amide monomer, ethanol, water, initiators, silica, silane coupling agent (2.3)	Kuraray Noritake Dental, Tokyo, Japan
Ultra-Etch (G019)	Etching agent	35% phosphoric acid, glycol, cobalt aluminate blue spinel	Ultradent Products, South Jordan, UT, USA
Z100 Universal Restrative (1312131)	Composite resin	bis-GMA, TEGDMA, silane-treated ceramic, benzotri-azolyl methylphenol	3M Oral Care, St. Paul, MN, USA

bis-GMA: 2,2-bis［p-(2-hydroxy-3-methacryloxy propoxy) phenyl］propane; HEMA: 2-hydroxyethyl methacrylate; 10-MDP: 10-methacryloyloxydecyl dihydrogen phosphate; TEGDMA: triethylene glycol dimethacrylate

air pressure of 0.3 MPa.

Thirty specimens were prepared for each adhesive for initial bond strength testing, and 40 specimens were prepared for each adhesive for bond fatigue strength testing. Additionally, 20 specimens were prepared for each adhesive for surface free energy measurements. Half of the specimens for each adhesive were phosphoric acid-etched for 15 s before application of the adhesive (etch-and-rinse mode), while the other half were not etched (self-etch mode). The specimens were prepared under ambient laboratory conditions of 23 ± 2℃ and $50\pm10\%$ relative humidity.

3．Initial bond strength testing

Stainless steel (SUS304) rings with an inner diameter of 2.4 mm, an outer diameter of 4.8 mm, and a height of 2.6 mm were used to bond a composite to the dentin. The bonding side of each metal ring was treated with a 3% solution of paraffin in hexane. Each dentin surface was treated with the universal adhesive in etch-and-rinse or self-etch mode according to the manufacturer's instructions. A custom fixture was used to position and hold the stainless steel ring over the bonding site as the composite was placed into the ring using a condensing instrument. The composite was then light-cured for 40 s using a quartz-tungsten-halogen (QTH) curing unit (Spectrum 800 Curing Unit; Dentsply Caulk, Milford, DE, USA) set at a light intensity of 800 mW/cm^2. The bonded specimens were then stored in 37℃ distilled water for 24 h before testing.

A chisel-shaped metal rod was used to apply the load to the metal ring (mold-enclosed method) immediately adjacent to the flat dentin surface. Fifteen specimens per group were loaded to failure using an all-electric dynamic test instrument (ElectroPuls E1000; Instron, Canton, MA, USA) at a crosshead speed of 1 mm/min. Initial bond strength (MPa) was calculated from the peak load at failure divided by the bonded surface area.

4．Bond fatigue strength testing

A staircase method was used to perform the bond fatigue strength tests using the all-electric dynamic test instrument.[11] In the staircase method, the initial stress level was set to half of the measured initial bond strength and was applied to the first specimens. The fatigue load was applied to the metal ring using a sine wave at a frequency of 20 Hz for 50,000 cycles or until failure occurred. If the first specimen survived the application of 50,000 cycles, a new second specimen was tested for the same number of cycles at a stress level that was about 10% higher. If the first specimen failed, the stress level was reduced by the same amount for the second specimen. This procedure was repeated for 20 specimens, raising and lowering the stress based on survival or failure at each loading force. The test specimens were immersed in water at room temperature (23 ± 2℃) during the testing.

5．Surface free energy measurement

The dentin surfaces were prepared as described above. Each dentin surface was treated with universal

adhesive in etch-and-rinse or self-etch mode in accordance with the manufacturer's instructions, and the uncured adhesive layer was removed by three set of alternating rinses of acetone and distilled water. The contact angles of the specimens were then measured to analyze the surface free energy characteristics of each adhesive-treated surface. Phosphoric acid-etched and ground dentin surfaces were also measured. The surface free energy characteristics of the specimens were determined by measuring the contact angle formed with the surface by the three test liquids of known surface free energy parameters: 1-bromonaphthalene, diiodomethane, and distilled water. For each test liquid, the equilibrium contact angle (θ) was measured using the sessile drop method under ambient laboratory conditions, as described earlier, using a contact angle measurement apparatus (DM 500; Kyowa Interface Science, Saitama, Japan) for ten specimens per group. The apparatus was fitted with a charge-coupled device camera to enable automatic measurement. A standardized $1.0\,\mu l$ drop of each test liquid was placed on the treated dentin surface, and a profile image was captured after 500 ms using the apparatus. The contact angle was then calculated using the $\theta/2$ method, using the built-in interface measurement and analysis system (FAMAS; Kyowa Interface Science). The surface free energy (γ_s) and its parameters for solids $(\gamma_s^d, \gamma_s^p, \text{ and } \gamma_s^h)$ were calculated using the formulae described by Hata et al.[14], again using the built-in software (FAMAS). The dispersion force (γ_s^d) represents the weakest intermolecular force between apolar molecules. The polar (non-dispersion) force (γ_s^p) represents the electric and metallic interactions, in addition to the dipolar interactions. Besides these two parameters of γ_s, the hydrogen-bonding force (γ_s^h), which relates to the water and hydroxyl components, was calculated.

6．Scanning electron microscopy observation of bonding interface

Representative scanning electron microscopy (SEM) micrographs of the resin-dentin interfaces for three specimens per group were obtained using field-emission SEM (ERA 8800FE; Elionix, Tokyo, Japan). A rectangular $(4\times2\times1\,\text{mm})$ section of dentin was removed from each molar for SEM observations of the bonding interface. The dentin surface was prepared as described above for specimen preparation. The dentin surface was treated with the adhesive according to the manufacturer's instructions in etch-and-rinse or self-etch mode. The resin composite was then placed and light-irradiated for 40 s using the QTH curing unit from a standardized distance of 1 mm. For the composite/dentin interfaces, bonded specimens were embedded in epoxy resin (Epon 812; Nisshin EM, Tokyo, Japan) and then stored at 37℃ for 24 h. Each bonded specimen was then sectioned near its center, and the surfaces of the cut halves were polished with a sequence of SiC papers (#180-, #320-, #600-, #1,200-, #2,000-, and #4,000-grit) using a grinder-polisher. Finally, the surface was polished with a soft cloth using $1.0\,\mu\text{m}$ particle diameter diamond paste (DP-Paste; Struers, Ballerup, Denmark). SEM specimens of the composite-dentin interfaces were dehydrated by first immersing them in ascending concentrations of aqueous *tert*-butanol (50% for 20 min, 75% for 20 min, 95% for 20 min, and 100% for 2 h) and then transferring them from the final 100% bath to a freeze-drying apparatus (Model ID-3; Elionix) for 30 min. The polished surfaces were etched for 30 s using an argon ion beam (Type EIS-200ER; Elionix) directed perpendicular to the surface at an accelerating voltage of 1.0 kV and an ion current density of $0.4\,\text{mA/cm}^2$. The surfaces were then coated with a thin film of gold in a vacuum evaporator (Quick Coater Type SC-701; Sanyu Electron, Tokyo, Japan) and observed using field-emission SEM at an operating voltage of 10 kV.

7．Statistical analysis

Initial bond strength data were analyzed with one-way analysis of variance (ANOVA) followed by Tukey's *post hoc* honestly significant difference (HSD) test. The bond fatigue strength data were analyzed using a modified *t*-test with a Bonferroni correction and custom software. The $\gamma_s, \gamma_s^d, \gamma_s^p,$ and γ_s^h data were analyzed using one-way ANOVA along with Tukey's HSD test. All statistical analyses, apart from the bond fatigue strength data analysis, were conducted using statistical software (SPSS Statistics Ver. 13; International Business Machines, Armonk, NY, USA), applying a significance level of 0.05.

Results

The initial bond strength of the universal adhesive in each etching mode is shown in Table 2. The initial bond strength of the universal adhesive was not significantly influenced by the etching mode (p＝0.606).

Table 2   Initial bond strength of universal adhesives to dentin using etch-and-rinse and self-etch modes

Code	Etch-and-rinse mode	Self-etch mode
CU	27.3 (4.2)[a]	28.1 (4.2)[a]

Unit: MPa. Values in parentheses indicate standard deviations. Same small letter indicates no significant difference (p>0.05).

Table 3   Bond fatigue strength of universal adhesives to dentin using etch-and-rinse and self-etch modes

Code	Etch-and-rinse mode	Self-etch mode
CU	13.9 (1.9)[a]	14.4 (1.7)[a]

Unit: MPa. Values in parentheses indicate standard deviations. Same small letter indicates no significant difference (p>0.05).

Table 4   Surface free energy characteristics of universal adhesive-treated dentin using etch-and-rinse and self-etch modes

Code	Etch-and-rinse mode				Self-etch mode			
	γ_s	γ_s^d	γ_s^p	γ_s^h	γ_s	γ_s^d	γ_s^p	γ_s^h
baseline	41.1 (2.5)[a]	37.8 (1.5)[a]	1.1 (1.6)[a]	2.2 (1.1)[a]	68.8 (3.6)[a]	41.0 (1.4)[a]	2.8 (2.3)[a]	25.0 (2.4)[a]
CU	39.2 (2.4)[a]	37.2 (0.8)[a]	1.1 (1.8)[a]	0.9 (2.1)[b]	64.1 (2.9)[b]	40.2 (1.1)[a]	2.5 (1.5)[a]	21.4 (2.0)[b]

Unit: mN/m. γ_s, surface free energy; γ_s^d dispersion force; γ_s^h, hydrogen-bonding force; γ_s^p, polar force. The same letters in a column indicate no statistically significant difference (p>0.05).

The bond fatigue strength for the universal adhesive in each etching mode is shown in Table 3. The bond fatigue strength of the universal adhesive was not significantly influenced by the etching mode.

The surface free energy parameters of the universal adhesive-treated dentin are shown in Table 4. The baseline in etch-and-rinse mode exhibited significantly lower γ_s and γ_s^h values than in self-etch mode (p<0.001 for γ_s and γ_s^h). Changes in the γ_s^d and γ_s^p values of the universal adhesive-treated dentin were not significantly decreased (γ_s^d: $p=0.279$ for etch-and-rinse mode, $p=0.571$ for self-etch mode; γ_s^p: $p=1.000$ for etch-and-rinse mode, $p=0.734$ for self-etch mode) by the adhesive application, in contrast to γ_s and γ_s^h in self-etch mode, whose values were significantly decreased (γ_s: $p=0.004$; γ_s^h: $p=0.002$).

Representative SEM images of the composite-dentin interfaces of etch-and-rinse samples and self-etch samples are shown in Fig. 1. The thickness of the layer of universal adhesive was −10 μm. For each tested adhesive, the composite-dentin interface showed excellent adaptation to dentin regardless of etching mode. However, deeper penetration of adhesives into the dentinal tubules was observed in etch-and-rinse mode due to removal of the smear layer and opening of the dentinal tubules.

Discussion

In the present study, etching mode did not affect the dentin bond fatigue resistance of the universal adhesive, and thus the first null hypothesis was not rejected. A recent study[15], which used the same research design to study enamel bonding, reported that the bond fatigue resistance of universal adhesives was significantly higher in etch-and-rinse mode than in self-etch mode. The results of the present and previous studies suggest that the use of etch-and-rinse or selective etching modes with universal adhesives is more effective than that of self-etch mode from the viewpoint of bond fatigue resistance, in agreement with a systematic review of earlier laboratory bond strength evaluations[16].

The results for interfacial characteristics showed that the baseline γ_s, γ_s^d, γ_s^p, and γ_s^h values for dentin in etch-and-rinse mode were significantly lower than in self-etch mode. These results indicate that the wettability, hydrophilicity, and degree of polarization of phosphoric acid-etched dentin might be lower than those of ground dentin. Tay et al.[17] reported that the dehydra-
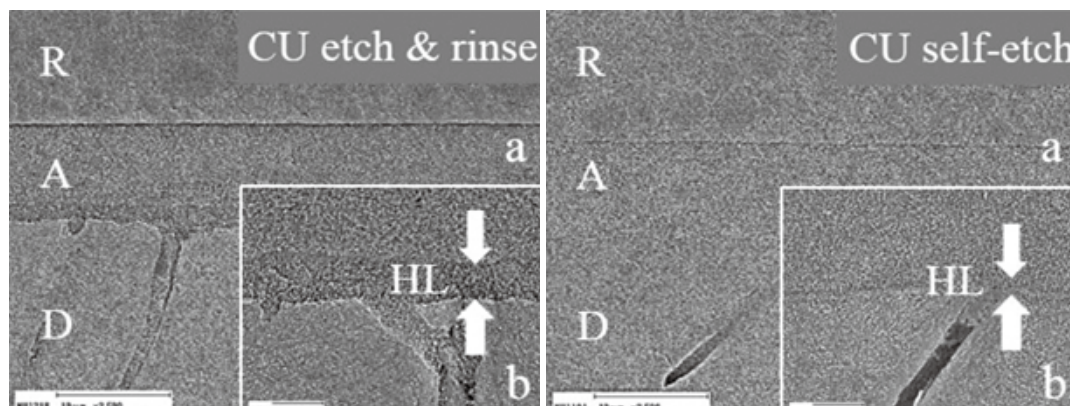
Fig. 1 Scanning electron microscopy images of the composite-dentin interface
One panel as CU etch & rinse and the other panel as CU self-etch at （a）2,500× and （b）10,000×
magnifications. A, adhesive; D, dentin; HL, hybrid layer; R, resin composite.

tion of demineralized dentin resulted in osmosis of water content from deeper dentin, leading to weaker bonding due to osmotic blisters and hydrolysis of the adhesive itself. However, etching mode did not influence the dentin bond fatigue resistance of the universal adhesive in the present study. In our SEM observations of adhesive interfaces, deeper penetration of the adhesive into the dentinal tubules was observed in etch-and-rinse mode due to removal of the smear layer and opening of the dentinal tubules by phosphoric acid etching, despite the lower wettability of the dentin. These deeper resin tags, lying perpendicular to shear stress, may have contributed somewhat to the cyclic fatigue resistance of adhesive interfaces. Additionally, bond fatigue testing in this study was performed with a frequency of 20 Hz and a cycling period of 50,000 cycles, but only for ~40 min, which may not be a sufficiently long testing period. Hence, the influence of osmosis of water content from deeper dentin, resulting in osmotic blisters and hydrolysis of adhesive, might have been reduced due to the short testing period compared to tests using long-term water storage or thermal cycling.

For the universal adhesive employed in this study, 10-MDP is a key technological factor for chemical bonding with dentin substrate, regardless of the bonding strategy employed. The adhesion-decalcification concept[18] claimed that the functional group of 10-MDP interacts ionically with calcium in dentin, forming a chemically bonded structure of 10-MDP and calcium salt layers on the dentin surface. As the long carbonyl chain of 10-MDP is relatively hydrophobic[19], a hydrophobic layer would cover the dentin surface due to the

layered structure of 10-MDP and calcium salt. A greater extent of chemical bonding to the dentin surface should therefore create a more hydrophobic surface. Only the γ_s^h value of adhesive-treated dentin in etch-and-rinse mode was significantly lower than the baseline, although both γ_s and γ_s^h values were decreased after adhesive application in self-etch mode. Thus, the second null hypothesis was rejected. A previous study[13] reported that interfacial characteristics were influenced by reactions between acidic functional monomers and calcium in tooth substrates; thus the present results are consistent with those of previous studies. Based on the different tendencies observed in the changes in interfacial characteristics between baseline and adhesive-treated dentin, the chemical interactions in self-etch mode might be much stronger than those in etch-and rinse mode.

Another interpretation of the results of bond fatigue testing might be supported by these surface free energy changes. Even with the deeper penetration of resin tags, lower reactivity between 10-MDP and collagen fibrils might reduce the stability of the bond, adding to the effects of the lower wettability of the adherend surface. However, further research is needed to clarify the contribution to dentin bond durability of the interaction between the functional resin monomer and naked collagen.

The clinical implication of this study is that although many Japanese clinicians use universal adhesive in selective etching mode, there is not much need to worry about exposure of dentin to phosphoric acid when the clinician places a direct composite filling with

this adhesive.

Conclusion

1. The initial bond strengths and bond fatigue strengths were not significantly influenced by etching mode.

2. The baseline in etch-and-rinse mode exhibited significantly lower γ_s and γ_s^h values than in self-etch mode. Only the γ_s^h value of adhesive-treated dentin in etch-and-rinse mode was significantly lower than the baseline, while both the γ_s and γ_s^h values were decreased after adhesive application in self-etch mode.

3. Based on SEM observations, the adaptation of the interface to dentin was excellent for both etching modes.

References

1) Van Meerbeek B, Yoshihara K, Van Landuyt K, Yoshida Y, Peumans M. From Buonocore's pioneering acid-etch technique to self-adhering restoratives. A status perspective of rapidly advancing dental adhesive technology. J Adhes Dent 2020; 22: 7-34.

2) Cuevas-Suárez CE, de Oliveira da Rosa WL, Vitti RP, da Silva AF, Piva E. Bonding strength of universal adhesives to indirect substrates: A meta-analysis of in vitro studies. J Prosthodont 2020; 29: 298-308.

3) Saikaew P, Matsumoto M, Chowdhury AFMA, Carvalho RM, Sano H. Does shortened application time affect long-term bond strength of universal adhesives to dentin?. Oper Dent 2018; 43: 549-558.

4) Kumagai RY, Hirata R, Pereira PNR, Reis AF. Moist vs over-dried etched dentin: FE-SEM/TEM and bond strength evaluation of resin-dentin interfaces produced by universal adhesives. J Esthet Restor Dent 2020; 32: 325-332.

5) Tsujimoto A, Barkmeier WW, Takamizawa T, Watanabe H, Johnson WW, Latta MA, Miyazaki M. Comparison between universal adhesives and two-step self-etch adhesives in terms of dentin bond fatigue durability in self-etch mode. Eur J Oral Sci 2017; 125: 215-222.

6) Nagarkar S, Theis-Mahon N, Perdigão J. Universal dental adhesives: Current status, laboratory testing, and clinical performance. J Biomed Mater Res B Appl Biomater 2019; 107: 2121-2131.

7) Erickson RL, De Gee AJ, Feilzer AJ. Effect of pre-etching enamel on fatigue of self-etch adhesive bonds. Dent Mater 2008; 24: 117-123.

8) Barkmeier WW, Erickson RL, Latta MA. Fatigue limits of enamel bonds with moist and dry techniques. Dent Mater 2009; 25: 1527-1531.

9) Scheidel DD, Takamizawa T, Bakmeier WW, Erickson RL, Tsujimoto A, Miyazaki M. Effect of frequency on the fatigue strength of dentin bonds. J Oral Sci 2016; 58: 539-546.

10) Tsujimoto A, Barkmeier WW, Erickson RL, Takamizawa T, Latta MA, Miyazaki M. Influence of the number of cycles on shear fatigue strength of resin composite bonded to enamel and dentin using dental adhesives in self-etching mode. Dent Mater J 2018; 37: 113-121.

11) Tsujimoto A, Barkmeier WW, Erickson RL, Fischer NG, Markham MD, Takamizawa T, Latta MA, Miyazaki M. Shear fatigue strength of resin composite bonded to dentin at physiological frequency. Eur J Oral Sci 2018; 126: 316-325.

12) Yoshida Y, Yoshihara K, Nagaoka N, Hayakawa S, Torii Y, Ogawa T, Osaka A, Van Meerbeek B. Self-assembled nano-layering at the adhesive interface. J Dent Res 2012; 91: 376-381.

13) Inoue N, Tsujimoto A, Takimoto M, Ootsuka E, Endo H, Takamizawa T, Miyazaki M. Surface free-energy measurements as indicators of the bonding characteristics of single-step self-etching adhesives. Eur J Oral Sci 2010; 118: 525-530.

14) Hata T, Kitazaki Y, Saito T. Estimation of the surface energy of polymer solids. J Adhes 1987; 21: 177-194.

15) Nagura Y, Tsujimoto A, Barkmeier WW, Watanabe H, Johnson WW, Takamizawa T, Latta MA, Miyazaki M. Relationship between bond fatigue durability and surface free energy characteristics of universal adhesives to enamel. Eur J Oral Sci 2018; 126: 135-145.

16) Rosa WL, Piva E, Silva AF. Bond strength of universal

adhesives: a systematic review and meta-analysis. J Dent 2015; 43: 765‒776.

17) Tay FR, Pashley DH, García-Godoy F, Yiu CK. Single-step, self-etch adhesives behave as permeable membranes after polymerization. Part Ⅱ. Silver tracer penetration evidence. Am J Dent 2004; 17: 315‒322.

18) Yoshioka M, Yoshida Y, Inoue S, Lambrechts P, Vanherle G, Nomura Y, Okazaki M, Shintani H, Van Meerbeek B. Adhesion/decalcification mechanisms of acid interactions with human hard tissues. J Biomed Mater Res 2002: 59: 56‒62.

19) Van Landuyt KL, Yoshida Y, Hirata I, Snauwaert J, De Munck J, Okazaki M, Suzuki K, Lambrechts P, Van Meerbeek B. Influence of the chemical structure of functional monomers on their adhesive performance. J Dent Res 2008; 87: 757‒761.

Original Article

Development of Chairside Dry Heat Sterilizer Using Halogen Lamps as a Thermal Radiation Source

Keisuke SAIGUSA, Yukihiro TAKAHASHI*,

Munehiro MAEDA and Masaru IGARASHI

Department of Endodontics, The Nippon Dental University, School of Life Dentistry at Tokyo
*Department of Microbiology, The Nippon Dental University, School of Life Dentistry at Tokyo

Abstract

Purpose: A chairside dry heat sterilizer using halogen lamps as a heat radiation source was developed, and its potential for clinical application was investigated.

Methods: The temperature in the sterilization chamber was measured in two groups: one group in which the central temperature was set and maintained at 330℃, and another group in which the central temperature continuously increased. Then, changes in the physical properties of a stainless-steel K-file irradiated with the lamp were examined by observing the surface by scanning electron microscope and by bending and torsion tests. Finally, sterilization tests were conducted using spore-forming bacteria and indigenous oral bacteria.

Results: The temperature in the light condensing area stabilized after about 20 s, with little effect on the physical properties of the K-file. Sterilization of spore-forming bacteria took several tens of seconds, while that of indigenous oral bacteria took 3-5 s on a paper point and 7-10 s on a cotton ball.

Conclusion: It is suggested that the chairside dry heat sterilization using a thermal radiation source is useful for dental materials.

Key words: simple dry heat sterilizer, halogen lamp, stainless-steel K-file, strength test, spore-forming bacteria

Introduction

Aseptic treatment in dentistry is one of the most important principles to improve treatment outcomes and prevent the spread of infection via treatment instruments. In particular, endodontic treatment requires thorough removal of bacterially infected tooth structures and antiseptic treatment of healthy dentin. In addition, root canal treatment possesses the risk of contamination by blood and saliva during the procedure, and also by necrotic tissue that has been infected by bacteria, making it necessary to re-disinfect the treatment instruments during the procedure.

In recent years, from the perspective of nosocomial infection, dental care workers have needed to be especially careful about their own infection potential to prevent bacterial infections caused by methicillin-resistant *Staphylococcus aureus*, *Pseudomonas aeruginosa*, and *Treponema pallidum*[1,2]. Viral infections include infections caused by viruses of the herpesvirus family, hepatitis B and C viruses, and human immunodeficiency virus, and these microorganisms have also been detected in dental pulp and periodontal tissues[3-5]. Recently, severe acute respiratory syndrome coronavirus 2 (SARS-CoV-2) has caused a worldwide pandemic and the infection is still spreading, so patients must be treated with caution during dental care[6,7].

Small sharp instruments such as reamers and files, which are frequently used in endodontics, are classified as critical instruments and are sterilized by gas or high-pressure steam sterilization before use[8]. However, once they come into contact with fingers, saliva, or infected dentin, bacterial contamination of the instruments is inevitable, and because these instruments are used repeatedly during the procedure, frequent sterilization during treatment is necessary.

Many endodontic dry heat sterilizers that can be used chairside have been described in the literature, including 1) devices using molten tin-based alloys, 2) devices using salt as a medium, 3) bead sterilizers using small glass beads or metal balls, 4) electric furnace-type dry heat sterilizers with heaters wrapped around quartz tubes, and 5) sterilizers that heat brass blocks with slits[9-18]. However, sterilizers that use molten metal or small balls, such as glass beads, introduce the possibility that the metal or balls will become attached

to the sterilized instrument and be transported directly into the root canal, resulting in blockage of the canal[11,12], harm to the human body due to heavy metal poisoning, and burns due to scattering of hot material.

Meanwhile, other sterilizers also have problems, such as unbalancing the table of the dental unit due to the excessive weight of the entire sterilizer, media spillage when the sterilizer is tipped over, and salt coagulation due to humidity in hot salt sterilizers. Furthermore, all sterilizers take time to heat the media, so advance preparation is necessary. Finally, in recent years, opportunities for home-visit dental care, in addition to dental care in the clinic, have been increasing, and thus there is a demand for easy, safe, and portable sterilizers that can be brought into a typical residence.

In this study, we developed a simple dry heat sterilizer that uses halogen lamps as a thermal radiation source to convert electrical energy into thermal energy and directly apply it to materials to be sterilized in the form of electromagnetic waves. Then, we investigated the characteristics of the sterilizer to determine its potential for clinical application.

Materials and Methods

1．Experimental equipment

An overview of the prototype sterilizer and peripheral apparatus is shown in Fig. 1. The prototype sterilizer was composed of two metal plates, each 154 mm in width by 70 mm in height, and two heat sinks, each 100 mm in width by 70 mm in height. These were combined on a metal chassis measuring 180 mm wide by 120 mm deep by 55 mm tall. A hole 1 cm in diameter was made in the center of the upper metal cover, and halogen lamps were installed in the heat sinks.

A halogen lamp spot heater (HSH-30, Fintech, Hyogo, Japan) with a focal length of 40 mm, a light condensing area diameter of 10 mm, and power of 75 watts was used for the experiment. Irradiation was carried out in both directions on opposite sides of the device's coaxial axis, and the material to be sterilized was placed in the irradiation field in the middle of the heater. The voltage was supplied by a 100 V household power supply, which was converted to 24 V for use, and the current was set at 3.125 A.

In Fig. 2, K-type thermocouples (Φ 0.3 mm) were placed alternately facing each other at 5-mm intervals

a

b
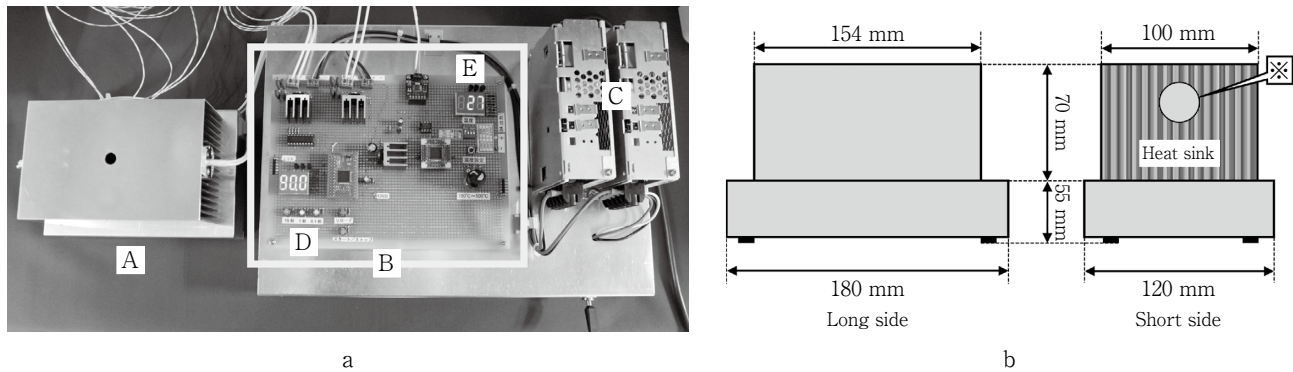
Fig. 1

(a) Overview of prototype sterilizer and peripheral apparatus：(A) Prototype sterilizer,(B) Control apparatus,(C) Power supply unit, (D) Irradiation switch, (E) Temperature control apparatus

(b) Schematic diagram of prototype sterilizer （※：Base of the halogen lamp）

a

b
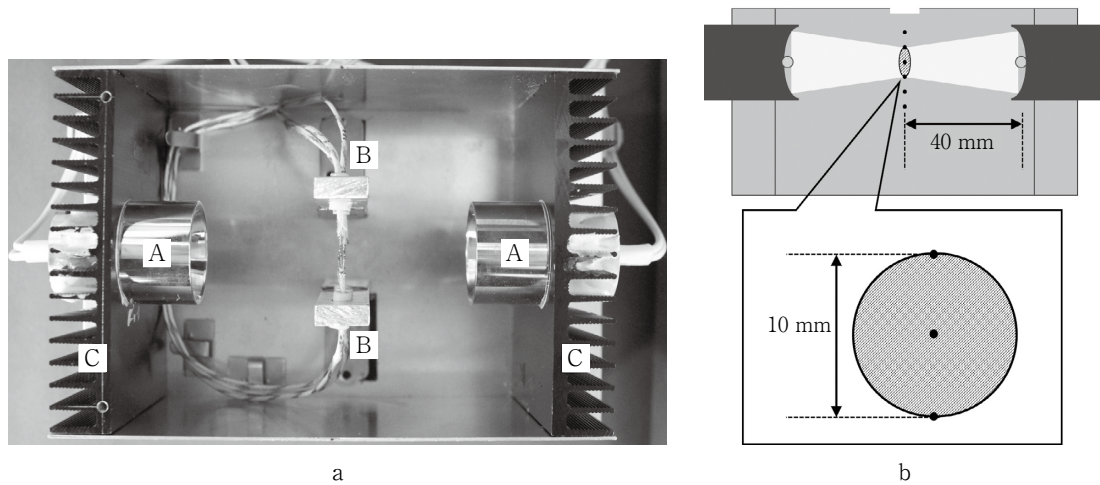
Fig. 2

(a) Prototype sterilizer (Fig. 1, A), top view：(A) Halogen lamps, (B) K-type thermocouples, (C) Heat sinks

(b) Cross-sectional schematic diagram of the prototype sterilizer：the entire circle is the light condensing area, and the circumference is the outer edge. The black points represent the tips of the K-type thermocouples （depths of 10, 15, 20, 25, 30, and 35 mm from the top）.

up to 35 mm from the side of the apparatus to measure the temperature of the sterilization area. The light condensing area （10 mm） at the focus of the halogen lamp was set at a depth of 15–25 mm from the hole, with 15 and 25 mm at the outer edge of the light condensing area and 20 mm at the center of the light condensing area.

The irradiation time could be set from 0.1 to 99.9 s at 0.1-s intervals, and a countdown system was adopted. There was also a temperature control switch that could be set from 100℃ to 500℃ in 1℃ increments. Two settings for halogen lamp irradiation were established:

Ⅰ: When the control switch is turned on, the lamp cycles on and off to reach and maintain the set temperature automatically.

Ⅱ: When the control switch is turned off, continuous irradiation is performed and the temperature increases until the switch is turned off.

2. Experimental details

The following items were investigated to determine the effects of this device on endodontic instruments and materials.
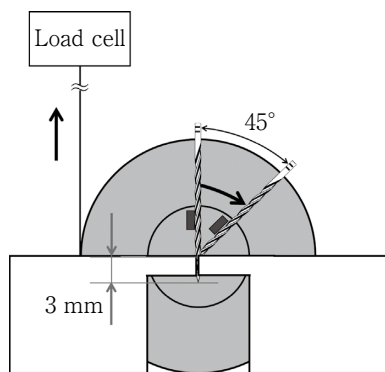
Fig. 3 Bending test machine
The first 3 mm of the file tip is fixed with a chuck, and the bending torque is measured when the file is bent to 45°.

Fig. 4 Torsion test machine
The first 3 mm of the file tip is fixed with a chuck, the file is twisted until it breaks, and the torsion torque and rotation angle at the time of failure are measured.

1) Measurement of temperature in the light condensing area

The K-type thermocouples placed inside the sterilizer were used to record the temperature change over time at 100-ms intervals when the temperature was controlled at 330℃ with setting Ⅰ and when the temperature was continuously increased with setting Ⅱ. The irradiation time was set to 90 s for both settings.

The measurement data were recorded on a PC (Inspiron 15 7000 Gaming, DELL, Round Rock, TX, USA) using a data logger (NR-1000, KEYENCE, Osaka, Japan). Temperature measurements were performed at room temperature (25℃) and humidity (55%).

2) Surface observation of K-files after heat irradiation

The surface of #40 stainless-steel hand K-files (MANI, Tochigi, Japan) was observed under a scanning electron microscope (SEM, S-4000, Hitachi, Tokyo, Japan) after halogen lamp irradiation to detect any change in the surface properties.

Five experimental groups were established. The first group was subjected to natural air cooling to room temperature after 5 s of irradiation, and this cycle was repeated 10 times at setting Ⅱ. The second and third groups were subjected to the same treatment, but at irradiation times of 10 s and 15 s. In addition, two control groups were set. An untreated group was used as a negative control and a flame-treated group was used as a positive control. In the flame-treated group, the blade was set at the position of the oxidizing flame of the gas burner (about 1,500℃) and heated for 10 s by grasping

the top, then the K-file was allowed to cool by natural air cooling to room temperature, and this process was repeated 10 times. We observed the surface changes by SEM for each group (n=1).

3) Strength testing of files after heat irradiation

The changes in physical properties of the files after irradiation with halogen lamps were tested according to the international standard ISO 3630-1[19] for small dental instruments and judged according to the standard values of ISO 3630-5.[20] Two types of #15–40 stainless-steel hand K-file were used for the test: K-file and Senseus K-FlexoFile (Dentsply Sirona, Charlotte, NC, USA). Since there was a risk of bias with a single type of sample, we made a comprehensive judgment by comparing two K-files with their respective untreated groups.

Non-irradiated files were used as a control group, and the experimental group consisted of files that were irradiated 10 times with halogen lamps for 10 s at setting Ⅱ (n=10 for each group). All instruments were allowed to stand at room temperature (25℃) for 30 min after each irradiation before the next irradiation. Before each test, the handle of the file was removed with wire cutters at the point where it was attached to the instrument shaft.

(1) Bending test (ISO 3630-1)

The bending test machine and test method are shown in Fig. 3. A section of the K-file up to 3 mm from the tip was fixed vertically in the chuck section of the bending test machine and rotated at a speed of 100 mm/min to induce bending. The maximum bending torque was measured and the average value of 10 files was used as the maximum bending torque (mN・m).
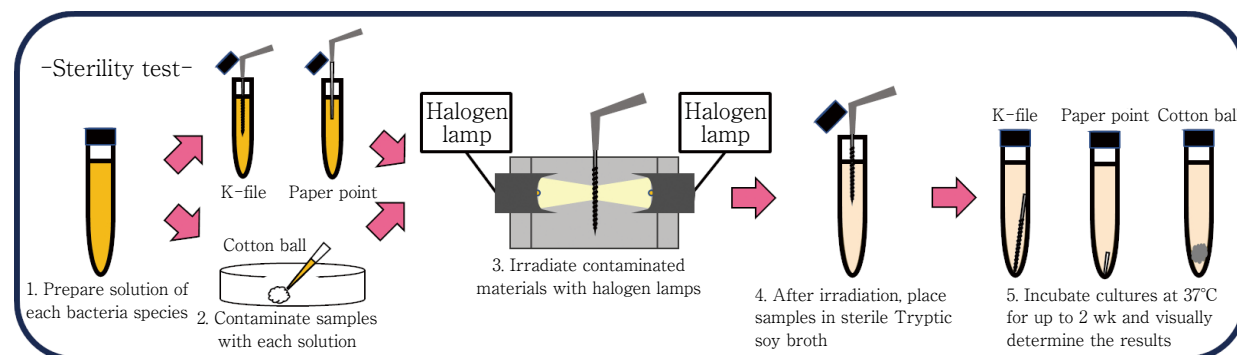
Fig. 5 Sterilization test procedure

（2）Torsion test（ISO 3630-1）

The torsion test machine and test method used are shown in Fig. 4. Each sample was set in the chuck of the motor, and a section of the file up to 3 mm from the tip was fixed in the chuck on the opposite side. The torque measuring device on the top of the machine was connected to the torsion testing machine by a wire, and the motor was operated at 100 mm/min. The average value of 10 files was used as the maximum torsional torque（mN・m）and fracture angle（°）.

4）Heat sterilization tests for K-files, paper points, and cotton balls

Various microorganisms were applied to different dental materials to evaluate the sterilization effectiveness. *Bacillus atrophaeus* ATCC9372 was used because it is regarded as an indicator organism for dry heat sterilization in ISO 11138-4[21]. *Fusobacterium nucleatum* ATCC23726, *Streptococcus intermedius* NCTC11324, *Actinomyces oris*（formerly known as *A. viscosus*）T14V[22], and *Streptococcus mutans* MT8148[23] were used as representative of indigenous oral bacteria. In addition, *Escherichia coli* W3110 was also included, for a total of six bacteria species used in the experiment.

B. atrophaeus and *F. nucleatum* were purchased from the American Type Culture Collection（ATCC）, and *S. intermedius* was purchased from the National Collection of Type Cultures（NCTC）. *E. coli* W3110 was obtained from the Institute of Medical Science, University of Tokyo.

First, only *B. atrophaeus* was inoculated in 50 ml of Shaeffer's medium[24] as a spore-forming medium, and cultured at 37℃ with shaking for 24 h. The spores were then removed from the shaking incubator and stored at room temperature for 1 wk. After confirming sufficient spore formation by Wirtz's spore staining method, the spores were collected by centrifugation at 3,000×g for 15 min, washed three times with sterile distilled water, and then heat-treated at 75℃ for 30 min to kill the vegetative form bacteria. Other bacteria were inoculated in brain heart infusion（BHI: Becton, Dickinson and Company, Sparks, MD, USA）broth and incubated at 37℃ for 24 h.

For experimental samples, we used a #40 stainless-steel hand K-file, #40 sterile paper points（Absorbent Paper Points, Zipperer, Germany）, and cotton balls with a diameter of 3 mm（Micro Cotton Ball #3, Iwatsuki, Tokyo, Japan）. The K-file was cut with wire nippers just below the handle, and the cotton balls were removed from their container, placed in sterilization bags, and sterilized by high-pressure steam in an autoclave for the experiments.

The procedure of the sterilization test is shown in Fig. 5. The K-file was immersed up to 16 mm from the tip of the blade in a bacterial solution adjusted to 1.0×10^8 colony forming units（CFU）/ml for each species. Contaminating bacteria on the paper points and cotton balls were prepared at approximately 2.0×10^3 CFU/ml. The paper points were immersed in 2.0×10^6 CFU/ml of bacterial solution up to 10 mm from the tip（about 1 μl）, and the cotton balls were contaminated by dropping 10 μl of 2.0×10^5 CFU/ml bacterial solution. The cotton balls were then placed in a sterile Petri dish for 30 min at 37℃ to dry them before use in the experiments.

For the K-files, the irradiation time was set to 0［Control（＋）］, 3, 5, 7, and 10 s with setting Ⅱ for all bacteria. For the paper and cotton samples, setting Ⅰ was used, and the irradiation time was set to 0［Control（＋）］, 3, 5, 7, 10, 15, 20, 30, and 40 s for *B. atrophaeus* and 0, 3, 5, 7, and 10 s for other bacteria（n＝20 for each
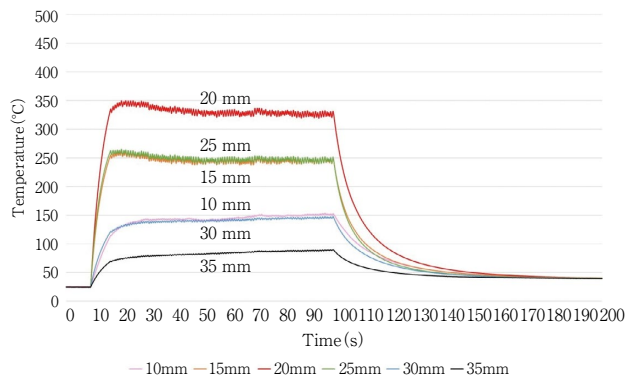
Fig. 6 Temperature measurement during irradiation at setting Ⅰ

Irradiation was started 10 s after the start of temperature measurement.

Fig. 7 Temperature measurement during irradiation at setting Ⅱ

Irradiation was started 10 s after the start of temperature measurement.

group). The test samples were irradiated with halogen lamps and incubated in sterile Tryptic soy broth (Becton, Dickinson and Company) at 37℃ for 24 h, 48 h, 72 h, 1 wk, and 2 wk, the results were visually checked, and those with increased turbidity or precipitation were judged as positive for culture. For each group, the number of samples that were culture negative was counted, divided by 20 (the total number of samples), and multiplied by 100 to calculate the culture negative achievement rate.

The paper points were cut 10 mm from the contaminated tip before being fed into the sterilizer.

3. Statistical analysis of strength

Student's *t*-test was performed on the data obtained from the strength tests. The statistical significance level was set at less than 5%, and IBM SPSS ver. 25 was used as the statistical software.

Results

1. Temperature measurement of sterilization area

The temperature of the sterilization area was measured for 90 s when the temperature was controlled to around 330℃ with setting Ⅰ (Fig. 6). When this temperature was reached, the control apparatus could not react quickly enough, and the center temperature rose to 349℃. However, 20 s after the start of control, the temperature stabilized at around 330℃. The amplitude during each on/off switching cycle was about 10℃, which maintained the temperature at around 325–335℃
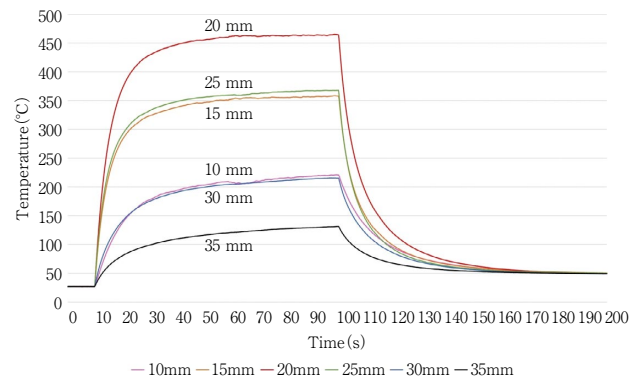
until the end of irradiation.

At 15 mm and 25 mm, which were the outer edges of the condensing area, the temperature rose to approximately 260℃ and remained at around 240–250℃ until the end of irradiation. The temperature dropped sharply outside the condensing area, reaching only 120–150℃ at 10 mm and 30 mm and 70–90℃ at 35 mm.

In setting Ⅱ, continuously increasing irradiation was performed for 90 s, and the results were measured over time (Fig. 7). In the light condensing area at a depth of 15–25 mm, the temperature rose rapidly as soon as irradiation started, reaching 275℃ at the center and 215–226℃ at the outer edge 5 s after the start of irradiation. After another 10 s, the temperature reached 368℃ at the center and 280–289℃ at the outer edge, and after 15 s, 408℃ at the center and 307–317℃ at the outer edge. The highest temperatures after 90 s of irradiation were 464℃ at the center and 367℃ at the outer edge.

2. Surface observation of K-files after heat irradiation

The surface of each file was observed by SEM (Fig. 8). The flame-treated group showed a loss of continuity due to the collapse of the file edge, with the metal on the file surface peeling off. In the group irradiated by the halogen lamp, there was no major change in the surface properties of the files irradiated for 5, 10, and 15 s compared with the untreated group, either by visual inspection without magnification or in the SEM images.

Flame treatment group ［Control(＋)］

Untreated group ［Control(－)］

5 s irradiation repeated 10 times group

10 s irradiation repeated 10 times group

15 s irradiation repeated 10 times group
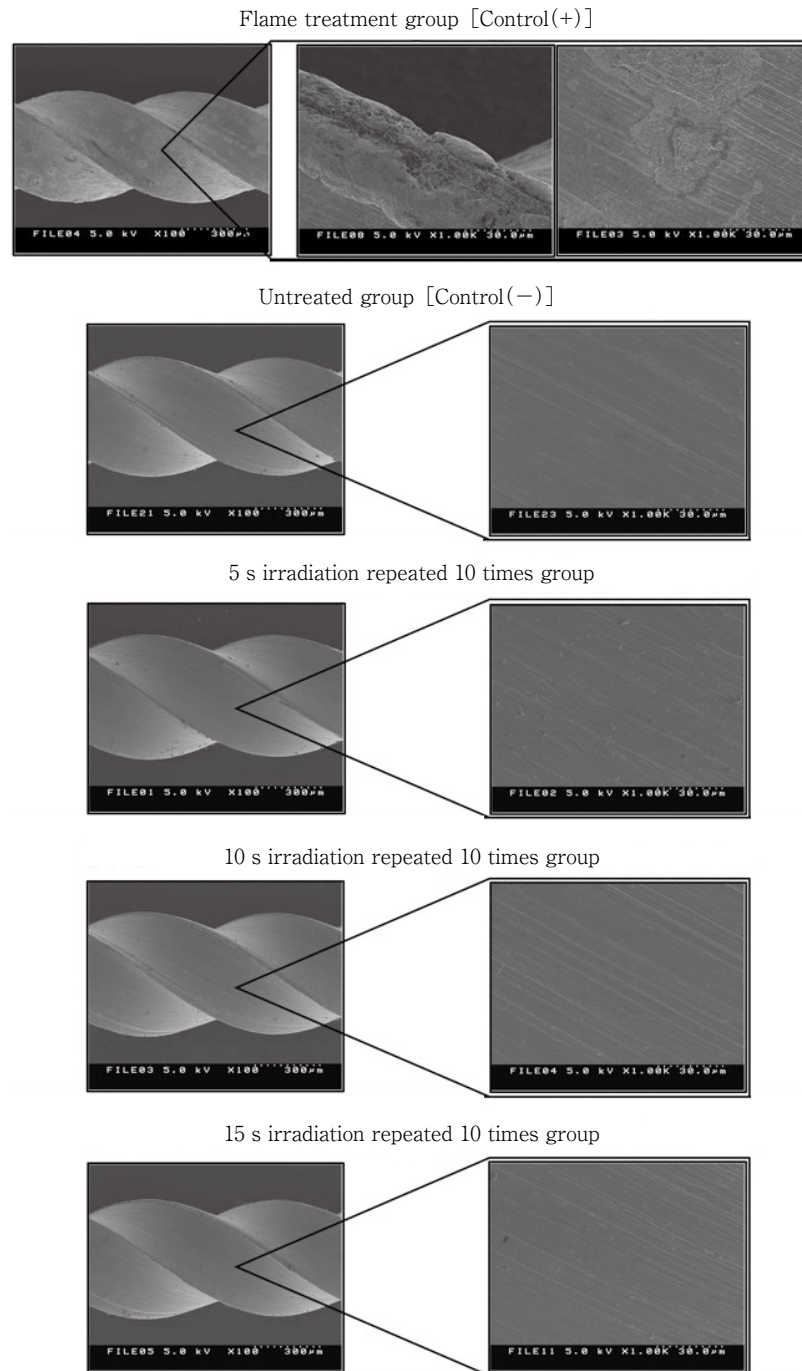
Fig. 8 Surface observation by SEM of K-file irradiated by halogen lamp

3．Strength testing of K-files after heat irradiation

The results of the strength tests are shown in Fig. 9.

1）Bending test

The torques required to bend the files up to 45°are shown in Fig. 9A and B. There was a significant difference between the control and irradiated groups for the #15 MANI K-files （$p < 0.05$）, and there was no significant difference between the groups for the Senseus K-FlexoFile. The bending torque values in both groups were within the ISO standard values.

2）Torsion test

The maximum torque and fracture angle until fracture when torsion was applied to the file are shown in Fig. 9C-F. For the #25 MANI K-file, results for the irradiated group were significantly lower than those for the untreated group, and for the #35 MANI K-file, results
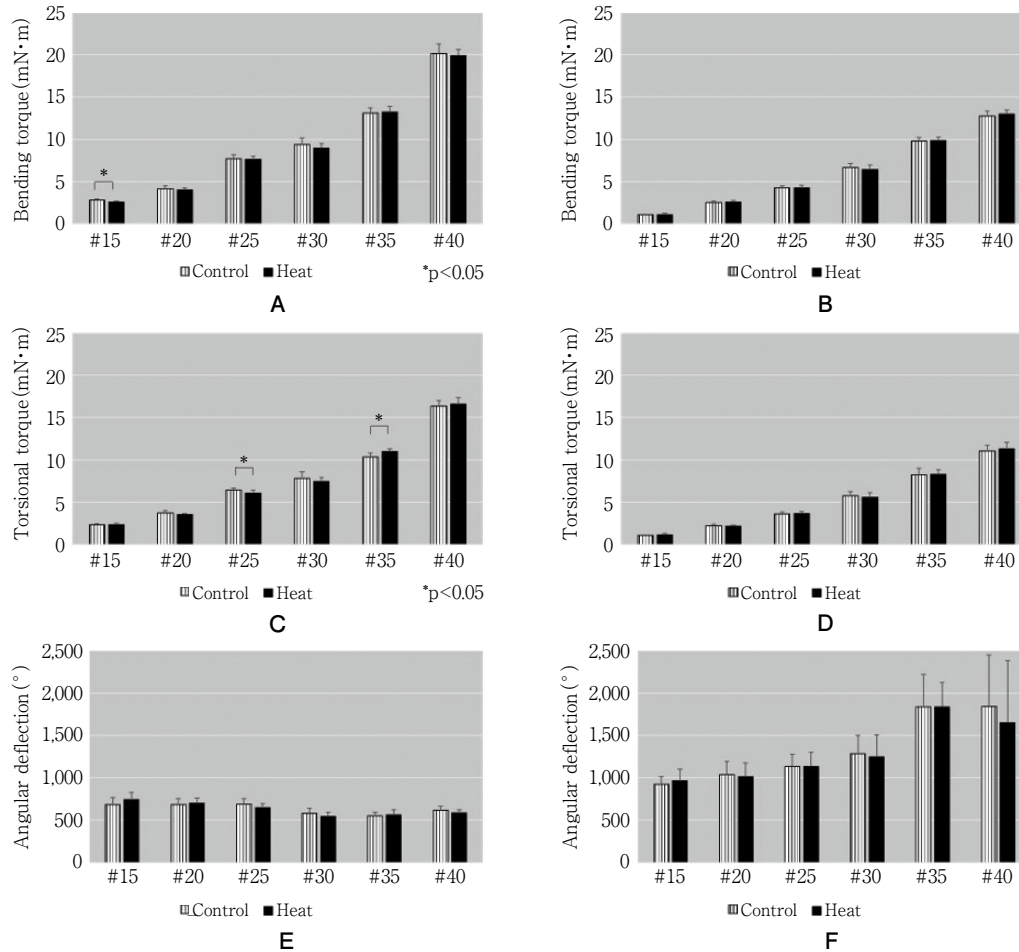
Fig. 9 Bending test and torsion test results （p＜0.05, n＝20）

（A）MANI K-file bending test results ；（B）Senseus K-FlexoFile bending test results ；

（C),（E）MANI K-file torsion test results ；（D),（F）Senseus K-FlexoFile torsion test results

for the untreated group were significantly lower than those for the irradiated group （p＜0.05）. The torque failure values for both groups were within the ISO standard values.

There was no significant difference between the groups for Senseus K-FlexoFile, but only one of the 10 #40 K-files had a fracture angle below the ISO standard of 360°. Therefore, 10 additional tests were conducted in accordance with the standard, and all of them were confirmed to meet the standard.

4. Sterilization tests

The results of the sterilization tests are shown in Tables 1-3. The culture results for K-files were all negative after 10 s of irradiation for *B. atrophaeus* and after 7 s for other bacteria. Results for the paper points were negative after 30 s for *B. atrophaeus*, after 5 s for *S. mutans* and *A. oris*, and after 3 s for other bacteria.

The culture results for cotton balls were all negative after 40 s for *B. atrophaeus*, after 10 s for *S. mutans, A. oris*, and *F. nucleatum*, and after 7 s for other bacteria.

Discussion

Most conventional simple dry heat sterilizers provide sterilization heat through a heating medium, such as glass pellets or molten metal, and it takes several minutes for the heating medium to rise to the sterilization temperature. In contrast, the prototype of the simple dry heat sterilizer used in this study heats the materials to be sterilized by directly radiated heat, which has the advantage of eliminating the need to turn on the power supply and heat the medium beforehand because there is no heating medium. Therefore, it is possible to rapidly heat an object by turning on the power and

Table 1　Sterilization test results of K-file（%）

Species and Irradiation		24 h	48 h	72 h	1 wk	2 wk	Species and Irradiation		24 h	48 h	72 h	1 wk	2 wk
B. atrophaeus	0 s	0	0	0	0	0	*E. coli*	0 s	0	0	0	0	0
	3 s	0	0	0	0	0		3 s	60	60	60	60	60
	5 s	70	0	0	0	0		5 s	65	65	65	65	65
	7 s	80	35	30	30	30		7 s	100	100	100	100	100
	10 s	100	100	100	100	100		10 s	100	100	100	100	100
Species and Irradiation		**24 h**	**48 h**	**72 h**	**1 wk**	**2 wk**	**Species and Irradiation**		**24 h**	**48 h**	**72 h**	**1 wk**	**2 wk**
S. mutans	0 s	0	0	0	0	0	*S. intermedius*	0 s	0	0	0	0	0
	3 s	90	80	80	80	80		3 s	80	80	80	80	80
	5 s	95	95	95	95	95		5 s	95	95	95	95	95
	7 s	100	100	100	100	100		7 s	100	100	100	100	100
	10 s	100	100	100	100	100		10 s	100	100	100	100	100
Species and Irradiation		**24 h**	**48 h**	**72 h**	**1 wk**	**2 wk**	**Species and Irradiation**		**24 h**	**48 h**	**72 h**	**1 wk**	**2 wk**
A. oris	0 s	100	0	0	0	0	*F. nucleatum*	0 s	0	0	0	0	0
	3 s	100	0	0	0	0		3 s	0	0	0	0	0
	5 s	100	90	65	65	65		5 s	85	85	85	85	85
	7 s	100	100	100	100	100		7 s	100	100	100	100	100
	10 s	100	100	100	100	100		10 s	100	100	100	100	100

The percentages of negative achievement rate are indicated（n＝20）.

Table 2　Sterilization test results of paper point（%）

Species and Irradiation		24 h	48 h	72 h	1 wk	2 wk	Species and Irradiation		24 h	48 h	72 h	1 wk	2 wk
B. atrophaeus	0 s	0	0	0	0	0	*E. coli*	0 s	0	0	0	0	0
	3 s	0	0	0	0	0		3 s	100	100	100	100	100
	5 s	15	0	0	0	0		5 s	100	100	100	100	100
	7 s	25	25	25	25	25		7 s	100	100	100	100	100
	10 s	50	50	50	50	50		10 s	100	100	100	100	100
	15 s	60	60	55	55	55	**Species and Irradiation**		**24 h**	**48 h**	**72 h**	**1 wk**	**2 wk**
	20 s	75	65	65	65	65	*S. intermedius*	0 s	0	0	0	0	0
	30 s	100	100	100	100	100		3 s	100	100	100	100	100
	40 s	100	100	100	100	100		5 s	100	100	100	100	100
Species and Irradiation		**24 h**	**48 h**	**72 h**	**1 wk**	**2 wk**		7 s	100	100	100	100	100
S. mutans	0 s	0	0	0	0	0		10 s	100	100	100	100	100
	3 s	100	95	65	65	65	**Species and Irradiation**		**24 h**	**48 h**	**72 h**	**1 wk**	**2 wk**
	5 s	100	100	100	100	100	*F. nucleatum*	0 s	0	0	0	0	0
	7 s	100	100	100	100	100		3 s	100	100	100	100	100
	10 s	100	100	100	100	100		5 s	100	100	100	100	100
Species and Irradiation		**24 h**	**48 h**	**72 h**	**1 wk**	**2 wk**		7 s	100	100	100	100	100
A. oris	0 s	100	0	0	0	0		10 s	100	100	100	100	100
	3 s	100	35	35	35	35							
	5 s	100	100	100	100	100							
	7 s	100	100	100	100	100							
	10 s	100	100	100	100	100							

The percentages of negative achievement rate are indicated（n＝20）.

Table 3 Sterilization test results of cotton ball（%）

Species and Irradiation		24 h	48 h	72 h	1 wk	2 wk	Species and Irradiation		24 h	48 h	72 h	1 wk	2 wk
B. atrophaeus	0 s	0	0	0	0	0	*E. coli*	0 s	0	0	0	0	0
	3 s	0	0	0	0	0		3 s	10	10	10	10	10
	5 s	0	0	0	0	0		5 s	95	80	80	80	80
	7 s	0	0	0	0	0		7 s	100	100	100	100	100
	10 s	0	0	0	0	0		10 s	100	100	100	100	100
	15 s	0	0	0	0	0	Species and Irradiation		24 h	48 h	72 h	1 wk	2 wk
	20 s	0	0	0	0	0	*S. intermedius*	0 s	0	0	0	0	0
	30 s	45	45	45	45	45		3 s	60	25	25	25	25
	40 s	100	100	100	100	100		5 s	95	95	95	95	95
Species and Irradiation		24 h	48 h	72 h	1 wk	2 wk		7 s	100	100	100	100	100
S. mutans	0 s	0	0	0	0	0		10 s	100	100	100	100	100
	3 s	15	0	0	0	0	Species and Irradiation		24 h	48 h	72 h	1 wk	2 wk
	5 s	100	45	30	25	25	*F. nucleatum*	0 s	0	0	0	0	0
	7 s	100	80	65	55	55		3 s	10	0	0	0	0
	10 s	100	100	100	100	100		5 s	70	50	50	50	50
Species and Irradiation		24 h	48 h	72 h	1 wk	2 wk		7 s	75	70	70	70	70
A. oris	0 s	100	0	0	0	0		10 s	100	100	100	100	100
	3 s	100	0	0	0	0							
	5 s	100	60	45	45	45							
	7 s	100	95	95	95	95							
	10 s	100	100	100	100	100							

The percentages of negative achievement rate are indicated（n＝20）.

pressing the irradiation switch.

In our prototype sterilizer, the time from pressing the "on" switch to stabilizing the temperature in the light condensing area was about 20 s. It was reported that it takes 9 min for the temperature to stabilize at 230℃ for glass beads, 5 min for salt, and 6 min for molten metal, which are conventional heating media[13]. Therefore, the setup time was greatly reduced, and the sterilizer could be used immediately. This feature is useful not only in daily clinical practice, but also in home-visit dental care if the device can be made smaller.

In addition, it is possible to set the temperature at the center of the light condensing area with a control switch and select setting Ⅰ, which controls the temperature by cycling the lamp, or setting Ⅱ, which performs continuously increasing irradiation. The paper points and cotton balls, which have poor thermal conductivity, were irradiated with setting Ⅰ, while K-files, which are stainless steel and have good thermal conductivity, were irradiated with setting Ⅱ.

The reason why the temperature was 330℃ in set-ting Ⅰ, which is slightly higher than that of conventional sterilizers（200–280℃）[9-18], is that the prototype sterilizer reflects more of the radiant heat projected onto the sterilized materials compared with the conventional type that uses a heating medium, and not all of the heat energy incident on the materials can be used. This is also the reason why the core temperature of N.I. dry heat sterilizers using radiation heat has been increased to around 360℃ in the past[16].

There is no clear ISO standard for simple dry heat sterilizers, and each sterilizer is designed with its own optimal temperature. The temperature difference between the center of the light condensing area and the outer edge of the light condensing area was 80℃. Although the temperature at the outer edge was not lower than the temperature of a conventional sterilizer, the temperature of the sterilized material may be lower than the apparent temperature for paper and cotton products in a sterilizer with low thermal energy efficiency. Currently, almost no sterilizers available on the market can heat K-files up to 330℃, and N.I. sterilizers have only been reported to heat cotton plugs and paper

points[16].

In this study, we observed the surface of the heated files and performed bending and torsion tests according to ISO 3630-1 to observe the changes in physical properties (Figs. 7 and 8). Compared with the untreated group, images of the flame-treated group showed metal peeling off the surface of the file and the blade disintegrating and blunting due to heat, while the halogen lamp-irradiated group showed no major changes.

It has long been believed that sensitization (a chromium deficiency phenomenon caused by grain precipitation due to chromium carbonization on the surface of the file), which is the cause of intergranular corrosion in 18-8 stainless steel, occurs when steel is heated for a long time at 500–800℃. In this experiment, the temperature was about 410℃ even after the longest irradiation of 15 s, so it is thought that the files were undamaged because the temperature was not high enough to cause grain precipitation[25].

In the bending tests, torque was significantly lower in the MANI #15 K-file, and in the torsion tests, torque was significantly lower in the MANI #25 K-file with respect to the untreated group. However, in both tests, the torque did not decrease significantly compared to the untreated group, and the ISO standard values[20] were met, so the K-files would still be acceptable for clinical use.

There was no significant difference in the fracture angle among all groups, but one Senseus K-FlexoFile #40 fractured at an angle under the ISO standard value. The additional 10 pieces tested in accordance with the standard all exceeded the standard value. The results of these strength tests are in agreement with those of Asakura[26], who reported that the mechanical properties of K-files were not affected until they were heated at 400℃ for 1 h in an electric furnace.

In the sterilization test, we used *B. atrophaeus* (Gram-positive bacteria), which is an indicator bacterium for dry heat sterilization and has the ability to form spores; *S. mutans*, *S. intermedius*, and *A. oris* as Gram-positive bacteria indigenous to the oral cavity; and *F. nucleatum* as Gram-negative bacteria. In addition, *E. coli* was used as a general Gram-negative bacterium. The amount of bacteria applied to the paper points and cotton balls was set at 2.0×10^3 CFU/ml, under the assumption that these materials would be used before provisional sealing at the end of treatment,

because the number of glove bacteria in the second half of treatment, just before the working length was determined and provisionally sealed, has been reported to be approximately $1.0–3.0 \times 10^3$ CFU[27].

For the paper points, negative cultures were obtained after 3–5 s of irradiation for non-spore-forming bacteria, but after 30 s for spore-forming *B. atrophaeus*. Because the central temperature of the condensing area rises to 330℃, this area seems to be able to kill bacteria in a short time. However, the temperature decreases away from the center, and the temperatures of the ends of the samples (tip of the paper point and edge of the cut) located in the outer edge reach only 240–250℃. Therefore, the spores that survive there could germinate.

Cotton balls were culture negative after 7–10 s of irradiation for non-spore-forming bacteria, but took 40 s for spore-forming *B. atrophaeus*. The longer time required for a negative culture compared to the paper points for all species was thought to be due to the fact that the depth from the surface to the center of the cotton ball required more time for heat conduction, allowing interior bacteria to survive.

In the K-files, the length of contamination was 16 mm, some of which was not placed within the condensing area, and despite the large number of contaminating bacteria, the culture was negative after 10 s for spore-forming *B. atrophaeus* and after 7 s for other bacteria species. This is probably due to the good thermal conductivity of the metal, unlike paper or cotton. Because it is rare to come into contact with highly thermostable bacteria in general dental practice, the results confirmed that clinical sterilization could be achieved by irradiating the K-files for 7 s with setting Ⅱ, and the paper points for 5 s and small cotton balls for 10 s with setting Ⅰ at the temperature settings used in this study.

The results show that it was able to quickly and safely heat the materials to be sterilized and achieve sterilization in the light condensing area. This prototype sterilizer had the necessary control boards and equipment in order to achieve sufficient performance. However, since some equipment could be omitted in actual clinical applications, it is possible to reduce the size of the sterilizer, and since there is no heating medium compared to the conventional type, it is possible to reduce the weight. Moreover, the lack of a heat-

ing medium prevented the material from being bent when it was inserted into the sterilization area and eliminated contamination of the material by a heating medium. The results also suggest that this sterilizer is effective for infected root canal treatment, where a large amount of necrotic pulp or infected dentin is handled, or where contamination is suspected due to small instruments falling outside the clean area or being exposed to saliva. Moreover, although they do not come into direct contact with the sterilized materials, the internal walls of the equipment can be sterilized by autoclaving if they are assembled, with the exception of the halogen lamps, which require wiring, so maintenance is considered possible.

However, as with conventional sterilizers, it is necessary to insert long instruments, such as tweezers or K-file handles, that are not heat resistant to direct light exposure. In addition, sterilization of materials exposed to a large amount of microorganism contamination will require a conventional autoclave. The bacterial count set for this study corresponds to that observed during clinical procedures, and it is therefore desirable to sterilize any suspected contaminated items after cleaning them with gauze.

In addition, the temperature tended to drop rapidly away from the center of the light condensing area. Thus, this instrument is effective for sterilizing small areas contaminated during use, and conventional methods are required to achieve complete sterilization of the entire instrument. Once used, instruments should only be used for the same patient, and autoclaves or dry heat sterilizers should be used to sterilize instruments between patients.

Conclusion

1. In setting I in which the central temperature of the condensing area was maintained, the temperature was stable at a central of around 330℃ and an outer edge of around 250℃ after irradiation for 20 s.

2. In setting II with continuous irradiation, the center temperature reached 368℃ and the outer edge temperature increased to around 280℃ after irradiation for 10 s.

3. In SEM observation of the irradiated K-file, there was no change compared to unirradiated file.

4. In the bending test and the torsion test of the

K-file, there was a tendency that no significant difference was observed between the conditions with and without irradiation.

5. The time required for 100% of the spore-forming bacteria to be sterilized was 10 s for the K-file, 30 s for the paper point, and 40 s for the cotton ball. For other bacterial species, it took 7 s for the K-file, 3 to 5 s for the paper point, and 7 to 10 s for the cotton ball.

These results suggest that this sterilizer is effective as used in this experiment, which was conducted under the assumption of clinical procedures.

References

1) Klevens RM, Gorwitz RJ, Collins AS. Methicillin-resistant *Staphylococcus aureus*: a primer for dentists. J Am Dent Assoc 2008; 139: 1328-1337.

2) Volgenant CMC, de Soet JJ. Cross-transmission in the dental office: Does this make you ill? Curr Oral Health Rep 2018; 5: 221-228.

3) Glick M, Trope M, Bagasra O, Pliskin ME. Human immunodeficiency virus infection of fibroblasts of dental pulp in seropositive patients. Oral Surg Oral Med Oral Pathol 1991; 71: 733-736.

4) Li H, Chen V, Chen Y, Baumgartner JC, Machida CA. Herpesviruses in endodontic pathoses: association of Epstein-Barr virus with irreversible pulpitis and apical periodontitis. J Endod 2009; 35: 23-29.

5) Sabeti M, Slots J. Herpesviral-bacterial coinfection in periapical pathosis. J Endod 2004; 30: 69-72.

6) Meng L, Hua F, Bian Z. Coronavirus disease 2019 (COVID-19): Emerging and future challenges for dental and oral medicine. J Dent Res 2020; 99: 481-487.

7) Amato A, Caggiano M, Amato M, Moccia G, Capunzo M, De Caro F. Infection control in dental practice during the COVID-19 pandemic. Int J Environ Res Public Health 2020; 17: 4769.

8) Centers for Disease Control and Prevention. Summary of infection prevention practices in dental settings: Basic expectations for safe care. Atlanta: Centers for Disease Control and Prevention, US Dept of Health and Human Services; October 2016. https://www.cdc.gov/oralhealth/infectioncontrol/pdf/safe-care2.pdf. (cited 2019. 3. 1)

9) Stewart GG, Williams NB. A preliminary report on the efficacy of molten metal for sterilization of root canal instruments and materials. Oral Surg Oral Med Oral

Pathol 1950; 3: 256-261.

10) Findlay J. A report on the efficacy of molten metal and ball bearings as media for sterilisation. Br Dent J 1955; 98: 318-323.

11) Grossman LI. Hot salt sterilizer. Br Dent J 1956; 100: 283.

12) Oliet S, Sorin S, Brown H. A temperature analysis of thermostatically controlled root canal sterilizers using molten metal, glass beads, or salt. Oral Surg Oral Med Oral Pathol 1958; 11: 37-42.

13) Yasuoka M, Ideguchi Y, Hiramine K, Osada T. A study of hot salt sterilizer for root canal instruments. Jpn J Conserv Dent 1975; 18: 282-291.(in Japanese)

14) Spring PN. Bacteriologic evaluation of the glass bead sterilizer for endodontics. Oral Surg Oral Med Oral Pathol 1959; 12: 353-357.

15) Kitajima K, Eguchi M, Kitano Y, Ezura A, Igarashi M, Kawasaki K. A study on the efficacy for the sterilization of a newly-designed electric glass bead sterilizer with digital thermometer. Jpn J Conserv Dent 1993; 36: 241-251.(in Japanese)

16) Tanaka I, Kojima K, Suzuki K, Matsuda J, Nakamura H. A study of a special electric drying sterilizer. —An improved drying apparatus of N.I. system—. Jpn J Conserv Dent 1976; 19: 323-331.(in Japanese)

17) Tamazawa K, Horiuchi H. A new endodontic sterilizer using a heated metal slit. Jpn J Conserv Dent 1980; 23: 209-212.(in Japanese)

18) Sawada K, Yazaki M, Kanda M, Suda H, Sunada I. A study on the efficacy for the sterilization of SL sterilizer. Jpn J Conserv Dent 1981; 24: 246-251.(in Japanese)

19) International Organization for Standardization. ISO 3630-1: 2019 (E) Dentistry—Root-canal instruments—part 1: General requirements and test methods, 2019.

20) International Organization for Standardization. ISO 3630-5: 2020 (E) Dentistry—Endodontic instruments—part 5: Shaping and cleaning instruments, 2020.

21) International Organization for Standardization. ISO 11138-4: 2017 (E) Sterilization of health care products—Biological indicators—Part 4: Biological indicators for dry heat sterilization processes, 2017.

22) Cisar JO, Vatter AE, Clark WB, Curl SH, Hurst-Calderone S, Sandberg AL. Mutants of *Actinomyces viscosus* T14V lacking type 1, type 2, or both types of fimbriae. Infect Immun 1988; 56: 2984-2989.

23) Okahashi N, Sasakawa C, Yoshikawa M, Hamada S, Koga T. Cloning of a surface protein antigen gene from serotype *c Streptococcus mutans*. Mol Microbiol 1989; 3: 221-228.

24) Bott KF, Davidoff-Abelson R. Altered sporulation and respiratory patterns in mutants of *Bacillus subtilis* induced by acridine orange. J Bacteriol 1966; 92: 229-240.

25) Umemura F. Non-destructive evaluation method for degree of sensitization of stainless steel. J Jpn Weld Soc 1987; 56: 411-416.

26) Asakura T. The effect of heating temperature for the cutting efficiency of the K-file for an enlargement of a root canal. J Fukuoka Dent Coll 2002; 29: 169-180.(in Japanese)

27) Niazi SA, Vincer L, Mannocci F. Glove contamination during endodontic treatment is one of the sources of nosocomial endodontic *Propionibacterium acnes* infections. J Endod 2016; 42: 1202-1211.

Development of Multilayered Dental Pulp Cell Sheets and Consideration for Calcification Ability

Katofumi Koyanagi, Munehiro Maeda, Miki Sekiya,
Taro Nishida and Masaru Igarashi

Department of Endodontics, The Nippon Dental University, School of Life Dentistry at Tokyo

Abstract

Purpose: The purpose of this study was to analyze the calcification characteristics of three-dimensional （3D） culture of multi-layered dental pulp cell （DPC） sheets that have potential application in pulp regeneration and evaluation of dental materials and pharmaceuticals.

Methods: DPC were isolated from third molars extracted from three healthy patients aged 18-30 years old. DPC sheets were constructed using a temperature-responsive culture dish （UpCell） and a gelatin stamp （Cell Stamp for UpCell）. Histological examination of three-layer and six-layer DPC sheets was performed using hematoxylin and eosin staining（HE）. DPC sheets on mineral trioxide aggregates（MTA）were observed using a scanning electron microscope （SEM） to examine the microstructure. The LOX-1 probe was used to examine the effects of hypoxia. Calcification ability was analyzed by real-time PCR and Alizarin Red S staining （ARS）. In this study, two-dimensional （2D） culture （monolayer） served as a control.

Results: Thick multilayered cell sheets were confirmed under the macroscopic view and with HE. The SEM images showed that the DPC sheets covered the MTA. Higher osteo/odontogenic differentiation was seen in the multi-layered cell sheets than in the monolayer cell sheets. The expression levels of alkaline phosphatase （ALP）, type Ⅰ collagen （COL1A1）, osteocalcin （OCN）, and dentin sialoprotein （DSPP） genes were higher in the DPC sheets. With ARS, characteristic nodules of mineralization were observed in the cell sheets.

Conclusion: DPC sheets possessed higher mineralizing ability than the monolayer sheets. Cell sheets may be useful for comparative examination of pharmaceuticals, materials, and pulp regeneration in a 3D environment.

Key words: dental pulp cell （DPC）, osteo/odontogenic differentiation, three-dimensional culture, cell sheets

Introduction

In recent years, three-dimensional (3D) culture has been performed using various methods. It has been reported that 3D culture provides results that closely mimic natural tissues as compared to those of two-dimensional (2D) culture for accurate modeling of living organisms[1] and analysis of medicines[2,3]. In dentistry, 3D cultures can be used to assess biocompatibility of dental materials[4,5] and for regeneration of pulp[6] and periodontal ligament[7], using scaffolds[8]. However, hypoxia, promotion of calcification in the spheroid structure[9], and a decrease in viability due to a decrease in oxygen and nutrient supply can occur due to the scaling-up of the 3D structure[10]. Therefore, there may be underestimation or overestimation of the results when evaluating drugs and materials. In view of these facts, we wondered if it would be possible to perform 3D culture that maintains a specified thickness that does not cause hypoxia without using a scaffold and that focuses on cell sheet engineering. Cell sheet engineering refers to the use of a temperature-responsive culture dish (UpCell) to collect cell sheets that retain extracellular matrix without using enzymes such as trypsin from monolayer culture, and to construct 3D structures by layering these cell sheets[11]. It is possible to collect cell sheets that retain the binding and extracellular matrix and stack these cell sheets to construct a 3D structure[11]. In recent years, cell sheet technology has been clinically tested in humans[12,13]. However, there are few studies on the effects of calcification and hypoxia in cell sheets that retain the specified thickness by multi-layering of dental pulp cell (DPC) sheets using UpCell. Therefore, we used a gelatin stamp (CellStamp for UpCell) to stack cell sheets and analyze the characteristics of DPC sheets for application in pulp regeneration and evaluation of dental materials and pharmaceuticals.

Materials and Methods

1．Cell isolation and culture

In this study, DPC was collected from three third molars of three healthy patients (18–30 years old) who had undergone orthodontic treatment, following a protocol approved by the Institutional Review Board of The Nippon Dental University, School of Life Dentistry at Tokyo with informed consent. DPC was cultured according to the method described by Huang et al[14]. Pulp tissues were minced and digested in a solution containing 3 mg/ml collagenase type Ⅰ (Sigma, St. Louis, MO, USA) and 4 mg/ml dispase (Gibco, Invitrogen, Carlsbad, CA, USA) at 37℃ for 60 minutes. Cell suspensions were obtained using a 70 μm strainer and then seeded in 60 mm culture dishes at 37℃ under 5% CO_2 and cells with passage numbers of 3–6 were used in all experiments. The growth medium (GM) used was as follows; minimum essential medium α (MEM-α, Gibco), 10% fetal bovine serum (FBS, Hyclone, Logan, UT, USA), 100 units/ml penicillin G, 100 μg/ml streptomycin (Wako Pure Chemical Industries, Ltd., Osaka, Japan), 2 mmol/l L-glutamine (Wako), and 100 μmol/l L-ascorbicacid-2-phosphate (Sigma). The osteo/odontogenic differentiation medium (OM) used was as follows: 10 nmol/l dexamethasone (Sigma), 10 mmol/l β-glycerophosphate (Sigma), 50 μg/ml L-ascorbic acid phosphate (Sigma), and 10 nmol/l 1,25 dihydroxyvitamin D3 (Cayman Chemical, Ann Arbor, MI, USA).

2．Laminating procedure for the DPC sheets

DPC sheets were laminated by a modified procedure of the method described by Haraguchi et al[15] and the number of seeded cells was determined with reference to the manufacturer's protocol. DPC was seeded at a cell density of 1.5×10^5/well into a 24-well UpCell (CellSeed, Tokyo, Japan) and incubated for 5 days in GM, then the 7.5% gelatin stamp (CellStamp for UpCell; CellSeed, Tokyo, Japan) was placed in the well and left at 25℃ for 30 minutes. The cell sheets were transferred to a gelatin gel, which was then transferred to the next well. This process was repeated to create multiple layers. After the stacking was complete, the gelatin gel was heated at 37℃ for 30 min to dissolve the gelatin and was washed three times in the medium (Fig. 1).

3．Observation by hematoxylin and eosin (HE) staining

The monolayer, three-layer, and six-layer cell sheets in the GM were cultured on a polytetrafluoroethylene membrane for 3 days and fixed with 10% neutral formalin. Then, the cell sheets were embedded with optimal cutting temperature (OCT) frozen compound and a 7 μm section was cut from the OCT blocks and stained with HE. HE was observed using an optical microscope.

①Preparation of gelatin stamp

②For UpCell

・7.5% gelatin stamp

Repeat 3 times

③Placement on UpCell

In case of 6 layers

④Incubate at 23 ℃ for 30 min

⑤24 well plate Dissolution of gelatin (37℃, 30 min)

⑥In culture medium 3 washes

Used for experiments
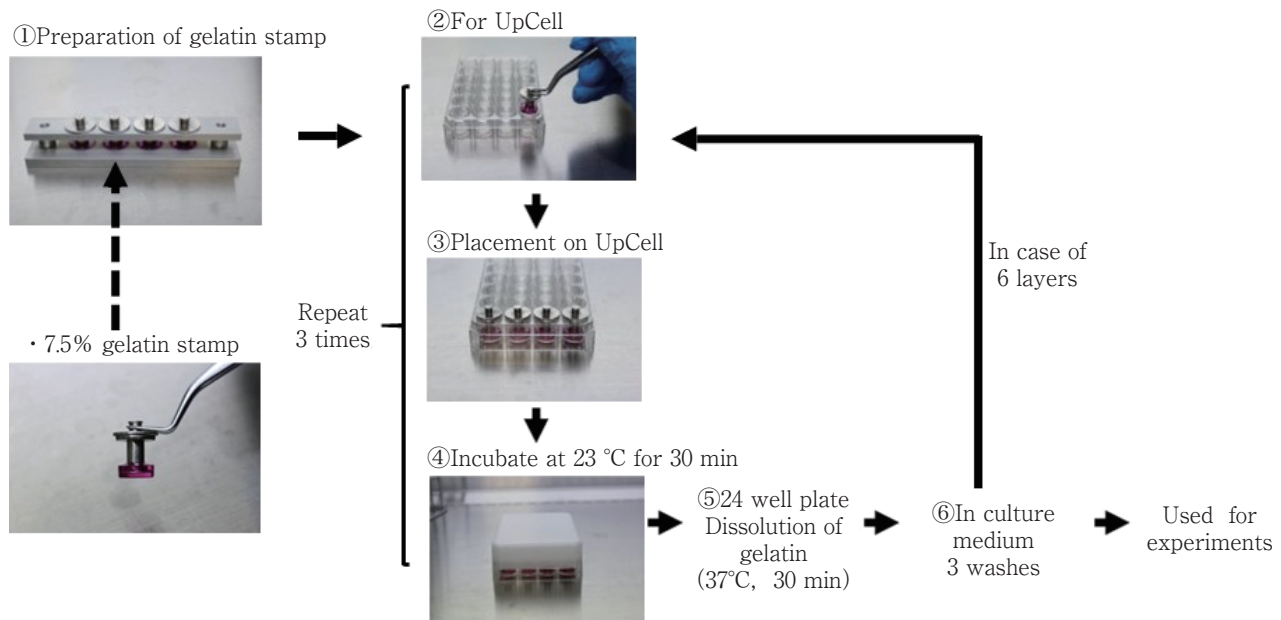
Fig. 1　Procedure for laminating cell sheets

　①Gelatin gel（7.5%）was prepared by molding and placed on a 24-well UpCell plate. ②-④Cells were attached to the bottom of the gelatin stamp at 23℃ for 30 min, and the process was repeated three times to make three-layer sheets. Six-layer sheets were prepared by layering a three-layer sheet on top of another three-layer sheet after dissolving the gelatin. ⑤Gelatin was dissolved by heating at 37℃ for 30 min in the 24 well plate. ⑥Cell sheets were washed 3 times with GM.

4．Observation by scanning electron microscopy（SEM）

The monolayer, three-layer, and six-layer cell sheets in the GM were cultured on MTA（ProRoot MTA; Densply Tulsa Dental Specialties, Johnson City, TN, USA）with a diameter of 6 mm for 3 days. The samples were fixed with 2.5% glutaraldehyde solution for 30 min and post-fixed with 1% osmium tetroxide for 2 h at room temperature. The samples were then dehydrated with 50, 70, 80, 90, 95%, and 99.5% ethanol for 10 min, followed by replacement with t-butanol and freeze-drying. The samples were observed using SEM.

5．Alizarin Red S staining

The monolayer, three-layer, and six-layer cell sheets were cultured in the OM for 21 days, washed with phosphate-buffer solution, and fixed with 10% neutral formaldehyde at room temperature for 15 min. After washing twice with dH_2O, 300 ml/well of 40 mmol/l ARS（pH 4.1）was added, incubation at room temperature was performed for 20 min, then the wells were washed with 1 ml dH_2O 4 times for 5 min each. The samples were observed using an optical microscope and macroscopic views. Three random points on the well were measured by ImageJ software to determine the

mean size of calcification（n=3）.

6．Analysis of hypoxia

Monolayer, three-layer, and six-layer cell sheets were cultured in the OM for 3 days, and the hypoxia probe solution LOX-1（Medical & Biological Laboratories, Aichi, Japan）was used in the medium at a final concentration of 2 μ/l. The cells were observed under a fluorescence microscope（Carl Zeiss LSM 700, Oberkochen, Germany）.

7．Real-time polymerase chain reaction（PCR）analysis

Monolayer, three-layer, and six-layer sheets were cultured in the GM and collected at 3, 7, and 14 days. Total RNA was extracted using TRIzol reagent（Thermo Fisher Scientific, Waltham, MA, USA）and Maxwell RSC simplyRNA Cells Kit（Promega Corporation, Madison, WI, USA）according to the manufacturer's instructions. Complementary DNA synthesis was performed from total RNA（1 μg）using SuperScript VILO Master Mix（Life Technologies, Foster City, CA, USA）. Real-time PCR was performed with a THUNDERBIR Probe qPCR Mix（TOYOBO, Osaka, Japan）using a StepOnePlus real-time PCR system（Applied Biosystems Waltham, MA, USA）under the following condi-

Table 1   Sequences of human primers used for real-time PCR

Genes	Upper primers	Lower primers
ALP	5′-TCCCTGATGTTATGCATGAGC-3′	5′-CGAGAGTGAACCATGCCA-3′
OCN	5′-CGCCTGGGTCTCTTCACT-3′	5′-CTCACACTCCTCGCCCTAT-3′
COL1A1	5′-TTCTGTACGCAGGTGATTGG-3′	5′-GACATGTTCAGCTTTGTGGAC-3′
DSPP	5′-TGACACATTTGATCTTGCTAGGA-3′	5′-TTTGGGCAGTAGCATGGG-3′
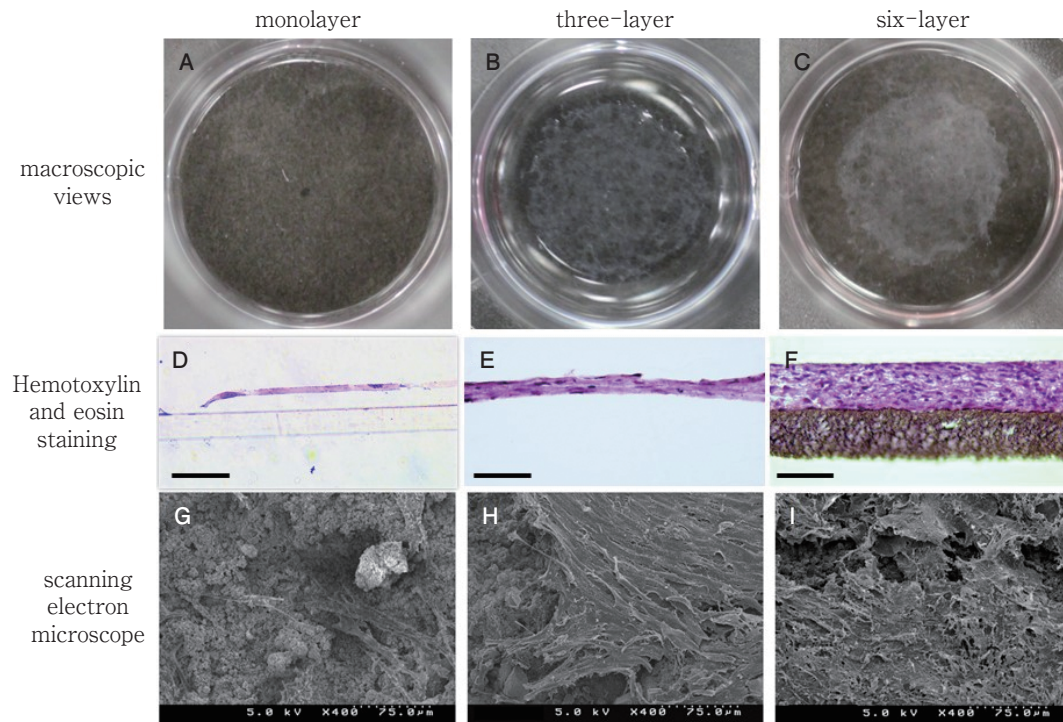
Fig. 2   Histological and SEM findings of cell sheets

     Macroscopic views of the monolayer (A), three-layer (B), and six-layer (C) cell sheets. Hemotoxylin and eosin staining of the monolayer (D), three-layer (E), and six-layer (F) cell sheets. Scanning electron microscope view of the monolayer (G), three-layer (H), and six-layer (I) cell sheets.

     Scale bar＝50 μm

tions: 95℃ for 3 min, followed by 40 cycles at 95℃ for 15 s. The primers for gene amplification were subjected to 40 cycles at 60℃ (45s) for alkaline phosphatase (*ALP*), type Ⅰ collagen (*COL1A1*) and osteocalcin (*OCN*) and at 62℃ (45s) for dentin sialoprotein (*DSPP*). *β-actin* (NM_001101.2) was used as an endogenous control. The primer sequences used are shown in Table 1.

8．Statistical Analysis

     Statistical significance was analyzed using one-way analysis of variance followed by Tukey's test. Data were expressed as mean±standard deviation, and p＜0.05 was considered statistically significant.

Results

1．Histological analysis

     The macroscopic view revealed membranous cell sheets with a thickness of three and six layers. The thickness of the monolayer, three-layer, and six-layer cell sheets, as seen with HE staining, was approximately 7 μm, 25 μm, and 45 μm, respectively. For SEM, when the cell suspension was seeded on the sample, the cells were scattered and attached to the MTA, but on the cell sheets, an image covering the sample was observed (Fig. 2).

2．Analysis of hypoxia

The monolayer cell sheets showed a few LOX-1 positive cells. More hypoxic cells were observed in the six-layer cell sheets than in the monolayer and three-layer cell sheets（Fig. 3）.

3．Alizarin Red S staining

Several nodules of mineralization were observed in the three-layer and six-layer cell sheets but not in the monolayer sheets. In addition, the nodules of mineral-

monolayer   three-layer   six-layer
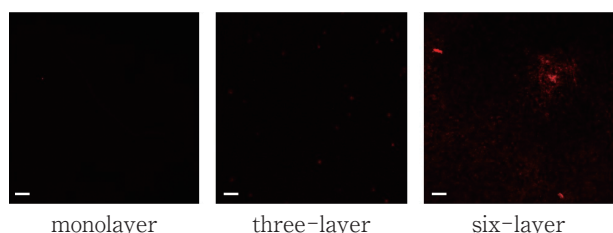
Fig. 3 Analysis of hypoxia

24-well viewed from above hypoxia was detected with the LOX-1 probe in the monolayer, three-layer, and six-layer cell sheets.

Scale bar＝100 μm

ization were larger in the six-layer cell sheets（1,573.4± 669.1 μm^2）than in the three-layer sheets （895.4±269.7 μm^2）（Fig. 4）.

4．Real-time PCR

The expression of *ALP* was upregulated in the monolayer, three-layer, and six-layer cell sheets at day 7 and downregulated at day 14, but tended to be significantly higher in the three-layer and six-layer cell sheets than in the monolayer sheets （p＜0.05）. The expression of *COL1A1* was upregulated in the monolayer, three-layer, and six-layer cell sheets on day 7 and was significantly higher in the six-layer cell sheets than in the monolayer sheets. The expression of *OCN* was upregulated in the monolayer, three-layer, and six-layer cell sheets at day 14 and was significantly higher in the six-layer （p＜0.05）cell sheets than in the three-layer and monolayer sheets. The expression of *DSPP* was upregulated in the monolayer, three-layer, and six-layer cell sheets at day 14 and was significantly higher in the six-layer （p＜0.05）cell sheets than in the three-layer and monolayer cell sheets （Fig. 5）.
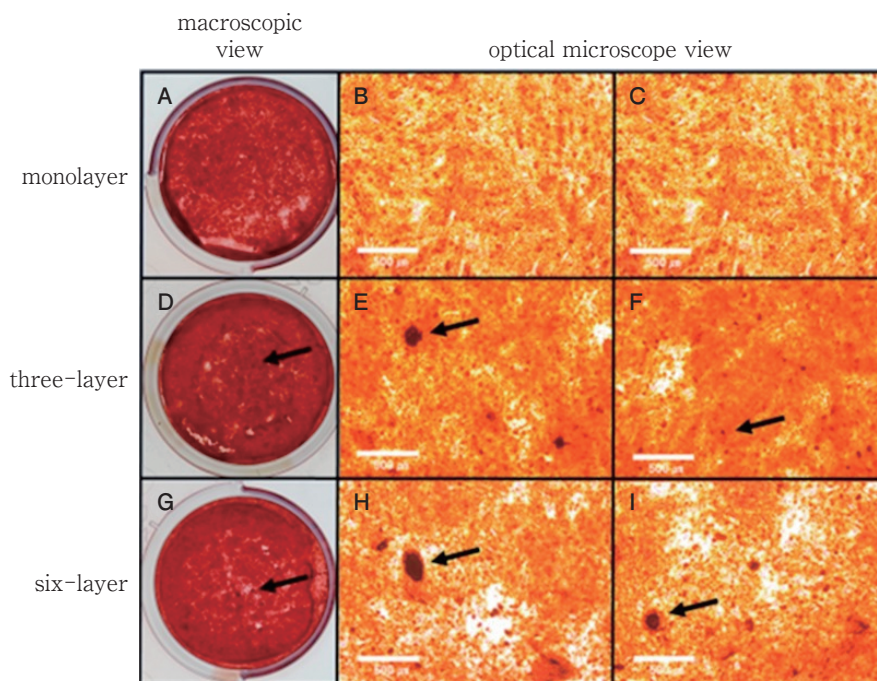
Fig. 4 Macroscopic and optical views

Macroscopic view of Alizarin Red S staining of the monolayer （A）, three-layer （D）, and six-layer （G） cell sheets in the 24-well plate. Optical microscope view of the monolayer （B, C）, three-layer （E, F）, and six-layer （H, I） cell sheets. Nodules of mineralization （indicated with black arrows） can be observed in relation to the three-layer and six-layer cell sheets.

Scale bar＝500 μm

○ : monolayer　⊘ : three-layer　⊞ : six-layer
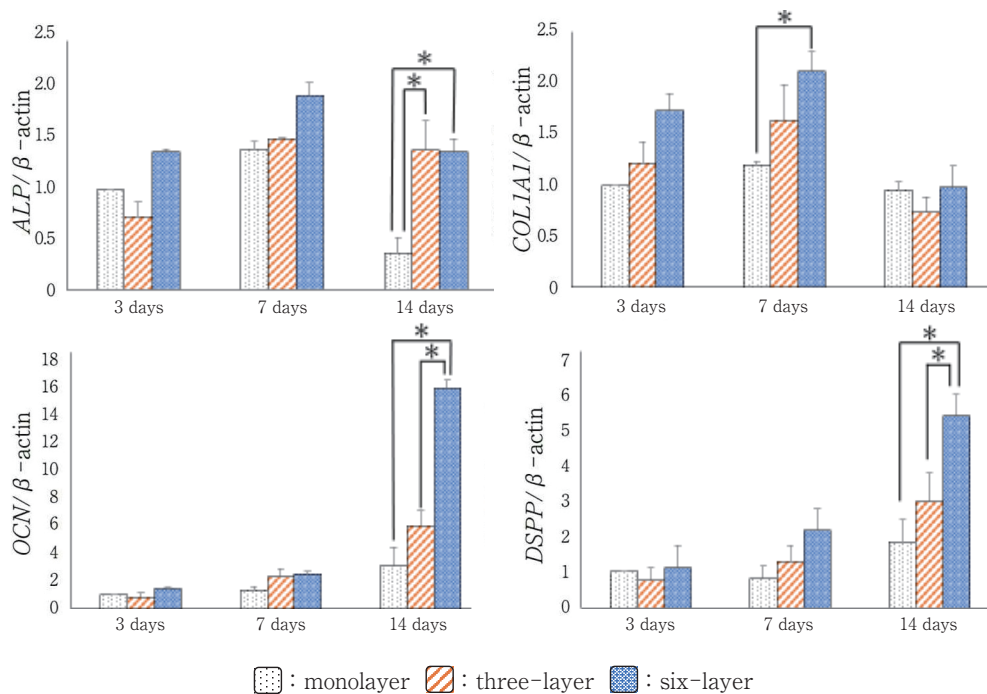
Fig. 5　Real-time PCR analysis of mineralization related marker genes

Real-time polymerase chain reaction was performed for *ALP, COL1A1, OCN*, and *DSPP* (n＝3). The results of two independent experiments performed in triplicate are expressed as the mean（±SD）（＊：p＜0.05）.
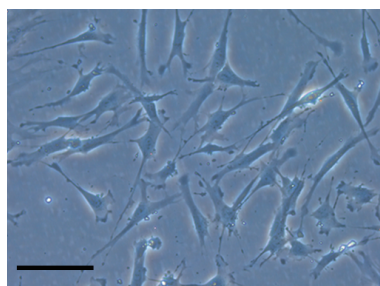
Fig. S1　Phase contrast image of DPC

Scale bar=100 μm
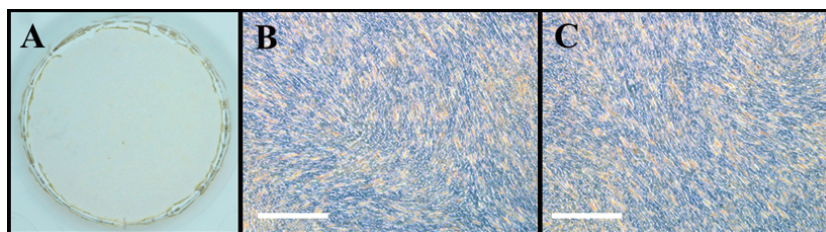
Fig. S2　Macroscopic and optical views

Macroscopic view of ARS of the monolayer（A）was cultured in the GM for 21 days. Optical microscope view of the monolayer（B, C）. Calcification was not observed（Scale bar=500 μm）.

Discussion

In the present study, it was possible to fabricate cell sheets to form in membranous by multilayering, as shown by Kikuchi et al[16]. In addition, some studies on MTA have reported the necessity of direct contact between cells and MTA for their differentiation into odontoblast-like cells[17]. Based on these studies, if it is possible to cover the MTA as shown by SEM, it may be possible to analyze the interaction with cells that occurs in the surface layer of the material in more detail and to study the material properties in an environment similar to that *in vivo*. Considering the mineralization-associated marker gene, after the initial expression of calcification and in *ALP*, which is an important factor for mineral deposition[18], downregulation was observed after 14 days in the monolayer sheets, while the levels were high in the three-layer and six-layer sheets, which may have been due to the occurrence of heterogeneous calcified areas within the sheets. *COL1A1*, a major collagen in dentin and bone matrix, also showed a similar trend. The expression of *OCN*, a non-collagenous protein and a marker of osteo/odontogenic differentiation, and *DSPP*, a representative marker of odontogenic differentiation, was also higher in the multilayered sheets. The expression trends of the markers were consistent with those seen in previous studies[19]. The above-described upregulation of the mineralization-related marker and increased nodular calcification seen with ARS were observed, especially in the six-layer sheets. This may have been due to the thickness of the cells (as seen with HE), causing the expansion of hypoxic areas and the upregulation of mineralization-associated marker expression[20] induced by localized hyper-calcified areas and hypoxic areas in ARS. However, when considered in terms of materialogical characterization, since many dental materials are often compared with cells for their odontogenic induction[21], a comparative study of calcification-related factors using six-layer sheets may result in an overestimation of calcification. Therefore, we hypothesized that a 3D culture with about three layers would not be affected by scaffolding or hypoxia and would allow us to perform comparative material studies in a 3D environment similar to that *in vivo*. In addition, there is a correlation between LOX-1 and hypoxia-inducible factor-1α (HIF-1α)[22]. The effect of hypoxia on cells may cause activation of angiogenesis[23] by inducing vascular endothelial growth factor (VEGF) expression related to HIF-1α, which may be advantageous for pulp regeneration by transplantation. The above results suggest that cell sheet technology may be further developed by changing the application depending on the thickness of the cell sheets.

Note that there were some limitations to this study. We were not able to produce stable cell sheets. Therefore, it is necessary to consider a more appropriate protocol.

In the future, we plan to conduct a more detailed study to investigate the material science of multilayered cell sheets with DPC for regeneration of dental pulp.

Conclusion

DPC sheets possessed higher mineralizing ability than monolayer sheets. Cell sheets may be useful for comparative examination of pharmaceuticals, materials, and pulp regeneration in a 3D environment.

The authors have no conflicts of interest directly relevant to the content of this article.

Supplemental Date

DPC image (Fig. S1) and ARS staining control (Fig. S2) were added as Supplemental Date.

References

1) Antoni D, Burckel H, Josset E, Noel G. Three-dimensional cell culture: a breakthrough in vivo. Int J Mol Sci 2015; 16: 5517–5527.
2) Perche F, Torchilin VP. Cancer cell spheroids as a model to evaluate chemotherapy protocols. Cancer Biol Ther 2012; 13: 1205–1213.
3) Ravi M, Paramesh V, Kaviya SR, Anuradha E, Solomon FD. 3D cell culture systems: advantages and applications. J Cell Physiol 2015; 230: 16–26.
4) Widbiller M, Lindner SR, Buchalla W, Eidt A, Hiller KA, Schmalz G, Galler KM. Three-dimensional culture of dental pulp stem cells in direct contact to tricalcium silicate cements. Clin Oral Investig 2016; 20: 237–246.
5) Pérard M, Le Clerc J, Watrin T, Meary F, Pérez F, Tri-

cot-Doleux S, Pellen-Mussi P. Spheroid model study comparing the biocompatibility of Biodentine and MTA. J Mater Sci Mater Med 2013; 24: 1527–1534.

6) Itoh Y, Sasaki JI, Hashimoto M, Katata C, Hayashi M, Imazato S. Pulp regeneration by 3-dimensional dental pulp stem cell constructs. J Dent Res 2018; 97: 1137–1143.

7) Raveendran NT, Vaquette C, Meinert C, Ipe DS, Ivanovski S. Optimization of 3D bioprinting of periodontal ligament cells. Dent Mater 2019; 35: 1683–1694.

8) Kim NR, Lee DH, Chung PH, Yang HC. Distinct differentiation properties of human dental pulp cells on collagen, gelatin, and chitosan scaffolds. Oral Surg Oral Med Oral Pathol Oral Radiol Endod 2009; 108: 94–100.

9) Yamamoto M, Kawashima N, Takashino N, Koizumi Y, Takimoto K, Suzuki N, Saito M, Suda H. Three-dimensional spheroid culture promotes odonto/osteoblastic differentiation of dental pulp cells. Arch Oral Biol 2014; 59: 310–317.

10) Novosel EC, Kleinhans C, Kluger PJ. Vascularization is the key challenge in tissue engineering. Adv Drug Deliv Rev 2011; 63: 300–311.

11) Kobayashi J, Kikuchi A, Aoyagi T, Okano T. Cell sheet tissue engineering: Cell sheet preparation, harvesting/manipulation, and transplantation. J Biomed Mater Res A 2019; 107: 955–967.

12) Nishida K, Yamato M, Hayashida Y, Watanabe K, Yamamoto K, Adachi E, Nagai S, Kikuchi A, Maeda N, Watanabe H, Okano T, Tano Y. Corneal reconstruction with tissue-engineered cell sheets composed of autologous oral mucosal epithelium. N Engl J Med 2004; 351: 1187–1196.

13) Iwata T, Yamato M, Washio K, Yoshida T, Tsumanuma Y, Yamada A, Onizuka S, Izumi Y, Ando T, Okano T. Periodontal regeneration with autologous periodontal ligament-derived cell sheets—a safety and efficacy study in ten patients. Regen Ther 2018; 9: 38–44.

14) Huang GT-J, Shagramanova K, Chan SW. Formation of odontoblast-like cells from cultured human dental pulp cells on dentin in vitro. J Endod 2006; 32: 1066–1073.

15) Haraguchi Y, Shimizu T, Sasagawa T, Sekine H, Sakaguchi K, Kikuchi T, Sekine W, Sekiya S, Yamato M, Umezu M, Okano T. Fabrication of functional three-dimensional tissues by stacking cell sheets in vitro. Nat Protoc 2012; 7: 850–858.

16) Kikuchi T, Shimizu T, Wada M, Yamato M, Okano T. Automatic fabrication of 3-dimensional tissues using cell sheet manipulator technique. Biomaterials 2014; 35: 2428–2435.

17) Paranjpe A, Smoot T, Zhang H, Johnson JD. Direct contact with mineral trioxide aggregate activates and differentiates human dental pulp cells. J Endod 2011; 37: 1691–1695.

18) Golub EE, Boesze-Battaglia K. The role of alkaline phosphatase in mineralization. Current opinion in Orthopaedics 2007; 18: 444–448.

19) Bakopoulou A, Leyhausen G, Volk J, Tsiftsoglou A, Garefis P, Koidis P, Geurtsen W. Comparative analysis of in vitro osteo/odontogenic differentiation potential of human dental pulp stem cells (DPSCs) and stem cells from the apical papilla (SCAP). Arch Oral Biol 2011; 56: 709–721.

20) Li L, Zhu YQ, Jiang L, Peng W, Ritchie HH. Hypoxia promotes mineralization of human dental pulp cells. J Endod 2011; 37: 799–802.

21) Emara R, Elhennawy K, Schwendicke F. Effects of calcium silicate cements on dental pulp cells: A systematic review. J Dent 2018; 77: 18–36.

22) Zhang S, Hosaka M, Yoshihara T, Negishi K, Iida Y, Tobita S, Takeuchi T. Phosphorescent light-emitting iridium complexes serve as a hypoxia-sensing probe for tumor imaging in living animals. Cancer Res 2010; 70: 4490–4498.

23) Amemiya K, Kaneko Y, Muramatsu T, Shimono M, Inoue T. Pulp cell responses during hypoxia and reoxygenation in vitro. Eur J Oral Sci 2003; 111: 332–338.

Original Article

Inhibitory Mechanisms of S-PRG Eluate and S-PRG Filler against Volatilization of Hydrogen Sulfide

Sami Omagari[1], Nao Taniguchi[2, 3], Yoshiyuki Yokogawa[4],
Masahiro Yoneda[1], Shigeru Yamamoto[1], Takashi Hanioka[2]
and Takao Hirofuji[1]

[1]Department of General Dentistry, Fukuoka Dental College
[2]Department of Preventive and Public Health, Fukuoka Dental College
[3]Oral Medicine Research Center, Fukuoka Dental College
[4]Graduate School of Engineering, Department of Mechanical and Physical Engineering, Osaka City University

Abstract

Purpose: The aim of this study was to elucidate the inhibitory mechanism of a surface pre-reacted glass-ionomer（S-PRG）eluate and S-PRG filler against volatilization of hydrogen sulfide（H_2S）.

Methods: The immediate inhibitory activity of S-PRG eluate on H_2S volatilization was assessed by mixing with a solution of sodium hydrogen sulfide（NaHS）in equal amounts for 5 min, and measuring the gaseous concentration of H_2S by gas chromatography. Subsequently, changes in the concentration of H_2S in the gaseous and liquid phases, as well changes in the pH in the liquid phase, were examined following the addition of S-PRG eluate, S-PRG filler, spherical silica, and potassium bicarbonate（$KHCO_3$）.

Results: S-PRG eluate inhibited 31.6% of H_2S volatilization in the reaction mixed with NaHS solution but with no significant difference（p＝0.065）. Following the addition of S-PRG eluate to the H_2S solution, the concentration of H_2S was reduced by 20% in the gaseous phase and increased by 5% in the liquid phase. There was no change in the gaseous concentration of H_2S in the reaction supplemented with spherical silica, whereas the gaseous concentration of H_2S was reduced in the reaction supplemented with $KHCO_3$, similar to that with S-PRG filler. The pH of the liquid phase was 5.77 in the H_2S solution, 6.01 in that with spherical silica, 7.07 in that with S-PRG filler, and 8.50 in that with $KHCO_3$.

Conclusion: The results of this study suggest that the inhibitory effect of S-PRG eluate and S-PRG filler on H_2S volatilization might be due to their buffering ability.

Key words: buffering ability, hydrogen sulfide, oral malodor, S-PRG filler

Introduction

Oral malodor, or bad breath, is one of the major complaints from patients visiting dental clinics, behind only dental caries and periodontitis. Clinical causes of oral malodor include periodontitis, poor oral hygiene, tongue debris, deep caries, inadequately fitted restorations, endodontic lesions, and low salivary flow[1-4]. The major compounds involved in oral malodor are volatile sulfur compounds (VSCs), and approximately 90% of the VSCs in mouth air are hydrogen sulfide (H_2S) and methyl mercaptan (CH_3SH)[5]. VSCs are produced by oral bacteria in the oral cavity during metabolism of the sulfur-containing amino acids cysteine and methionine[6]. Gram-negative anaerobes are important producers of VSCs[7-9]. Persson et al.[7] evaluated the capacity of 163 culturable oral bacterial strains to produce VSCs; all bacterial strains tested formed H_2S from L-cysteine, whereas less than one-third of the strains produced CH_3SH from L-methionine. Periodontal pathogens isolated from subgingival plaque, such as *Porphyromonas gingivalis*, *Prevotella intermedia*, *Tannerella forsythia*, and *Treponema denticola*, have been shown to generate significant amounts of H_2S and CH_3SH[8]. An examination of the microbiota composition in tongue biofilms of individuals without periodontitis, or only a slight degree of periodontitis, suggested that the major species of H_2S-producing bacteria are *Veillonella*, *Actinomyces*, and *Prevotella*[9].

Dental restorative material containing surface pre-reacted glass-ionomer (S-PRG) filler has recently been shown to possess both anti-dental plaque and anti-bacterial properties[10-15]. S-PRG filler can both release and recharge fluoride ions (F), as well as release other ions, including strontium (Sr), silicon (Si), boron (B), sodium (Na), and aluminum (Al)[16]. S-PRG filler and released ions have anti-demineralization and re-mineralization effects[17,18]. Previous studies concerning the anti-cariogenicity of S-PRG filler have reported that the eluate of S-PRG filler inhibits bacterial growth, adhesion, and gene expression related to sugar metabolism of *Streptococcus mutans*[10,12]. We have been studying the effect of S-PRG eluate on oral microbiota including periodontopathic bacteria[14,15]. S-PRG eluate has been shown to suppress the protease and gelatinase activities of *P. gingivalis*, as well as the coaggregation between *P. gin-*

givalis and *Fusobacterium nucleatum*[14], to inhibit biofilm formation and disrupt mature biofilms; however, its anti-bacterial activity was limited[15]. In further clinical trials, oral rinsing and tongue cleaning with S-PRG eluate reduced oral malodor compared to the control[15]. Since the reduction of oral malodor occurred immediately after oral rinsing with S-PRG eluate, it is thought that S-PRG eluate suppresses oral malodor by an immediate mechanism that does not involve anti-biofilm, anti-bacterial, or anti-enzyme actions. The purpose of this study was to investigate whether S-PRG eluate and S-PRG filler suppress oral malodor independent of their effect on oral bacteria, and to clarify the underlying mechanism.

Materials and Methods

1．Preparation of S-PRG eluate and S-PRG filler

The S-PRG eluate (lot 031501K; Shofu Inc., Kyoto, Japan) and S-PRG filler (lot 120501; Shofu Inc.) used in this study were generated as previously described[18,19]. S-PRG eluate was prepared with S-PRG filler under the specific conditions that produce the highest concentration of each ion[19]. Elemental analysis of ions released from S-PRG filler (Al, B, Na, Si, and Sr) was performed using inductively coupled plasma atomic emission spectroscopy (ICP-AES; ICPS-8000, Shimadzu Co., Kyoto, Japan) and fluoride ion electrodes (fluoride electrode, Model 9609BN; pH/ion meter, Model 720A; Orion Research Inc., MA, USA)[14]. The ion concentrations of S-PRG eluate used to evaluate the immediate inhibitory effect of S-PRG eluate on gaseous H_2S were as follows: Al, 1.5 ppm; B, 890.5 ppm; Na, 368.2 ppm; Si, 6.0 ppm; Sr, 78.4 ppm; and F^-, 105.0 ppm.

2．Immediate inhibitory effect of S-PRG eluate on gaseous H_2S

Gaseous H_2S was prepared from a dilute aqueous solution of sodium hydrogen sulfide (NaHS). Chlorides of two metal ions released from S-PRG filler, $AlCl_3$ and $SrCl_2$, were prepared as 1 mol/l aqueous solutions. Then, 2 ml of S-PRG eluate, 1 mol/l $AlCl_3$ solution, or 1 mol/l $SrCl_2$ solution was added to 2 ml of 10^{-5}% NaHS solution in 15 ml tubes, which were sealed and incubated at room temperature for 5 min. Then, 1 ml of the gas phase was collected and analyzed using a gas chromatograph (model GC2014; Shimadzu Co.). Distilled water (d-water) and 1 mol/l $ZnCl_2$ solution were used
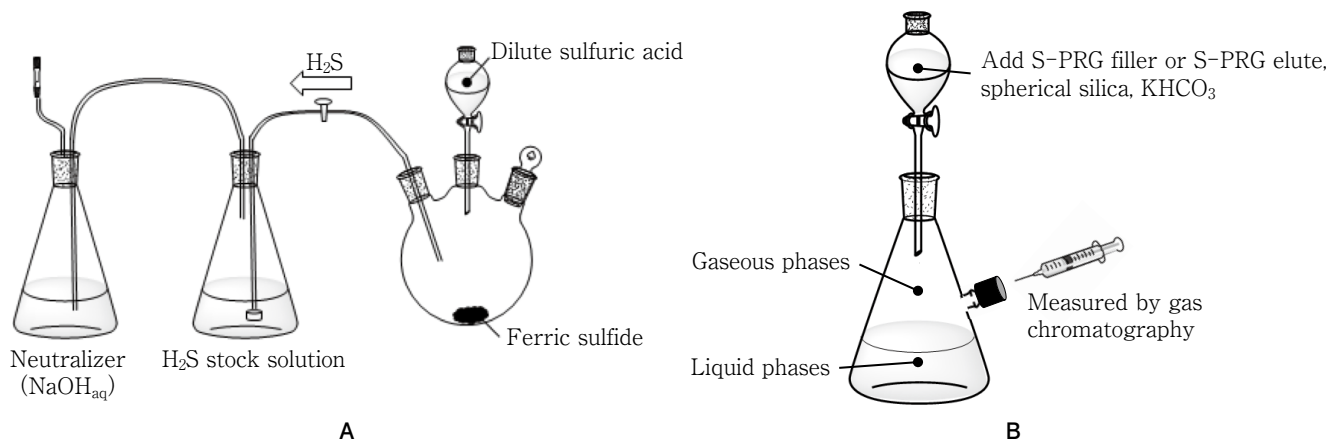
Fig. 1 Hydrogen sulfide (H₂S) gas generator (A) and equipment for preparation of the H₂S solution (B)

as negative and positive controls, respectively. All test reagents were obtained from FUJIFILM Wako Pure Chemical Co.(Osaka, Japan). The experiments were repeated at least three times.

3. Preparation of H_2S solution

H_2S gas was produced by adding dilute sulfuric acid through a dropping funnel into a four-necked flask containing ferric sulfide. H_2S gas was transferred into an Erlenmeyer flask and bubbled through 150 ml of Milli-Q water to obtain a stock solution of H_2S (Figure 1A). The H_2S stock solution was removed by syringe and transferred to an Erlenmeyer flask containing 100 ml Milli-Q water, and rotated at 400 rpm for 1 h to obtain a solution of H_2S with a concentration of 500 ppb (Figure 1B). Finally, 2 μl of the liquid and 30 μl of the gas in the headspace of the H_2S solution were tested by gas chromatography to confirm that the concentration of H_2S was 500 ppb.

4. Changes in H_2S concentration in the gaseous and liquid phases following addition of S-PRG eluate

The changes in H_2S concentration in the gaseous and liquid phases following addition of 0.5 ml S-PRG eluate to 100 ml of H_2S solution (500 ppb) in an Erlenmeyer flask were measured by gas chromatography (GC-14B; Shimadzu Co.) at 0, 1, 2, 3, and 4 h. Then, 30 μl was sampled from the headspace as a gaseous phase sample, 2 μl was sampled from the reaction mixture as a liquid phase sample, and the H_2S concentration was measured.

5. Changes in H_2S concentration in the gaseous phase and pH in the liquid phase following addition of S-PRG filler

The H_2S concentration in the gaseous phase and pH in the liquid phase were measured at 0, 0.5, 1, 2, and 3 h following the addition of 0.1 g S-PRG filler, 0.1 g spherical silica, or 0.1 g potassium bicarbonate($KHCO_3$) to 100 ml of H_2S solution (500 ppb) in an Erlenmeyer flask.

6. Changes in H_2S concentration in the liquid phase following addition of S-PRG filler by the methylene blue method

In a previous study, S-PRG filler was added to H_2S solution and the changes in H_2S concentration in the liquid phase were examined by the methylene blue method[20]. Immediately following the addition of S-PRG filler in the above experiment (initial), as well as at 0.5, 1, 2, and 3 h, a 0.1 ml sample was taken from the liquid phase as a test solution. Briefly, 0.1 ml test solution was added to 10 ml distilled water in a 15 ml stoppered test tube; 1 ml p-aminodimethylaniline dichloride (10 mmol/l in 10 N H_2SO_4) and 1 ml $FeCl_3$ (20 mmol/l in 1% H_2SO_4) were also added (Figure 2). After incubation at room temperature for 15 min, the absorbance was measured at 665 nm using an ultraviolet-visible-near-infrared spectrophotometer (V-550; Jasco Co., Tokyo, Japan). Measurement of only the reagent without the test solution was used as the baseline.

7. Statistical analysis

Welch's t-test was used to evaluate the immediate inhibitory effects of metal ions and S-PRG eluate on H_2S volatilization compared to the addition of d-water(negative control). Differences were considered to be significant at $p < 0.05$. Statistical analyses were carried out
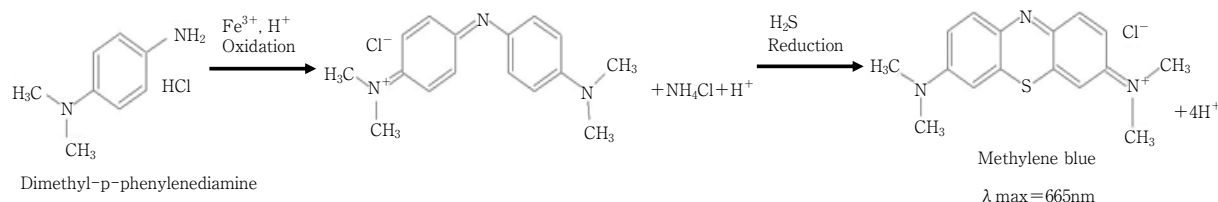
Fig. 2 Methylene blue method

Under acidic conditions, H_2S produces methylene blue by the reaction of p-aminodimethylaniline hydrochloride with iron (III) chloride as an oxidizing agent. Since methylene blue has a maximum absorption wavelength of 665 nm, it is possible to quantify H_2S using absorptiometry.
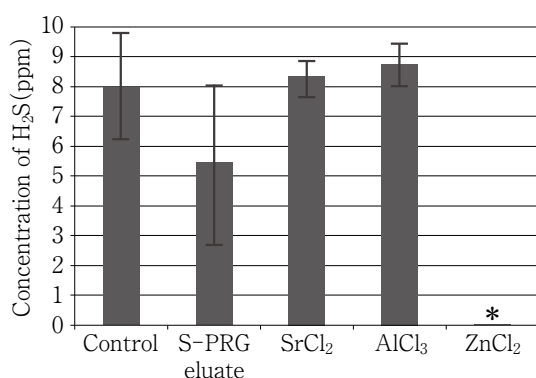
Fig. 3 Immediate inhibitory effect of surface pre-reacted glass-ionomer (S-PRG) eluate on gaseous H_2S

Bars show mean±standard error. S-PRG eluate inhibited 31.6% of H_2S volatilization (p= 0.065), while $AlCl_3$ and $SrCl_2$ did not inhibit H_2S volatilization. The aqueous solution of $ZnCl_2$ almost completely inhibited H_2S volatilization (＊：p＜0.001).

using the R software package (ver. 3.6.1.; http://www.R-project.org).

Results

1．Direct inhibitory effect of S-PRG eluate on gaseous H_2S

In the reaction mixed with the 10^{-5}% NaHS solution, neither aqueous solutions of $AlCl_3$ (−9.68%) nor $SrCl_2$ (−4.63%) inhibited H_2S volatilization, whereas S-PRG eluate inhibited H_2S volatilization by 31.6% (p=0.065) (Figure 3). The aqueous solution of $ZnCl_2$ almost completely inhibited H_2S volatilization (99.9%, p＜0.001).
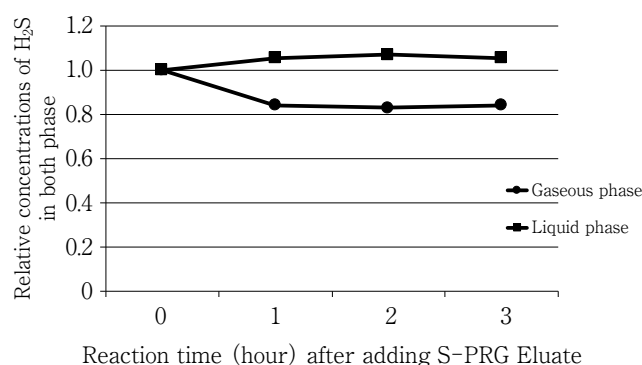
Fig. 4 Changes in H_2S concentration in the gaseous and liquid phases following addition of S-PRG eluate (representative data)

The concentration of H_2S in the gaseous phase (filled circles) decreased by 20%, while that in the liquid phase (filled squares) increased by 5%.

2．Changes in H_2S concentration in the gaseous and liquid phases, and pH, following addition of S-PRG eluate or S-PRG filler

Although the reproducibility was confirmed by repeated experiments, the reaction was easily affected by the temperature and the measured values varied, and thus representative data are shown. One hour after S-PRG eluate was added to the H_2S solution (500 ppb) and stirred at 400 rpm, the concentration of H_2S in the gaseous phase decreased by 20%, while that in the liquid phase increased by 5% (Figure 4); these concentrations remained unchanged after 4 h. Following the addition of S-PRG filler, the concentration of H_2S in the gaseous phase decreased by approximately 70% after 1 h, and by approximately 80% after 3 h (Figure 5). As shown in Figure 5, the reaction with $KHCO_3$ resulted in a similar decrease in the concentration of H_2S in the gaseous phase as that following the addition of S-PRG filler. By contrast, the addition of spherical silica did not
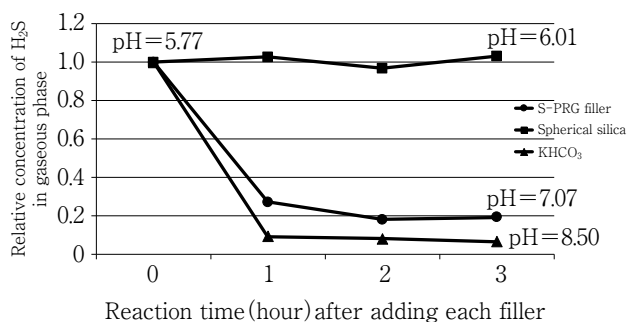
Fig. 5 Changes in H₂S concentration in the gaseous and liquid phases, and in pH, following addition of S-PRG filler (filled circles)

The concentration of H₂S in the gaseous phase decreased by 80% after 3 h. The reaction with KHCO₃ (filled triangles) resulted in a decrease in H₂S concentration in the gaseous phase similar to that following addition of S-PRG filler. The addition of spherical silica (filled squares) did not affect the concentration of H₂S in the gaseous phase. Representative data are shown.
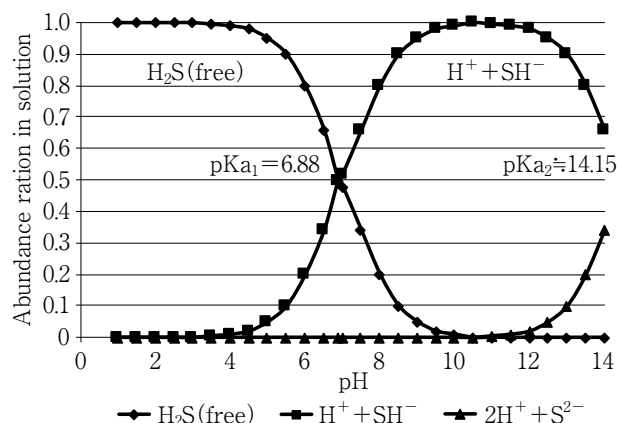
Fig. 7 Relative abundance of each dissociated species of H₂S at each pH
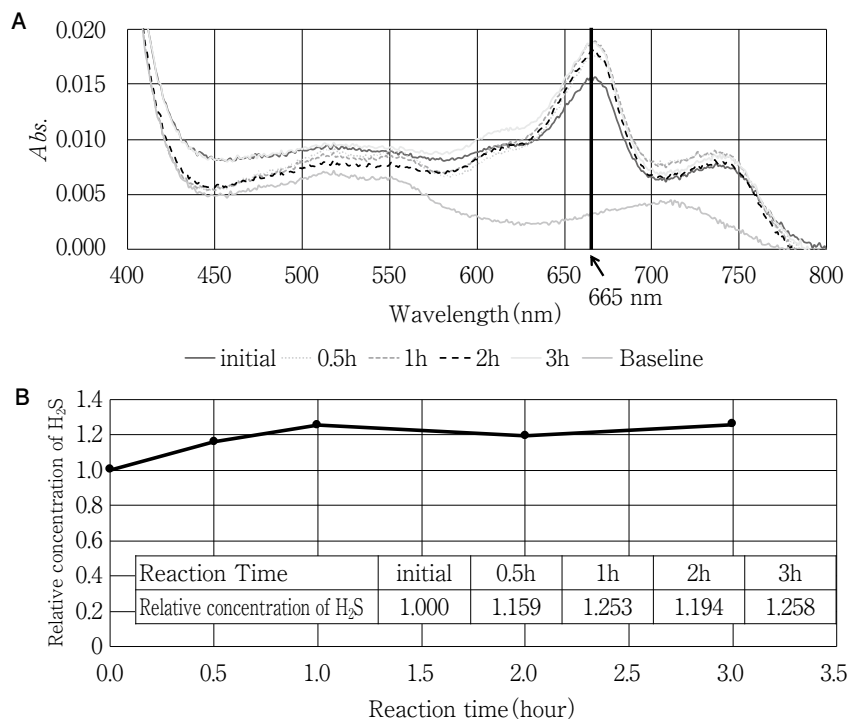
Fig. 6 Effect of addition of S-PRG filler on H₂S concentration in liquid phase (A) Changes in H₂S concentration in the liquid phase following addition of S-PRG filler by the methylene blue method. (B) Changes in relative concentration of H₂S in the liquid phase measured by the absorbance at 665 nm. Representative data are shown.

affect the concentration of H₂S in the gaseous phase. The pH values in the liquid phase prior to the reaction, and 3 h after the addition of S-PRG filler, KHCO₃, and

spherical silica, were 5.77, 7.07, 8.50, and 6.01, respectively. The concentration of H₂S in the liquid phase was examined with the methylene blue method (Figure 6

A). The relative concentration of H_2S in the liquid phase increased by 15.9%, 25.3%, 19.4%, and 25.8% at 0.5, 1, 2, and 3 h after the addition of S-PRG filler (Figure 6B).

Discussion

We previously reported that metal ions such as Ag^+, Cd^{2+}, Cu^{2+}, and Zn^{2+} inhibit H_2S volatilization by chemical binding[21]. In both previous and current experiments, Sr^{2+} and Al^{3+} did not inhibit volatilization of H_2S. On the other hand, S-PRG eluate inhibited 31.6% of H_2S volatilization in the reaction mixed with 10^{-5}% NaHS. S-PRG eluate immediately inhibited H_2S volatilization by a mechanism distinct from its action on bacteria and chemical binding by metal ions. In terms of the anti-bacterial action of S-PRG filler on *S. mutans*, it has been reported that borate and fluoride ions are among the ions released from the filler[22]. Sr^{2+} are also often taken up by enamel and are considered to be involved in the inhibitory effect of S-PRG eluate on the demineralization of enamel[23]. In that study, the absorption of multiple ions from S-PRG filler eluate into the tooth structure occurred much faster than that of each ion alone. As described above, S-PRG filler is characterized by its ability to allow the released ions to act in concert with multiple ions, rather than acting alone. However, we conclude that suppression of the volatilization of H_2S does not occur via a chemical bond, since no reaction occurs with the ions alone.

The pH of S-PRG eluate is approximately 7.8[19]. Therefore, we focused on the buffering effect of S-PRG filler and S-PRG eluate. S-PRG filler, $KHCO_3$, and spherical silica were added to an aqueous solution of H_2S, and the concentration of H_2S in the gas phase and pH in the liquid phase were measured. The concentration of H_2S in the gas and liquid phases respectively decreased and increased when $KHCO_3$ and S-PRG filler were added, which makes the aqueous solution weakly alkaline. The effects of pH were considered in these experiments. In the reaction vessel, the gas-liquid and acid dissociation equilibria are in equilibrium (Figure 7):
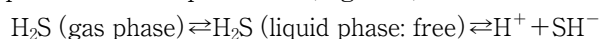
H_2S (gas phase) $\rightleftarrows H_2S$ (liquid phase: free) $\rightleftarrows H^+ + SH^-$
Also, when limited to solution only,

H_2S (liquid phase) $\rightleftarrows H^+ + SH^-$

Since its acid dissociation constant (pK_{a1}) is 6.88, the equilibrium tends to dissociate ions when the pH of the solution rises, and H_2S (liquid phase: free) in the liquid phase may decrease. Since the H_2S aqueous solution is weakly acidic, H_2S (liquid phase: free) $> H^+ + SH^-$ in the liquid phase before the material is charged, but when the pH of the liquid phase is > 6.88, H_2S (liquid phase: free) $< H^+ + SH^-$. In other words, H_2S (liquid phase: free) in the liquid phase decreases in an environment with pH > 6.88, and H_2S in the gas phase may move to the liquid phase. The concentration of H_2S in the gas and liquid phases was examined every hour for 3-4 h, and the reaction was nearly complete after 1 h following the addition of both S-PRG filler and S-PRG eluate. The reaction occurred rapidly, as the concentration of H_2S in the gas phase decreased by 31.6% after 5 min in the mixing experiment with NaHS. The concentration of H_2S in the gas phase is believed to be lower in S-PRG filler than in S-PRG eluate, because the S-PRG filler continued to release ions to maintain the buffer capacity.

Conclusion

In conclusion, the weak inhibitory effect of S-PRG eluate and S-PRG filler on H_2S volatilization might be due to their buffering ability. Oral malodor might be suppressed by complex mechanisms of S-PRG eluate and filler that include anti-biofilm, anti-bacterial, and anti-enzyme actions against bacteria as well as a non-bacterial buffer action.

Conflict of interest

The authors declare that they have no competing interest.

References

1) Suzuki N, Fujimoto A, Yoneda M, Watanabe T, Hirofuji T, Hanioka T. Resting salivary flow independently associated with oral malodor. BMC Oral Health 2016; 17: 23.

2) Morita M, Wang HL. Association between oral malodor and adult periodontitis: a review. J Clin Periodontol 2001; 28: 13–19.

3) Yoneda M, Naito T, Suzuki N, Yoshikane T, Hirofuji T. Oral malodor associated with internal resorption. J Oral Sci 2006; 48: 89–92.

4) Garret NR. Poor oral hygiene, wearing dentures at night, perceptions of mouth dryness and burning, and lower educational level may be related to oral malodor in denture wearers. J Evid Based Dent Pract 2010; 10: 67–69.

5) Tonzetich J. Direct gas chromatographic analysis of sulphur compounds in mouth air in man. Arch Oral Biol 1971; 16: 587–597.

6) Scully C, Porter S, Greenman J. What to do about halitosis. BMJ 1994; 308: 217–218.

7) Persson S, Edlund MB, Claesson R, Carlsson J. The formation of hydrogen sulfide and methyl mercaptan by oral bacteria. Oral Microbiol Immnuol 1990; 5: 195–201.

8) Suzuki N, Yoneda M, Takeshita T, Hirofuji T, Hanioka T. Induction and inhibition of oral malodor. Mol Oral Microbiol 2019; 34: 85–96.

9) Washio J, Sato T, Koseki T, Takahashi N. Hydrogen sulfide-producing bacteria in tongue biofilm and their relationship with oral malodor. J Med Microbiol 2005; 54: 889–895.

10) Saku S, Kotabe H, Scougall-Vilchis RJ, Ohashi S, Hotta M, Horiuchi S, Hamada K, Asaoka K, Tanaka E, Yamamoto K. Antibacterial activity of composite resin with glass-ionomer filler particles. Dent Mater J 2010; 29: 193–198.

11) Han K, Takenaka S, Okuji T. Evaluation of selected properties of a prototype S-PRG filler containing root canal sealer. J Conserv Dent 2007; 50: 713–720. (in Japanese)

12) Nomura R, Morita Y, Matayoshi S, Nakano K. Inhibitory effect of surface pre-reacted glass-ionomer (S-PRG) eluate against adhesion and colonization by *Streptococcus mutans*. Sci Rep 2018; 8: 5056.

13) Takakusaki K, Fueki K, Tsutsumi C, Tsutsumi Y, Iwasaki N, Hanawa T, Takahashi H, Takakuda K, Wakabayashi N. Effect of incorporation of surface pre-reacted glass ionomer filler in tissue conditioner on the inhibition of *Candida albicans* adhesion. Dent Mater J 2018; 8: 453–459.

14) Yoneda M, Suzuki N, Masuo Y, Fujimoto A, Iha K, Yamada K, Iwamoto T, Hirofuji T. Effect of S-PRG eluate on biofilm formation and enzyme activity of oral bacteria. Int J Dent 2012; 2012: 814913.

15) Suzuki N, Yoneda M, Haruna K, Masuo Y, Nishihara T, Nakanishi K, Yamada K, Fujimoto A, Hirofuji T. Effects of S-PRG eluate on oral biofilm and oral malodor. Arch Oral Biol 2014; 59: 407–413.

16) Nakatuka T, Yasuda Y, Kimoto K, Mizuno M, Negoro N. Dental fillers. United States Patent No. 6620861; 2003.

17) Shiiya T, Mukai Y, Tomiyama K, Teranaka T. Anti-demineralization effect of a novel fluoride-releasing varnish on dentin. Am J Dent 2012; 25: 347–350.

18) Ito S, Iijima M, Hashimoto M, Tsukamoto N, Mizoguchi I, Saito T. Effects of surface pre-reacted glass-ionomer fillers on mineral induction by phosphoprotein. J Dent 2011; 39: 72–79.

19) Fujimoto Y, Iwasa M, Murayama R, Miyazaki M, Nagafuji A, Nakatsuka T. Detection of ions released from S-PRG fillers and their modulation effect. Dent Mater J 2010; 29: 392–397.

20) Yano M. Quantification of hydrogen sulfide in hot spring water using methylene blue absorptiometry. Annual Report of the Hyogo Prefectural Institute of Public Health and Environmental Sciences 2002; 1: 181–186.

21) Suzuki N, Nakano Y, Watanabe T, Yoneda M, Hirofuji T, Hanioka T. Two mechanisms of oral malodor inhibition by zinc ions. J Appl Oral Sci 2018; 26: e20170161.

22) Miki S, Kitagawa H, Kitagawa R, Kiba W, Hayashi M, Imazato S. Antibacterial activity of resin composites containing surface pre-reacted glass-ionomer (S-PRG) filler. Dent Mater 2016; 32: 1095–1102.

23) Ogawa A, Wada T, Mori Y, Uo M. Time dependence multi-ion absorption into human enamel from surface pre-reacted glass-ionomer (S-PRG) filler eluate. Dent Mater J 2019; 38: 707–712.

Original Article

Clinical Assessment of Resin-coating Technique for Dentin after Cavity Preparation

Hanemi Tsuruta, Shusuke Kusakabe,
Michael F Burrow* and Toru Nikaido

Department of Operative Dentistry, Division of Oral Functional Science and Rehabilitation,
Asahi University School of Dentistry
*Restorative Dental Sciences, Faculty of Dentistry, University of Hong Kong

Abstract

Purpose: Many studies have been conducted on the resin-coating technique for indirect restorations, and its efficacy has been reported. This study investigated the clinical course of cases with the resin-coating technique for dentin after inlay cavity preparation and examined the efficacy of the technique clinically.

Methods: Twenty cases in 18 patients visiting one of three dental clinics that were collaborating with this investigation between September 2014 and October 2019 were evaluated. The patients were treated using the resin-coating technique by applying a thin coating material (Hybrid Coat II, HC II) after inlay cavity preparation. Patient dental and medical records as well as clinical information that included tooth site, procedures, materials used, and clinical symptoms before, during, and after the procedures and at the time of recall were obtained using set clinical evaluation criteria.

Results: Fifty percent of the restorations were performed in premolars and 50% in molars. Local anesthesia was used in all cases except one. Resin coating was performed using HC II alone in 40% of cases and HC II combined with a flowable resin in 60% of cases. After inlay placement, 95% of the cases (19 cases) had a favorable outcome. Of the 10 cases (50%) where the patient experienced pain on cold water stimulation before treatment, nine cases had a favorable outcome; however, in one case pain on drinking cold water persisted and the patient then presented with pulpal symptoms, thereby requiring a pulpectomy.

Conclusion: The results demonstrate the clinical efficacy of the resin-coating technique using HC II on inlay cavity preparations.

Key words: resin-coating technique, Hybrid Coat II, inlay cavity preparation

Introduction

In recent years, the use of direct composite restorations in molars has improved with the advancement of adhesive materials and technologies. Currently, a composite restoration can be promptly performed by preparing the cavity such that only the 'caries-infected' dentin is removed and 'caries-affected' dentin is preserved, thereby protecting the remaining dentin and pulp. However, for extensive carious lesions in molars where the restoration is subjected to greater occlusal loading and the restorations may need to protect cusps, an indirect restoration such as an inlay or onlay can be selected. Generally, the degree of dentin exposure after preparation for an indirect restoration is much greater.

The resin-coating technique was introduced based on the idea of direct composite resin restorations and the application of a reliable adhesive system for indirect restorations. The resin-coating technique is used to cover the dentinal surface exposed after cavity preparation for an indirect restoration such as an inlay or crown with an adhesive system for protecting the exposed dentin and pulp[1-4]. Specifically, coating the exposed dentinal surface immediately before impression-taking with an adhesive system aims to form a thin film on the dentinal surface which helps protect the pulp and improves adhesion of the resin cement to the dentin, thereby improving the marginal seal[1]. By using the resin-coating technique, few adhesive failures of restorations at the dentinal interface occur due to the improvement in the adhesion of the resin cement to the dentin. This also leads to a decrease in the frequency of marginal and bacterial leakage which has been reported[2,5-13]. Conservation of tooth structure, decreased patient discomfort, and a favorable clinical course of indirect restorations have also been reported[1,2,14-19].

In Japan, the resin-coating technique for preparing vital abutment teeth has been covered under the Japanese national health insurance system since December 2019 and its use is expected to become more common. On the other hand, the clinical application of the resin-coating technique is still being improved[20]. Laboratory studies have demonstrated its superior performance; a clinical study on the resin-coating technique for crown preparation of vital teeth reported that the resin coating is a reliable treatment[21]. However, no clinical study has evaluated the resin coating for cavity preparations. Therefore, this retrospective study investigated the clinical performance of inlay restorations placed using a resin-coating technique in collaboration with three dentists who routinely employ the resin-coating technique for vital teeth, and assessed the validity and efficacy of the procedure.

Materials and Methods

1．Materials for resin coating

The composition of Hybrid Coat II (HC II Sun Medical, Moriyama, Japan), a resin coating material used in this study, is shown in Table 1. HC II is the next version of HC (Sun Medical), which has been available in the market since January 2010. HC II was developed on the concept of a one-step bonding agent, which consists of a one-bottle bonding agent and a dedicated sponge[22]. When HC II is used, a dedicated sponge containing adhesion promoters is used to apply the bonding material to the tooth surface. In Japan, HC II has been covered under the Japanese national health insurance system since December 2019 as a material for resin coating of prepared surfaces of vital abutment teeth.

2．Methods for investigation

This study was approved by the Ethics Committee of Asahi University School of Dentistry (approval number 32007). The study was conducted in collaboration with three dentists in private practice who frequently perform vital tooth inlay restorations using the resin-coating technique. The outline of the clinical study and its methods were explained to the dentists and their consent to join the study was obtained.

The study included 18 patients (ten males, eight females; mean age, 51.4 years old) visiting one of the three dentists between September 2014 and October 2019. Patient records were identified for those who received an inlay for a vital tooth. The age of the patients is shown in Table 2. Nineteen cases in 18 patients who could be followed up after the restoration and who also consented to join the investigation were investigated.

Immediately after the cavity preparation, the prepared tooth was resin-coated using HC II followed by impression-taking. At the next visit, an inlay was placed with a resin cement.

Table 1   Composition and usage of resin-coating material

Brand	Manufacturer	Composition	Procedure
Hybrid Coat Ⅱ (HC Ⅱ)	Sun Medical (Moriyama, Japan)	liquid：acetone, MMA, 4-META others, water Powder in coat sponge/micro-brush sponge：aromatic amine, aromatic sulfinate	①Liquid stirring and mixing with a coat sponge/micro-brush sponge ②After applying the mixed solution for 10 s, air-blowing for 5 s ③Light irradiation for 5 s

MMA：methyl methacrylate, 4-META：4-methacryloxyethyl trimellitate anhydride

Table 2   Baseline information of the participants

Category	Sex		Age （yrs）					Treatment tooth	
	Male	Female	20–29	30–39	40–49	50–59	60–69	Premolar	Molar
Number of cases (Percentage)	10 (55.6)	8 (44.4)	1 (5.6)	3 (16.7)	4 (22.2)	3 (16.7)	7 (38.9)	10 (50.0)	10 (50.0)
	Total 18		Average 51.4					Total 20	

We used a clinical investigation proforma to obtain basic information about each patient （age, sex）, the intervention site and investigated procedures such as whether local anesthesia had been administered, if pulp protection had been provided, methods for resin coating, the resin cement used for adhesion, and any clinical symptoms before, during, and after the restorative procedure and at the time of latest recall based on the dental records. Personal information including patient name and address was excluded from the data forms to maintain anonymity.

3．Data collection and analysis

After the investigation was completed, the evaluation forms were collected from the dentists. When there was any doubt about the information provided in the form, the dentist who completed it was asked directly for confirmation and clarification. Thereafter, all data were collated and analyzed.

Results

The results of the investigation are shown in Table 3. In this study, the restorations were performed on premolars in 10 cases （50%） （five cases on maxillary premolars and five cases on mandibular premolars） and molars in 10 cases （50%） （three cases on maxillary molars and seven cases on mandibular molars）. The average period between cavity preparation and inlay placement and between inlay placement and recall was 11 days and 289 days, respectively. The total period of the investigation was 10 months on average.

Before commencing the cavity preparation, local anesthesia was used in all cases except one. Also, local anesthesia was used for inlay placement in 10% of the cases.

The resin-coating technique was performed on each cavity using a single application of HC Ⅱ in eight cases （40%）and a combination of HC Ⅱ with a flowable resin composite in 12 cases （60%）. No case required direct pulp capping during the cavity preparation. The restorations comprised inlays covered under insurance in 14 cases （70%） （metal inlay in 12 cases and a resin composite inlay in one case） and self-financed inlays in six cases （30%） （hybrid resin inlay in one case, gold alloy inlay in two cases, ceramic inlay in two cases, and a zirconia inlay in one case）.

In 19 cases（95%）, a dual-cure resin cement was used for the cementation, SA Luting Plus （Kuraray Noritake Dental, Tokyo, Japan）, G-Luting（GC, Tokyo, Japan）, and other dual-cure resin cements described as listed in the clinical data forms. In one case （5%）, Super-Bond C & B （Sun Medical）, a methyl methacrylate-based resin cement, was used.

After inlay placement, the clinical outcome was determined to be favorable in 19 cases （95.0%）. Although discomfort such as pain on drinking cold water was observed before treatment in nine cases （45%）, the outcome was determined to be favorable

Table 3 Evaluation outcomes collected from the protocols

	Content of survey		Number of cases (Percentage of cases)
Local anesthesia	Cavity preparation	Yes	19 (95.0)
		No	1 (5.0)
	Inlay placement	Yes	2 (10.0)
		No	18 (90.0)
Resin-coating procedure	Single application of HC Ⅱ		8 (40.0)
	Combination of HC Ⅱ with a flowable resin		12 (60.0)
Resin cement	MMA-based resin cement		1 (5.0)
	Dual-cure resin cement		19 (95.0)
Restoration category under the national insurance system		Approved	14 (70.0)
		Not approved	6 (30.0)
Adverse event after placement of the restoration		No	19 (95.0)
		Yes	1 (5.0)

after treatment in eight of the nine cases. Of the cases where discomfort was experienced before treatment, pain on drinking cold water persisted after treatment and even at the time of recall occurred in only one case, which subsequently required a pulpectomy 155 days after the commencement of treatment (Table 3).

Discussion

The results of this study showed that as cavity preparation for vital teeth was accompanied by the cutting of intact dentin, local anesthesia needed to be used for cavity preparation in almost all cases. Some studies have indicated that damage to the pulp is associated with the cutting of vital dentin when using an air-turbine hand piece[23,24]. If protecting the vital tooth structures is prioritized based on the idea of minimally invasive dentistry, a direct composite restoration should be selected for caries treatment. However, when an inlay restoration is inevitably selected as the treatment of choice, the tooth preparation should be carefully performed while using air-water spray from the handpiece and a very light touch preparation to minimize damage to the pulp. On the other hand, local anesthesia was not used in one case. The reason was not unclear, but cutting intact dentin might have been minimal in this case. According to Fusayama's concept[25], local anesthesia is not necessary if cutting is limited only for 'caries-infected' and 'caries-affected' dentin.

A favorable outcome free of any discomfort after placement of the restoration in 95% of cases was determined, which indicated that the resin-coating technique was effective after cavity preparation in vital teeth. The clinical outcomes were favorable in 8/9 cases that originally presented with pain upon cold water stimulation before the treatment. The resin-coating technique was able to protect the prepared dentin surface and isolated it from pain-causing stimuli. However, one case still experienced pain on cold water exposure at the time of recall and finally presented with pulpal symptoms, thereby requiring a pulpectomy. Currently, it is challenging to accurately diagnose the pulp response of a tooth where the patient experiences discomfort. In cases requiring a pulpectomy, it is difficult to diagnose the pulpal condition for an inlay restoration. Under the current circumstances, in cases with discomfort due to pulpal sensitivity, the restoration should be performed after recovery from the discomfort. In cases requiring a restoration, it is crucial to carefully perform the restorative procedures after providing the patient with an adequate explanation of the benefits and risks of the procedure and then obtaining consent.

The resin-coating technique may improve the bonding performance of resin cement to dentin for indirect restorations and also enhance the marginal seal between the restoration and the cavity wall[26-28]. This evaluation used dual-cure resin cements for luting restorations in most cases. Such cements are routinely used for the luting of tooth-colored restorations, such as resin composite and ceramic inlay/onlay restorations,

because the light-curing of the cement effectively improves the bond strength of the tooth-colored restorations to the underlying tooth structure. On the other hand, self-cure resin cements, such as Super-Bond C & B, should ideally be used for metal inlay restorations. It was reported, however, that the immediate dentin bond strength of Super-Bond C&B was significantly lower than that of dual-cure resin cements, but after 24 h a high bond strength could be achieved[29]. Further investigation of the clinical outcomes of restorations cemented with various types of resin cement, including cement removal after restoration placement, is required to expand the current evidence base[30,31].

Resin coating was performed by using HC Ⅱ alone in 37% of cases and HC Ⅱ combined with a flowable resin in 63% of cases. As the coating with HC Ⅱ forms a thin coating of approximately 5 μm thickness per application, HC Ⅱ does not alter the overall contour of the prepared surface[18,32,33]. Meanwhile, when HC Ⅱ is combined with a flowable resin, any undercuts within the cavity preparation can be easily blocked out by placement of the flowable resin. In this study, interviews after collecting the evaluation forms confirmed that the cavity morphology had been modified by the additional use of a flowable resin. In addition, it has been reported that HC Ⅱ combined with a flowable resin improved the adhesion of a resin cement to dentin[4,10,11,34,35]. Resin coating using HC Ⅱ alone is suitable for cases requiring high-precision preparation methods, such as crown preparation of abutment teeth for a fixed prosthesis. On the other hand, resin coating using HC Ⅱ combined with a flowable resin is suitable for cases requiring smooth and stress concentration-free cavity forms such as resin or ceramic inlays.

The resin-coating technique has been covered by the Japanese national health insurance system for the preparation of vital teeth since 2019, however, it does not include inlay and onlay cavities. The results of this study revealed the efficacy of the resin-coating technique on inlays and onlays. It is strongly hoped that the resin-coating technique will be covered within the insurance system for inlay and onlay cavities in the future. This study verified the short-term clinical outcomes of the resin-coating technique; however, its long-term clinical outcomes need to be investigated.

Conclusion

1. Local anesthesia was used for cavity preparation in a vital tooth in almost all cases.

2. The outcome was favorable after placing the restoration with the resin-coating technique using HC Ⅱ alone and HC Ⅱ combined with a flowable resin in 95% of cases.

3. Of the nine patients who experienced discomfort before the procedure, the clinical outcome was favorable in eight cases (89%); however, discomfort persisted in one case, which required a pulpectomy (11%).

4. These results revealed that the resin-coating technique using HC Ⅱ was effective in protecting the dentin and pulp after cavity preparation.

Conflict of Interest

The authors declare that there are no potential conflicts of interest with regard to the publication of this article.

References

1) Nikaido T, Tagami J, Yatani H, Ohkubo C, Nihei T, Koizumi H, Maseki T, Nishiyama Y, Takigawa T, Tsubota Y. Concept and clinical application of the resin-coating technique for indirect restorations. Dent Mater J 2018; 37: 192–196.

2) Hu J, Zhu Q. Effect of immediate dentin sealing on preventive treatment for postcementation hypersensitivity. Int J Prosthodont 2010; 23: 49–52.

3) Santana VB, de Alexandre RS, Rodrigues JA, Ely C, Reis AF. Effects of immediate dentin sealing and pulpal pressure on resin cement bond strength and nanoleakage. Oper Dent 2016; 41: 189–199.

4) Magne P. Immediate dentin sealing: a fundamental procedure for indirect bonded restorations. J Esthet Res Dent 2005; 17: 144–154.

5) Magne P, Kim TH, Cascione D, Donovan TE. Immediate dentin sealing improves bond strength of indirect restorations. J Prosthet Dent 2005; 94: 511–519.

6) Ishii N, Maseki T, Nara Y. Bonding state of metal-free CAD/CAM onlay restoration after cyclic loading with and without immediate dentin sealing. Dent Mater J 2017; 36: 357–367.

7) Islam M, Takada T, Weerasinghe DS, Uzzaman MA, Foxton RM, Nikaido T, Tagami J. Effect of resin coating on adhesion of composite crown restoration. Dent Mater J 2006; 25: 272–279.

8) Okuda M, Nikaido T, Maruoka R, Foxton RM, Tagami J. Microtensile bond strengths to cavity floor dentin in indirect composite restorations using resin coating. J Esthet Res Dent 2007; 19: 38-46.

9) Giannini M, Takagaki T, Bacelar-Sá R, Vermelho PM, Ambrosano GM, Sadr A, Nikaido T, Tagami J. Influence of resin coating on bond strength of self-adhesive resin cements to dentin. Dent Mater J 2015; 34: 822-827.

10) de Andrade OS, de Goes MF, Montes MA. Marginal adaptation and microtensile bond strength of composite indirect restorations bonded to dentin treated with adhesive and low-viscosity composite. Dent Mater 2007; 23: 279-287.

11) Santos-Daroz CB, Oliveira MT, Góes MF, Nikaido T, Tagami J, Giannini M. Bond strength of a resin cement to dentin using the resin coating technique. Braz Oral Res 2008; 22: 198-204.

12) van den Breemer CR, Özcan M, Pols MR, Postema AR, Cune MS, Gresnigt MM. Adhesion of resin cement to dentin: effects of adhesive promoters, immediate dentin sealing strategies, and surface conditioning. Int J Esthet Dent 2019; 14: 52-63.

13) Brigagão VC, Barreto LFD, Gonçalves KAS, Amaral M, Vitti RP, Neves ACC, Silva-Concílio LR. Effect of interim cement application on bond strength between resin cements and dentin: immediate and delayed dentin sealing. J Prosthet Dent 2017; 117: 792-798.

14) Turkistania A, Sadr A, Shimada Y, Nikaido T, Sumi Y, Tagami J. Sealing performance of resin cements before and after thermal cycling: Evaluation by optical coherence tomography. Dent Mater 2014; 30: 993-1004.

15) Feitosa VP, Medina AD, Puppin-Rontani RM, Correr-Sobrinho L, Sinhoreti MA. Effect of resin coat technique on bond strength of indirect restorations after thermal and load cycling. Bull Tokyo Dent Coll 2010; 51: 111-118.

16) van den Breemer CRG, Özcan M, Cune MS, van der Giezen R, Kerdijk W, Gresnigt MMM. Effect of immediate dentine sealing on the fracture strength of lithium disilicate and multiphase resin composite inlay restorations. J Mech Behav Bio Mater 2017; 72: 102-109.

17) Ashy LM, Marghalani H, Silikas N. In vitro evaluation of marginal and internal adaptations of ceramic inlay restorations associated with immediate vs delayed dentin sealing techniques. Int J Prosthodont 2020; 33: 48-55.

18) Hironaka NGL, Ubaldini ALM, Sato F, Giannini M, Terada RSS, Pascotto RC. Influence of immediate dentin sealing and interim cementation on the adhesion of indirect restorations with dual-polymerizing resin cement. J Prosthet Dent 2018; 119: 678.e1-678.e8.

19) Hofsteenge JW, Hogeveen F, Cune MS, Gresnigt MMM. Effect of immediate dentine sealing on the aging and fracture strength of lithium disilicate inlays and overlays. J Mech Behav Biomed Mater 2020; 110: 103906.

20) Nikaido T, Yoda A, Foxton RM, Tagami J. A resin coating technique to achieve minimal intervention in indirect resin composites: A case report. Int Chin J Dent 2003; 3: 62-68.

21) Kusakabe S, Tsuruta H, Uno M, Burrow MF, Nikaido T. Clinical assessment of resin-coating technique applied to exposed dentin after crown preparation. Dent Mater J; doi: 10. 4012/dmj. 2021-029〔Epub ahead of print〕.

22) Nikaido T, Nakaoki Y, Ogata M, Foxton R, Tagami J. The resin-coating technique. Effect of a single-step bonding system on dentin bond strengths. J Adhes Dent 2003; 5: 293-300.

23) Farah RI. Effect of cooling water temperature on the temperature changes in pulp chamber and at handpiece head during high-speed tooth preparation. Res Dent Endod 2018; 44: e3.

24) Oztürk B, Uşümez A, Oztürk AN, Ozer F. In vitro assessment of temperature change in the pulp chamber during cavity preparation. J Prosthet Dent 2004; 91: 436-440.

25) Fusayama T. Clinical guide for removing caries using a caries-detecting solution. Quintessence Int 1988; 19: 397-401.

26) Takahashi R, Nikaido T, Ariyoshi M, Kitayama S, Sadr A, Foxton RM, Tagami J. Thin resin coating by dual-application of all-in-one adhesives improves dentin bond strength of resin cements for indirect restorations. Dent Mater J 2010; 29: 615-622.

27) Jayasooriya PR, Pereira PN, Nikaido T, Burrow MF, Tagami J. The effect of a "resin coating" on the interfacial adaptation of composite inlays. Oper Dent 2003; 28: 28-35.

28) Murata T, Maseki T, Nara Y. Effect of immediate dentin sealing applications on bonding of CAD/CAM ceramic onlay restoration. Dent Mater J 2018; 37: 928-939.

29) Burrow MF, Nikaido T, Satoh M, Tagami J. Early bonding of resin cements to dentin, ─Effect of bonding environment. Oper Dent 1996; 21: 196-202.

30) Kitasako Y, Burrow MF, Nikaido T, Tagami J. Effect of resin-coating technique on dentin tensile bond strengths over 3 years. J Esthet Restor Dent 2002; 14: 115-122.

31) Shinagawa J, Inoue G, Nikaido T, Ikeda M, Burrow MF, Tagami J. Early bond strengths of 4-META/MMA-TBB resin cements to CAD/CAM resin composite. Dent Mater J 2019; 38: 28-32.

32) Jayasooriya PR, Pereira PN, Nikaido T, Tagami J. Efficacy of a resin coating on bond strengths of resin cement to dentin. J Esthet Restor Dent 2003; 15: 105-113.

33) Ghiggi PC, Steiger AK, Marcondes ML, Mota EG, Bur-

nett LH Jr, Spohr AM. Does immediate dentin sealing influence the polymerization of impression materials? Eur J Dent 2014; 8: 366–372.

34） de Carvalho MA, Lazari-Carvalho PC, Polonial IF, de Souza JB, Magne P. Significance of immediate dentin sealing and flowable resin coating reinforcement for unfilled/lightly filled adhesive systems. J Esthet Restor Dent 2021; 33: 88–98.

35） Sultana S, Nikaido T, Matin K, Ogata M, Foxton RM, Tagami J. Effect of resin coating on dentin bonding of resin cement in class Ⅱ cavities. Dent Mater J 2007; 26: 506–513.

The Shaping Advantage of M-wire Compared with Conventional Nickel-titanium Rotary Instruments in Heavy Curvature Canals

Akito KASAHARA, Mika TANAKA-SATO,
Noriko MUTOH and Nobuyuki TANI-ISHII

Department of Pulp Biology and Endodontics, Kanagawa Dental University

Abstract

Background: The purpose of this study was to evaluate the shaping advantage of M-wire NiTi ProTaper NEXT（PTN）compared with a conventional NiTi ProTaper Universal（PTU）file in heavy curvature canals. The shaping ability was measured by the amount of canal cutting and transportation between the PTN and conventional PTU.

Methods: Root canal shaping by the PTN and PTU was classified into two experimental groups according to the final tip size, ISO #25 or ISO #40. Eighty-four J-shaped root canals（10°, 20°, 30° apical curvature）in resin blocks were used.

Results: After adjusting for the level and canal wall side, the mean transportation did not significantly decrease between the PTN and PTU with ISO #25. Significantly less deviation occurred with the PTN and PTU between 10° and 30° using ISO #40.

Conclusions: The PTN improves file flexibility and enables accurate canal shaping for heavy curvature canals.

Key words: M-wire, ProTaper NEXT, ProTaper Universal, shaping ability, apical curvature

Introduction

Rotary dental files with a NiTi alloy containing 56% (wt) Ni and 44% (wt) Ti have significantly changed root canal preparation. The NiTi alloy has a cubic crystal structure with an austenite phase above the shape recovery temperature[1]. The austenite phase changes to martensite under force and temperature, but when the stress is released, the phase returns to austenite[2,3]. Consequently, the NiTi alloy has a shape memory effect and super-elasticity without plastic deformation, which is advantageous for instruments used for root canal preparation.

Given the development of NiTi endodontic instruments targeted at root canals with complex anatomical configurations, the shape memory and super-elastic properties of such NiTi instruments have helped prevent endodontic accidents (such as ledges, root canal perforations, apical transportation, and file fractures)[4,5]. Currently, unique heat and mechanical treatments can be used to complement the mechanical properties of NiTi alloys to improve flexibility and fatigue resistance.

In 2007, Sportwire LLC (Langley, OK, USA) developed a unique heat treatment process with the aim of producing a more flexible NiTi alloy with better fatigue resistance than conventional NiTi alloys[6]. Additionally, Berendt developed a NiTi composition in which trace elements of less than 1% were added to produce a NiTi alloy[7]. Under a heat treatment process, the M-wire alloy converts to a rhombohedral (R) phase (intermediate temperature phase between austenite and martensite) and the elasticity changes with the change from austenite to martensite. Therefore, the flexibility of a NiTi endodontic file can be enhanced by modification[8,9]. Additionally, NiTi alloy converted to the R phase is conventionally produced by cutting; however, NiTi files are produced by a non-cutting rolling step, thereby increasing the file fatigue resistance and fracture resistance.

The ProTaper NEXT (PTN) file used in this study is a next-generation model of ProTaper Universal (PTU), which is a modification of the conventional NiTi alloy PTU and uses M-wire. PTN was developed as a file suitable for severely curved root canals given its increased flexibility and fracture resistance. Compared with PTU, the PTN suppresses the occurrence of micro-cracks during root canal formation[10,11]. Root canal wall displacement after cutting[12-15], fatigue resistance[16-18], and file breakage resistance[19] of PTN have been previously studied to determine the shaping ability. However, no report has objectively compared the different curvature canal range and shaping ability of PTN with a PTU in the same shaping system. The purpose of this study was to analyze the advantages of the PTN and the relationship between the amount of canal wall removed and canal center transportation compared with a PTU.

Materials and Methods

1．Simulated root canal block and experimental design

Eighty-four simulated J-shaped canal blocks with a curvature of 10°, 20°and 30° (apical diameter/taper: 15/06, root canal length 19 mm (working length), Nissin Plastic Training Block S4-U1, Nissin, Kyoto, Japan) were used. Three J-shaped canal blocks with different angles (S4-U1-10°, 20°, 30°) were cut at 19.0 mm (S4-U1-10°), 18.5 mm (S4-U1-20°), and 18.0 mm (S4-U1-30°) from the root canal orifice at the top of the model by IsoMet (Buehler, Tokyo, Japan) and adjusted to allow apical foramen penetration (Fig. 1).

We used a PTN file (Dentsply Sirona, Ballaigues, Switzerland) made by M-wire and a PTU file (Dentsply Sirona) as a control.

For root canal preparation, there were two final apical sizes for four groups, ISO #25 (1: PTN, 2: PTU) and ISO #40 (3: PTN, 4: PTU). Using a J-shaped canal block, measurements were made by classifying the blocks into two groups. The apical size and file taper (diameter increase amount/mm) of each NiTi file were PTN X1 (17/04), X2 (25/06), X3 (30/07), X4 (40/06), and PTU F1 (20/04), F2 (25/06), F3 (30/06), and F4 (40/06), which were used to set the final apical size to ISO #25 and #40.

Three curvature blocks (10°, 20°, 30°; each n＝7) were used, giving a total of 21 canal blocks for each of the ISO #25 (1: PTN, 2: PTU) and ISO #40 (3: PTN, 4: PTU) groups. Therefore, 84 canal blocks were tested. All root canal models were attached to the Endo Training Model Castillo (VDW, Frankfurt, Germany), and root canal preparation was performed in a situation where the root canal morphology could not be confirmed.
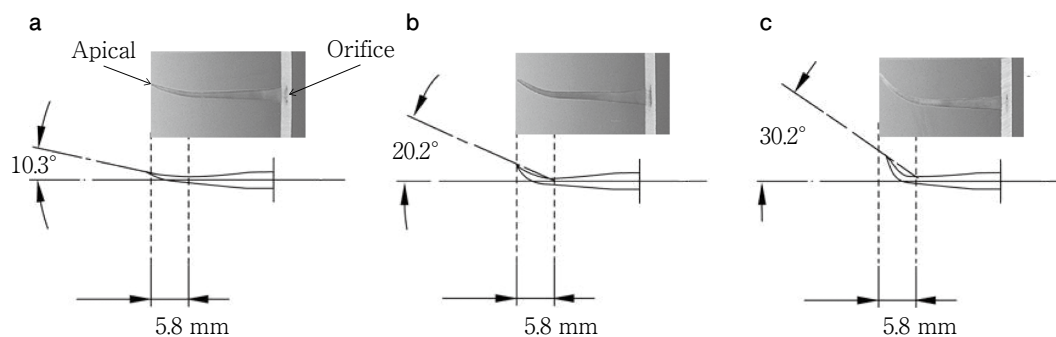
Fig. 1 J-shaped canal blocks made of clear resin with diameter of 0.15 mm, taper of 06, and apical curvatures of (a) 10°, (b) 20°, and (c) 30°.

2．Root canal preparation

The canals were first scouted with an ISO #15 stainless-steel K-file (Dentsply Sirona) to check patency and to precisely determine the working length (19 mm). The canal preparation was performed by a single operator (specialist of JEA and JCD) using the Ni-Ti (PTN, PTU) files in strict accordance with the manufacturer's recommendations for each system.

Before starting root canal preparation with the PTN and PTU files, flare formation in the upper third of all root canal orifice openings and smooth file guide path creation (glide path) up to the root apex were performed. Flare formation was performed using PTN SX and PT SX files, which are used for straight line formation only. Furthermore, the glide path was confirmed up to #15 using an ISO #15 stainless-steel K file (Dentsply Sirona). All NiTi files were washed with purified water using a dedicated engine (X Smart plus, Dentsply Sirona), and 1 ml of EDTA-gel Glide (Dentsply Sirona) was applied to the NiTi files.

Root canal preparation using PTN and PTU files was performed by a single dentist with more than 7 years of experience using NiTi rotary files. The following procedure was performed and files were exchanged after every five root canal formations.

1) ISO #25 PTN: Using two X1 and X2 files sequentially, select the X Smart plus PTN mode (300 rpm, 2.0 Ncm), perform root canal cleaning with 2 ml of distilled water by plastic syringe when exchanging files, and reach the working length (19 mm) of the X2 file to complete the root canal formation.

2) ISO #25 PTU: Using S1 (17/02), S2 (20/04), F1 and F2 files in sequence, select the PT mode (250 rpm, 3.0-1.0 Ncm), perform root canal cleaning with 2 ml of distilled water when exchanging files, and let the F2 file

reach its working length.

3) ISO #40 PTN: Using X1, X2, X3, and X4 files in sequence, select the PTN mode (300 rpm, 2.0 Ncm), perform root canal cleaning with 2 ml of distilled water when exchanging files, and let the X4 file reach its working length.

4) ISO #40 PTU: Using S1, S2, F1, F2, F3, and F4 files in sequence, select the PT mode (250 rpm, 3.0-1.0 Ncm), perform root canal cleaning with 2 ml of distilled water when exchanging files, and save the F4 file after it reaches its working length.

3．Evaluation of the canal shaping

The amount of resin removed in the outer and inner sides of the curved root canal was compared. A stereoscopic microscope (SZX16, Olympus, Tokyo, Japan) and a digital camera (DP71, Olympus) were used for the measurement. The transparent root canal models before and after root canal preparation were superimposed with digital images, and the resulting images were transferred to a PC and measured. The measurement points were 1, 2, 3, 4, and 5 mm from the apex, and the increase in the root canal width on the outer and inner sides was measured and statistical processing was performed (Fig. 2).

Root canal center transportation was measured as the amount of root canal wall cutting in the outer and inner sides of the curved root canal, and the median displacement of the root canal before and after preparation was measured. We measured ①the distance between shaping and original inner canal wall, ②the distance between shaping and original outer canal wall, and ③the canal width of the shaped canal. The canal center transportation was calculated as the centering ratio using the equation ①−②/③[16]. The shaping becomes more centered as the centering ratio
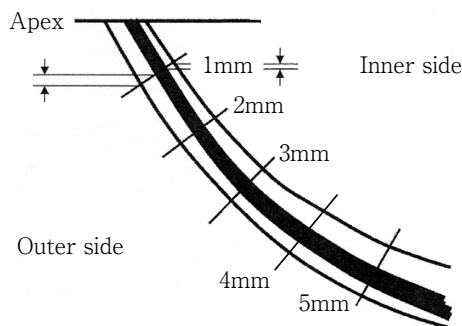
Fig. 2

Pre-instrumentation and post-instrumentation images were superimposed and the difference between the canal configuration before and after instrumentation was measured in each of the five traced levels.

approaches zero.

4. Statistical analysis

The amount of root canal wall cutting and root canal transportation was measured using statistical analysis using one-way analysis of variance and a multiple comparison test using the Bonferroni-Dunn test. The level of significance was set at $p < 0.05$.

Results

The root canal shaping ability was evaluated according to the amount of resin removed and the root canal transportation. In experimental groups 1 to 4, the amount of resin removed was shown by comparing PTN and PTU for each curvature (10°, 20°, 30°; Figs. 3-5). The root canal transportation was classified by PTN and PTU files (Tables 1 and 2).

1. Shaping ability of the final apical size ISO #25

The removal of resin by PTN decreased in both the inner and outer sides in the ISO #25 curvatures of 10° to 30° compared with the PTU (Fig. 3-a, 4-a, 5-a). Meanwhile, the amount of resin removed by PTU on the inner and outer sides was small at 10° to 20° curvatures. The amount of resin removed by PTU increased slightly at the 30° curvature: the apex side was 1 mm on the outer side, and the apical side was 4 mm and 5 mm on the inner side, although the difference was not significant (Fig. 5-a).

The change in the root canal transportation for both PTN and PTU was within 0.02 mm for all root canals with a curvature of 10°to 30° (Table 1).

2. Shaping ability of the final apical size ISO #40

Even with ISO #40 and PTN, the amount of resin removed from the inner and outer sides was less than those in the PTU group for all root canals with a curvature of 10°to 30° (Fig. 3-b, 4-b, 5-b). For ISO #40 and PTN, the amount of resin removed was significantly less than that of the PTU group at 1-5 mm on the inner side with a curvature of 10° (Fig. 3-b) and 1 mm on the outer side at 30° (Fig. 5-b). The amount of resin removed by PTN only increased from 4 to 5 mm on the inner side compared with the outer side at 20° (Fig. 4-b) and 30° (Fig. 5-b). This tendency was similar to that of the PTU group. The amount of resin removed by PTU with ISO #40 significantly increased by 1 mm on the apex side for all curvatures, and the cutting amount on the inner side increased from 4 to 5 mm on the apex side (p<0.05) (Fig. 5-b).

The change in the root canal transportation was less than 0.05 mm with the 10° to 20° curvatures using PTN, but 0.06 mm at the apex 4 to 5 mm into the root with the 30° curvature. The transportation further significantly increased to 0.08 mm (p<0.05) (Table 2).

In contrast, the root canal transportation of PTU showed a displacement of 0.1 mm or more on the outer side of the apex side at 1 mm in all the root canals with a curvature of 10°to 30°. In the PTU, the canal transportation on the inner side increased to 0.07 mm and 0.08 mm at 3 and 4 mm, respectively, even with a curvature of 10°, and the inner side displacement of the root canal of 30° also increased to 0.07 mm and 0.08 mm at 4 and 5 mm, respectively (Table 2).

Discussion

The mechanical properties of the NiTi file depend on the processing method of the file and the surface finishing method, but it has been reported that the change in crystal structure by the heat treatment process affects the flexibility of NiTi alloys[9,20-22]. The PTU used in this study has super-elasticity by the stress-induced transformation of the martensitic phase with a monoclinic crystal structure to the austenite phase, which is the cubic crystal structure of a conventional NiTi alloy[23]. Meanwhile, PTN, which is a NiTi alloy processed into M-wire by heating and cooling, coexists with austenite, martensite, and R phases, and has a monoclinic marten-
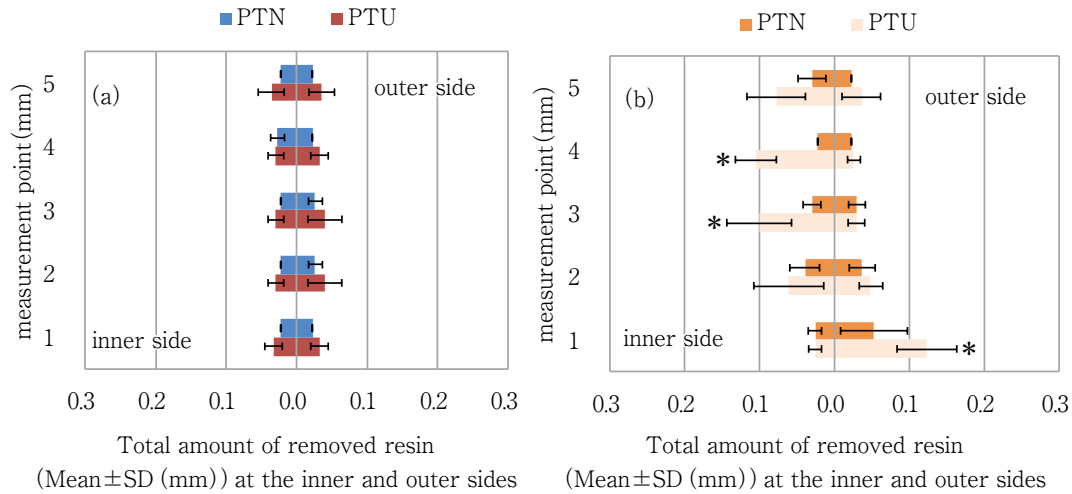
Fig. 3　Total amount of removed resin (mm) at the different levels after root canal preparation for 10° apical curvature canals by (a) ISO #25 PTN, ISO #25 PTU, and (b) ISO #40 PTN, ISO #40 PTU

＊：Significant difference between PTN and PTU (p＜0.05)

Fig. 4　Total amount of removed resin (mm) at the different levels after root canal preparation for 20° apical curvature canals by (a) ISO #25 PTN, ISO #25 PTU, and (b) ISO #40 PTN, ISO #40 PTU

＊：Significant difference between PTN and PTU (p＜0.05)

site phase and R phase[16-18]. Because the elastic modulus is less than that of the austenite phase, the initial flexibility is improved. Additionally, the M-wire NiTi alloy is more flexible than the conventional NiTi alloy because the austenite phase undergoes a martensitic transformation due to the stress on the file when forming a curved root canal. The stress load on the file is reduced, which reduces file corruption[19].

In this study, the usefulness of the M-wire NiTi alloy

was analyzed by comparing the cutting characteristics of PTN and PTU under a stress load (formation of a curved root canal). The root canal formation using root canal models with different apex curvatures of 10° to 30° was analyzed with final apical sizes of ISO #25 and ISO #40. There was a large difference in the displacement of the root canal wall between the groups. In the ISO #25 group, there was no significant difference in the amount of resin removed or canal transportation
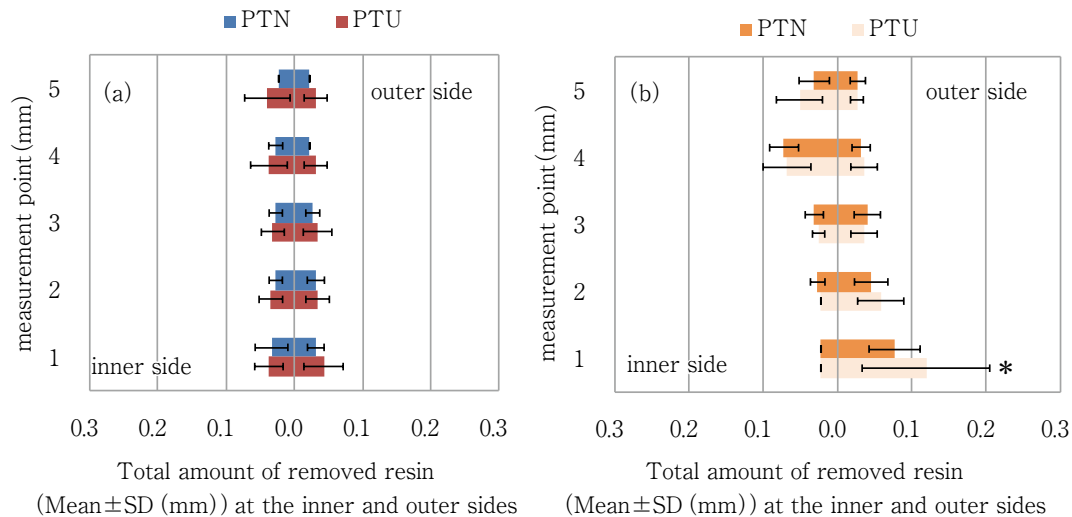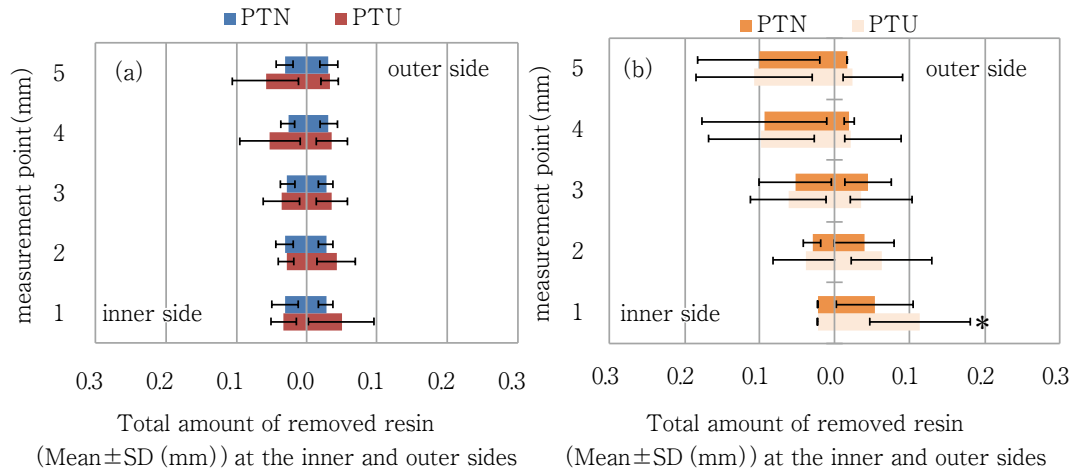
Fig. 5　Total amount of removed resin (mm) at the different levels after root canal preparation for 30° apical curvature canals by (a) ISO #25 PTN, ISO #25 PTU, and (b) ISO #40 PTN, ISO #40 PTU

∗：Significant difference between PTN and PTU (p＜0.05)

Table 1　Statistical analysis of canal transportation at different levels after root canal preparation using a final apical size of ISO #25 in 10°, 20°, and 30° apical curvature models by PTN and PTU.

	PTN			PTU		
apical curvature	10°	20°	30°	10°	20°	30°
level (mm)						
1	0.00±0.00	0.00±0.01	0.00±0.01	0.00±0.00	−0.01±0.01	−0.02±0.01
2	0.00±0.00	−0.01±0.00	0.00±0.01	−0.01±0.01	0.00±0.00	−0.01±0.01
3	−0.02±0.00	0.00±0.01	0.00±0.00	−0.01±0.01	0.00±0.00	0.00±0.01
4	−0.02±0.00	−0.01±0.01	0.02+0.01	−0.01±0.00	0.01±0.00	0.02±0.01
5	0.00±0.00	0.00±0.00	0.00±0.01	0.01±0.01	0.01±0.01	0.03±0.02

Mean±SD (mm)

Table 2　Statistical analysis of canal transportation at different levels after root canal preparation using a final apical size of ISO #40 in 10°, 20°, and 30° apical curvature models by PTN and PTU.

	PTN			PTU		
apical curvature	10°	20°	30°	10°	20°	30°
level (mm)						
1	−0.03±0.02*	−0.05±0.01*	−0.05±0.03*	−0.10±0.02*	−0.10±0.03*	−0.13±0.03*
2	0.00±0.01	−0.02±0.01	−0.02±0.02	0.01±0.02	−0.04±0.01	−0.05±0.02
3	0.00±0.01*	−0.01±0.01	−0.01±0.01	0.07±0.02*	−0.01±0.01	0.01±0.01
4	0.00±0.00*	0.04±0.01	0.07±0.03	0.08±0.01*	0.03±0.01	0.07±0.02
5	0.01±0.01	0.05±0.00	0.08±0.03	0.04±0.01	0.03±0.01	0.08±0.03

Mean±SD (mm)

∗：Significant difference between PTN and PTU (p＜0.05)

associated with the change in the bending angle in PTN and PTU.

In the ISO #25 group, the amount of resin removed by PTN and PTU was 1 to 5 mm from the apex of the inner and outer sides for curved root canal angles of 10°, 20°, and 30°. The measured value was less than 0.05 mm. Furthermore, the root canal transportation was less than 0.05 mm and both files could form the root canal and maintain the original anatomical root canal morphology. The NiTi file with an ISO #25 tip showed that the shaping ability of the conventional and M-wire type NiTi alloy files were similar and useful for root canal preparation of curved root canal angles between 10° to 30°.

In the ISO #40 group, the amount of resin removed significantly changed depending on the root canal curvature between the PTN and PTU files. The PTU increased the lateral displacement by 1 mm from the apex, and by 4 mm and 5 mm from the apex in the inside of the root canal between the 10° to 30° canals. The risk of transportation and canal perforation in the curved root canal was observed. However, the PTN maintained the original root canal morphology when the amount of resin removed in the inner and outer sides was 1 to 3 mm and from the apex was 0.1 mm or less between the 10° to 30°canals. For the 30° curvature canal, the inner side cutting of 4 mm and 5 mm from the apex tended to be as high as that of the PTU. The PTN obtained by converting the NiTi alloy into the R phase by heat processing improved the root canal followability and suppressed the transport on the outer side of the apex. It is necessary to be careful of accidents, such as strip perforation during root canal formation on the inner side, when using the 30° curvature.

Because the PTN and PTU used in this study are similar file systems for complete root canal formation with multiple lines, the flexibility of the M-wire NiTi alloy is useful for proper root canal formation. Additionally, the M-wire type NiTi alloy single file preparation system (Reciproc, WaveOne file) completes root canal formation with only one file, the root canal wall displacement is less than that by the PTU, and the root canal transportation is reduced. Additionally, the PTN is reported to retain anatomical morphology[9,23]. Finally, the PTN has excellent fatigue resistance and torsion resistance regardless of the difference in file systems used for root canal preparation.

Conclusion

The amount of canal wall removed and transported by M-wire ISO #40 PTN was less than that by the conventional ISO #40 PTU in 10° to 30° curvature canals and the original root canal form was maintained, although there was no significant difference in the shaping ability for curvature canals by both PTN and PTU of ISO #25. The M-wire PTN improves file flexibility and enables accurate canal shaping for wide and heavy curvature canals.

References

1) Thompson SA. An overview of nickel-titanium alloys used in dentistry. Int Endod J 2000; 33: 297–310.
2) Lee JH, Park JB, Andreason GF, Lakes RS. Thermomechanical study of NiTi alloys. J Biomed Mater Res 1988; 22: 573–588.
3) Serene TP, Adams JD, Saxena A. Nickel-titanium instruments: Applications Endodontics. St. Louis: Ishiyaku Euro America Inc.
4) Walia HM, Brantley WA, Gerstein H. An initial investigation of the bending and torsional properties of Nitinol root canal files. J Endod 1988; 14: 346–351.
5) Kazemi RB, Stenman E, Spångberg LS. A comparison of stainless steel and nickel-titanium H-type instruments of identical design: torsional and bending tests. Oral Surg Oral Med Oral Pathol Oral Radiol Endod 2000; 90: 500–506.
6) Zinelis S, Darabara M, Takase T, Ogane K, Papadimitriou GD. The effect of thermal treatment on the resistance of nickel-titanium rotary files in cyclic fatigue. Oral Surg Oral Med Oral Pathol Oral Radiol Endod 2007; 103: 843–847.
7) Berendet C. Method of preparing Nitinol for use in manufacturing instrument with improved fatigue resistance.

US patent Application 20070072147 AI.

8) Alapati SB, Brantley WA, Iijima M, Clark WAT, Phil D, Kovarik L, Buie C, Liu J, Johnson WB. Metallurgical characterization of a new nickel-itanium wire for rotary endodontic instruments. J Endod 2009; 35: 1589–1593.

9) Pereira ESJ, Peixoto IFC, Viana ACD, Oliveira II, Gonzalez BM, Buono VTL, Bahia MGA. Physical and mechanical properties of a thermomechanically treated NiTi wire used in the manufacture of rotary endodontic instruments. Int Endod J 2012; 45: 469–474.

10) De-Deus G, Belladonna FG, Souza EM, Silva EJ, Neves Ade A, Alves H, Lopes RT, Versiani MA. Micro-computed tomographic assessment on the effect of ProTaper Next and Twisted File Adaptive systems on dentinal cracks. J Endod 2015; 41: 1116–1119.

11) Saha SG, Vijaywargiya N, Saxena D, Saha MK, Bharadwaj A, Dubey S. Evaluation of the incidence of microcracks caused by Mtwo and ProTaper Next rotary file systems versus the self-adjusting file: A scanning electron microscopic study. J Conserv Dent 2017; 20: 355–359.

12) Hiran-us S, Pimkhaokham S, Sawasdichai J, Ebihara A, Suda H. Shaping ability of ProTaper NEXT, ProTaper Universal and iRace files in simulated S-shaped canals. Aust Endod J 2016; 42: 32–36.

13) Gagliardi J, Versiani MA, de Sousa-Neto MD, Plazas-Garzon A, Basrani B. Evaluation of the shaping characteristics of ProTaper Gold, ProTaper NEXT, and ProTaper Universal in curved canals. J Endod 2015; 41: 1718–1724.

14) Wu H, Peng C, Bai Y, Hu X, Wang L, Li C. Shaping ability of ProTaper Universal, WaveOne and ProTaper Next in simulated L-shaped and S-shaped root canals. BMC Oral Health 2015; 15: 27. doi: 10.1186/s12903-015-0012.

15) Tavanafar S, Gilani PV, Saleh AM, Schäfer E. Shaping ability of ProTaper Universal, ProTaper NEXT and WaveOne Primary in severely curved resin blocks. J Contemp Dent Pract 2019; 20: 363–369.

16) Özyürek T, Yılmaz K, Uslu G. The effects of autoclave sterilization on the cyclic fatigue resistance of ProTaper Universal, ProTaper Next, and ProTaper Gold nickel-titanium instruments. Restor Dent Endod 2017; 42: 301–308.

17) Topçuoğlu HS, Topçuoğlu G, Akti A, Düzgün S. In vitro comparison of cyclic fatigue resistance of ProTaper Next, HyFlex CM, OneShape, and ProTaper Universal instruments in a canal with a double curvature. J Endod 2016; 42: 969–971.

18) Uygun AD, Kol E, Topcu MK, Seckin F, Ersoy I, Tanriver M. Variations in cyclic fatigue resistance among ProTaper Gold, ProTaper Next and ProTaper Universal instruments at different levels. Int Endod J 201; 49: 494–499.

19) Fernández-Pazos G, Martín-Biedma B, Varela-Patiño P, Ruíz-Piñón M, Castelo-Baz P. Fracture and deformation of ProTaper Next instruments after clinical use. J Clin Exp Dent 2018; 10: e1091–e1095.

20) Pereira ES, Gomes RO, Leroy AM, Singh R, Peters O. Mechanical behavior of M-wire and conventional NiTi wire used to manufacture rotary endodontic instruments. Dent Mater 2013; 29: e318–e324.

21) Gutmann JL, Gao Y. Alteration in the inherent metallic and surface properties of nickel-titanium root canal instruments to enhance performance, durability and safety: a focused review. Int Endod J 2012; 45: 113–128.

22) Braga LC, Silva AC, Buono VT, Bahia MG. Impact of heat treatments on the fatigue resistance of different rotary nickel-titanium instruments. J Endod 2014; 40; 1494–1497.

23) Câmara AS, Martins RC, Viana ACD, Leonardo PT, Buono VTL, Bahia MGA. Flexibility and torsional strength of ProTaper and ProTaper Universal rotary instruments assessed by mechanical tests. J Endod 2009; 35: 113–116.

Original Article

Influence of Surface Moisture on the Bond Strength
of a Universal Adhesive in the Etch-and-rinse Mode

Runa Sugimura, Akimasa Tsujimoto*, Kei Iwase,
Shun Katsuki, Ahmad Alkhazaleh*, Olajide Obe*,
Toshiki Takamizawa and Masashi Miyazaki

Department of Operative Dentistry, Nihon University School of Dentistry
*Department of Operative Dentistry, University of Iowa College of Dentistry

Abstract

Purpose: This study aimed to investigate the effect of surface moisture on the enamel and dentin bonding performances of a universal adhesive in the etch-and-rinse mode based on shear bond strength（SBS）tests.

Methods: Enamel and dentin surfaces were prepared（moist and dry conditions）using bovine mandibular incisors and treated with the universal adhesive Clearfil Universal Bond Quick（CU）using the etch-and-rinse mode. Resin composite was condensed into a plastic mold clamped to a fixture against the adherend surfaces and light-cured for 40 s. The bonded specimens（n＝15）were either stored in distilled water at 37℃ for 24 h or underwent 10,000 thermal cycles between 5℃ and 55℃ before the SBS tests. The universal adhesive interfaces in the etch-and-rinse mode were observed via scanning electron microscopy（SEM）.

Results: The CU's enamel and dentin bond strengths were not influenced by the surface moisture, regardless of the storage condition. Based on the SEM observations, surface moisture did not influence the widths of the adhesive and hybrid layers in the resin-dentin interfaces. However, the lengths of the resin tags in the moist group were longer than those in the dry group.

Conclusion: These findings indicated that the surface moisture content of the enamel and dentin might not significantly influence CU bonding performance regardless of the storage conditions. The presence of a new hydrophilic amide monomer in this universal adhesive might be a key factor that influences its bonding performances with enamel and dentin.

Key words: universal adhesive, surface moisture, etch-and-rinse mode

Introduction

Universal adhesives, in both etch-and-rinse and self-etch modes, have increased in popularity due to their versatility and relative ease of application[1]. Universal adhesives can be used as pretreatment agents for resin luting cements[2]; they can bond to various substrates without surface pretreatment[3] and can be used with reduced application time[4].

A recent systematic review on the laboratory bond strength of universal adhesives reported that the dentin bond strength of universal adhesives was not affected by the bonding strategy employed. In contrast, the enamel bond strength was lower in the self-etching mode than in the etch-and-rinse mode[1]. In addition, previous studies of universal adhesives demonstrated that the use of an etch-and-rinse mode for dentin bonding yields a bond strength equal to or greater than a self-etch mode[5-7]. These results suggested that universal adhesives might be more suitable for use in the etch-and-rinse mode than in the self-etch mode in some cases. However, there is no consensus on the optimal conditions for using universal adhesives in the etch-and-rinse mode; the ideal surface moisture condition for applying these adhesives has not been determined so far. The influence of surface moisture on the bonding performance of dental adhesive systems has long been discussed. A higher water content or over-drying of the demineralized dentin can degrade the quality of the adhesive layer and reduce the bond strength[8]. Previous studies have reported that the dentin bond strength of universal adhesives in the etch-and-rinse mode is not affected by surface moisture[9,10]. Nonetheless, the effect of surface moisture on the bonding of universal adhesives to enamel and dentin in the etch-and-rinse mode needs to be clarified.

This study aimed to investigate the influence of surface moisture on the bonding performance of a universal adhesive in the etch-and-rinse mode. The null hypotheses tested were as follows: 1) the surface moisture in phosphoric acid-etched enamel and dentin does not influence the bond durability of the universal adhesive, and 2) the surface moisture does not affect the interfacial morphology of the universal adhesive in the etch-and-rinse mode.

Materials and Methods

1．Study materials

The universal adhesive used in this study（Clearfil Universal Bond Quick ER; CU）was obtained from Kuraray Noritake Dental, Tokyo, Japan. Ultra-Etch（Ultradent Products, South Jordan, UT, USA）, a 35% phosphoric acid solution, was used as the etching agent, and Clearfil AP-X（Kuraray Noritake Dental）was used as the resin composite to fabricate the specimens（Table 1）.

2．Specimen preparation

The shear bond strengths of CU to enamel and dentin in the etch-and-rinse mode were measured using the notched-edge test specified by ISO 29022[11]. Bovine mandibular incisors were extracted from 2- to 3-year-old cattle. The roots were cut using a slow-speed saw equipped with a diamond-impregnated disk（Isomet, Buehler, Lake Bluff, IL, USA）, and the pulps were removed. Each tooth was then mounted in self-curing acrylic resin（Tray Resin II, Shofu, Kyoto, Japan）and placed underwater to limit the temperature rise caused by the exothermic polymerization of the resin. The dentin bonding surfaces were ground flat using a grinder-polisher（EcoMet 4, Buehler）with P120 and P400 silicon carbide（SiC）papers（Struers, Cleveland, OH, USA）under running water. The surfaces were then washed with an air-water spray and air-dried using a three-way syringe.

The prepared enamel and dentin adherent surfaces were etched with 35% phosphoric acid for 15 s before applying the adhesive. Subsequently, they were divided into two groups based on the level of moisture: *moist group*, where 2.5 μl of distilled water was applied to an area（diameter, 4 mm）and blot dried; and *dry group*, where 2.5 μl distilled water was applied to an area of similar diameter and air-dried for 5 s using a dental three-way syringe（distance, 5 cm above the surface; air pressure, 0.25 MPa）. The specimens were prepared under ambient laboratory conditions at 23℃±2℃ and 50%±10% relative humidity.

3．Shear bond strength testing

The prepared enamel and dentin surfaces from the two groups were treated with the universal adhesive per the manufacturer's instructions. After applying the adhesive to the tooth surface, a Bonding Mold Insert（2.38 mm in internal diameter and 2.5 mm in height,

Table 1 Materials used in this study

Material (Lot No.)	Type (Code)	Main components	Manufacturer
Clearfil Universal Bond Quick ER (9T0050)	Adhesive (CU)	bis-GMA, MDP, HEMA, hydrophilic amide monomer, filler, ethanol, water, NaF, photo initiators, chemical polymerizer, accelerator, silane coupling agent, others	Kuraray Noritake Dental, Tokyo, Japan
Ultra-Etch (A124)	Etching agent	35% phosphoric acid, glycol, cobalt aluminate blue spinel	Ultradent Products, South Jordan, UT, USA
Clearfil AP-X (380094)	Resin composite	bis-GMA, TEGDMA, silanated barium glass filler, silanated silica filler, silanated colloidal silica, CQ, pigments, others	Kuraray Noritake Dental, Tokyo, Japan

Ultradent Products) was clamped to a fixture against the adherend surfaces and filled with resin composite using a condensing instrument. The resin composite was light-cured for 40 s at a standardized distance of 1 mm using a quartz-tungsten halogen (QTH) curing unit (Optilux 501, Kerr, Orange, CA, USA). The light intensity (>600 mW/cm^2) of the QTH curing unit was monitored using a curing radiometer (Model 100, Kerr). The plastic mold was removed, and the bonded specimens were stored in distilled water at 37℃ for 24 h. The specimens were randomly allocated to two subgroups ($n=15$ each) as follows: those that did not undergo thermal cycling (no thermal cycling; 24 h) and those that underwent 10,000 thermal cycles (10,000 TC at 5℃ and 55℃). Thermal cycling was conducted using a thermal shock tester (TTS-1, Thomas Kagaku, Tokyo, Japan), and each cycle involved incubation in each water bath for 30 s with a transfer time of 5 s.

The shear bond strength (SBS) measurements were performed using a universal testing machine (5500R, Instron, Norwood, MA, USA) equipped with Test Base Clamp (Ultradent Products) at a crosshead speed of 1.0 mm/min. Crosshead Assembly (Ultradent Products) with a semicircular notch (diameter, 2.38 mm) was used for the measurements. The SBS values (MPa) were calculated by dividing the peak load at failure by the bonding area.

4. Failure mode analysis

After the SBS tests, a single experienced individual evaluated the bond failure sites via optical microscopy (SZH-131, Olympus, Tokyo, Japan; magnification, 20×). The failure mode was assessed based on the percentage of surface area (adhesive, resin, or substrate) observed on both the bonded resin composite cylinders

and the tooth bonding sites. The failure modes were classified as follows: adhesive failure at the interface; cohesive failure in the resin composite; cohesive failure in the enamel or dentin; and mixed failure.

5. Scanning electron microscopy observation

Representative micrographs of the resin-enamel and resin-dentin interfaces were obtained using field-emission scanning electron microscopy (SEM; ERA 8800FE, Elionix, Tokyo, Japan). Acid-base treatment was performed to visualize the resin tags and assess their length to dentinal tubules. The enamel and dentin surfaces were prepared (as described earlier), and the bonded specimens were stored in distilled water at 37℃ for 24 h. They were embedded in epoxy resin (Epon 812, Nisshin EM, Tokyo, Japan) and stored at 37℃ for an additional 24 h. Subsequently, the specimens were sectioned at the center, and the surfaces of the cut halves were polished using a grinder-polisher (#4,000-grit SiC paper). Finally, the surfaces were polished with a soft cloth using 0.25 μm-grit diamond paste (DP-Paste; Struers, Ballerup, Denmark) and ultrasonically cleaned for 3 min. The polished surfaces of specimens with the resin-dentin with acid-base treatment interfaces were etched with HCl solution (6 mol/l) for 25 s and deproteinized by immersion in 6% NaOCl solution for 3 min. The SEM specimens were dehydrated by immersing them in ascending concentrations of aqueous *tert*-butanol (50% for 20 min, 75% for 20 min, 95% for 20 min, and 100% for 2 h) and then transferring them to a freeze dryer (Model ID-3, Elionix) for 3 min. In order to enhance the visibility of the layers on the adhesive interfaces, the specimens' polished surfaces were etched for 30 s using an argon ion-beam (Type EIS-200ER, Elionix), which was directed perpen-

Table 2 Shear bond strength (MPa) and standard deviations (in parentheses) of the universal adhesive with their failure mode

Substrate	Surface wetness	24 h		10,000 TC	
		Bond strength (MPa)	Failure mode	Bond strength (MPa)	Failure mode
Enamel	Moist	33.4 (3.9)[a]	[100/0/0/0]	35.6 (4.7)[a]	[100/0/0/0]
	Dry	34.8 (5.0)[a]	[100/0/0/0]	36.9 (5.3)[a]	[100/0/0/0]
Dentin	Moist	21.2 (4.5)[b]	[93/0/7/0]	23.1 (4.7)[b]	[100/0/0/0]
	Dry	22.5 (4.8)[b]	[86/0/14/0]	24.4 (5.1)[b]	[100/0/0/0]

Same small letters indicate no significant differences ($p > 0.05$).
Percentage of failure mode[adhesive failure/cohesive failure in resin/cohesive failure in enamel or dentin/mixed failure]. There were no significant differences in failure mode with surface wetness or substrate.

dicular to the surface at an accelerating voltage of 1.0 kV and an ion current density of 0.4 mA/cm^2. The surfaces were then coated with a thin film of gold in a vacuum evaporator (Quick Coater Type SC-701, Sanyu Electron, Tokyo, Japan) and observed using field-emission SEM (operating voltage, 10 kV). The approximate lengths of the resin tags were measured on the images of the acid-base-treated resin-dentin interfaces.

6．Statistical analysis

The SBS data were analyzed using a two-way analysis of variance followed by Tukey's post hoc honestly significant difference test. Fisher's exact test was used for statistical analysis of the failure mode after SBS testing. The significance level in this study was set at $p < 0.05$. The statistical analysis was conducted using a commercial statistical software package (SPSS Statistics, IBM, Armonk, NY, USA).

Results

1．SBS

Table 2 shows the results for the effect of surface moisture on the SBS of CU in the etch-and-rinse mode. The SBS to the enamel was not influenced by the surface moisture, regardless of the storage condition. Furthermore, no significant difference ($p > 0.05$) in the SBS of the universal adhesive to dentin between the moist and dry groups was noted, regardless of the storage condition.

2．Failure mode

The results of the failure mode analysis for SBS after 24 h and 10,000 TC are shown in Table 2. Fisher's

exact tests did not reveal statistically significant differences in failure modes based on the surface moisture conditions or the substrate.

3．SEM observation of bonding interface

Figure 1 shows representative SEM micrographs of the control and etching groups. SEM observations of the resin-enamel and resin-dentin interfaces showed excellent adaptation, regardless of surface moisture. The thickness of the adhesive layers in the resin-enamel and resin-dentin interfaces ranged from 5 to 10 μm; a hybrid layer (thickness, approximately 2 μm) was visible in the resin-dentin interfaces. However, the surface moisture did not influence the widths of the adhesive and hybrid layers. In the SEM observations of the resin-dentin interfaces treated with an acid-base, the resin tags were identified and concentrated in the dentinal tubules. The length of the resin tag was dependent on the surface moisture condition of the dentin; the length in the moist group was longer (40-60 μm) than that in the dry group (30-50 μm).

Discussion

Clinicians try to control the surface moisture of the substrate after phosphoric acid etching when using universal adhesives in the etch-and-rinse mode. However, moisture control is dependent on the individual's interpretation of the most appropriate surface moisture condition for the procedure. This study investigated the influence of surface moisture on the bonding strengths of a universal adhesive to both enamel and dentin in the etch-and-rinse mode.
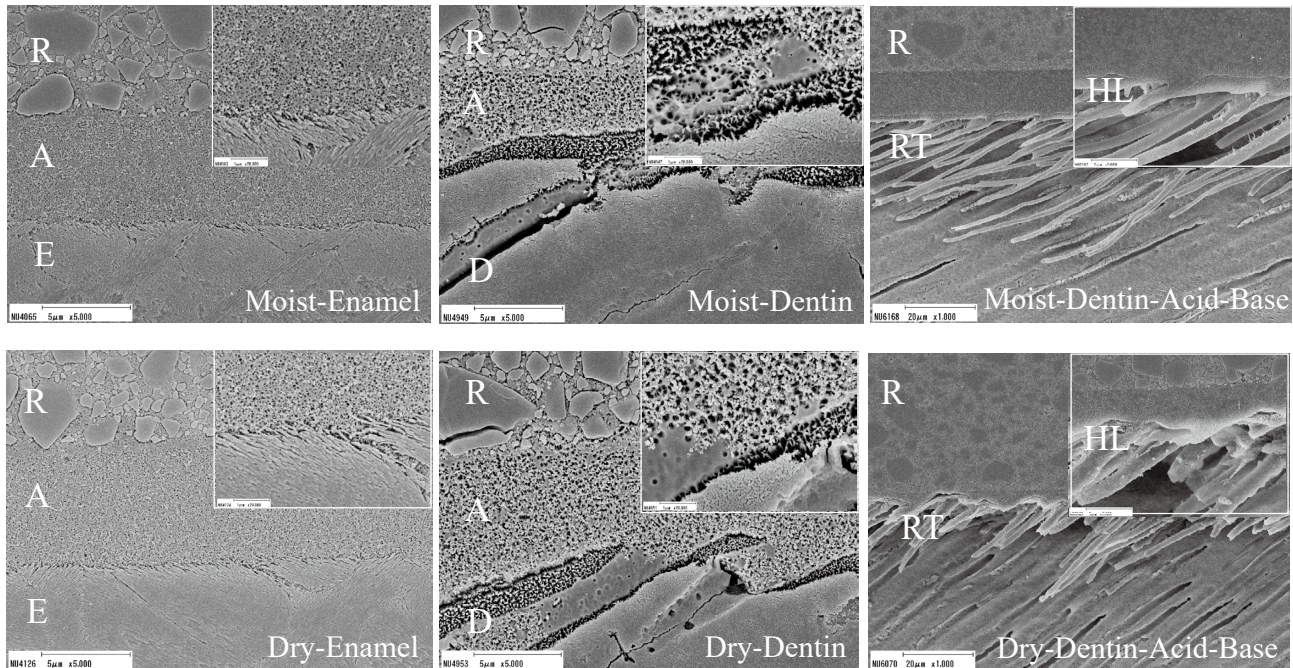
Fig. 1 Representative scanning electron microscopy images of resin-enamel, resin-dentin, and resin-dentin＋acid-base-treated interfaces

The left upper and lower images indicate representative resin-enamel interfaces. The upper and lower images in the middle indicate representative resin-dentin interfaces. The main images are at ×5,000 magnification. The smaller white rectangle indicates the location in the main images at ×20,000. The right upper and lower images indicate representative resin-dentin interfaces with acid-base treatment. The main images are at ×1,000 magnification. The smaller white rectangle indicates the location in the main images at ×5,000. A: adhesive; Acid-Base: acid-base treatment; D: dentin; E: enamel; HL: hybrid layer; R: resin; RT: resin tags.

The results of the present study suggested that the surface moisture of adherent surfaces did not affect the bond durability of CU in the etch-and-rinse mode. Therefore, the first null hypothesis that "surface moisture does not affect the bond durability of universal adhesives in the etch-and-rinse method" was not rejected. These results were consistent with those of a previous study[12], even when using the current universal adhesive. Phosphoric acid etching creates a micro-porous surface[13] and increases the surface free energy of enamel[14]. In contrast, in the case of the dentin, the surface becomes hydrophobic, and the surface free energy is decreased[15]. Previous studies have reported that the surface of the enamel etched with phosphoric acid is more "friendly" toward water than that of the dentin because the water is tightly trapped onto the surface owing to its structure and high surface free-energy[16]. This makes it difficult for the water to be removed by air-drying and the small difference in water content between the wet and dry enamel surfaces when compared to those of dentin.

On the other hand, the inorganic apatite crystals in the smear layer, superficial layer, and subsurface of the phosphoric acid-etched dentin are demineralized by etching and replaced by water. The intrinsic water-bound hydroxyl groups surround the collagen fibrils[17]. The water must surround the collagen fibrils to maintain the rigidity of the spaces between the fibrils, increase the adhesive penetration into the collagen network, and facilitate the interaction between the adhesive and the collagen. When the dentin surface becomes excessively dry, the collagen network collapses and shrinks, trapping water within the dentin tubules, resulting in poor interaction with the adhesive and reduced adhesive penetration[18]. In contrast, when the surface of the etched dentin is over-wet, the collagen network swells, and the interfibrillar space decreases, resulting in poor penetration of the adhesive into the dentinal tubules[19]. Furthermore, excessive moisture on the substrate causes phase separation of the adhesive[20] and poor polymerization[21], leading to hydrolysis and degradation of the adhesive layer. Thus, moisture con-

trol on the surface of demineralized dentin is an important factor determining the adhesive effect of the adhesive in the etch-and-rinse mode[22].

The effect of the surface moisture condition was visible in the SEM images of the resin tags in the acid-base-treated resin-dentin interface. Moreover, there were no differences in the widths of the adhesive and hybrid layers between the moist and dry groups at the resin-enamel or resin-dentin interfaces. The length of the resin tags in the acid-base-treated resin-dentin interfaces depended on the surface moisture conditions; the resin tags in the moisture group were longer than those in the dry group. However, no difference in the thickness of the hybrid layer was noted. Therefore, the second null hypothesis, "the interfacial morphology of CU in the etch-and-rinse mode does not differ depending on the surface moisture," was partially rejected.

In the present study, no relationship between the length of the resin tags and dentin bond durability of CU was observed. A previous study reported no correlation between the length of the resin tag and the adhesive strength of a two-step etch-and-rinse adhesive[23], but a strong correlation was observed with the thickness of the hybrid layer. In another study, the lengths of the resin tags in the case of the universal adhesives were significantly longer than those of the two-step etch-and-rinse adhesives; no relationship was observed between the length of the resin tag and the dentin bond strength[22]. Alternatively, according to Sugimura et al., there was an association between the length of the resin tags and the dentin bond durability of universal adhesives, and it was material dependent[24].

However, the length of the resin tags and the thickness of the hybrid layer alone cannot fully explain the results obtained in the present study because the effect of surface moisture on the bond durability to dentin might be dependent on the material used. The most likely reason for the difference between the results of this study and those of previous studies might be the composition of the adhesive used[9,10]. CU contains a new hydrophilic amide monomer, which is considered to be an important technical factor of this adhesive. It is used as an alternative to 2-hydroxyethyl methacrylate (HEMA). It exhibits a higher degree of polymerization than HEMA, thereby reducing water absorption, which is important to ensure adhesiveness under different surface wetting conditions. Therefore, the new hydrophilic amide monomer might reduce the effect of surface moisture on the bond durability of CU. By capturing the moisture from the substrate, the universal adhesive makes it more prone to demineralization and increases the chemical reactions between the adhesive and the substrate. Excess moisture in the adhesive will result in insufficient polymerization and a low-quality adhesive layer. In contrast, insufficient moisture in the adhesive will result in weak demineralization and poorer chemical reactions. Therefore, it is important to optimize the moisture content of the adhesive before applying it to the tooth substrate.

Nowadays, the principle of development differs among manufacturers, even for adhesives that belong to the same category. Therefore, the effect of surface moisture on bond durability in the etch-and-rinse mode can be overcome by adding special ingredients to the adhesive and optimizing the moisture content. However, there is little information about the influence of moisture condition on the bond performance of universal adhesives in the self-etch mode. Further research is needed to investigate the influence of moisture condition on bond performance when using universal adhesives in the self-etch mode.

Conclusion

1. The enamel and dentin bond strengths of CU were not influenced by the surface moisture, regardless of the storage condition.

2. SEM observations of the resin-enamel and resin-dentin interfaces showed excellent adaptation, regardless of the surface moisture. On the other hand, the lengths of the resin tags in the acid-base-treated resin-dentin interfaces differed according to the surface moisture conditions of the dentin.

Conflicts of interest

The authors declare no conflict of interest related to this paper.

References

1) Cuevas-Suárez CE, da Rosa WLO, Lund RG, da Silva AF, Piva E. Bonding performance of universal adhesives: An updated systematic review and meta-analysis. J Adhes Dent 2019; 21: 7–26.

2) Tsujimoto A, Barkmeier WW, Takamizawa T, Watanabe H, Johnson WW, Latta MA, Miyazaki M. Simulated localized wear of resin luting cements for universal adhesive systems with different curing mode. J Oral Sci 2018; 60: 29–36.

3) Siqueira F, Cardenas AM, Gutierrez MF, Malaquias P, Hass V, Reis A, Loguercio AD, Perdigão J. Laboratory performance of universal adhesive systems for luting CAD/CAM restorative materials. J Adhes Dent 2016; 18: 331–340.

4) Ahmed MH, Yoshihara K, Mercelis B, Van Landuyt K, Peumans M, Van Meerbeek B. Quick bonding using a universal adhesive. Clin Oral Investig 2020; 24: 2837–2851.

5) Nagarkar S, Theis-Mahon N, Perdigão J. Universal dental adhesives: Current status, laboratory testing, and clinical performance. J Biomed Mater Res B Appl Biomater 2019; 107: 2121–2131.

6) Takamizawa T, Barkmeier WW, Tsujimoto A, Berry TP, Watanabe H, Erickson RL, Latta MA, Miyazaki M. Influence of different etching modes on bond strength and fatigue strength to dentin using universal adhesive systems. Dent Mater 2016; 32: e9–e21.

7) Takamizawa T, Barkmeier WW, Tsujimoto A, Suzuki T, Scheidel DD, Erickson RL, Latta MA, Miyazaki M. Influence of different pre-etching times on fatigue strength of self-etch adhesives to dentin. Eur J Oral Sci 2016; 124: 210–218.

8) Yamamoto K, Suzuki K, Suwa S, Miyaji H, Hirose Y, Inoue M. Effects of surface wetness of etched dentin on bonding durability of a total-etch adhesive system: Comparison of conventional and dumbbell-shaped specimens. Dent Mater J 2005; 24: 187–194.

9) Perdigão J, Sezinando A, Monteiro PC. Laboratory bonding ability of a multi-purpose dentin adhesive. Am J Dent 2012; 25: 153–158.

10) Lenzi TL, Raggio DP, Soares FZM, Rocha Rde O. Bonding performance of a multimode adhesive to artificially-induced caries-affected primary dentin. J Adhes Dent 2015; 17; 125–131.

11) International Organization for Standardization. Dentistry-Adhesive-Notched-edge shear bond strength test,

ISO 29022 TR: 2013, Geneva.

12) Barkmeier WW, Erickson RL, Latta MA. Fatigue limits of enamel bonds with moist and dry techniques. Dent Mater 2009; 25: 1527–1531.

13) Zhu JJ, Tang AT, Matinlinna JP, Hägg U. Acid etching of human enamel in clinical applications: A systematic review. J Prosthet Dent 2014; 112: 122–135.

14) Tsujimoto A, Barkmeier WW, Takamizawa T, Watanabe H, Johnson WW, Latta MA, Miyazaki M. Influence of duration of phosphoric acid pre-etching on bond durability of universal adhesives and surface free-energy characteristics of enamel. Eur J Oral Sci 2016; 124: 377–386.

15) Yamauchi K, Tsujimoto A, Jurado CA, Shimatani Y, Nagura Y, Takamizawa T, Barkmeier WW, Latta MA, Miyazaki M. Etch-and-rinse vs self-etch mode for dentin bonding effectiveness of universal adhesives. J Oral Sci 2019; 61: 549–553.

16) Walls AW, Lee J, McCabe JF. The bonding of composite resin to moist enamel. Br Dent J 2001; 191: 148–150.

17) Pashley DH, Tay FR, Breschi L, Tjäderhane L, Carvalho RM, Carrilho M, Tezvergil-Mutluay A. State of the art etch-and-rinse adhesives. Dent Mater 2011; 27: 1–16.

18) Wang Y, Spencer P. Hybridization efficiency of the adhesive/dentin interface with wet bonding. J Dent Res 2003; 82: 141–145.

19) Mohan B, Kandaswamy D. A confocal microscopic evaluation of resin-dentin interface using adhesive systems with three different solvents bonded to dry and moist dentinan in vitro study. Quintessence Int 2005; 36: 511–521.

20) Tay FR, Gwinnett AJ, Wei SH. The overwet phenomenon: An optical, micromorphological study of surface moisture in the acid-conditioned, resin-dentin interface. Am J Dent 1996; 9: 43–48.

21) Toledano M, Cabello I, Yamauti M, Giannini M, Aguilera FS, Osorio E, Osorio R. Resistance to degradation of res-in-dentin bonds produced by one-step self-etch adhesives. Microsc Microanal 2012; 18: 1480–1493.

22) Iwami Y, Yamamoto H, Kawai K, Ebisu S. Effect of enamel and dentin surface wetness on shear bond strength of composites. J Prosthet Dent 1998; 80: 20–26.

23) Anchieta RB, Oliveira FG, Sundfeld RH, Rahal V, Machado LS, Alexandre RS, Sundefeld ML, Rocha EP. Analysis of hybrid layer thickness, resin tag length and their correlation with microtensile bond strength using a total etch adhesive to intact dentin. Acta Odontol Latinoam 2011; 24: 272–278.

24) Sugimura R, Tsujimoto A, Hosoya Y, Fischer NG, Barkmeier WW, Takamizawa T, Latta MA, Miyazaki M. Surface moisture influence on etch-and-rinse universal adhesive bonding. Am J Dent 2019; 32: 33–38.

Original Article

Removal of Biofilm from Titanium Surfaces Using 400-kHz Ultrasound

Takashi TAKIGUCHI, Junki YAMADA,
Masanori SATO* and Matsuo YAMAMOTO

Department of Periodontology, Showa University School of Dentistry
*Honda Electronics Co., Ltd.

Abstract

Purpose: Peri-implantitis is a microbial infectious disease that is similar to periodontal disease. Although one of the most important procedures for managing peri-implantitis is to remove dental biofilm from titanium surfaces, this is less than adequate when the procedure is conducted using conventional dental devices. Ultrasound in the MHz range generates vibration in water, thereby accelerating water molecules through which debris on the surface of an object can be removed. The objective of this study was to investigate the effectiveness of ultrasonic water flow in removing plaque from titanium specimens.

Methods: Sound pressure was measured by the beam pattern distribution and a hydrophone. The optimum applied power and irradiation conditions were determined based on the relationship between artificial plaque removal effect and sound pressure. Plaque biofilms were formed over a period of 72 h on the surfaces of titanium specimens attached to custom-made stents fixed to the buccal surfaces of the molar and premolar teeth of volunteers. In this experiment, the titanium surfaces were exposed to an ultrasonic water flow of 400 kHz, with a sound pressure of 0.6 MPa, for 180 s. After cleaning by the ultrasonic water flow, the titanium surfaces were examined by a scanning electron microscope. For each specimen, the residual plaque biofilm areas were evaluated as percentages of the surface scanned.

Results: The sound pressure measurements were confirmed to be reasonably accurate based on the calculated results of the beam pattern distribution. The artificial plaque was removed in a sound pressure-dependent manner. The total proportions of residual plaque biofilm were 22.8% (median) and 7.05% (median) on mirror-finished and rough surfaces, respectively. The difference in residual plaque biofilm compared to the condition before treatment on both the mirror-finished and rough surfaces was judged to be significant at *p<0.05. Furthermore, the ultrasonic water flow completely destroyed the bacterial chains on the titanium specimens.

Conclusions: This study demonstrated that the 400-kHz, 0.6-MPa sound pressure ultrasonic water flow cleaning device can effectively remove plaque biofilm from titanium surfaces.

Key words: ultrasonics, vibrational acceleration, sound pressure, biofilm

Introduction

Peri-implantitis is a microbial infectious disease that is similar to periodontal disease. One of the most important procedures for managing peri-implantitis is the removal of dental biofilm from titanium surfaces. Biofilm consists of microbes enclosed within extracellular polymeric substances such as polysaccharides, proteins, and nucleic acids. Biofilm formation can be observed on the surfaces of medical devices such as venous catheters, heart valves, coronary stents, and dental implants[1,2]. The biofilm formed around dental implants follows a similar pattern of microbial colonization as that formed on natural teeth[3]. Microbiological evidence of biofilm-related peri-implant infection has been reported in the literature[4,5]. Peri-implant mucositis and peri-implantitis were reported as new dental diseases affecting implants[6,7]. Although thorough bacterial reduction is necessary to treat peri-implant diseases, it is difficult to eliminate bacteria from a dental implant surface using conventional tools such as tooth brushes and ultrasonic scalers[8,9], which is because the implant's roughness is in the order of micrometers.

Ultrasonic scalers have an advantage with respect to the removal of plaque and calculus, but they also carry the risk of scratching the surface of dental implants[10,11]. Therefore, it is necessary to develop a device for cleaning dental plaque from rough surfaces.

Ultrasonic cleaning is an efficient method to remove unwanted particles from an object by generating high-frequency mechanical oscillations in water or a solvent. The cleaning mechanism is based on cavitation and vibrational acceleration within the washing fluid. Ultrasonic cleaners that operate at frequencies below 100 kHz primarily depend on this cavitation mechanism[12]. This type of ultrasonic cleaner is suitable for removing particles with sizes in the order of several microns and is used, for example, for cleaning optics and precision parts. Cleaners in the MHz range are operated at very high frequencies above 1 MHz, and these depend on the vibrational acceleration mechanism[13]. At these frequencies, particles measuring $\leq 0.3\,\mu\mathrm{m}$ in diameter can be removed[14]. This type of cleaner relies on high-frequency acceleration force and is used, for example, for cleaning photo masks or silicon wafers in the manufacture of semiconductors[14–16].

Recently, we focused on developing a new cleaning system operating at a midrange frequency, in which 400-kHz ultrasound was superposed on a water flow from a nozzle. The ultrasonic water flow (UWF) worked as a medium not only for propagating ultrasound but also for transporting debris detached by the ultrasonic action[17].

The present study aimed to explore whether it is possible to use the developed UWF system to remove biofilm from titanium surfaces.

Materials and Methods

1．Ultrasonic water flow

UWF is a non-contact high-frequency ultrasonic cleaning system that removes dental biofilm from the minute structures of implants without cavitation or contact damage.

Figure 1 depicts a schematic of the experimental setup of the UWF system. The washing fluid is supplied to the device from a water tank, in which ultrasonic waves (frequency: 400 kHz; input power: 0–25 W) are propagated. The diameter of the ultrasonic transducer is 30 mm. The nozzle's outlet diameter is 6 mm. The vibrator case is tapered toward an outflow port, and the washing fluid through which the ultrasonic waves propagate impinges upon the specimen.

The UWF device was mounted on an arm that could be adjusted along three axes to ensure reproducibility. In the present experiment, the variation in sound pressure with the working distance was measured and the optimal working distance was determined for the cleaning test. Figure 2 shows images of the UWF device. Since the UWF device is to be used in the mouth for this application, the water flow rate was chosen to be approximately 300 ml/min. Although it was observed that the water flow remained rectilinear, it developed into a spray after a working distance of ≥ 60 mm (Fig. 2).

2．Sound pressure simulation

Figure 3 shows a simulated ultrasonic beam pattern under the free-boundary condition in water. The ultrasonic field was calculated using the ring function method[18] at a frequency of 400 kHz (wavelength 3.75 mm), a transducer size of $\phi = 30$ mm, and a sound velocity of 1,500 m/s. The maximum sound pressure area appears around 50–80 mm from the transducer.
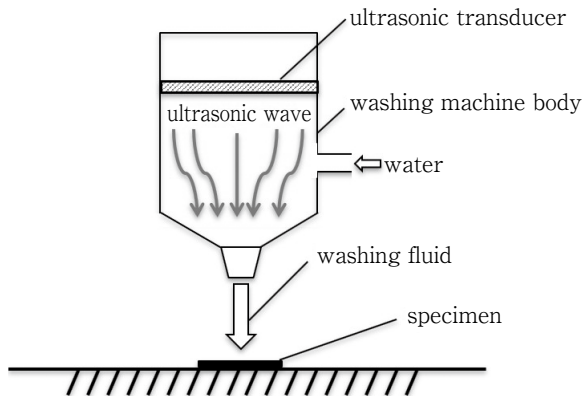
Fig. 1　The UWF system

This simulation shows the profile of the sound pressure that we experimentally measured using hydrophones.

3．Measurement of sound pressure

The sound pressure distribution in the UWF system was measured using a hydrophone（ONDA HNR-0500; with −250 kHz to 1 MHz calibration）. Figure 4 shows the waveform of the sound pressure p_{0-p} of the UWF system.

The measurements were performed for various input settings and various distances from the transducer.

In the present experiment, the sound pressure was measured as a function of working distance for various input powers, and an optimal condition was determined for the cleaning test.

4．Cleaning experiment for artificial plaque
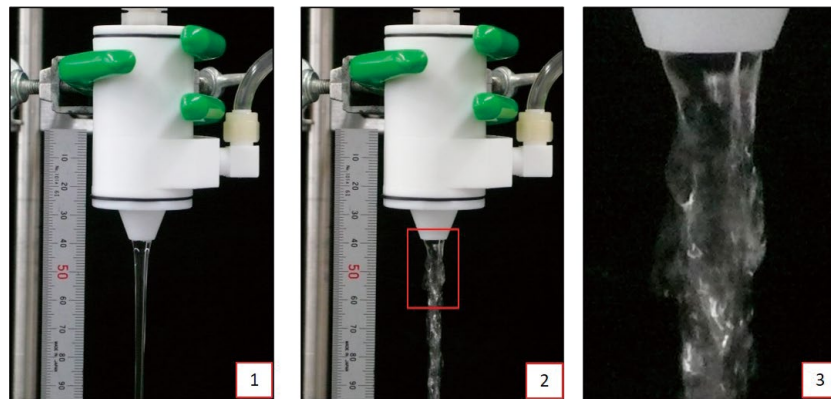
The cleaning effects of various input powers were

Fig. 2　Images of UWF
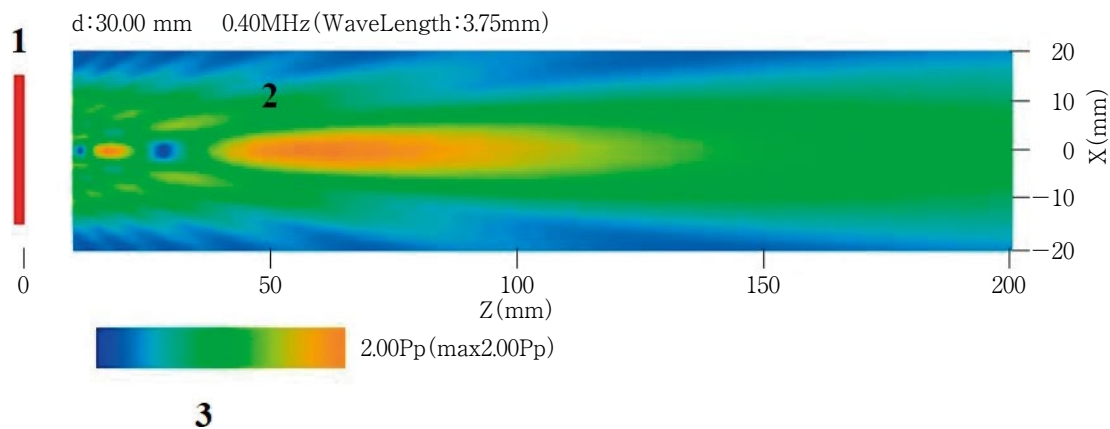1：Water flow, 2：Ultrasonic water flow, 3：Ultrasonic water flow (Close-up view)

Fig. 3　Simulated beam pattern in the free-boundary condition
1：Ultrasonic transducer, 2：Maximum sound pressure of the ultrasonic wave, 3：Level of sound pressure. The maximum（peak）pressure（Pp）is 2.00.
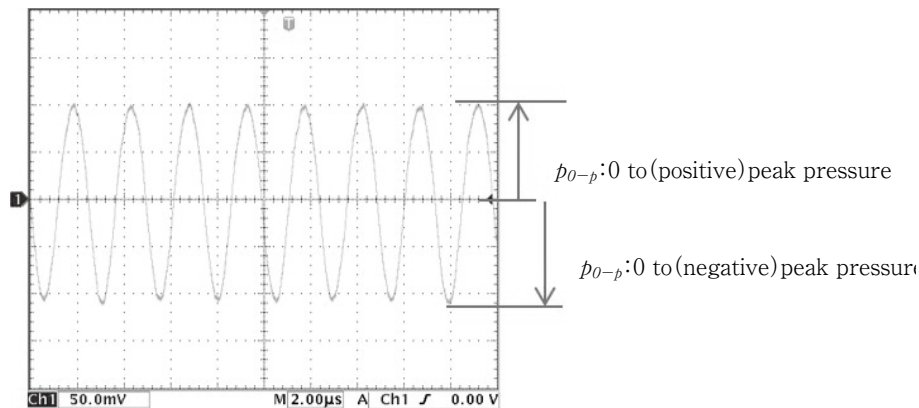
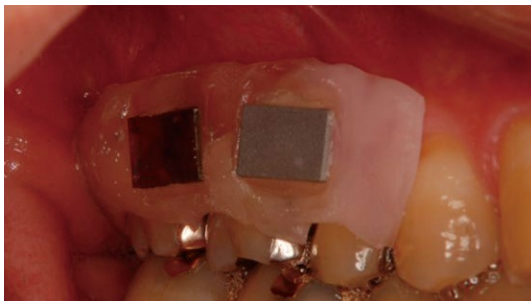**Fig. 4** Waveform of the sound pressure

Fig. 5 Titanium test plate placed in the mouth
 Plaque biofilm was formed on the titanium specimens in situ over a period of 72 h (rough surface and mirror-finished surface, 5 mm×7 mm) at the buccal site of the molar and premolar teeth on custom-made stents.

investigated using artificial plaque on a titanium specimen. The input power to the ultrasonic transducer ranged from 5 to 25 W, and the washing time was 60 s. The area of artificial plaque remaining on the titanium specimen after cleaning was measured using a digital optical microscope. The residual artificial plaque (RAP) in the scanned area was defined as the percentage of the area that retained the artificial plaque after cleaning. This area was measured by setting a threshold value for the color.

5．Cleaning experiment for biofilm

1 ）Biofilm formation on titanium specimens

Figure 5 illustrates the position of the titanium plates fixed to a removable custom-made stent placed in the mouth of a volunteer. The specimens were placed at the buccal sites of molar and premolar teeth in the mouths of five male subjects for 72 h to allow plaque biofilm to form on them[19] and were removed only during eating or brushing. They were then analyzed for biofilm formation and removal using UWF treatment. The study protocol was approved by the ethics committee of the Showa University School of Dentistry, and written informed consent was obtained from all participants（No. 2011‑013）.

The surface characteristics of the titanium specimens were similar to those of commercial dental implants (Setio, GC Corporation, Japan). Two types of surface were examined, a mirror-finished surface and a sandblasted rough surface. The sandblasted surface was hydrophilic, grade IV, with a surface roughness Ra＝2.54 μm and Rz＝11.87 μm.

2 ）Estimation of the area covered by the residual plaque biofilm

The titanium specimens were subjected to water flow alone or to UWF, and in each case the area covered by residual plaque biofilm (RPB) was measured as the percentage of the area of a randomly selected scanned surface using a digital microscope (VHX‑2000, KEYENCE, Japan). To compare the RPBs, the initial area covered by the plaque biofilm was defined as 100% RPB[20].

6．Scanning electron microscope observations

After the application of UWF, the titanium specimens were fixed in glutaraldehyde ［2.5% phosphate-buffered saline (PBS)］ for 30 min and then rinsed in PBS. Then, the samples were fixed in osmic acid（1% PBS) for 30 min at 4℃ and subsequently dehydrated in a graded ethanol series（50%‑100% for 10 min). Finally, the samples were dried in a critical point drying machine (HCP-2, Hitachi, Japan). All samples were mounted on scanning electron microscope (SEM) sample stubs (E-1030, Hitachi) and sputtered with platinum. The plaque biofilm was analyzed using an S‑4700 SEM

(Hitachi) at ×350 magnification.

7．Sample size calculation

Sample size was calculated using EZR (Saitama Medical Center, Jichi Medical University, Japan) and by performing power analysis for RPB on titanium specimens. The sample size was calculated for a＝0.05 and b/a ratio＝0.8, and the effect of size was calculated using the mean and SD of the variables. The analysis indicated that a sample of five subjects was needed.

8．Statistical analysis

The results are presented as median values with the top 25th and the bottom 25th percentiles (first and third quartiles) rather than as mean and standard deviation. Statistical analyses were performed using EZR, which is a graphical user interface for R (The R Foundation for Statistical Computing, Vienna, Austria). The Mann-Whitney U test was used to evaluate the differences in RPB, and the Wilcoxon signed-rank test was used to compare differences between the initial plaque biofilm (IPB) and RPB. The correlation was analyzed using Spearman's correlation test. A p value of ＜0.05 was considered to be significant.

Results

Figure 6 depicts the relationship between the negative and positive peak pressures of the sound pressure waveform in the UWF system. The sound pressure measurements were confirmed to be reasonably accurate based on the calculated results of the beam pattern distribution (Fig. 6A). An increase in sound pressure can be observed at distances ＞50 mm from the ultrasonic transducer (Fig. 6A). Therefore, the work distance for the artificial plaque cleaning test was chosen as 50 mm. The absolute values of the negative and positive peak pressures were approximately equal. As shown in Figure 6B, when the input setting was changed from 5 to 25 W, the sound pressure increased depending on the input power. For example, the maximum sound pressure was 0.6 MPa when the input power was 15 W.

Figure 7A shows a painted titanium specimen before (left) and after (right) cleaning. The input power to the ultrasonic transducer was −5–25 W, and the cleaning time was 60 s. As depicted in Figure 7A, metallic colors indicate the areas from which artificial plaque had been removed. Although the nozzle outlet diameter was 6
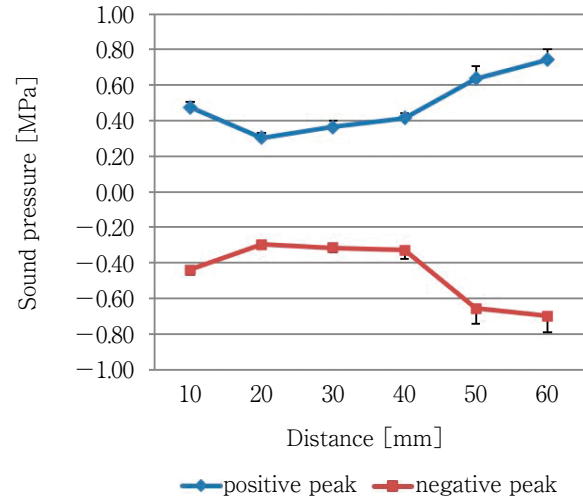

Fig. 6A　Axial position and sound pressure field measured in the water flow using a hydrophone
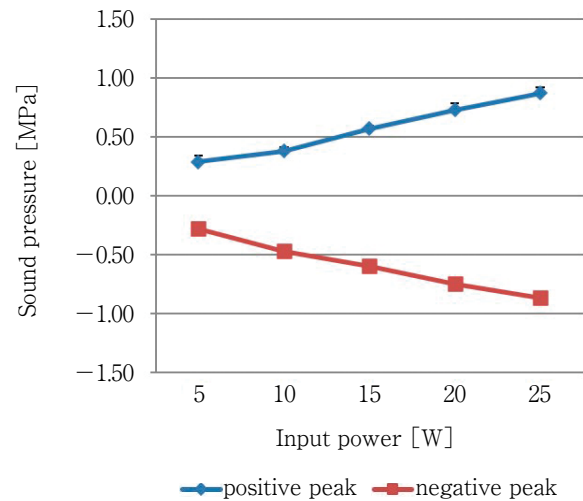

Fig. 6B　Sound pressure-input curves obtained by hydrophone

mm, the area cleaned by the UWF was considerably larger. Figure 7B shows the percentages of RAPs for various input powers. Water flow without ultrasonic waves was unable to remove any of the artificial plaque. As shown in Figure 7B, when the input setting was changed from 5 to 25 W, the RAP declined with an increase in the input power; for example, the RAP was 60% when the input power was 15 W. There was a negative correlation between the RAP rate and the input power. Based on these results, the device conditions used for evaluating the removal of dental biofilm were set as follows: the input power was 15 W and the
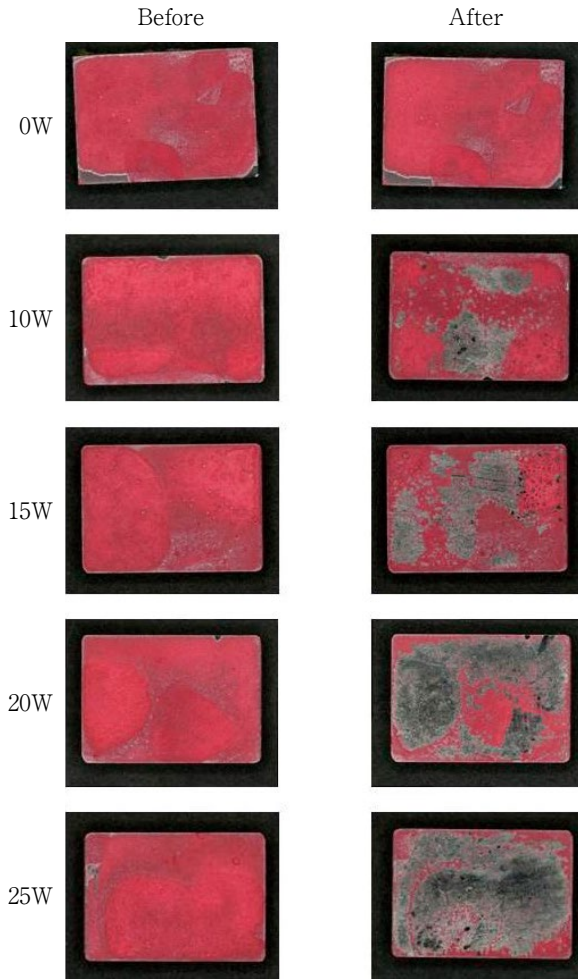
Before   After

0W

10W

15W

20W

25W

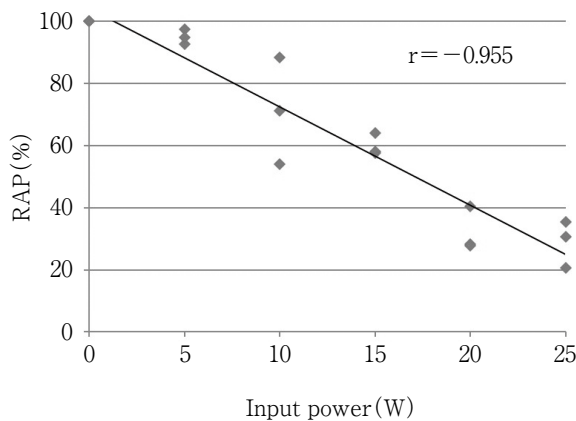**Fig. 7A**   Cleaning experiment for artificial plaque

Fig. 7B   Correlation of the RAP areas and input
            power

The cleaning effects of various input powers were investigated using artificial plaque on a titanium specimen. The input power to the ultrasonic transducer ranged from 5 to 25 W, and the washing time was 60 s. RAP declined with increase in the input power. There was a negative correlation between the RAP and the input power.

distance from the transducer to the specimen surface was 50 mm.

Figures 8A and 8B show optical images of the initial titanium surface. Both types of specimen (i.e., those with a mirror-finished surface and those with a rough surface) exhibited an erythrosine-stained plaque biofilm coverage of 100% after 72 hours of intraoral exposure (Figs. 8C and 8D). The titanium specimens were subjected to UWF under the abovementioned conditions, and digital microscopic photographs of each surface revealed the removal of plaque biofilm (Figs. 8E and 8F). Biofilm removal was observed after approximately 45 s from the initiation of UWF. Plaque removal was found to increase in a time-dependent manner for up to 180 s. All stained specimens were improved similar to that in the initial titanium surface.

The total RPBs after cleaning on the mirror-finished and rough surfaces were 22.8% (median) and 7.05% (median), respectively (Fig. 9). A significant decrease in RPB after the application of UWF was confirmed by comparison with the surfaces before treatment. Eight specimens were included in each group.

The clean titanium specimens showed a flat (Fig. 10A) or sharp-edged surface (Fig. 10B). The specimens exhibited a thick dental biofilm (Figs. 10C and 10D); in particular, the specimen with a rough surface was entirely coated (Fig. 10D). The plaque biofilm could not be removed by normal water flow treatment, and it remained intact with only a slight disturbance of the surface (Figs. 10E and 10F). However, the UWF treatment removed not only the plaque biofilm but also the water-insoluble glucans from both types of surface (Figs. 10G and 10H). The grooves and peaks on the rough titanium surface were visible after the UWF treatment (Fig. 10H). There were no alterations in the surfaces of the specimens treated by UWF.

Discussion

Sound pressure estimation based on input power
Regarding the estimation of sound pressure from the input power, sound pressure, p_{0-p}, is represented using the electric input power E (W) and the electromechanical coupling factor, η (%), as follows:

$$p_{0-p} = 1.4 \times \sqrt{\frac{E \times \eta^2}{S} \times \rho c} \cdots \cdots (1)$$

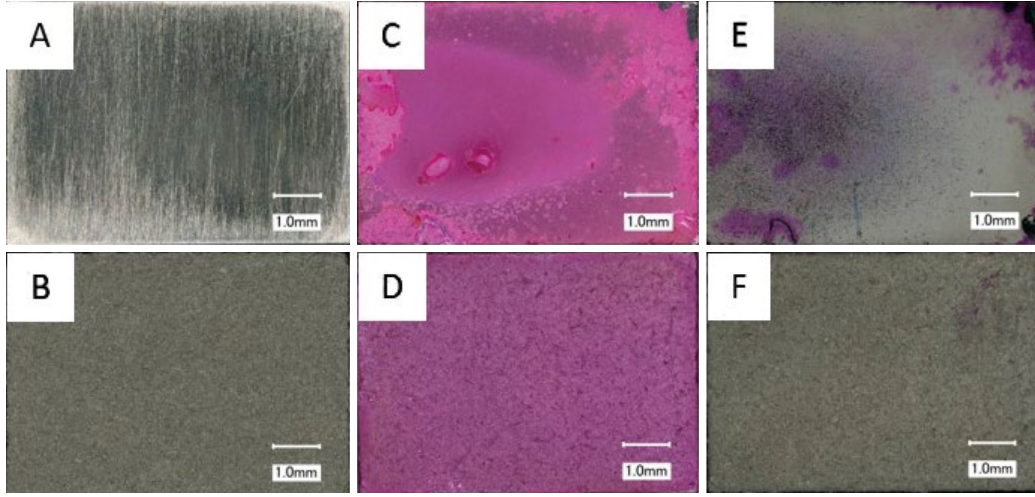where, S is the effective area of the transducer (m²),

Fig. 8　Optical images of plaque biofilm removal by the ultrasonic water flow
Control specimens of titanium with a mirror-finished surface（A）and a rough surface（B）.
Plaque biofilm formed on the titanium surfaces after 72 h（C, D）. Surfaces after treatment by
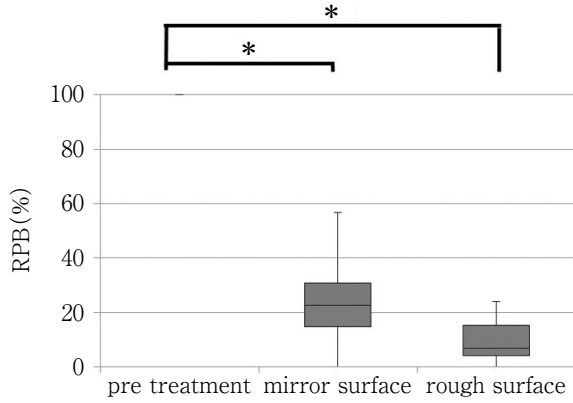ultrasonic water flow for 3 min（E, F）. Magnification：×100

Fig. 9　The RPB areas after ultrasonic water treatment of the specimens
　The total RPBs are 22.8%（median）and 7.05% （median）on the mirror-finished and rough surfaces, respectively. There is a significant decrease in the RPB when compared to its value before treatment for both the mirror-finished and rough surfaces.
＊：p＜0.05, Mann-Whitney U test（n＝8）.

$\rho = 1 \times 10^3 \text{kg/m}^3$ is the density of water, and $c = 1,500$ m/s is the speed of sound in water. If the effective diameter of the transducer is assumed to be 0.02 m and electromechanical coupling factor, η, is assumed to be 0.5, at the electric input power E＝15 W, we obtain

$$p_{0-p} = 1.4 \times \sqrt{\frac{3.75}{201 \times 10^{-6}} \times 1.5 \times 10^6}$$

$$= 0.236 \text{（MPa）} \cdots\cdots (2)$$

From Figure 4, if we assume that the sound pressure is around 2.5 times greater at the focal point, the sound pressure 0.23 MPa becomes 0.59 MPa at the focal point. The measured value was 0.6 MPa.

Therefore, the acceleration α associated with a frequency of 400 kHz is determined using equation（3）as follows:

$$\alpha = -2\pi f \frac{p_{0-p}}{\rho c} = -2\pi \times 400 \times 10^3 \times \frac{0.6 \times 10^6}{1.5 \times 10^6} =$$

$$-1.0 \times 10^6 (m/s^2) \cdots\cdots (3)$$

This value is approximately 100,000 times the gravitational acceleration g （＝9.8 m/s^2）.

The mechanism involved in ultrasonic cleaning in the MHz range is related to the magnitude of vibrational acceleration in the washing fluid[13]. We combined an ultrasonic cleaner at 400 kHz with flowing water to produce an UWF system that is capable of effectively removing dental biofilm from titanium surfaces. The enhanced cleaning effect of this setup may be due to the sound pressure derived from vibrational acceleration in the fluid.

In the simulation illustrated in Figure 3, a region of high sound pressure is observed at distances of ≥50 mm from the transducer, and the beam pattern of the high-frequency ultrasound has a narrow directivity angle, which is characteristic of high-frequency ultrasonic cleaners. In addition, the sound pressure measurements depicted in Figure 6 indicate that the sound
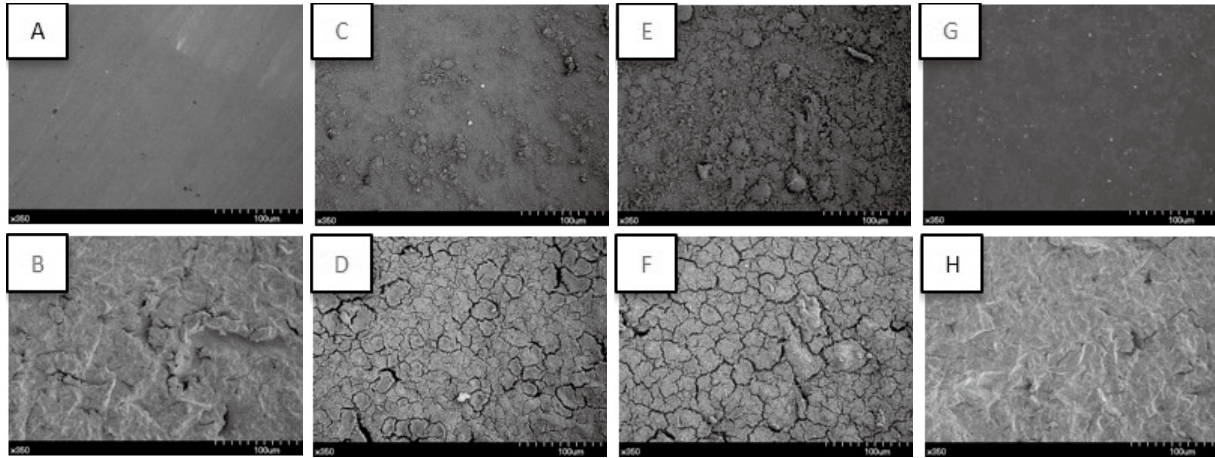
Fig. 10 SEM micrographs of plaque biofilm on titanium surfaces

Control specimens of titanium with a mirror-finished surface（A）and a rough surface（B）. Untreated titanium surfaces covered by dense bacterial biofilm（C, D）. Micro-structured titanium surfaces treated with a water jet demonstrating little or no disruption of the bacterial chain（E, F）. Titanium surfaces after exposure to ultrasonic water flow for 3 min, resulting in complete disruption of the bacterial chain and also removal of the water-insoluble glucans（G, H）.（Magnification：×350）

pressure reaches its maximum value at a distance of 50 mm from the transducer, and when the input power is set to 15 W, the sound pressure is also stable. This stable sound pressure could be measured in all directions if sufficient flowing water was obtained. Therefore, this suggests that the same effect can be expected in the human oral cavity. However, it is considered that a nozzle tip needs to be developed to transmit the ultrasonic energy of the flowing water to a narrow part of the oral cavity. Hence, these values were determined to be the optimal conditions for the experiment.

The efficiency of ultrasonic cleaning depends on the sizes of the particles to be removed and the frequency of the ultrasound. Low-frequency（~28–200 kHz）ultrasonic cleaners are suitable for removing particles with $\geq 10\,\mu m$ diameter, and high-frequency（~1 MHz）ultrasonic cleaners can easily remove much smaller particles measuring $\leq 0.3\,\mu m$ in diameter[14,21,22]. The 400-kHz ultrasonic cleaner used in this study is commonly applied to remove particles measuring ~0.2–5$\,\mu m$ in diameter, corresponding to the size of bacteria[23]. Furthermore, oral bacteria are electrostatically attached to the tooth or implant surfaces and can be removed by vibrational acceleration. Therefore, we suggest that a high-frequency or a midrange-frequency ultrasonic cleaner is most suitable for removing plaque biofilm. The use of UWF was effective in removing biofilm from titanium surfaces（Fig. 9）. This removal effect was

due to the vibrational acceleration of the washing fluid. It is thought that the vibrational acceleration and washing fluid exert a synergistic effect on the biofilm removal. The result of smaller RPB areas on UWF-treated rough surfaces may have been caused by ultrasonic waves propagating in the thread gap. In addition, the ultrasonic waves may have reflected off the uneven surface and effectively peeled off the biofilm.

SEM observations of both mirror-finished and rough surfaces showed that titanium surfaces covered by dental biofilm recovered almost to their original state in terms of both biofilm content and surface characteristics after the UWF treatment. The results also demonstrated that even the biofilm from the crests and troughs of threaded implants could be removed using the proposed cleaning system（Fig. 10）, whereas conventional devices such as hand scalers, toothbrushes, and ultrasonic scalers cannot reach such minute structures since the diameters of the working parts are generally too large.

In general, the damage caused by ultrasonic cleaners depends on their frequency, with higher frequencies causing greater damage. In this study, there were no changes to the titanium surfaces treated using the UWF system.

Cleaning procedures with conventional devices, which require contact with the dental implant, can increase the surface roughness of titanium, thereby

affecting microbial colonization and inducing the formation of plaque[10,11,24]. Our proposed technique avoids this disadvantage.

Therefore, the advantages of the UWF system can be summarized as follows: 1) it can remove dental biofilm from minute structures, 2) the use of a higher frequency in this system implies that there is less cavitation damage, and 3) it is a non-contact cleaning system that does not cause additional damage. However, a future task is to reduce the size of the UWF device and the amount of water as the ultrasonic transducer is large.

Conclusion

We demonstrated a novel UWF cleaning mechanism that can efficiently remove plaque biofilm without altering the characteristics of the titanium surface. In our experiment, titanium surfaces were exposed to UWF with a water flow rate of 300 ml/min, an ultrasonic frequency of 400 kHz, and an input power of 15 W (sound pressure of 0.6 MPa). The proposed UWF mechanism can be applied to devices for the maintenance of dental implants.

Conflict of Interest

The authors declare they have no financial interest, either directly or indirectly, in the products or information described in this article.

References

1) Costerton JW, Montanaro L, Arciola CR. Biofilm in implant infections: its production and regulation. Int J Artif Organs 2005; 28: 1062-1068.

2) Costerton JW, Montanaro L, Arciola CR. Bacterial communications in implant infections: a target for an intelligence war. Int J Artif Organs 2007; 30: 757-763.

3) Agerbaek MR, Lang NP, Persson GR. Comparisons of bacterial patterns present at implant and tooth sites in subjects on supportive periodontal therapy. Clin Oral Implants Res 2006; 17: 18-24.

4) Rams TE, Link CC Jr. Microbiology of failing dental implants in humans: electron microscopic observations. J Oral Implantol 1983; 11: 93-100.

5) Kalykakis GK, Mojon P, Nisengard R, Spiekermann H, Zafiropoulos GG. Clinical and microbial findings on osseo-integrated implants; comparisons between partially dentate and edentulous subjects. Eur J Prosthodont Restor Dent 1998; 6: 155-159.

6) Lindhe J, Meyle J, Group DoEWoP. Peri-implant diseases: Consensus Report of the Sixth European Workshop on Periodontology. J Clin Periodontol 2008; 35: 282-285.

7) Heitz-Mayfield LJ. Peri-implant diseases: diagnosis and risk indicators. J Clin Periodontol 2008; 35: 292-304.

8) Albouy JP, Abrahamsson I, Persson LG, Berglundh T. Implant surface characteristics influence the outcome of treatment of peri-implantitis: an experimental study in dogs. J Clin Periodontol 2011; 38: 58-64.

9) Claffey N, Clarke E, Polyzois I, Renvert S. Surgical treatment of peri-implantitis. J Clin Periodontol 2008; 35: 316-332.

10) Sato S, Kishida M, Ito K. The comparative effect of ultrasonic scalers on titanium surfaces: an in vitro study. J Periodontol 2004; 75: 1269-1273.

11) Baek SH, Shon WJ, Bae KS, Kum KY, Lee WC, Park YS. Evaluation of the safety and efficiency of novel metallic ultrasonic scaler tip on titanium surfaces. Clin Oral Implants Res 2012; 23: 1269-1274.

12) Morita K. Ultrasonic cleaning. Kindai Henshu, Tokyo 1989.

13) Kim JO, Choi S, Ho Kim J. Vibroacoustic characteristics of ultrasonic cleaners. Applied Acoustics 1999; 58: 211-228.

14) Mayer A, Shwartzman S. Megasonic cleaning: A new cleaning and drying system for use in semiconductor processing. J Electron Mate 1979; 8: 855-864.

15) Busnaina AA, Gale GW. Ultrasonic and megasonic particle removal. Proc Precis Clean 1995; 15: 347-359.

16) Hatano H, Kanai S. High-frequency ultrasonic cleaning tank utilizing oblique incidence. IEEE Trans Ultrason Ferroelectr Freq Control 1996; 43: 531-535.

17) Honda Keisuke. Ultrasonic cleaning device. U. S Patent 4,834, 124 May 30, 1989.

18) Ohtsuki S. Calculation method for the nearfield of a sound source with ring function. J Acoust Soc Jpn 1974; 30: 76-81.

19) Rimondini L, Fare S, Brambilla E, Felloni A, Consonni C, Brossa F, Carrassi A. The effect of surface roughness on early in vivo plaque colonization on titanium. J Peri-

odontol 1997; 68: 556-562.

20) Schwarz F, Sculean A, Romanos G, Herten M, Horn N, Scherbaum W, Becker J. Influence of different treatment approaches on the removal of early plaque biofilms and the viability of SAOS2 osteoblasts grown on titanium implants. Clin Oral Investig 2005; 9: 111-117.

21) Busnaina A, Taylor J, Kashkoush I. Measurement of the adhesion and removal forces of submicrometer particles on silicon substrates. J Adhes Sci Technol 1993; 7: 441-455.

22) Kashkoush I, Busnaina A. Submicron particle removal using ultrasonic cleaning. Particulate Science and Technology 1993; 11: 11-24.

23) Listgarten M. Structure of the microbial flora associated with periodontal health and disease in man: A light and electron microscopic study. J Periodontol 1976; 47: 1-18.

24) Shafagh I. Plaque accumulation on cast gold complete crowns polished by a conventional and an experimental method. J Prosthet Dent 1986; 55: 339-342.

Effect of Root Canal Transportation by Minimally Invasive Endodontic Shaping of Canal Orifice Dentin

Kazuyuki Tsubaki, Mai Utsunomiya, Kaori Shimojima,
Noriko Mutoh and Nobuyuki Tani-Ishii

Department of Pulp Biology and Endodontics, Kanagawa Dental University

Abstract

Background: The purpose of this study was to analyze the effect of minimally invasive (MI) shaping of canal orifice dentin by evaluating the shaping characteristics of TruNatomy (TN), which was developed as a Ni-Ti file capable of MI endodontics.

Methods: A J-shaped canal model was used to compare prepared final canal morphology using a minimally invasive shaping TN file and a conventional shaping ProTaper NEXT (PTN) file. The TN files used in the experiment were classified into two groups: no straight-line access (group A) and straight-line access (group B). The PTN files of the control were also classified into two groups: no straight-line access (group C) and straight-line access (group D), and the increase in canal width and the median displacement (transportation) were compared.

Results: Analysis of the canal width by TN showed that the displacement on the inner side increased by 5 mm in both groups A and B, but the displacement on the outer side increased at the other measurement sites. In groups C and D using PTN, the displacement on the inner side increased by 3–5 mm. On the other hand, the displacement on the outer side increased by 8 mm, and the displacement in group D increased. The canal transportation using TN was 0.1 mm or less in both groups A and B, although preparation by PTN showed significant transport to the inner side by 3–5 mm and outer side of 8 mm in group D compared to groups A and B.

Conclusion: TN shaping was shown to preserve tooth structure and canal geometry without straight-line access. It was confirmed that TN, which was developed based on the concept of MI Endo, enables accurate root canal shaping and reduces transportation.

Key words: canal transportation, shaping ability, straight-line access, TruNatomy, ProTaper NEXT

Introduction

It has been reported that endodontic treated teeth have a higher risk of fracture depending on the morphology and amount of residual tooth substance[1-3]. Seo et al.[4] reported that 79% of vertical root canal fractured teeth were endodontic treated teeth. Endodontic treated teeth and root canal fractures have been shown to be related to stress during root canal shaping[5]. Dentin cracks that occur during root canal shaping are thought to be the cause of vertical root canal fracture along with long-term disinfectant administration in the root canal and excessive vertical filling pressure during root canal obturation[6].

In recent years, minimally invasive endodontics (MI Endo) has been advocated, and root canal shaping by minimal dentin removal that preserves the dentin on the canal orifice reduces root canal fracture[7, 8]. In the basic process of canal shaping, straight-line access is one of the most important procedures and is a prerequisite step for shaping and obturation[9-11]. The removal of infected dentin at the canal orifice by straight-line access and reduction of the degree of root canal curvature facilitate accurate root canal shaping. However, straight-line access has been reported to be associated with excessive shaping of the orifice dentin, reducing both dentin stiffness and fracture resistance[12, 13]. It has been reported that preservation of orifice dentin of the upper one-third of the root canal is more important than preservation of crown occlusal surface dentin to prevent root canal fracture[14, 15]. It has also been reported that contouring of the access cavity by MI Endo is related to the structural maintenance of the crown dentin, but the relationship between minimally invasive access to the cervical dentin and the fracture resistance of the root is controversial[16-18]. However, root canal shaping by MI Endo of orifice dentin is reported to maintain high fracture resistance compared to root canal shaping by straight-line access[19].

Currently, MI Endo[20] is being used mainly on the west coast of the United States in order to prevent root canal fracture, unlike the conventional root canal preparation method. MI Endo aims to maximally preserve dentin and also influences caries diagnosis, treatment choices, access cavity design, and root canal or restoration choices[21, 22]. The access cavity is considered to

be a prerequisite for improving the prognosis of endodontic treatment because it enables apical closure by proper root canal filling by maintaining the apical root canal morphology during root canal preparation[23]. However, next-generation Ni-Ti files, microscopy, and cone-beam computed tomography enable dentists to make access cavities as minimally invasive as possible and maintain the dentin structure of the tooth being treated.

The TruNatomy (TN; Dentsply Sirona, Ballaigues, Switzerland) file was designed based on the concept of MI Endo and was developed to enable accurate root canal shaping without straight-line access, and rotates at high speed. It is a unique thin Ni-Ti wire with a maximum flute diameter of 0.8 mm instead of 1.2 mm, which is commonly used in other Ni-Ti files. Also, it has a regression taper and an off-centered parallelogram cross section in the file system as used by Peters et al.[24]. The TN file consists of a file system designed according to the conventional ProTaper NEXT (PTN, Dentsply Sirona) file. Since the PTN file[25] is used based on the conventional root canal shaping concept that requires straight-line access, it can be compared with the minimally invasive shaping TN file as a control for this study. The physical characteristics of PTN files have been reported to be extremely flexible[26, 27]. Similar to PTN, the TN file is constructed with a cross-sectional form in which the file cutting surface is off-centered, but the characteristics of the alloy are different. Although the tapers of both TN and PTN files are variable, both have a 6% taper for the apical 3 mm. In addition, the file system has a similar format, but the PTN file tip sizes are X1 (#17), X2 (#25), and X3 (#30), while the TN file tip sizes are Small (#20), Prime (#26), and Medium (#36). Both file systems are usually designed to complete root canal shaping with two files: X1 and X2 for PTN, Small for TN, and Prime for cases of pulpectomy in the root canal.

The purpose of this study was to evaluate the characteristics of canal preparation by TN based on the MI Endo concept. For the evaluation, root canals were prepared using a minimally invasive cutting type TN and a conventional cutting type PTN, and the total amount of removed root canal wall and the canal transportation were measured and compared. The results clarified the relationship between straight-line access during root canal preparation and final canal morphology.

Materials and Methods

1．Operator and test canal model

The canal preparation was performed by a single operator (specialist of JEA and JCD) using Ni-Ti (PTN) files in strict accordance with the manufacturer's recommendations for each system.

For the experiment, a total of 40 J-type root canal models (curvature 30°, apex diameter #15, taper 02, canal length 16.5 mm: End Training block canals, Dentsply Sirona) made by epoxy resin were used. All root canal models were attached to the Endo Training Model Castillo (VDW, Frankfurt, Germany), and root canal preparation was performed in a situation where the root canal morphology could not be confirmed.

2．Root canal preparation

To analyze the effect of straight-line access on the final canal morphology after root canal preparation, TN and PTN files were compared. The TN files used in the experiment were classified into two groups: no straight-line access (group A) and straight-line access (group B). The PTN files of the control were also classified into two groups: no straight-line access (group C) and straight-line access (group D), and the increase in root canal width and the canal transportation were compared. In each experimental group, the PTN Access Opener XA of the PTN file system was used for the straight-line access group, and the Orifice 5 (OM) of the TN file system was used for the no straight-line group to enlarge the root canal orifice.

In each experimental group, the final preparation morphology was set to TN Prime (file tip diameter #26/average taper 04 (Variable: V): ISO #26/04V) and PTN file X2 (ISO #25/06). Figure 1 shows the dimensions of the TN and PTN files, and Table 1 shows the files used up to the root canal preparation in each experimental group.

For root canal preparation by TN in the experimental group, after confirming penetration to the apex with a stainless-steel K file #10 (Dentsply Sirona) before the start of root canal preparation, straight-line access was made using Orifice Modifier 20/08 to shape the canal orifice. The experimental TN group was classified into no straight-line group A using Orifice Modifier 20/08 for the root canal orifice opening, and straight-line group B using TN Access Opener XA. Then, a glide
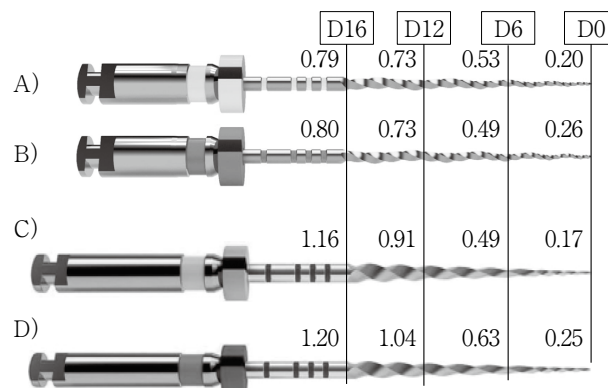

Fig. 1　The dimensions of TN (A：Small 20/04 V, B：Prime 26/04 V) and PTN (C：X1 17/04, D：X2 25/06) files

path was formed by TN Glider. Root canal preparation by TN was shaped using X Smart plus (Dentsply Sirona) by the following procedure. For root canal preparation, shaping was performed with TN Small (20/04V), then TN Prime (26/04V), with both files set to 500 rpm and 1.5 Ncm, and three vertical movement operations were performed. The working length was reached in 3 cycles as 1 cycle, then root canal preparation was completed by cleaning the root canal with 2 ml of distilled water (DW) at the end of each cycle.

In the control group using PTN, penetration to the apex with K file #10 was confirmed before the start of root canal preparation. After confirmation of penetration, the group was classified into no straight-line group C using Orifice Modifier 20/08, and straight-line group D using PTN Access Opener XA. Then, a glide path was formed in the TN Glider group (n=20). Root canal formation by PTN was performed using X Smart plus by the following procedure. For root canal preparation by PTN, two X1 (17/04) and X2 (25/06) files were used, with both files set to 300 rpm and 2.0 Ncm. The first X1 and second X2 files were penetrated to the working length three times, then root canal preparation was completed by cleaning the root canal with 2 ml of DW at the end of each cycle.

3．Evaluation of root canal morphology

The amount of root canal morphological displacement was analyzed by measuring the total amount of removed root canal wall on the outer and inner sides of the curved root canal. A stereoscopic microscope (SZX16; Olympus, Tokyo, Japan) and a digital camera (DP71; Olympus) were used for measurement, transpar-

Table 1 The files used up to root canal preparation in each experimental group

Experimental Group	Ni-Ti file system Straight-line (＋/－)	Scout	Orifice open	Glide path	Preparation Start file	Preparation Final file
A	TruNatomy Straight-line (－)	#10	O. Modifier 20/08	Glider 17/02 V	Small 20/04 V	Prime 26/04 V
B	TruNatomy Straight-line (＋)	#10	A. Opener XA	Glider 17/02 V	Small 20/04 V	Prime 26/04 V
C	ProTaper NEXT Straight-line (－)	#10	O. Modifier 20/08	Glider 17/02 V	X1 17/04	X2 25/06
D	ProTaper NEXT Straight-line (＋)	#10	A. Opener XA	Glider 17/02 V	X1 17/04	X2 25/06
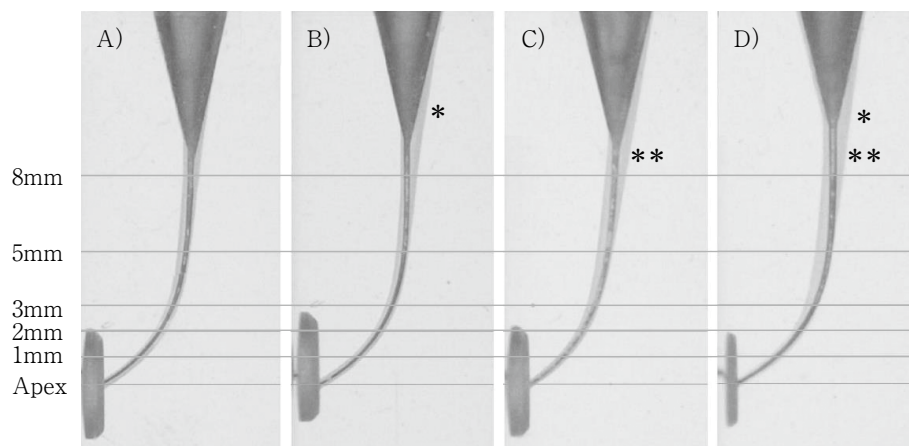
Fig. 2 Superimposition of pre- and post-preparation images
TN no straight-line group (A), TN straight-line group (B), PTN no straight-line group (C), and PTN straight-line group (D). ＊：Straight-line access, ＊＊：Final preparation by PTN X2 file.

ent root canal models pre- and post-preparation were superimposed on digital images, and the obtained image data was captured on a PC for measurement. Measurements were performed using software (WinRoof; Tokyo, Japan) (Fig. 2). To measure the amount of root canal wall shaping in the root canal model, the positions were set at 1, 2, 3, 5, and 8 mm from the apex as the measuring unit, and the root canal width was increased on each of the outer and inner canal sides. The distance from the root canal wall of pre- to post-preparation and the median root canal value as canal transportation were measured and statistically processed.

4．Statistical processing

The measured values of root canal wall cutting were statistically processed with a risk factor of 5% using one-way ANOVA, Bonferroni-Dunn multiple comparison test, and Mann-Whitney U test (comparative analysis between two groups).

Results

The root canal morphology in post-preparation was evaluated by measuring the increase in root canal width and the median displacement on the inner and outer sides at positions 1, 2, 3, 5, and 8 mm from the apex. Comparing the prepared canal morphology (Fig. 2) of the canal models in pre- and post-root preparation of groups A, B, C, and D, flare formation on the canal orifice was not observed in group A without straight-line access. However, in group C in which straight-line access was not formed, flare formation on the canal orifice was observed similar to that in groups B and D in which straight-line access was formed. Furthermore, in group D with straight-line access, an increasing ten-
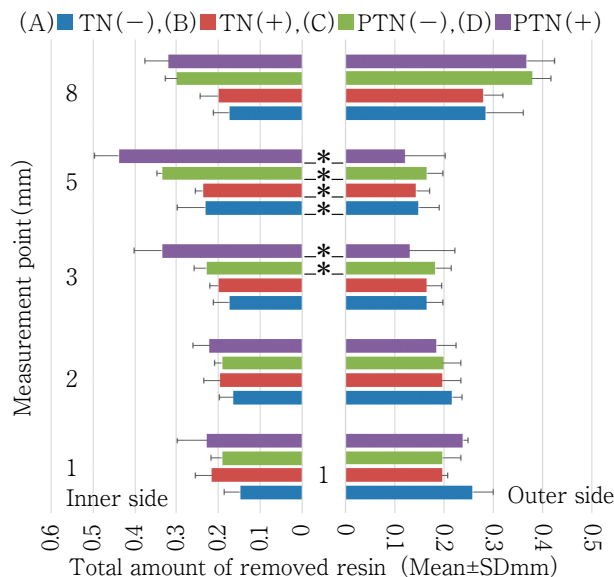
(A)■TN(−),(B)■TN(+),(C)■PTN(−),(D)■PTN(+)

Fig. 3 Total amount of removed canal wall (mm) at the different levels in post-preparation

TN no straight-line group (A), TN straight-line group (B), PTN no straight-line group (C), and PTN straight-line group (D). ＊：Significant difference (p＜0.05).

(A)■TN(−),(B)■TN(+),(C)■PTN(−),(D)■PTN(+)

Fig. 4 Canal transportation at different levels from apex in post-preparation

TN no straight-line group (A), TN straight-line group (B), PTN no straight-line group (C), and PTN straight-line group (D). ＊：Significant difference (p＜0.05) between TN (A, B) and PTN (D).

dency was observed in the amount of cutting on the inner side at the start position of the curve of 3-5 mm.

The results of measuring the total amount of removed root canal wall are shown in Fig. 3 and canal transportation is shown in Fig. 4 for all experimental groups.

According to the results of analyzing the increase in total amount of root canal wall removed by TN, the displacement on the inner side increased at the measurement site by 5 mm at the start position of root canal curvature in both groups A and B, but the displacement on the outer side increased at other measurement sites. On the other hand, in both groups C and D, the displacement on the inner side at the measurement site increased by 3-5 mm, on the outer side by 8 mm, and the displacement of group D increased in particular (Fig. 3).

The median displacement as canal transportation by TN was 0.1 mm or less at all measurement sites in both groups A and B. The median displacement by PTN was significant: 3-5 mm to the inner side at the measurement site in group D compared to groups A and B, and 8 mm to the outer side. On the other hand, the median displacement of group C was not significantly different from that of groups A and B (Fig. 4).
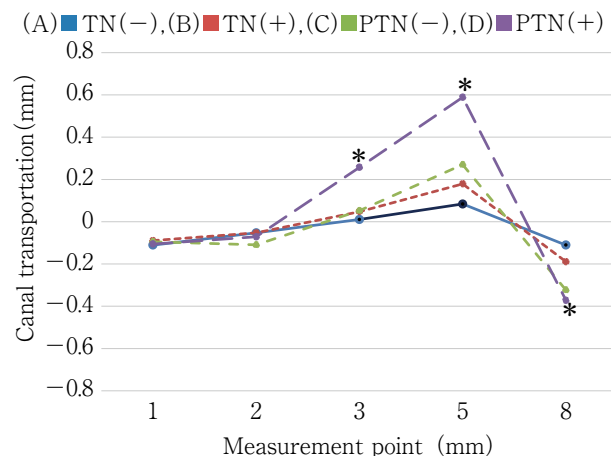
Discussion

Regarding endodontic treated teeth, it has been suggested that the treatment process itself such as access cavity preparation and root canal enlargement has a risk of causing root canal fracture, and in particular, a relationship between the distribution of occlusal stress and root canal fracture has been reported[28]. To reduce the risk of root canal fracture, the concept of MI Endo with minimal access cavity and root canal preparation using Ni-Ti files is recommended. It is essential to negotiate the root canal using a K file at the start of root canal preparation, to obtain anatomical root canal information such as curvature, calcification, apical foramen diameter, and root canal length. Furthermore, when preparing curved root canals, removal of the orifice dentin ridge is considered to be the most important step, facilitating file insertion to the apical foramen. That is, the removal of dentin ridges by straight-line access and the establishment of glide paths have been regarded as essential techniques for the safe use of Ni-Ti files.

On the other hand, it has been reported that straight-line access, which has been considered the basis of root canal preparation, reduces fracture resistance and causes root canal fracture due to excessive cutting of orifice dentin. Endodontic treated teeth have high

stress concentration in the cervical region[29, 30], and excessive cutting of orifice dentin is considered to be a factor that increases the susceptibility to fracture[31]. These study reports have shown that minimizing flare formation due to straight-line access may reduce the risk of cervical fracture. In addition, a straight-line access unformed root canal causes stress dispersion in the orifice dentin when normal stress is applied to the occlusal surface, whereas the straight-line access formed root canal concentrates stress and has weak fracture resistance[19]. The results showed that endodontic treated teeth using MI Endo were less susceptible to cervical fracture. Previous studies have suggested that the preservation of orifice dentin may be correlated with long-term maintenance of occlusal function in endodontic treated teeth[14, 15].

Previous research reports have discussed the need for straight-line access in root canal preparation. For straight-line access unformed root canals, it is likely to be difficult to limit the operation of instruments and directly reach a direct view due to the reduction of the surgical field at the start of root canal preparation. Inadequate morphological following ability may result. The present study analyzed the relationship between the final canal morphology by Ni-Ti preparation and straight-line access, and accurate root canal preparation was possible even with MI Endo, which reduces the risk of root canal fracture. The 30° curvature of the curved root canal model used in this study was selected because it is easy to obtain the effect of reduced curvature due to straight-line access.

Furthermore, the TN used in this study was developed with the concept of MI Endo, which maintains a high occlusal strength of endodontic treated teeth by forming a root canal with minimally invasive shaping. The results showed that TN enables proper root canal preparation without straight-line access. The increase in root canal width and the median displacement in TN canal preparation were measured. Even when comparing the no straight-line access group (A) and the straight-line access group (B), no significant difference was observed between the increase in root canal width and the median displacement using TN. Accurate canal preparation was shown to require no straight-line access.

On the other hand, a comparison of the PTN with the no straight-line access group (C) and the straight-line access group (D) revealed interesting results. The increase in root canal width and the median displacement in the group without PTN straight-line access (C) showed the same amount of displacement of 1–3 mm at the apex as in groups A and B by TN. Furthermore, the displacement by TN in groups A and B increased by 5 mm only on the inner side and by 8 mm on the outer side, but no significant difference was observed, and straight-line access was not formed even in root canal preparation by PTN. It was shown that proper root canal preparation is possible. Since the PTN X2 file has a large taper, flare of the upper one-third of the root canal is formed even in the no straight-line access group (C) when using X2, similar to the straight-line access formation, at the apex. It was also shown that accurate root canal preparation was possible.

In addition, at 1–2 mm on the apical side, accurate root canal preparation was possible in both the TN and PTN groups regardless of the presence or absence of straight-line access, and the median root canal value was also the same.

This result shows that both TN and PTN files have a 6% taper up to 3 mm on the apical side, TN (apical 0, 1, 2, 3 mm = #26, #32, #38, #44) and PTN (apical 0, 1, 2, 3 mm = #25, #31, #37, #43). The fact that the file diameters were the same may have had an effect. On the other hand, the displacement on the inner side of 3, 5 and 8 mm significantly increased, showing a tendency of straightening on the inner side of the curved root canal in the PTN straight-line access group (D). This result is considered to be due to the difference in flexibility and file taper (4 mm or more from the apex) between the PTN file and the TN file. Peters et al. reported that TN was more fatigue resistant and showed significantly more predictable torque and threading-in force compared with PTN[24].

It was shown that root canal preparation by PTN that formed the straight-line access, which was considered to be essential for maintaining the anatomical root canal morphology, straightened the curved root canal on the inner side.

The PTN has two files, X1 and X2, which can obtain the final root canal morphology that enables sufficient root canal cleaning and root canal filling, and at the same time, the elasticity of the file itself is improved. The files are easy to use and are expected to reduce accidents, and are used clinically. The PTN files are

characterized by having a rectangular cross section and always cutting at only two points in contact with the root canal wall in order to reduce the bite into the wall. Therefore, PTN is the most frequently used file system in Europe and the United States because there are few accidents during root canal preparation and accurate root canal preparation is possible even in curved root canals. The TN file system was constructed with a similar system based on PTN, and was designed to have a final root canal morphology that can be filled with root canals using two files, Small and Prime. However, since there is no straight-line access, the root canal following ability of the apical curved root canal may be inadequate due to the restricted instrument operation in the limited field. The results of this study showed that there is no need for straight-line access, which has been considered essential for accurate root canal preparation. Insufficient flare preparation in the upper part of the root canal when straight-line access is not formed suggests the difficulty of root canal cleaning and the effect of insufficient pressurization of root canal obturation. However, for root canal preparation by minimally invasive shaping type TN, it is recommended to use a dedicated needle with an improved tip for root canal cleaning and pressure root canal obturation or single-point root canal obturation with a dedicated gutter core by root canal obturation. In recent years, a bioceramic sealer has been developed for root canal obturation, and has been reported to have excellent biological properties such as hard tissue forming ability in addition to biocompatibility and non-cytotoxicity[32]. In particular, bioceramic sealers are expected to have a higher tight-sealing chain than other sealers by forming hard tissue at the dentin interface and apical foramen. Currently, the root canal obturation method uses multiple chemically and physically stable gutta-percha cones to tightly seal the root canal by lateral and vertical obturation with heated gutta-percha. The obturation method has been established and good clinical results have been reported. However, the single-point root canal filling method[33] using a bioceramic sealer capable of root canal preparation and hard tissue formation, which reduces the risk of root canal fracture due to minimally invasive cutting type TN, will follow the flow of endodontic treatment in the future. The possibility of shifting to MI Endo was shown.

Conclusion

Root canal preparation by TN was shown to maintain the original anatomical root canal morphology without straight-line access. The minimally invasive shaping type TN developed based on the concept of MI Endo enables accurate root canal preparation and reduces the amount of root canal displacement after root canal preparation due to the shape and flexibility of the file.

References

1) Fransson H, Dawson VS, Frisk F, Bjørndal L, EndoReCo O, Kvist T. Survival of root-filled teeth in the Swedish adult population. J Endod 2016; 42: 216–220.

2) Aquilino SA, Caplan DJ. Relationship between crown placement and the survival of endodontically treated teeth. J Prosthet Dent 2002; 87: 256–263.

3) Pratt I, Aminoshariae A, Montagnese TA, Williams KA, Khalighinejad N, Mickel A. Eight-year retrospective study of the critical time lapse between root canal completion and crown placement: its influence on the survival of endodontically treated teeth. J Endod 2016; 42: 1598–1603.

4) Seo DG, Yi YA, Shin SJ, Park JW. Analysis of factors associated with cracked teeth. J Endod 2012; 38: 288–292.

5) Liu R, Kaiwar A, Shemesh H, Wesselink PR, Hou B, Wu MK. Incidence of apical root cracks and apical dentinal detachments after canal preparation with hand and rotary files at different instrumentation lengths. J Endod 2013; 39: 129–132.

6) Fain WD. Tooth fractures and cracks. J Am Dent Assoc 2021; 152: 423–424.

7) Krishan R, Paqué F, Ossareh A, Kishen A, Dao T, Friedman S. Impacts of conservative endodontic cavity on root canal instrumentation efficacy and resistance to fracture assessed in incisors, premolars, and molars. J Endod 2014; 40: 1160–1166.

8) Moore B, Verdelis K, Kishen A, Dao T, Friedman S. Impacts of contracted endodontic cavities on instrumentation efficacy and biomechanical responses in max-

illary molars. J Endod 2016; 42: 1779–1783.

9) Goerig AC, Michelich RJ, Schultz HH. Instrumentation of root canals in molars using the step-down technique. J Endod 1982; 8: 550–554.

10) Swindle RB, Neaverth EJ, Pantera EA Jr, Ringle RD. Effect of coronal-radicular flaring on apical transportation. J Endod 1991; 17: 147–149.

11) Torabinejad M. Passive step-back technique. Oral Surg Oral Med Oral Pathol 1994; 77: 398–401.

12) Lang H, Korkmaz Y, Schneider K, Raab WH. Impact of endodontic treatments on the rigidity of the root. J Dent Res 2006; 85: 364–368.

13) Tang W, Wu Y, Smales RJ. Identifying and reducing risks for potential fractures in endodontically treated teeth. J Endod 2010; 36: 609–617.

14) Pierrisnard L, Bohino F, Renault P, Barquins M. Corono-radicular reconstruction of pulpless teeth: a mechanical study using finite element analysis. J Prosthet Dent 2002; 88: 442–448.

15) Clark D, Khademi JA. Case studies in modern molarendodontic access and directed dentin conservation. Dent Clin North Am 2010; 54: 275–289.

16) Tang W, Wu Y, Smales RJ. Identifying and reducing risks for potential fractures in endodontically treated teeth. J Endod 2010; 36: 609–617.

17) Reeh ES, Messer HH, Douglas WH. Reduction in tooth stiffness as a result of endodontic and restorative procedures. J Endod 1989; 15: 512–516.

18) Pradeep P, Kumar VS, Bantwal SR, Gulati GS. Fracture strength of endodontically treated premolars: an in-vitro evaluation. J Int Oral Health 2013; 5: 9–17.

19) Yuan K, Niu C, Xie Q, Jiang W, Gao L, Huang Z, Ma R. Comparative evaluation of the impact of minimally invasive preparation vs. conventional straight-line preparation on tooth biomechanics: a finite element analysis. Eur J Oral Sci 2016; 124: 591–596.

20) Burllein S, Schafer E. Minimally invasive endodontics. Quintessence Int 2015; 46: 119–124.

21) Murdoch-Kinch CA, Mclean ME. Minimally invasive dentistry. J Am Dent Assoc 2003; 134: 87–95.

22) Gutamann JL. Minimally invasive dentistry (Endodontics). J Conserv Dent 2013; 16: 282–283.

23) Kenneth MH, Stephen C. Cohen's pathways of the pulp.

10th ed. St. Louis: Elsevier, 2011; 137–138.

24) Peters OA, Arias A, Choi A. Mechanical properties of a novel nickel-titanium root canal instrument: Stationary and dynamic tests. J Endod 2020; 46: 994–1001.

25) Arias A, Singh R, Peters OA. Torque and force induced by ProTaper Universal and ProTaper Next during shaping of large and small root canals in extracted teeth. J Endod 2014; 40: 973–976.

26) Nguyen HH, Fong H, Paranjpe A, Flake NM, Jonson JD, Peters OA. Evaluation of the resistance to cyclic fatigue among ProTaper Next, ProTaper Universal, and Vortex Blue rotary instruments. J Endod 2014; 40: 1190–1193.

27) Shim KS, Oh S, Kum K, Kim YC, Jee KK, Chang SW. Mechanical and metallurgical properties of various nickel-titanium rotary instruments. Biomed Res Int 2017; 2017: 4528601 doi: 10.1155/2017/4528601

28) Chen G, Fan W, Mishra S, El-Atem A, Schuetz MA, Xiao Y. Tooth fracture risk analysis based on a new finite element dental structure models using micro-CT data. Comput Biol Med 2012; 42: 957–963.

29) Al-Omiri MK, Rayyan MR, Abu-Hammad O. Stress analysis of endodontically treated teeth restored with post-retained crowns: a finite element analysis study. J Am Dent Assoc 2011; 142: 289–300.

30) Belli S, Eraslan O, Eraslan O, Eskitascioglu G. Effect of restoration technique on stress distribution in roots with flared canals: an FEA study. J Adhes Dent 2014; 16: 185–191.

31) Sathorn C, Palamara JE, Palamara D, Messer HH. Effect of root canal size and external root surface morphology on fracture susceptibility and pattern: a finite element analysis. J Endod 2005; 31: 288–292.

32) Sanz JL, Rodríguez-Lozano FJ, Llena C, Sauro S, Forner L. Bioactivity of bioceramic materials used in the dentin-pulp complex therapy: A systematic review. Materials 2019; 12: 1015. doi: 10.3390/ma12071015

33) Yu YH, Kushnir L, Kohli M, Karabucak B. Comparing the incidence of postoperative pain after root canal filling with warm vertical obturation with resin-based sealer and sealer-based obturation with calcium silicate-based sealer: a prospective clinical trial. Clin Oral Investig 2021; 25: 5033–5042.

Original Article

Study on Evaluation of Cavity Preparation Using Non-contact High-speed 3-D Shape Measuring Device

Saeko Okumura, Hiroaki Tanimoto, Kenzo Yasuo, Naohiro Iwata, Kazushi Yoshikawa and Kazuyo Yamamoto

Department of Operative Dentistry, Osaka Dental University

Abstract

Introduction: In dental education, it has long been essential to master cavity preparation techniques by training with models, both during basic and clinical training before college graduation as well as during clinical practice as dentists. However, the instruction given is subjective depending on the instructor, with variations in instruction contents and evaluations, and it has long been pointed that quantification is difficult. Effective and efficient education and instruction as well as reproducible and objective evaluations are essential. Therefore, this study examined the objective evaluation and grading of Class II metal inlay cavity by a computer system using a non-contact high-speed 3-D shape measuring device.

Subjects and methods: Ten dental residents at the Department of Operative Dentistry, Osaka Dental University Hospital were recruited as subjects. A jaw model containing an artificial tooth for training was used to conduct cavity preparation for a mesial Class II metal inlay on the mandibular right first molar tooth within 30 minutes. After preparation, an evaluation was conducted by this system and by nine instructors at the Department of Operative Dentistry with 7 to 28 years of clinical experience. A free description column for the evaluation and instruction items was provided as part of the evaluation by instructors. Feedback was given based on the results, and a total of five sessions of cavity preparation were conducted at two-month intervals. Pearson's correlation coefficient was used in the correlation analysis of the evaluation results.

Results: Reanalysis was conducted by excluding the seven points which had the largest deductions in the evaluation using the measuring device. As a consequence, a significant positive correlation with the number of preparations was observed. There was also a significant positive correlation with the evaluation by instructors. A comparison of the evaluations by the measuring device and by the instructors showed a significant positive correlation.

Conclusion: The measuring device can consistently and objectively evaluate Class II metal inlay cavity preparation equivalent to evaluations by multiple instructors with long clinical experience. It was also shown that a curriculum using evaluations by the measuring device and instructors effectively improved the skills of the dental residents. Incorporating evaluation by the measuring device may be an effective method for reducing the burden on instructors and length of the instruction period.

Key words: objective evaluation, cavity preparation, dental education

Introduction

In the field of dental education, it has long been essential for students to master tooth-cutting techniques. In particular, the technique used to prepare a cavity for metal inlay, which is an indirect repair method, greatly affects the prognosis after treatment. Conventionally, students learn the basic skills of metal inlay cavity preparation by repeatedly training using mannequins and jaw models during undergraduate basic and clinical training before college graduation as well as during clinical practice as residents. At present, there are no other methods of evaluation or instruction; both of these approaches are subjective, depending on the instructor or medical advisor. An instructor with experience and skills who has mastered cavity preparation techniques is thus required for evaluation and instruction. However, students often become confused due to differences in the instructions given by each instructor, as well as variations in contents and evaluations. In addition, providing instruction in the clinical field requires much time and effort, sometimes resulting in failure to provide sufficient instruction[1].

Cavity preparation techniques are often evaluated based on subjective observation of outline and depth of the cavity by the instructor. Even the same instructor may sometimes give different evaluation results[2–5] since quantification is difficult[6], and the lack of objectivity in evaluation methods has been pointed out in the past[6,7]. Some have reported that effective and efficient education and instruction as well as reproducible evaluations are essential[2,3,8–10]. In addition, with the use of 3-D shape measuring devices, it is now possible to measure the data on cavity preparation in a short period[1,11,12].

This study examined the consistency of objective evaluations by instructors by using a computer system featuring non-contact high-speed 3-D shape measurement to perform objective evaluations and grading. The usefulness and practicality of a curriculum using this system was also examined.

Subjects and Methods

1．Subjects

The subjects were ten dental residents undergoing clinical training at the Department of Operative Den-

tistry, Osaka Dental University Hospital, which is a controlled postgraduate education institution.

2．Methods

A jaw model (D16FE-500H (GSF)-MF, Nissin Dental Products Inc, Kyoto), in which an artificial tooth for training (A5SA-500#46, Nissin Dental Products Inc.) with special processing on melamine was inserted as the mandibular right first molar tooth, was attached to the simulator (DR-H Ni: MO, Nissin Dental Products Inc.) (Figs. 1 and 2). The task was to form a mesial Class Ⅱ metal inlay cavity (within 30 minutes). A period of two minutes to visually observe the example tooth (Fig. 3) was given, and the subjects were not allowed to check the example during cavity preparation. As cutting tools, diamond burs (#401, #301, #F215, #201, SHOFU Inc, Kyoto), and steel burs (UA, No. 701, No. 702, No. 703 Steel, Beldenta Supply Inc, Switzerland) were used (Fig. 4). The formed cavity was measured and evaluated with the 3-D shape measuring device (hereafter, "evaluation by measuring device"), and was evaluated by nine instructors belonging to the Department of Operative Dentistry with 7 to 28 years of clinical experience (hereafter, "evaluation by instructors"). A column for free description on evaluation and instruction items was provided as part of the evaluation by instructors (Table 1). Feedback was given to each student based on the results after evaluation. Cavity preparation was conducted at two-month intervals in the curriculum, with a total of five cavity preparation sessions, followed by measurement, evaluation, grading and feedback. Informed consent was orally given to participants in the research and the freedom to refuse participation was guaranteed. Pearson's correlation coefficient was used in the correlation analysis between the evaluation by measuring device and the evaluation by instructors.

3．Grading evaluation methods

1）Cavity preparation evaluation system and measurement principle

The system used in this study consisted of a 3-D shape measuring device (J. Morita Mfg. Corp, Kyoto; hereafter, "SURFLACER") (Figs. 5 and 6), a personal computer (Latitude E5430, DELL, Tokyo) equipped with the measuring device control software and cavity preparation skill evaluation software, and a printer (LP-S520, EPSON, Tokyo)[1]. The system measured the formed cavity using SURFLACER. It superimposed the
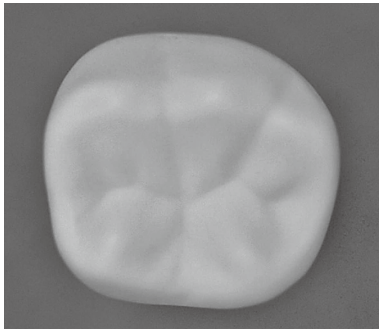
Fig. 1 Artificial tooth for training
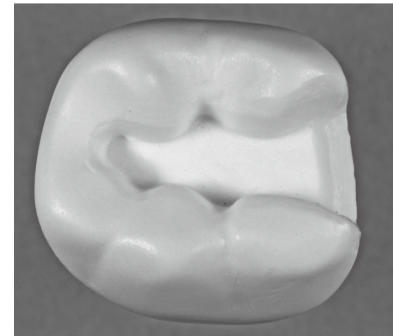

Fig. 2 Simulator, jaw model

Fig. 3 Example tooth

Fig. 4 Burs that were used

example tooth cavity shape data that was registered in advance and the shape data for the formed cavity, and executed evaluation and grading on the computer using the different date.

The principle of measurement was as follows. The laser was irradiated on the formed tooth attached to the special jig and the slit light of the laser was received by two CMOS cameras. The 3-D coordinate values on the specimen were obtained by triangulation measurement using the slit-ray projection method. Computer calculations were made based on these 3-D data to convert them into an image[1,13]. The basic triangulation measurement principle using the slit-ray projection method is shown in Fig. 7. The optical axis of the laser projection part was positioned at angle θ to the optical axis of the CMOS camera detection part. Since image formation point P' on the horizontal image of the CMOS camera changes when the position of the intersection point P moves from camera center O, it is possible to calculate height Z（height of actual object）as displacement Z from the camera center by reading the position of image point P'.

Table 1 Instructor evaluation items and allocation of points

Cavity outline	Allocation of points
1．Size（width）of the cavity outline	
□ Too large（too wide）	10
□ Rather large（wide）	20
□ Appropriate	35
□ Rather small（narrow）	25
□ Too small（too narrow）	15
2．Is the cusp ridge retained?	
□ Retained	30
□ Somewhat retained	25
□ Difficult to say	18
□ Retention rather failed	12
□ Not retained	5
3．Does the cavity outline include the pit and fissure?	
□ Included	30
□ Somewhat included	25
□ Difficult to say	18
□ Rather not included	12
□ Not included	5

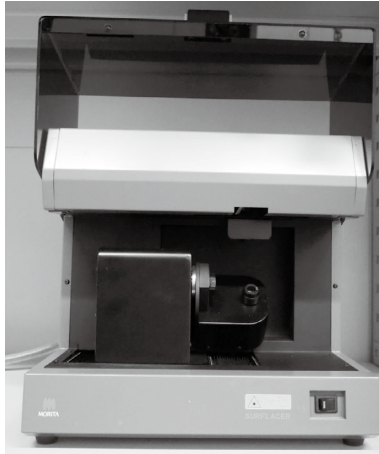| Cavity depth	Allocation of points
4．Cavity bottom dept	
□ Too shallow	35
□ Somewhat shallow	40
□ Appropriate	95
□ Somewhat deep	40
□ Too deep	20

Free description column
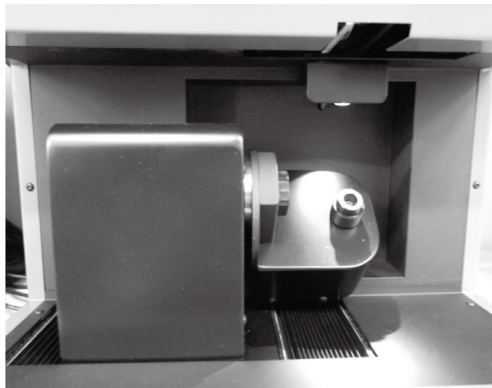
Fig. 5 SURFLACER

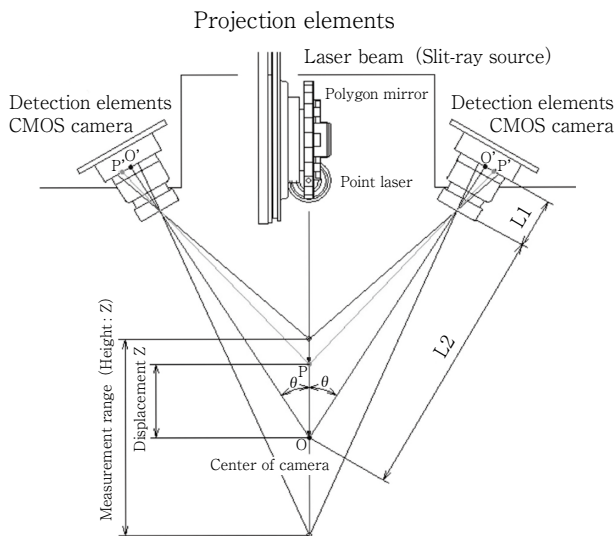**Fig. 6** Attachment part of SURFLACER for artificial tooth for training

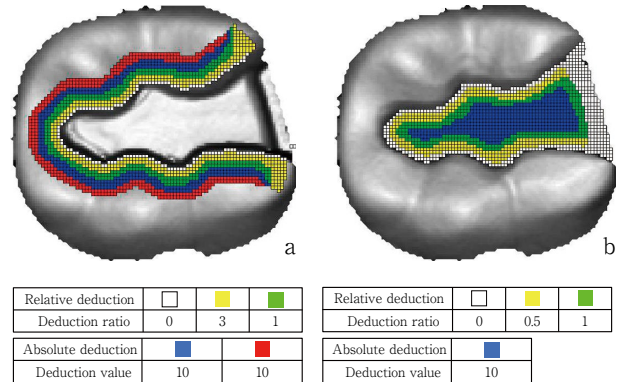**Fig. 7** Slit-ray projection method measurement principles

Fig. 8 Evaluation map for outside and inside the cavity
a. Outside the cavity   b. Inside the cavity

Table 2 Cavity depth evaluation map

Insufficient cutting		Excessive cutting	
Shallowness (mm)	Deduction ratio	Depth (mm)	Deduction ratio
0.00–0.10	0.00	0.00–0.10	0.00
0.10–0.20	3.00	0.10–0.20	0.25
0.20–0.30	1.00	0.20–0.30	3.00
0.30–0.40	1.00	0.30–0.40	1.00
0.40–0.50	1.00	0.40–0.50	1.00
0.50–	0.00	0.50–	0.00

2）Setting the criteria for evaluation with the measuring device

A cavity that satisfied the requirements for a metal inlay cavity[14,15] was formed as the example tooth. It is necessary to incorporate the data on the example tooth in advance and set up the evaluation map based on the incorporated data in order to execute evaluation by the measuring device. The evaluation map is divided into the outline and depth of cavity. The cavity outline was set up by dividing it into maps to evaluate and grade the outer or inner side of the margin of the example tooth. The area outside the margin was considered as the excessive cutting area, and the area inside the margin as the insufficient cutting area, and the ratio of deduction and locations that could not be cut or that could not be left uncut were set up（Fig. 8, Table 2）. Regarding cavity depth, dental pulp exposure is a contraindication in clinical practice. Excessive cutting was therefore set with a larger deduction ratio than insufficient cutting.

Table 3　Score calculation formula for SURFLACER

Cavity outline evaluation score O＝(OE×OI)$^{1/2}$
Evaluation score for excessive cutting OE
＝100−excessive cutting deduction value
Evaluation score for insufficient cutting OI
＝100−insufficient cutting deduction value
Cavity depth evaluation score D＝(DE×DI)$^{1/2}$
Evaluation score for excessive cutting DE
＝100−excessive cutting deduction value
Evaluation score for insufficient cutting DI
＝100−insufficient cutting deduction value
Total evaluation score＝(O×D)$^{1/2}$

Table 4　Score calculation formula for instructor evaluation

Cavity outline evaluation score＝(evaluation item 1+2+3)
Cavity depth evaluation score＝evaluation item 4
Total evaluation score＝(outline score×depth score)$^{1/2}$

3) Setting the evaluation criteria for the evaluation by instructors

The evaluation by instructors was made using the same example tooth used for the evaluation by measuring device. The teeth formed by dental residents were assigned codes A through J so that the individuals could not be identified.

4) Score calculation in evaluation by measuring device and evaluation by instructors

Table 3 shows the score calculation formula for SURFLACER in the evaluation by measuring device. In addition, points for the outline and points for the depth of cavity were both calculated in the deduction method. Tables 1 and 4 show the evaluation items and allocation of points in the evaluation by instructors, and the score calculation formula. The average score resulting from five measurements and gradings on the example tooth after setting the criteria for the evaluation by measuring device was 95 points. Based on this, the point allocation was set so that the highest score would be 95 points for the third item in cavity outline and the first item in cavity depth. In accordance with clinical practice in a similar fashion to the setting for the evaluation by measuring device, both cavity outline and cavity depth were set so that a lower score was given when cutting was excessive. Settings were also made to minimize the variation in scores among the instructors based on the results of a preliminary experiment. The highest and lowest scores by the nine instructors were also excluded and the average of the other instructors was used as the score.

5) Feedback method

Feedback was given to the dental residents using the results of evaluation by measuring device (Figs. 9 and 10) and the results of evaluation by instructors. The parts in the evaluation by measuring device that are marked in red indicate excessive cutting, and those in blue indicate insufficient cutting. The results allow visualization into fine parts. The average score of the nine instructors was indicated for the evaluation by instructors, and the comments in the free description column were presented along with the score.

Results

The total score results of the evaluation by measuring device and the evaluation by instructors are shown in Table 5.

1. Objective evaluation by measuring device

The results of correlation analysis showed no significant difference between the number of preparations and evaluation by measuring device (Fig. 11) (NS). The average score was 60 points and the highest score 85 points. In the results, the largest deduction (−98 points) occurred at seven points (A-3, C-2, -3 and -5, F-3, G-3 and -4) due to the locations at which cutting or leaving uncut was a contraindication, resulting in especially low scores (Table 5). A breakdown of the scores at these seven points is shown in Table 6. Of the seven points, excessive cutting in cavity depth was considered
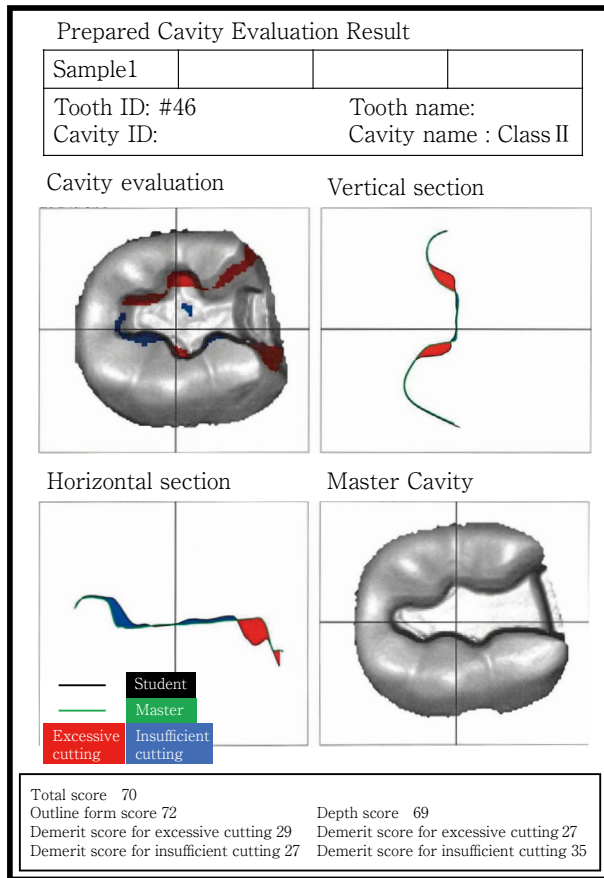
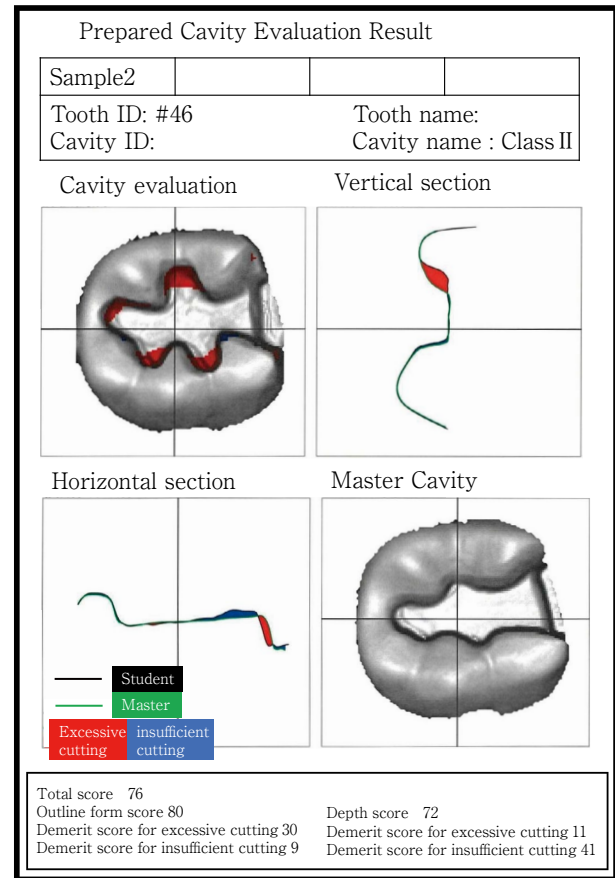**Fig. 9**   Measuring device evaluation results,
Example（1）

Fig. 10   Measuring device evaluation results,
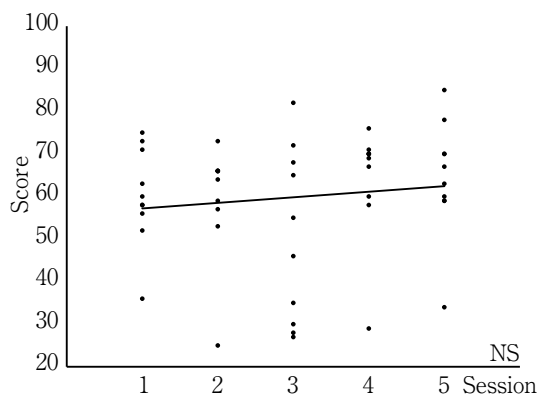Example（2）

Fig. 11   Measuring device evaluation score（by
preparation session）

a contraindication at six points and excessive cutting in cavity outline was a contraindication at one point. Correlation analysis was therefore conducted by excluding the above seven points, and the result showed a significant positive correlation between the number of preparations and evaluation by measuring device （Fig. 12）

（r＝0.32, p＜0.05）.

2．Objective evaluation by instructors

Correlation analysis showed a significant positive correlation between the number of preparations and evaluation by instructors （Fig. 13）（r＝0.30, p＜0.05）. The evaluation by instructors tended to be higher in both average score and highest score.

3．Comparison between evaluation by measuring device and evaluation by instructors

A scatter diagram of the evaluation by measuring device and the evaluation by instructors is shown in Fig. 14. Correlation analysis showed a significant positive correlation between the two evaluations （r＝0.41, p＜0.01）.

Discussion

For improving clinical dental skills, it is necessary to master the procedures in addition to learning the knowledge in order to conduct treatments. In dental

Table 5 Measuring device/instructor evaluation score results

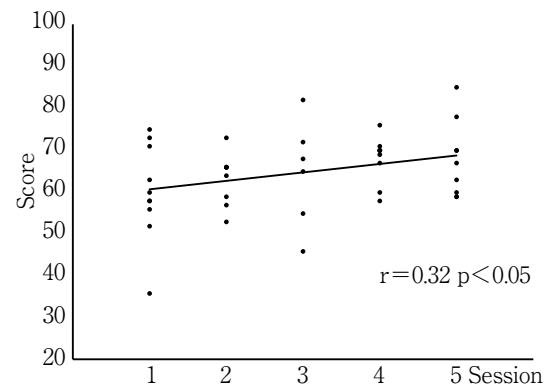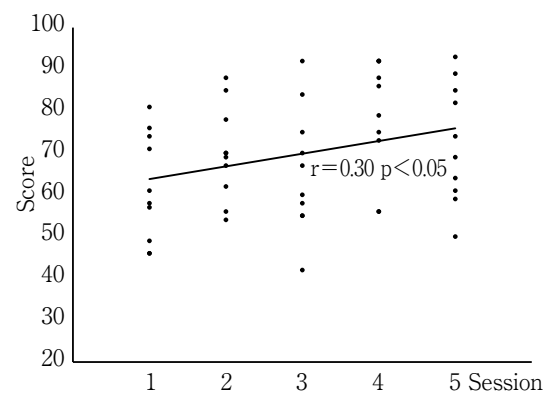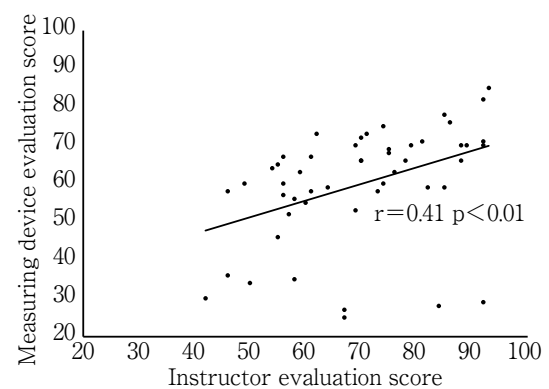|		1	2	3	4	5 (Session)
A	DS	52	66	30	70	70
	IS	57	70	42	79	69
B	DS	75	57	68	69	59
	IS	74	56	75	75	64
C	DS	60	25	28	70	34
	IS	49	67	84	92	50
D	DS	36	64	65	60	59
	IS	46	54	55	56	82
E	DS	63	66	55	71	60
	IS	76	78	60	92	74
F	DS	71	53	35	70	85
	IS	81	69	58	88	93
G	DS	56	59	27	29	70
	IS	58	85	67	92	89
H	DS	58	66	46	76	63
	IS	46	88	55	86	59
I	DS	73	66	72	67	67
	IS	71	70	70	56	61
J	DS	58	73	82	58	78
	IS	61	62	92	73	85

DS : Measuring device evaluation score, IS : Instructor evaluation score

Fig. 12 Measuring device evaluation score (by preparation session, with deletion of seven points)

Fig. 13 Instructor evaluation score (by preparation session)

Table 6 Score breakdown

	T	O	OE	OI	D	DE	DI
A-3	30	65	91	46	14	2	100
C-2	25	62	45	85	10	2	47
C-3	28	13	2	81	60	37	98
C-5	34	83	75	91	14	2	100
F-3	35	87	98	78	14	2	100
G-3	27	76	91	62	9	2	45
G-4	29	78	90	69	11	2	61

T : Total evaluation score, O : Cavity outline evaluation score, OE : Evaluation score for excessive cutting, OI : Evaluation score for insufficient cutting, D : Cavity depth evaluation score, DE : Evaluation score for excessive cutting, DI : Evaluation score for insufficient cutting

Fig. 14 Correlation diagram on measuring device evaluation score and instructor evaluation score

care, precise work must be conducted inside the confined space of the oral cavity. To acquire the skills to conduct diagnosis and treatment safely and precisely

within the oral cavity of the patient, it is important to repeatedly perform skill training in basic education and training. It is therefore necessary to evaluate skills
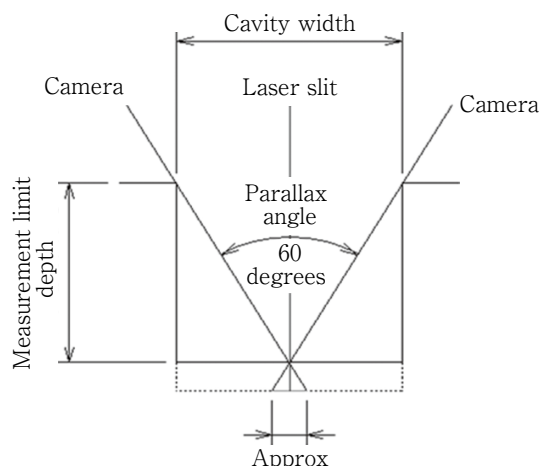
Fig. 15 Invisible area

Table 7 Measurable depth to cavity width

Cavity width（mm）	0.5	1.0	1.5	2.0	2.5
Measurable depth（mm）	0.45	0.90	1.35	1.80	2.25
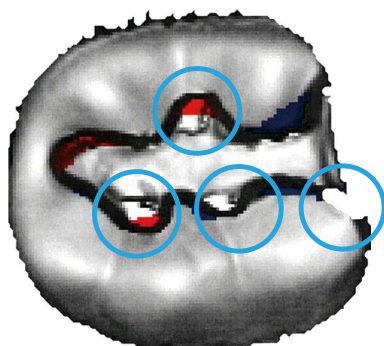
Fig. 16 Example of invisible
area display
〇：Invisible area

Cavity evaluation   Vertical section

Horizontal section   Master Cavity

Student
Master
Excessive cutting   Insufficient cutting

Measuring device evaluation score

Total score 28
Outline form score 13
Demerit score for excessive cutting 98
Demerit score for insufficient cutting 19

Depth score 60
Demerit score for excessive cutting 63
Demerit score for insufficient cutting 2

Instructor evaluation score
Total score 84
Outline form score 74
Depth score 95

Fig. 17 Results of evaluation by measuring device
and instructors（C-3）
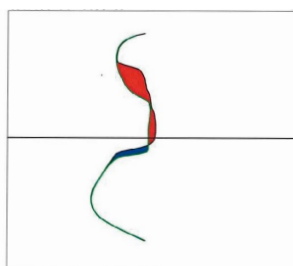
objectively, not based on the subjectivity of the instructor, and various attempts have been made[16-23]. Unlike knowledge that can be learned in the classroom, practical experience is essential for mastering the procedures. This is one of the reasons why clinical training is included as a requirement in curriculums for dental school students. Universities that teach dentistry thus have university hospitals where students can receive clinical training. However, the number of patients who participate in clinical training has declined dramatically in recent years due to changes in patients' attitudes toward medicine, etc., and many dentistry students face the risk of graduating and becoming dentists without
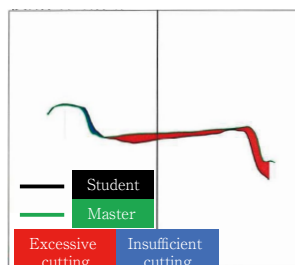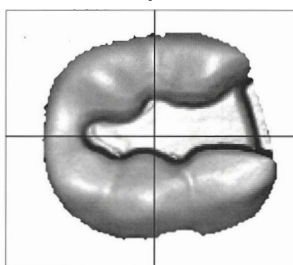
having sufficient practical experience as it is becoming increasingly difficult to gain sufficient clinical skills at outpatient hospitals. Therefore, this study compared objective evaluation by measuring device and objective evaluation by multiple instructors in cavity preparation for a Class Ⅱ metal inlay, and examined the usefulness and practicality of a skill education curriculum that adopted this system.

This study recruited dental residents who were undergoing clinical practice at the Department of Operative Dentistry, Osaka Dental University Hospital. The skills of a dental resident improve by both experience in diagnosis and treatment and self-improvement using jaw models on which they work during spare time from diagnosis and treatment. Accordingly, medical advisors assign patients to suit the skills of the dental resident. The study was therefore conducted within the extent that would not interfere with their diagnosis and treatment at two-month intervals. No significant difference in correlation was observed in total scores of evaluation by measuring device. It is considered that the maxi-

mum deduction at seven points (−98 points) affected the correlation results greatly (Table 5). The cut on locations uncut considered as contraindication were specified in the settings for the measuring device. As a result, large deductions occurred. As a significant positive correlation was observed by excluding these seven points, it was found that skills were improved by conducting evaluations by measuring device and giving feedback over time. It was also found that skills were improved by conducting evaluations by instructors and giving feedback over time, as a significant difference in correlation coefficient was observed in the evaluations by instructors. Based on these findings, this curriculum, which incorporates evaluation by measuring device and evaluation by instructors, is expected to be effective for improving the skills for cavity preparation.

Evaluation of cavity preparation with measuring devices has been used to ensure fairness for students and make feedback more objective[2,7,24-28]. Meanwhile, evaluations by instructors have also been examined, including whether importance should be placed on the cavity outline or depth, and what ratio of the two would be best[1]. Variations in evaluations among instructors were also observed in some of the formed teeth in this study. On the other hand, evaluation by measuring device is possible under certain conditions, as a detailed evaluation map can be set up and differences that cannot be judged by the human eye can be evaluated. However, there are areas that cannot be seen by the measuring device (Fig. 15), and the measurable depth varies depending on the cavity width (Table 7). If there are invisible areas within the cavity, it is impossible to evaluate the cavity depth in such areas, even though the cavity outline can be evaluated. In such cases, the cavity depth is evaluated based on the points in proximity to the invisible area that can be measured. That is, evaluation by an instructor is necessary for 3-D shape measurement using laser light, as the occurrence of invisible areas is unavoidable. The invisible areas can be recognized by experienced people, as they appear as white areas in the results (Fig. 16).

At C-3, which had the largest deduction in the evaluation by measuring device, the evaluation by instructors varied greatly with a tendency for high evaluations (Fig. 17). Comments in the free description column in the instructor evaluation included "it was well-formed," "slightly too large on the lingual side, but well-

done." Instructors tended to give a high evaluation as long as the tooth was formed with a good balance, even when parts that were subject to deduction had been cut. While dental residents may feel that evaluations done by measuring device under certain conditions are severe, it is considered better to evaluate under certain conditions when comparing changes over time. Since the evaluations by measuring device and by instructors showed a significant positive correlation, it was considered that the measuring device can perform evaluations that are similar to those by instructors.

It is possible to apply SURFLACER, which was used in this study, in basic training and clinical training before graduation in addition to the training of dental residents. By incorporating phantom training using this system, it is expected that students can experience more complete training as the limited skill training period can be utilized more effectively and the instructor can spend more time in instructing individual students. Furthermore, SURFLACER can be operated by the students or dental residents themselves, and they can receive instant self-feedback[29]. It is also considered that the system will help students study better on their own, as it can be used to visualize even the points of the formed tooth that are difficult to see with the eye, and make it easier to understand visually with coloring. Since reports have been published on using the system for training on abutment tooth preparation, caries removal and pulp chamber opening other than cavity preparation[2,29,30], it is considered that SURFLACER is an effective new method of skill training. Because the evaluation map on the example tooth can be freely set, another advantage of this system is that the severity of evaluation can be specified to suit the skill level of the student. It can be set to an easy level for basic training of students who have little experience in cavity preparation, and to a harder level as they gain experience from hospital training on the way to becoming dental residents. It may also be used by dentists as a self-improvement tool for ongoing training.

Conclusion

1. The non-contact high-speed 3-D shape measuring device can objectively evaluate Class Ⅱ metal inlay cavities, and can execute evaluations that are consistent with evaluations by multiple instructors with rich clini-

cal experience.

2．A curriculum that includes evaluation by measuring device and evaluation by instructors is effective for improving the skills of dental residents.

3．The incorporation of evaluation by measuring device may reduce the burden on instructors and the instruction period.

References

1) Hirata K, Nakashima M, Imura S, Yamamoto K, Sekine I, Moriwaki Y, Yoshida S. Application of noncontact high speed 3-D shape measuring system to restorative dentistry　Part 2 Development of cavity preparation assessment system. Jpn J Conserv Dent 1998; 41: 320-336.（in Japanese）

2) Yamaguchi T, Hosoya N, Kurachi Y, Yoshida T, Morito A, Koda S, Yamamoto T, Momoi Y. Objective evaluation of access cavity preparation. Jpn J Conserv Dent 2012; 55: 278-284.（in Japanese）

3) Yasunaga T, Kato S, Takaoka T, Nishi M, Miura M, Ebisu S. Uniformization of subjective evaluation on class Ⅰ inlay cavity. DSTS 1996; 91-98.（in Japanese）

4) Kimoto S, Matsuzawa M, Kubota M, Komatsu T, Yamaguchi M. Evaluation by objective structured clinical examination (OSCE) during pre-clinical practice for pediatric dentistry: A study of evaluation results by instructors and students. Bull Kanagawa Dent Col 2007; 42: 32-41.（in Japanese）

5) Itoh N, Osawa G, Ogawa T, Kawamura H, Nakaya H. Evaluation of scaling rootplaning in pre-clinical training program by objective structured clinical examination─Results of 6 years─. J Jpn Soc Periodontol 2010; 52: 429-433.（in Japanese）

6) Oka A, Murayama R, Takano R, Furuichi T, Sai K, Takeuchi Y, Seki K, Furuchi M, Kamimoto A, Masutani S. A study of cavity preparation training using digital data obtained by optical impression device. Journal of Japanese Society of the General Dentistry 2019; 11: 58-65.（in Japanese）

7) Torii M, Yasunaga T, Urano M, Takeshige F, Tsuchitani Y. Numerical evaluation of prepared cavity and its application to simulation training. The Japanese Journal of Ergonomics 1995; 31: 101-104.（in Japanese）

8) Taguchi Y, Takizawa T, Oka Y, Fujii N. A study of clinical training and evaluation for the preparation of a full-veneer crown. Ann Jpn Prosthodont Soc 2012; 4: 434-443.（in Japanese）

9) Quinn F, Keogh P, McDonald A, Hussey D. A pilot study comparing the effectiveness of conventional training and visual reality simulation in the skills acquisition of junior dental school. Eur J Dent Educ 2003; 7: 13-19.

10) Quinn F, Keogh P, McDonald A, Hussey D. A study comparing effectiveness of conventional training and virtual reality simulation in the skills acquisition of junior dental school. Eur J Dent Educ 2003; 7: 164-169.

11) Hirata K, Nakashima M, Imura S, Yamamoto K, Sekine I, Moriwaki Y, Yoshida S. Application of non-contact high speed 3-D shape measuring system to restorative dentistry　Part 1 Accuracy in measuring width and depth of standard cavity. Jpn J Conserv Dent 1997; 40: 287-293.（in Japanese）

12) Hirata K, Nakashima M, Imura S, Yamamoto K, Sekine I, Moriwaki Y, Yoshida S. Application of non-contact high speed 3-D shape measuring system to restorative dentistry　Part 3 Assessment of prepared cavity by points. Jpn J Conserv Dent 1998; 41: 337-342.（in Japanese）

13) Hirata K. Application of laser measuring system to dental education. JJSLSM 2003; 24: 168.（in Japanese）

14) Tagami J, Nara Y, Yamamoto K, Saito T. Operative Dentistry 21. 5th ed. Nagasue Shoten: Kyoto; 2017. 112-118.（in Japanese）

15) Kitamura C, Morotomi T. Required conditions for cavity preparation. Senda A, Miyazaki M, Hayashi M, Mukai Y, Saito T. Operative Dentistry. 7th ed. Ishiyaku Publishers, Inc.: Tokyo; 2019. 114-122.（in Japanese）

16) Kimura K. Studies on the development of the system using a digital camera for the evaluation of cavity preparations. J Hiroshima Univ Dent Soc 2004; 36: 24-36.（in Japanese）

17) Ibaraki Y, Haraguchi K, Tsukagoshi S, Odachi T, Nagai Y, Saito T, Kawakami T, Kobayashi F, Matsuda K. Rationalization and improving efficiency of dental clinical education using simulation systems. Jpn J Conserv Dent 2002; 45: 52-61.（in Japanese）

18) Kawamoto T. Application of a computer to dental education─Application to the lecture─. JJDEA 1995; 11: 97-100.（in Japanese）

19) Kawamoto M, Kitano T, Kawamoto T, Onchi Y, Kohmi

T, Inoue M, Narikawa K, Fujii B. Application of 3D computer-graphics to dental education　Part 1 Development of the trial teaching aids for bevel preparation of metal inlay cavity. JJDEA 1995; 11: 101-107.(in Japanese)

20) Gonda T, Maeda Y, Nokubi T. Multimedia support system for clinical prosthodontic education. The Journal of Osaka University Dental Society 1997; 42: 148-153.(in Japanese)

21) Kurachi Y. Objective evaluation of cavity preparation —Class Ⅱ cavity—. TUDJ 2002; 28: 95-107.(in Japanese)

22) Johnson L, Thomas G, Dow S, Stanford C. An initial evaluation of the Iowa Dental Surgical Simulator. J Dent Educ 2000; 64: 847-853.

23) Kota K, Ayukawa Y, Iwaku M. An introduction of computer to dental simulation system　Part 1 Evaluation methods for cutting pressure and prepared cavities. Jpn J Conserv Dent 1994; 37: 152. P-62.(in Japanese)

24) Yasukawa Y. The effectiveness of cavity preparation training using a virtual reality simulation system with or without feedback. J Stomatol Soc Jpn 2009; 76: 73-80.(in Japanese)

25) Yamada S, Ono Y, Sugiyama T, Watari M, Asari J, Mayahara M, Yanagisawa W, Futaki K, Sato M, Suzuki H, Maki K, Inoue M. Method of evaluation of preclinical tooth modeling practice in pediatric dentistry and automatic evaluation of 3D shape. Jpn J Ped Dent 2015; 53: 471-476.(in Japanese)

26) Wierinck E, Puttemans V, Swinnen S, Van Steenberghe D. Effect of augmented visual feedback from a virtual reality simulation system on manual dexterity training. Eur J Dent Educ 2005; 9: 10-16.

27) Welk A, Maggio MP, Simon JF, Scarbecz M, Harrison JA, Wicks RA, Gilpatrick RO. Computer-assisted learning and simulation lab with 40 DentSim units. Int J Comput Dent 2008; 11: 17-40.

28) Abe T, Okuyama Y, Kasahara S, Kimura K. Education effect on tooth preparation of visual feedback using computer graphics. Ann Jpn Prosthodont Soc 2009; 1: 123-129.(in Japanese)

29) Huiru Z, Shufeng J, Jianping S, Yanmei D. A cavity preparation evaluation system in the skill assessment of dental students. J Dent Educ 2016; 80: 930-937.

30) Wakamatsu N, Okano T, Kondo T, Hasegawa S, Iinuma M. Objective evaluation of abutment tooth preparation for preformed metal crowns for primary molars in Japanese preclinical training. Pediatr Dent J 2020; 30: 92-98.

Effects of Universal Adhesives on Dentin Adhesive Performance and Acid-base Resistance

Ryuta Ando[1], Takaaki Sato[1], Naoko Matsui[1],

Masaomi Ikeda[3], Noriko Hiraishi[1], Tomohiro Takagaki[1,2],

Toru Nikaido[1,2], Junji Tagami[1] and Yasushi Shimada[1]

[1]Department of Cariology and Operative Dentistry, Division of Oral Health Sciences, Medical and Dental Sciences Track,
Graduate School of Medical and Dental Sciences, Tokyo Medical and Dental University（TMDU）
[2]Department of Operative Dentistry, Division of Oral Functional Science and Rehabilitation,
Asahi University, School of Dentistry
[3]Clinical Oral Science, Department of Oral Health Care Sciences, Tokyo Medical and Dental University（TMDU）

Abstract

　Purpose: This study elucidated the dentin-bonding performance of three kinds of universal adhesive using the bond strength test and morphological observation under a scanning electron microscope（SEM）.

　Methods: OptiBond Universal（OPB）, Prime&Bond Universal（PBU）, and Clearfil Universal Bond Quick ER （UBQ） were used. For the microtensile bond strength（μTBS）test, human dentin was ground with #600-grit silicon carbide（SiC）paper, then an adhesive and built resin composite were applied. After water storage for 24 h, bonded teeth were sectioned into beam-shaped specimens. Specimens were divided into three sub-groups and exposed to 0, 5,000, or 10,000 thermal cycles. After the μTBS test, statistical differences were examined by multiple comparisons using t-tests with Bonferroni correction（$\alpha =0.05$）. For the acid-base resistant zone（ABRZ）observation, human molars were sectioned into dentin disks. Dentin surfaces were ground with #600-grit SiC paper. Following the application of the adhesive, a flowable resin composite was light-cured to make a dentin disk sandwich. After water storage, the acid and base challenges were conducted using a buffered demineralizing solution（pH=4.5）and 5% NaOCl（pH=10.5-12.9）. Then, the surface was covered by adhesive resin Super-Bond C&B. The specimens were sectioned to approximately 2 mm thickness, and polished. The polished surfaces were etched with an argon-ion beam, and gold-sputter coated for the morphological analysis of adhesive interface under SEM.

　Results: The results of μTBS tests depended on the thermal cycle challenges. After 10,000 cycles, the μTBS of all adhesives were significantly lower than those of the 0 cycle group. After 5,000 cycles, μTBS results showed different trends among the three groups. ABRZ observation showed that all groups formed ABRZ. A funnel-shaped erosion was clearly observed in OPB and PBU, but not in UBQ. On the other hand, funnel-shaped erosion was observed in UBQ, but not clearly.

　Conclusion: The bond strength test results and the interfacial morphological structure after the acid-base challenge depended on material components such as hydrophilic amide monomer, HEMA and NaF. The results of this study suggest that the bonding durability between universal adhesives and dentin depends on material components.

　Key words: universal adhesives, dentin bond strength, acid-base resistance zone

Introduction

The three-step bonding system consists of etching, priming, and bonding procedures. Due to the demand for simpler, more user-friendly, and less technique-sensitive adhesives, manufacturers have developed new adhesives used in one-step procedures[1,2]. Recently, one-step self-etch adhesive (SEA) systems called "multi-mode adhesive" or "universal adhesive" were released. With these adhesives, clinicians can choose one of three strategies (etch and rinse, selective enamel etch, or self-etch modes), depending on the clinical application, rendering the clinical procedure more user-friendly[3]. These bonding agents are also indicated to be used as silane for glass ceramics and primers for metal alloys and polycrystalline ceramics. This is why these adhesives are called "universal adhesives"[4]. Universal adhesives are a complex mixture of hydrophilic and hydrophobic compounds, water, and solvents such as ethanol and acetone, which can lead to poor adhesion and deterioration of the bonding interface[5].

To evaluate the bonding interface, not only the bond strength test but also morphological evaluation is often conducted. Primarily, a scanning electron microscope (SEM) examination provides valuable information for adequately understanding the mechanism of adhesive adhesion to teeth. SEM studies after acid and base challenges revealed the formation of an "acid-base resistant zone (ABRZ)" adjacent to the hybrid layer when dentin was treated with a SEA system[6]. However, there have been few comparative studies[7] on universal adhesives after acid and base challenges. In one study[7], a universal adhesive was employed to evaluate the bonding interface.

Therefore, the present study elucidated the dentin-bonding performance of three kinds of universal adhesive by the bond strength test and morphological observation under SEM. The null hypothesis of this study was that the material components of universal adhesives do not influence the durability of dentin bonding.

Materials and Methods

1．Materials used in this study

This study used three kinds of universal adhesive, OptiBond Universal (OPB; Kerr, Brea, CA, USA), Prime&Bond Universal (PBU; Dentsply Sirona, Charlotte, NC, USA), and Clearfil Universal Bond Quick ER (UBQ; Kuraray Noritake Dental, Tokyo, Japan). The characteristics of each adhesive are as follows. Regarding the functional monomers, OPB contains GPDM, PBU contains MDP and PENTA, and UBQ contains MDP. Additionally, PBU and UBQ contain a hydrophilic amide monomer, and only UBQ contains NaF. Table 1 provides a detailed description of the respective adhesives and application protocols. In this study, caries-free human third molars were collected according to the ethical protocol No. 2013-022 approved by the Human Research Ethics Committee of Tokyo Medical and Dental University. The teeth were stored in 0.1% thymol solution at 4℃, and used within six months after extraction.

2．Microtensile bond strength（μTBS）testing

1) Tooth specimen preparation

The outline of the μTBS test is schematically presented in Fig. 1. Thirty human third molars were selected for this part of the study. For each tooth, the coronal portion was removed to expose a flat mid-coronal dentin surface using a low-speed water-cooled diamond saw (Isomet; Buehler, Lake Bluff, IL, USA). The exposed dentin surface was ground for 30 s with #600-grit silicon carbide (SiC) paper under running water to produce standardized smear layers.

2) Bonding and restorative procedures

Thirty teeth were randomly divided into three groups (10 teeth per group) by type of adhesive. Each tooth was bonded according to the manufacturer's instructions (Table 1). After application, the specimens were air-dried for 5 s and cured with a light-emitting diode (LED) light-curing unit (VALO LED Curing Light, high-power mode at 1,400 mW/cm², Ultradent, South Jordan, UT, USA) for 10 s. Then, the resin composite (Clearfil AP-X, shade A2, Kuraray Noritake Dental) was built to a thickness of 2 mm and light-cured for 40 s using the light-curing unit. This operation was performed twice to build a resin composite block with a total thickness of 4 mm. After storage in 37℃ distilled water for 24 h, all bonded teeth were sectioned into beam-shaped specimens (surface area: 1.0×1.0 mm) using Isomet. Nine specimens were obtained from the center of each bonded tooth (9 beams per tooth).

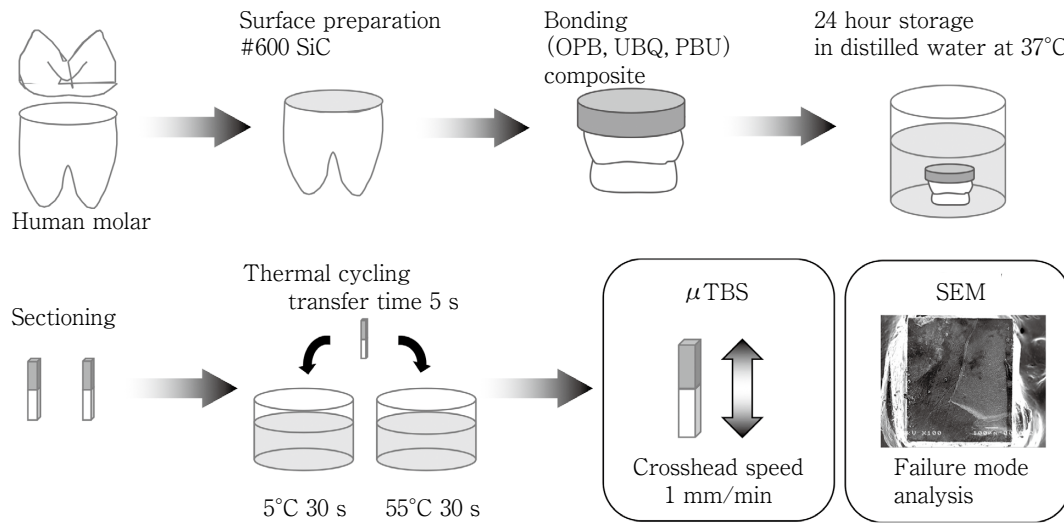The beam-shaped specimens in each group were ran-

Fig. 1 Schematic of specimen preparation methodology for μTBS

Table 1 Materials used in this study

	Code	Composition	Hydrophilic amide monomers	HEMA	NaF	Application time
Universal adhesive						
OptiBond Universal	OPB	GPDM, HEMA, dimethacrylate, acetone, ethanol, glycerol,	—	✓	—	OPB was applied for 20 s with agitation, then air-dried for 5 s.
Prime & Bond Universal	PBU	Phosphoric acid modified acrylate resin (MDP, PENTA), multifunctional acrylate, bifunctional acrylate (amide monomer), acidic acrylate, isopropanol, water, initiator	✓	—	—	PBU was applied for 20 s with agitation, then air-dried for 5 s.
Clearfil Universal Bond Quick ER	UBQ	MDP, HEMA, Bis-GMA, hydrophilic amide monomers, colloidal silica, silane coupling agent, sodium fluoride, dl-camphorquinone, ethanol, water	✓	✓	✓ (<0.1%)	UBQ was applied and immediately air-dried with no time lapse between steps.
Resin composite						
Clearfil AP-X		Bis-GMA, TEGDMA, silanated glass filler, silanated silica filler, silanated colloidal silica, di-camphorquinone, catalysts, accelerators, pigments				
Clearfil Majesty ES Flow		Silanate barium glass filler, silanate colloidal filler, TEGDMA, hydrophobic aromatic dimethacrylate, di-camphorquinone, accelerators, pigments				

GPDM : glycero-phosphate dimethacrylate, HEMA : 2-hydroxyethyl methacrylate, MDP : 10-methacryloyloxydecyl dihydrogen phosphate, PENTA : dipentaerythritol penta acrylate monophosphate, TEGDMA : triethylene glycol dimethacrylate, Bis-GMA : 2,2 bis［4-(2-hydroxy-3-methacrylyloxy-propoxy)-phenyl］propane.

domly divided into three subgroups, and exposed to 0, 5,000 or 10,000 thermal cycles (n=30, for each subgroup). The beams were cycled between two water baths at 5℃ and 55℃ with a dwell time of 30 s in each bath and a transfer time of 5 s using a thermal cycling device (K178-08, Tokyo Giken, Tokyo, Japan). After thermal cycling, each specimen was individually bonded to a tensile testing jig using cyanoacrylate adhesive (Model Repair II Blue, Dentsply-Sankin, Tokyo, Japan) mounted in a tabletop testing machine (EZ-SX, Shi-
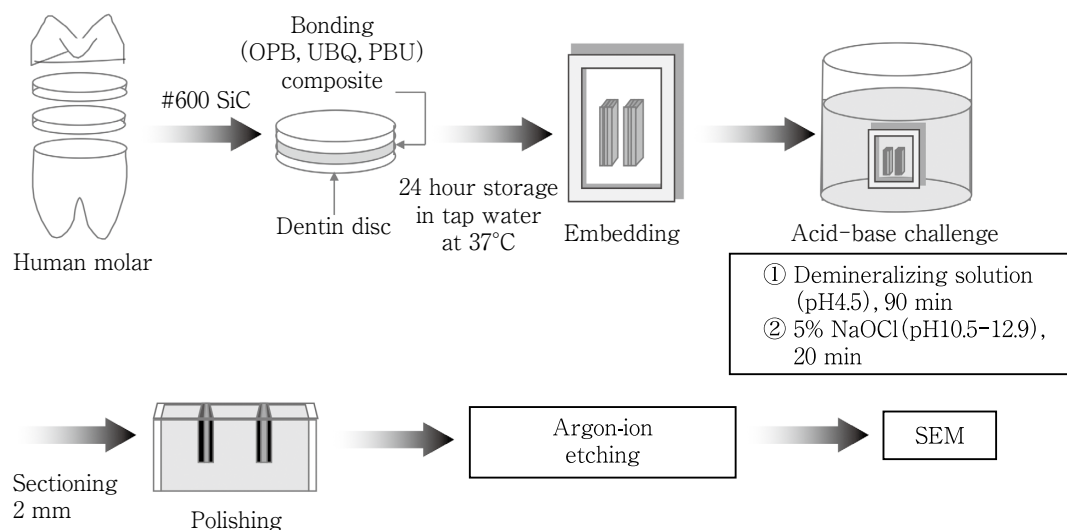
Fig. 2 Schematic of specimen preparation methodology for SEM

madzu, Kyoto, Japan) and subjected to the μTBS test at a crosshead speed of 1.0 mm/min (Fig. 1). The μTBS was derived by dividing the imposed force at the time of fracture by the bonded area (mm^2). Statistical differences were examined by multiple comparisons using t-tests with Bonferroni correction ($\alpha = 0.05$) in IBM SPSS Statistics for Windows, version 22.0 (IBM, Armonk, NY, USA).

After the μTBS test, the fractured specimens were observed under SEM (JSM-IT100, JEOL, Tokyo, Japan) to characterize their failure modes. Fractured specimens were classified as: (1) C-D: cohesive failure in dentin with ＞80% of total bonding area, (2) I-DA: interfacial failure between dentin and adhesive with ＞80% of total bonding area, (3) C-A: cohesive failure in adhesive with ＞80% of total bonding area, (4) Mix: mixed failure. Statistical differences were examined by Fisher's exact test and Chi-square test ($\alpha = 0.05$) in IBM SPSS Statistics for Windows, version 22.0.

3. SEM observation of the adhesive-dentin interface after acid-base challenge

The sample preparation for SEM examination of the ABRZ is illustrated in Fig. 2. Thirty human third molars were randomly divided into three groups (10 teeth per group). Each tooth was sectioned to obtain two 2 mm-thick dentin disks using Isomet. The dentin surfaces were ground with #600-grit SiC paper under running water to standardize the smear layers, and in the same way as the μTBS test, one of the three adhesives was applied. Following the adhesive application, a

flowable resin composite (Clearfil Majesty ES Flow, shade A2, Kuraray Noritake Dental) was placed between pairs of prepared dentin disks and light-cured to make a dentin disk sandwich. The bonded specimens were stored in distilled water at 37℃ for 24 h. Subsequently, the specimens were sectioned vertically at the dentin-adhesive interface and embedded in epoxy resin (Epoxicure 2 Resin, Buehler). Each specimen was first stored in 100 ml of a buffered demineralizing solution, containing 2.2-mmol/l $CaCl_2$, 2.2-mmol/l NaH_2PO_4, and 50-mmol/l acetic acid adjusted to pH 4.5, for 90 min to create an artificial secondary caries challenge. The specimens were then immersed in 5% NaOCl (pH＝ 10.5–12.9), which was prepared from 10% sodium hypochlorite solution (Yoneyama Yakuhin Kogyo, Osaka, Japan), using an ultrasonic cleaner for 20 min in an attempt to remove any demineralized dentin collagen fibrils, and rinsed with running water for 30 s. The edge of the dentin-adhesive interface could be easily damaged during specimen polishing. To prevent this, a self-cure adhesive resin, Super-Bond C&B (Sun Medical, Moriyama, Japan), was applied to the surface without any surface preparation[8]. The specimens were sectioned perpendicular to the dentin-adhesive interface, and reduced to approximately 2 mm thickness, then polished with diamond pastes (Struers A/S, Copenhagen, Denmark) down to 0.25 μm particle size. The polished surfaces were etched with an argon-ion beam (EIS-200ER, Elionix, Tokyo, Japan) at 1 kV, 0.2 mA/cm^2 for 30 s to bring the hybrid layer into sharp relief. The

Table 2 Microtensile bond strength (Mean±SD, MPa)

Group	Thermal cycle		
	0	5,000	10,000
OPB	67.5±13.2^A	58.6±10.0^B	47.4±11.6^C
PBU	62.4±8.2^{Aa}	57.5±10.6^{Bab}	52.8±9.8^{CDb}
UBQ	66.3±9.4^A	58.7±6.4^{Bc}	54.3±13.1^{Dc}

N=30, Mean and standard deviation (SD) of microtensile bond strength values (MPa).
Values within the same thermal cycle stage, marked with the same large superscripts, are not significantly different (p>0.05).
Values within the same material, marked with the same small superscripts, are not significantly different (p>0.05).

Table 3 Failure mode analysis

Group	Thermal cycle	Failure mode			
		C-D	I-DA	C-A	Mix
OPB	0	6^a	1^a	4^a	19^a
	5,000	11^a	0^a	8^a	11^a
	10,000	9^a	3^a	6^a	12^a
PBU	0	10^a	0^a	6^a	14^a
	5,000	13^a	1^a	12^a	4^a
	10,000	15^a	0^a	7^a	8^a
UBQ	0	11^a	2^a	0^a	17^a
	5,000	16^a	2^a	3^a	9^a
	10,000	15^a	1^a	6^a	8^a

C-D : cohesive failure in dentin with >80% of total bonding area, I-DA : interfacial failure between dentin and adhesive with >80% of total bonding area, C-A : cohesive failure in adhesive with >80% of total bonding area, Mix : mixed failure.
Numbers marked with the same small superscripts are not significantly different (p>0.05).

specimens were then gold-sputter coated, and morphological changes to the dentin-adhesive interface due to the acid-base challenge were observed under SEM[9,10].

Results

1. Microtensile bond strength (μTBS)

The μTBS values and failure modes are shown in Tables 2 and 3. Compared to each adhesive, the μTBS test results showed that the bond strength of the UBQ groups was significantly higher than that of the OPB groups after the 10,000 thermal cycle challenge (p<0.001). Regarding the bond strength of the 0 and 5,000 cycles groups, there were no significant differences among the three adhesive groups. In the OPB groups, the bond strength of the 0 cycle group was significantly higher than those of the 5,000 and 10,000 cycles groups (p<0.001). Moreover, the bond strength of the 5,000 cycles group was significantly higher than that of the 10,000 cycles group (p<0.001). In the UBQ groups, the bond strength of the 0 cycle group was significantly higher than those of the 5,000 and 10,000 cycles groups (p<0.001). However, there was no statistically significant difference in the bond strength between the 5,000 and 10,000 cycles groups (p>0.05). In the PBU groups, there was no statistically significant difference in the bond strength between the 0 and 5,000 cycles groups (p>0.05). Moreover, there was no difference in the bond strength of the 5,000 and 10,000 cycles groups (p>0.05). Meanwhile, the bond strength of the 0 cycle group was significantly higher than that of the 10,000 cycles group (p<0.001). Regarding the failure mode observation, there was no statistically significant differ-

ence in all groups.

2. SEM observations of ultra-structural features after acid-base challenge

Typical interface morphologies after the acid-base challenge are shown in Fig. 3. An outer lesion (OL), created by the dissolution of dentin due to the acid-base challenge, was observed in the three groups. The depth of OL ranged from 15 to 20 μm in all specimens. ABRZ was observed in all groups. The zone was approximately less than 1 μm thick. Moreover, a funnel-shaped erosion was observed at the junction of the dentin and bonding layer in all groups. A funnel-shaped erosion was clearly observed in OPB and PBU. On the other hand, a funnel-shaped erosion was observed in UBQ, but not clearly.

Discussion

For 5,000 thermal cycle challenges, μTBS results showed different trends among the three groups. Of the three universal adhesives, only the OPB group showed a statistically significant deterioration in μTBS at both 5,000 and 10,000 cycles. Both UBQ and PBU contain multifunctional hydrophilic amide monomers. A multifunctional hydrophilic amide monomer is more hydrophilic before polymerization and more hydrophobic after polymerization than previously used hydrophilic
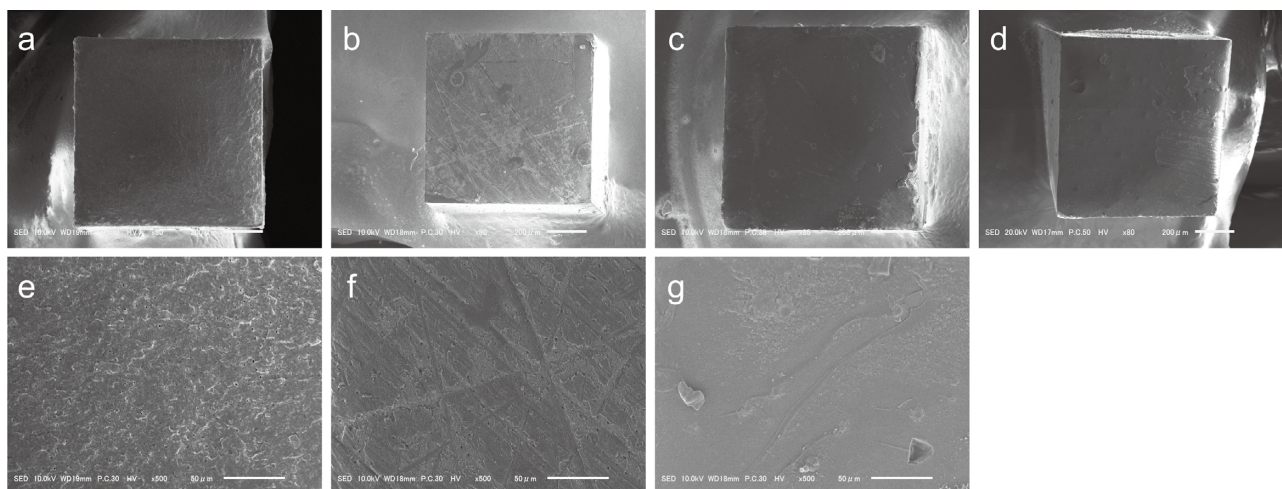
Fig. 3　Representative SEM images of failure site

(a) C-D：cohesive failure in the dentin with ＞80% of total bonding area, magnification of 80×. (b) I-DA：interfacial failure between dentin and adhesive with ＞80% of total bonding area, magnification of 80×. (c) C-A：cohesive failure in adhesive with ＞80% of total bonding area, magnification of 80×. (d) Mix：mixed failure, magnification of 80×. (e) C-D, magnification of 500×. (f) I-DA, magnification of 500×. (g) C-A, magnification of 500×.

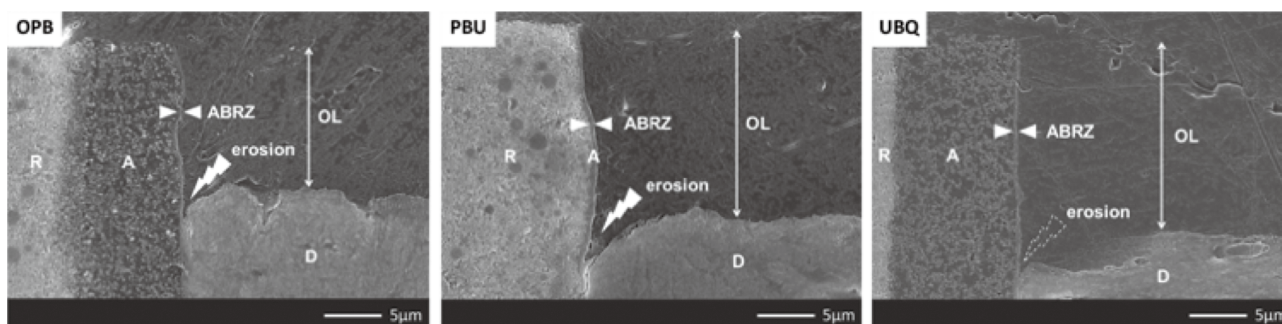**Fig. 4**　SEM images of dentin-adhesive interface after acid-base challenge, magnification of 3,500×

OL：outer lesion, R：resin composite, A：adhesive layer, D：dentin, ABRZ：acid-base resistant zone, OPB：SEM image of OptiBond Universal, PBU：SEM image of Prime&Bond Universal, UBQ：SEM image of Clearfil Universal Bond Quick ER.

ABRZ was observed in all groups. In OPB and PBU a funnel-shaped erosion was clearly observed at the junction of the dentin and bonding layer, whereas a funnel-shaped erosion was not clearly observed in UBQ.

monomers, and also has excellent mechanical properties[11]. Therefore, these characteristics of hydrophilic amide monomer might contribute to the bond strength after the thermal cycles of UBQ and PBU.

Furthermore, the PBU group results showed no statistically significant difference between 0 cycle and 5,000 cycles （p＞0.05）. In this study, only PBU does not contain 2-hydroxyethyl methacrylate （HEMA）. The hydrophilic monomer HEMA has been commonly incorporated into adhesive formulations to improve dentin bond strength because it enhances wetting of the dentin subsurface[12]. However, HEMA after polymerization exhibits hydrophilic properties, leading to water uptake after polymerization[13]. Thus, HEMA-containing SEAs are more hydrophilic[14], exhibit higher water sorption[15] and show an accelerated reduction in the mechanical properties of the adhesive layer during water storage[16]. Additionally, some studies[12,17–20] reported that HEMA reduces the long-term durability of adhesive. From the results of earlier studies and this study, it could be inferred that PBU showed more resistance to the thermal cycle test than other adhesives.

For dentin bonding, the hybridization theory has been widely accepted, in which a resin monomer pene-

trates into demineralized dentin and polymerizes *in situ*, resulting in the formation of a hybrid layer, which is an intermingling of resin with the collagen fibers of the dentin[21,22]. In 2004, Tsuchiya et al.[23] first reported a new zone adjacent to the visible hybrid layer in 2SEA characterized by the resistance to acid and base challenges, which was identified from a part of the hybrid layer by argon etching. This zone indicated higher microhardness than the hybrid layer, and was characterized by tooth-like structures under SEM observation[23]. Hence, it is different from the conventional hybrid layer and caries-inhibition zone in fluoride-releasing materials. It was therefore named "ABRZ," and is considered to play an important role in preventing secondary caries, sealing restoration margins, and promoting restoration durability[21]. However, ABRZ formation has been confirmed only in SEA systems, but not in etch and rinse systems[21,24]. Furthermore, it was reported that ABRZ is not formed depending on the type of functional monomer[25]. In this experiment, all groups formed ABRZ. Previous studies[7,26] demonstrated that ABRZ was formed using 2SEA containing MDP or GPDM. In this study, it was newly confirmed that GPDM contained in universal adhesives also forms ABRZ. Meanwhile, some researches[7,27] reported that it was difficult to detect the hybrid layer at the interface of 1SEA, even though the hybrid layer was detected with 2SEA. Similarly, the hybrid layer was not clearly observed using universal adhesives in this study. Some studies[7,26,28] reported that even if ABRZ is formed, a funnel-shaped erosion adjacent to ABRZ indicates a vulnerable region to acid-base attacks. It was reported that a universal adhesive that contains MDP creates ABRZ with a funnel-shaped erosion[7,26], and that a funnel-shaped erosion was not observed in 2SEA containing MDP or GPDM[7,26]. In contrast to 2SEA, in this study, all groups formed a funnel-shaped erosion, regardless of the type of functional monomer.

Universal adhesives contain hydrophobic monomers, hydrophilic monomers, water, and solvents in one bottle. Hence, universal adhesives are a complex mixture of hydrophilic and hydrophobic compounds and water, so they contain solvents such as ethanol or acetone to maintain miscibility[29,30]. Meanwhile, solvent and water evaporation is essential because residual solvent and water adversely affect the polymerization of the adhesive[12,31-34]. However, complete evaporation of the solvent and water is clinically difficult[35]. Therefore, the degree of polymerization of universal adhesives is generally inferior to that of 2SEAs[5]. These properties of universal adhesives could make a vulnerable region adjacent to the bonding interface, resulting in the formation of a funnel-shaped erosion after the acid-base challenge. In contrast, in this experiment, a funnel-shaped erosion was clearly observed in OPB and PBU, but not in UBQ. Previous studies of ABRZ[36,37] reported the formation of a slope shape, sloping upward to the end of the outer lesion, without a funnel-shaped erosion observed when using SEAs containing NaF. The formation of a slope shape indicates improved acid resistance. From these reports, NaF might improve the acid-base resistance adjacent to the bonding interface[36,37]. Meanwhile, the formation of a funnel-shaped erosion indicates that the acid-base resistance of the region directly below the ABRZ is reduced. In this experiment, a funnel-shaped erosion was not clearly observed in UBQ, probably because the decrease in acid-base resistance was compensated for by the inclusion of NaF. From these results, the null hypothesis of this study was rejected.

Conclusion

After thermal cycling, the bond strength test appeared to be influenced by the hydrophilic amide monomer (PBU and UBQ) or HEMA (OPB and UBQ). For SEM observation after the acid-base challenge, ABRZ formation was detected using universal adhesives containing MDP (PBU and UBQ) or GPDM (OPB). Moreover, a funnel-shaped erosion adjacent to ABRZ was not clearly observed in a universal adhesive containing NaF (UBQ), but was clearly observed in others (OPB and PBU). Therefore, the results of this study suggest that the durability of the bonding between universal adhesives and dentin depends on material components.

References

1) Seitoku E, Hoshika S, Ikeda T, Abe S, Tanaka T, Sano H. Bonding performance of a hydrophilic amide monomer containing adhesive to occlusal and cervical dentin. Materials (Basel) 2020; 13: 4727.

2) Van Meerbeek B, De Munck J, Yoshida Y, Inoue S, Vargas M, Vijay P, Van Landuyt K, Lambrechts P, Vanherle G. Buonocore memorial lecture. Adhesion to enamel and dentin: Current status and future challenges. Oper Dent 2003; 28: 215–235.

3) Perdigão J, Kose C, Mena-Serrano AP, De Paula EA, Tay LY, Reis A, Loguercio AD. A new universal simplified adhesive: 18-month clinical evaluation. Oper Dent 2014; 39: 113–127.

4) Giannini M, Makishi P, Ayres AP, Vermelho PM, Fronza BM, Nikaido T, Tagami J. Self-etch adhesive systems: A literature review. Braz Dent J 2015; 26: 3–10.

5) Sato T, Takagaki T, Hatayama T, Nikaido T, Tagami J. Update on enamel bonding strategies. Front Dent Med 2021; 2: 666379.

6) Nikaido T, Takagaki T, Sato T, Burrow MF, Tagami J. Fluoride-releasing self-etch adhesives create thick ABRZ at the interface. Biomed Res Int 2021; 2021: 9731280.

7) Guan R, Takagaki T, Matsui N, Sato T, Burrow MF, Palamara J, Nikaido T, Tagami J. Dentin bonding performance using Weibull statistics and evaluation of acid-base resistant zone formation of recently introduced adhesives. Dent Mater J 2016; 35: 684–693.

8) Inoue G, Nikaido T, Foxton RM, Tagami J. The acid-base resistant zone in three dentin bonding systems. Dent Mater J 2009; 28: 717–721.

9) Vicheva M, Sato T, Takagaki T, Baba Y, Ikeda M, Burrow MF, Nikaido T, Tagami J. Effect of repair systems on dentin bonding performance. Dent Mater J 2021; 40: 903–910.

10) Nakamoto A, Sato T, Matsui N, Ikeda M, Nikaido T, Burrow MF, Tagami J. Effect of fluoride mouthrinse and fluoride concentration on bonding of a one-step self-etch adhesive to bovine root dentin. J Oral Sci 2019; 61: 125–132.

11) Kuno Y, Hosaka K, Nakajima M, Ikeda M, Klein Junior CA, Foxton RM, Tagami J. Incorporation of a hydrophilic amide monomer into a one-step self-etch adhesive to increase dentin bond strength: Effect of application time. Dent Mater J 2019; 38: 892–899.

12) Van Landuyt KL, Snauwaert J, De Munck J, Peumans M, Yoshida Y, Poitevin A, Coutinho E, Suzuki K, Lambrechts P, Van Meerbeek B. Systematic review of the chemical composition of contemporary dental adhesives. Biomaterials 2007; 28: 3757–3785.

13) Ito S, Hashimoto M, Wadgaonkar B, Svizero N, Carvalho RM, Yiu C, Rueggeberg FA, Foulger S, Saito T, Nishitani Y, Yoshiyama M, Tay FR, Pashley DH. Effects of resin hydrophilicity on water sorption and changes in modulus of elasticity. Biomaterials 2005; 26: 6449–6459.

14) Yiu CK, King NM, Carrilho MR, Sauro S, Rueggeberg FA, Prati C, Carvalho RM, Pashley DH, Tay FR. Effect of resin hydrophilicity and temperature on water sorption of dental adhesive resins. Biomaterials 2006; 27: 1695–1703.

15) Malacarne J, Carvalho RM, de Goes MF, Svizero N, Pashley DH, Tay FR, Yiu CK, Carrilho MR, de Oliveira Carrilho MR. Water sorption/solubility of dental adhesive resins. Dent Mater 2006; 22: 973–980.

16) Takahashi M, Nakajima M, Hosaka K, Ikeda M, Foxton RM, Tagami J. Long-term evaluation of water sorption and ultimate tensile strength of hema-containing/-free one-step self-etch adhesives. J Dent 2011; 39: 506–512.

17) Van Landuyt KL, Snauwaert J, De Munck J, Coutinho E, Poitevin A, Yoshida Y, Suzuki K, Lambrechts P, Van Meerbeek B. Origin of interfacial droplets with one-step adhesives. J Dent Res 2007; 86: 739–744.

18) Itoh S, Nakajima M, Hosaka K, Okuma M, Takahashi M, Shinoda Y, Seki N, Ikeda M, Kishikawa R, Foxton RM, Tagami, J. Dentin bond durability and water sorption/solubility of one-step self-etch adhesives. Dent Mater J 2010; 29: 623–630.

19) Shinoda Y, Nakajima M, Hosaka K, Otsuki M, Foxton RM, Tagami J. Effect of smear layer characteristics on dentin bonding durability of HEMA-free and HEMA-containing one-step self-etch adhesives. Dent Mater J 2011; 30: 501–510.

20) Van Landuyt KL, Snauwaert J, Peumans M, De Munck J, Lambrechts P, Van Meerbeek B. The role of HEMA in one-step self-etch adhesives. Dent Mater 2008; 24: 1412–1419.

21) Matsui N, Takagaki T, Sadr A, Ikeda M, Ichinose S, Nikaido T, Tagami J. The role of MDP in a bonding resin of a two-step self-etching adhesive system. Dent Mater J 2015; 34: 227–233.

22) Gale MS, Darvell BW. Thermal cycling procedures for laboratory testing of dental restorations. J Dent 1999; 27: 89–99.

23) Tsuchiya S, Nikaido T, Sonoda H, Foxton RM, Tagami J. Ultrastructure of the dentin-adhesive interface after acid-base challenge. J Adhes Dent 2004; 6: 183–190.

24) Inoue G, Tsuchiya S, Nikaido T, Foxton RM, Tagami J. Morphological and mechanical characterization of the acid-base resistant zone at the adhesive-dentin interface of intact and caries-affected dentin. Oper Dent 2006; 31:

466–472.

25) Li N, Nikaido T, Takagaki T, Sadr A, Makishi P, Chen J, Tagami J. The role of functional monomers in bonding to enamel: Acid-base resistant zone and bonding performance. J Dent 2010; 38: 722–730.

26) Sato T, Takagaki T, Matsui N, Hamba H, Sadr A, Nikaido T, Tagami J. Morphological evaluation of the adhesive/enamel interfaces of two-step self-etching adhesives and multimode one-bottle self-etching adhesives. J Adhes Dent 2016; 18: 223–229.

27) Inoue G, Nikaido T, Sadr A, Tagami J. Morphological categorization of acid-base resistant zones with self-etching primer adhesive systems. Dent Mater J 2012; 31: 232–238.

28) Nikaido T, Takagaki T, Sato T, Burrow MF, Tagami J. The concept of super enamel formation—Relationship between chemical interaction and enamel acid-base resistant zone at the self-etch adhesive/enamel interface. Dent Mater J 2020; 39: 534–538.

29) De Munck J, Van Landuyt K, Peumans M, Poitevin A, Lambrechts P, Braem M, Van Meerbeek B. A critical review of the durability of adhesion to tooth tissue: Methods and results. J Dent Res 2005; 84: 118–132.

30) Van Landuyt KL, Peumans M, De Munck J, Lambrechts P, Van Meerbeek B. Extension of a one-step self-etch adhesive into a multi-step adhesive. Dent Mater 2006; 22: 533–544.

31) Suh BI, Feng L, Pashley DH, Tay FR. Factors contributing to the incompatibility between simplified-step adhesives and chemically-cured or dual-cured composites. Part iii. Effect of acidic resin monomers. J Adhes Dent 2003; 5: 267–282.

32) Frankenberger R, Strobel WO, Lohbauer U, Krämer N, Petschelt A. The effect of six years of water storage on resin composite bonding to human dentin. J Biomed Mater Res B Appl Biomater 2004; 69: 25–32.

33) Tay FR, Pashley DH, Suh BI, Hiraishi N, Yiu CK. Water treeing in simplified dentin adhesives—déjà vu? Oper Dent 2005; 30: 561–579.

34) Loguercio AD, Loeblein F, Cherobin T, Ogliari F, Piva E, Reis A. Effect of solvent removal on adhesive properties of simplified etch-and-rinse systems and on bond strengths to dry and wet dentin. J Adhes Dent 2009; 11: 213–219.

35) Ikeda T, De Munck J, Shirai K, Hikita K, Inoue S, Sano H, Lambrechts P, Van Meerbeek B. Effect of evaporation of primer components on ultimate tensile strengths of primer-adhesive mixture. Dent Mater 2005; 21: 1051–1058.

36) Kirihara M, Inoue G, Nikaido T, Ikeda M, Sadr A, Tagami J. Effect of fluoride concentration in adhesives on morphology of acid-base resistant zones. Dent Mater J 2013; 32: 578–584.

37) Kakiuchi Y, Takagaki T, Ikeda M, Sato T, Matsui N, Nikaido T, Burrow MF, Tagami J. Evaluation of MDP and NaF in two-step self-etch adhesives on enamel microshear bond strength and morphology of the adhesive-enamel interface. J Adhes Dent 2018; 20: 527–534.

Case Report

A Case of Non-surgical Root Canal Treatment Using an Operating Microscope on Type III-b Dens Invaginatus

Masashi Yamada[1,5], Kento Odaka[2,5], Norio Kasahara[3,5],
Satoru Matsunaga[4,5], Yoshiki Tamiya[1], Ryo Sako[1]
and Masahiro Furusawa[1]

[1]Department of Endodontics, Tokyo Dental College
[2]Department of Oral and Maxillofacial Radiology, Tokyo Dental College
[3]Histology and Developmental Biology and Clinical Pathophysiology, Tokyo Dental College
[4]Department of Anatomy, Tokyo Dental College
[5]Oral Health Science Center, Tokyo Dental College

Abstract

　Dens invaginatus is a developmental malformation, in which there is an infolding of enamel into dentin. It is prevalent in maxillary lateral incisors, with a relatively high incidence of 0.3-10%. However, the morphology is complex and therefore its diagnosis and treatment are difficult. We report a case of endodontic treatment of dens invaginatus with a root apex lesion by non-surgical root canal treatments using an operating microscope to preserve the pulp.

　Case report: The patient was a 23-year-old male. He had no spontaneous pain but had an abscess of the maxillary left lateral incisor. The pulp was diagnosed as reversible pulpitis. Transient pain occurred upon cold stimulation. Percussion and palpation pain were noted. The periodontal pocket depth was ≦3 mm all around the tooth. Dental X-rays showed invagination in the central part of the root canal and there were pathways of communication with the periodontal tissue at the root apex. CBCT was taken to understand the root canal morphology. Oehlers type III-b dens invaginatus was diagnosed, with apical periodontitis due to infection via the invagination despite a normal tooth pulp morphology. Therefore, root canal treatment of the invagination was performed using a microscope and pulp preservation was anticipated. Both oral and written informed consent were obtained from the patient prior to treatment, and a full explanation of the research purpose was given. A manual stainless-steel file was then used to explore the route through the pseudo-root canal and was passed through it, and the root canal length was measured with an electronic apex locator. After confirming that the root canal length was correct, the working length was set at a point 0.5 mm shorter than the root canal length. Preparation was performed using Ni-Ti rotary files. After final irrigation of the root canal, filling was performed with MTA cement. The entrance of the invagination was sealed with an adhesive resin.

　Course: The clinical symptoms disappeared after one year. The case was diagnosed as "healing" due to the diminishing apical radiolucency on dental X-ray and CBCT.

　Discussion: In this case, we were able to magnify the invagination to the minimum necessary by using an operating microscope. The use of MTA cement enabled tight sealing and protection of the pulp, which may have resulted in good healing.

　Conclusions: An operating microscope may be useful in the treatment of dens invaginatus.

Key words: dens invaginatus, Oehlers' type III-b, CBCT, operating microscope

Introduction

Dens invaginatus, also known as tooth within a tooth, is a condition in which there is invagination of the enamel and dentin of a tooth crown into the pulp cavity[1]; its mean prevalence is reported to be 0.3–10%. Around 90% of reported cases have involved the maxillary lateral incisors[2], and it has been shown to be more frequent in particular ethnic groups[3-5].

Although numerous different classification methods have been reported, Oehler's classification, which is based on the depth of incursion of the invagination and its positional relationship with the cementoenamel junction(CEJ), is generally used[5]. Studies of the prevalence of different classes have not identified any racial differences, with type I being the most frequent and type III the most uncommon[6,7]. This is also the case in Japanese patients[8]. Type III has two subtypes, with invaginations that communicate laterally with the periapical tissue designated as type III-a and those that communicate via the apical foramen as type III-b. Because these invaginations are completely separate from the pulp cavity, they may cause large apical lesions even in vital teeth. Such cases are difficult to treat and diagnose, but cases in which the tooth pulp has been conserved by successful treatment of the invagination in the same way as an infected root canal (pseudo-root canal) have been reported[9]. This report describes an attempt to conserve the tooth pulp of a type III-b dens invaginatus with an apical lesion that nevertheless exhibited a vital reaction by performing non-surgical root canal treatment using an operating microscope.

Case Report

Patient: 23-year-old man

Chief complaint: Unable to bite due to swelling of the gingiva of the left upper front teeth

Location: Maxillary left lateral incisor

General medical history: Nothing of note

History of present illness: The patient was examined for root canal treatment of a malformed tooth at the request of his previous dentist. A hole had appeared on the lingual side of the maxillary left lateral incisor two months before and this had been filled. The patient said that the gingiva had been swollen since the previous week. On inspection, the maxillary left lateral incisor had a wide tooth crown and a lingual-side composite resin filling, and the gingiva in the apical region was reddened (Figure 1-a). In terms of clinical symptoms, cold stimulation elicited transient pain, and the tooth exhibited a normal pulp reaction in comparison with that of the neighboring teeth, but percussion pain, apical palpation, and some mobility were evident. The periodontal pocket depth was ≤3 mm all around the tooth and some degree of tooth mobility was evident. On a panoramic X-ray image that the patient brought from the previous doctor, the maxillary left lateral incisor showed root hypertrophy, and its appearance suggested dens invaginatus. Dental X-ray imaging was therefore performed for further investigation(Figure 1-b), and an invagination that reached the apex of the root was found in the center of the tooth; there was no obvious caries-like radiolucency in the crown, but an apical radiolucency was apparent around the hypertrophic root apex. On the basis of these findings, Oehler's type III-b dens invaginatus was diagnosed, with apical periodontitis due to infection via the invagination despite a normal tooth pulp morphology. When embarking on treatment, additional cone-beam computed tomography (CBCT) was performed to evaluate the shape of the invagination and its positional relationship with the lesion(Figure 2). On the CBCT images, the enamel was invaginated from the incisal tip toward the apex and communicated with the periodontal tissue, so that the invagination appeared similar to a root canal (pseudo-root canal). In part of the interior of this pseudo-root canal, the enamel was partially cut off and the dentin was exposed. The apical radiolucency included the opening of the invagination, and a part of the buccal-side cortical bone defect was evident in the sagittal section. The slice data acquired by CBCT were used to create a three-dimensional (3D) reconstruction image and a 3D model for use in treatment planning. The 3D model was printed with a 3D printer(Objet260 Connex, Stratasys, Eden Prairie, MN, USA) using transparent biocompatible resin (MED610, Stratasys) (Figure 3).

On the 3D reconstruction image, there was no obvious communication between the main root canal and the pseudo-root canal. On the 3D-printed model, the pulp cavity was observed to surround the pseudo-root canal in a C-shape. The pulpal horn was present up to a comparatively high position. Based on these findings, a
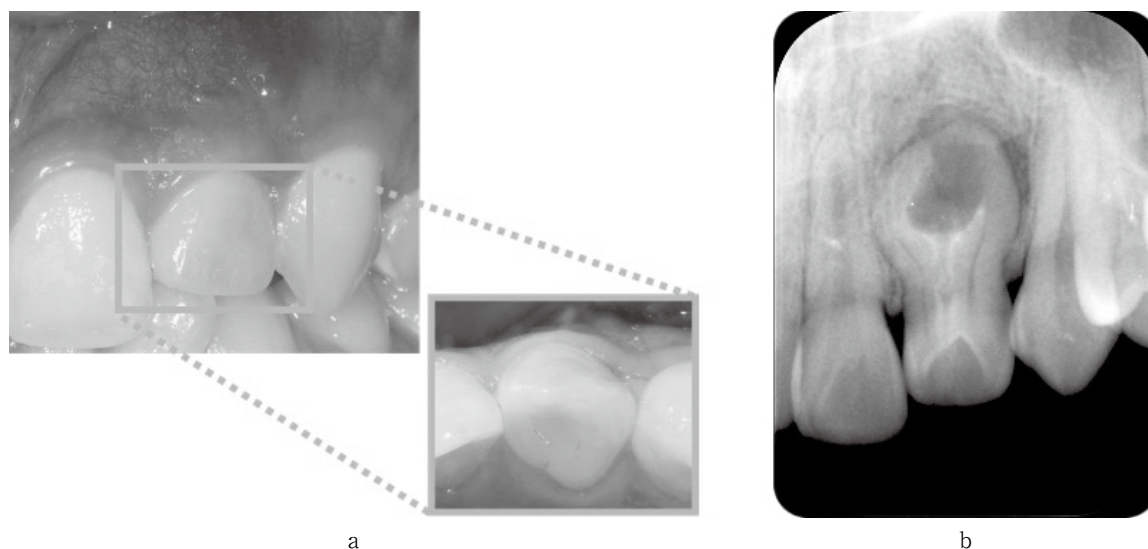
Fig. 1　Pre-treatment images of maxillary left lateral incisor
(a) Intraoral photographs showing a wide crown of the lateral incisor. (b) Dental X-ray image showing an enlarged root and an invagination penetrating to the root apex.
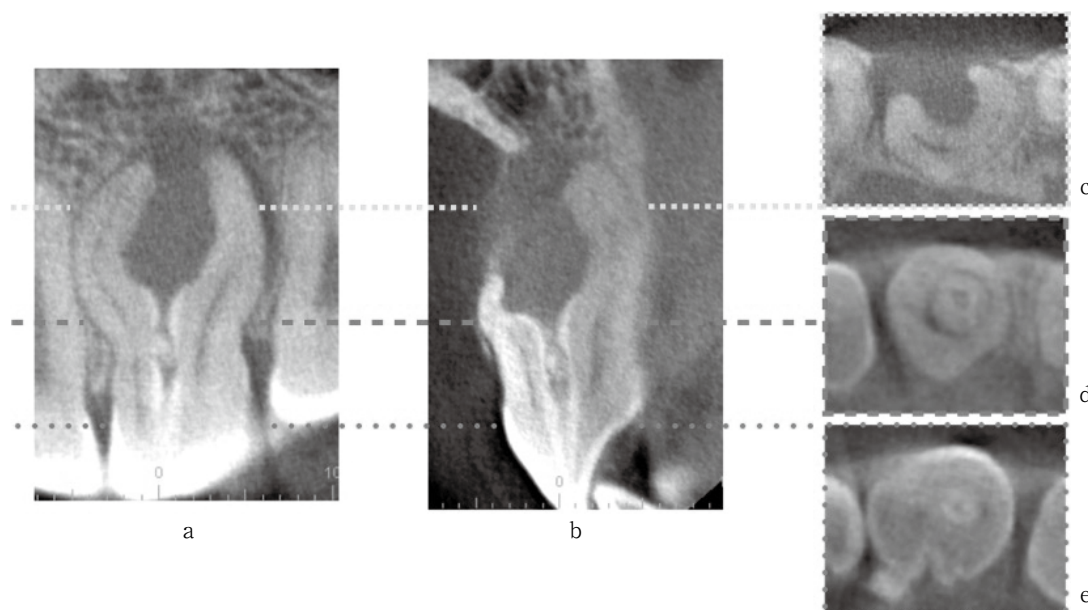

Fig. 2　Pre-treatment CBCT images of maxillary left lateral incisor
The cortical bone of the buccal side is missing.
(a) Frontal section. (b) Sagittal section. (c),(d) Transverse sections.

treatment plan was formulated consisting of non-surgical treatment under surgical microscopic observation, with the aim of preserving the pulp by treating the pseudo-root canal as a root canal.

In line with the Declaration of Helsinki, the purpose of the study and the treatment plan were explained orally and in writing to the patient, who, having fully understood them, consented to take part. Treatment was then started in compliance with the ethical regulations of Tokyo Dental College (Tokyo Dental College Ethics Committee approval no. 999).

Treatment: Root canal treatment of the pseudo-root canal.

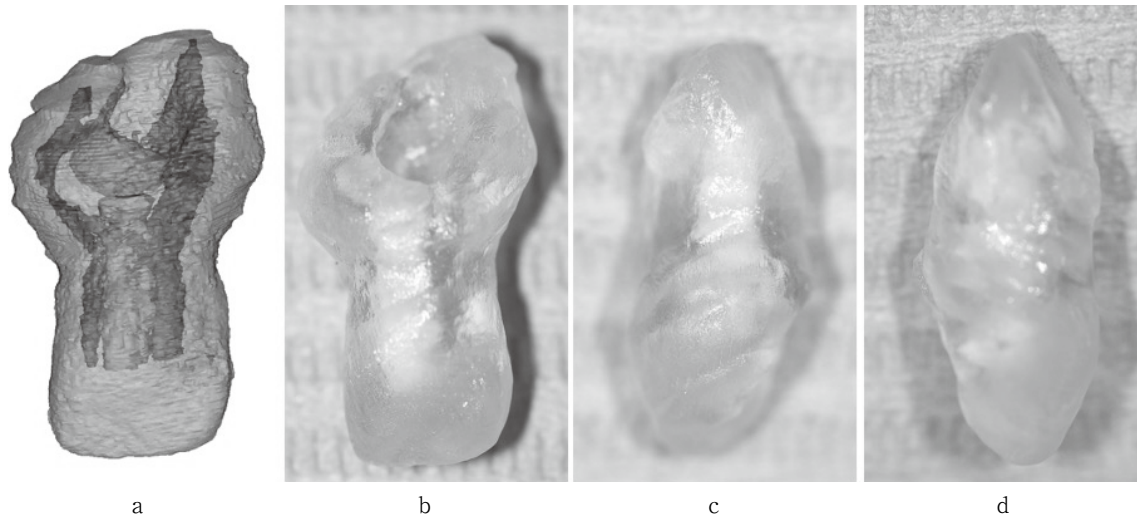The composite resin closing the invagination was

a   b   c   d

Fig. 3 3D construction images of maxillary left lateral incisors
(a) 3D construction image. (b) 3D printer output buccal-side model. (c) 3D printer output distal-side
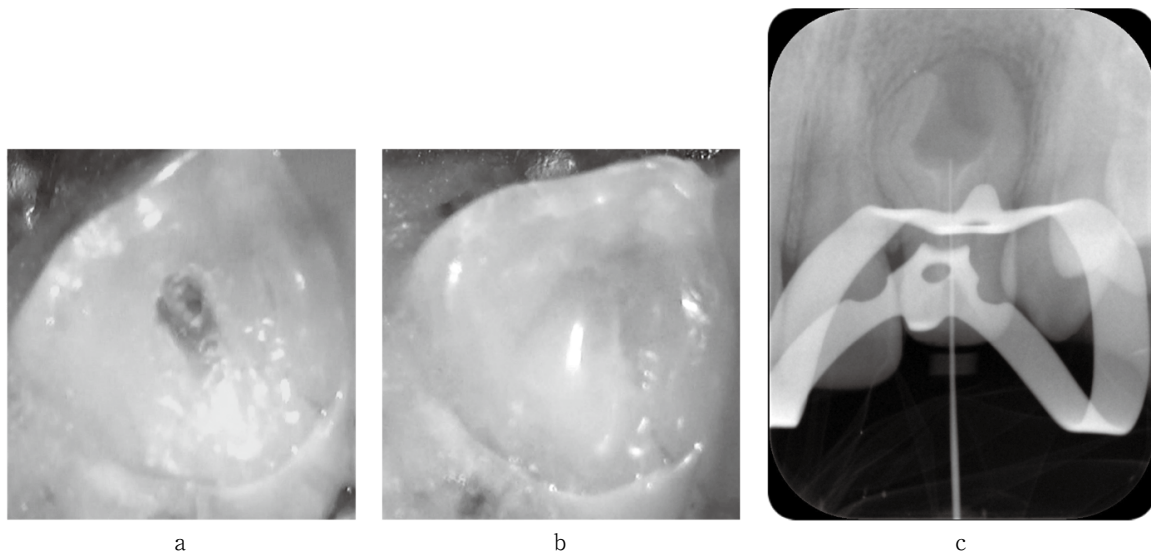model. (d) 3D printer output mesial-side model.

a   b   c

Fig. 4 Enlargement of the dens invaginatus opening and negotiation
(a) After enlargement of the dens invaginatus opening. (b) Drainage from the pseudo-root canal.
(c) Dental X-ray with a trial file at the root canal length.

removed with a diamond turbine bur, after which the enamel of the invagination was drilled away. A manual stainless-steel file was then used to explore the route through the pseudo-root canal and was passed through it. There was a purulent discharge from the pseudo-apex, which was aspirated using a root canal vacuum. When no more pus was discharged, an electronic apex locator was used to measure the length of the root canal. A file was inserted into the root canal up to this measured length, and a dental X-ray was taken to con-

firm that this length was in fact correct. The working length was then designated as a point 0.5 mm proximal to the root canal length (Figure 4). The hardness of the enamel in the upper part of the pseudo-root canal meant that the entrance had not been sufficiently enlarged, and this was therefore further enlarged using a diamond-coated ultrasonic tip. Because exploration with the manual file showed that the inner surface of the pseudo-root canal felt softer to drill, it was enlarged to #60 with a Ni-Ti rotary file (Hi-Flex CM, Coltene
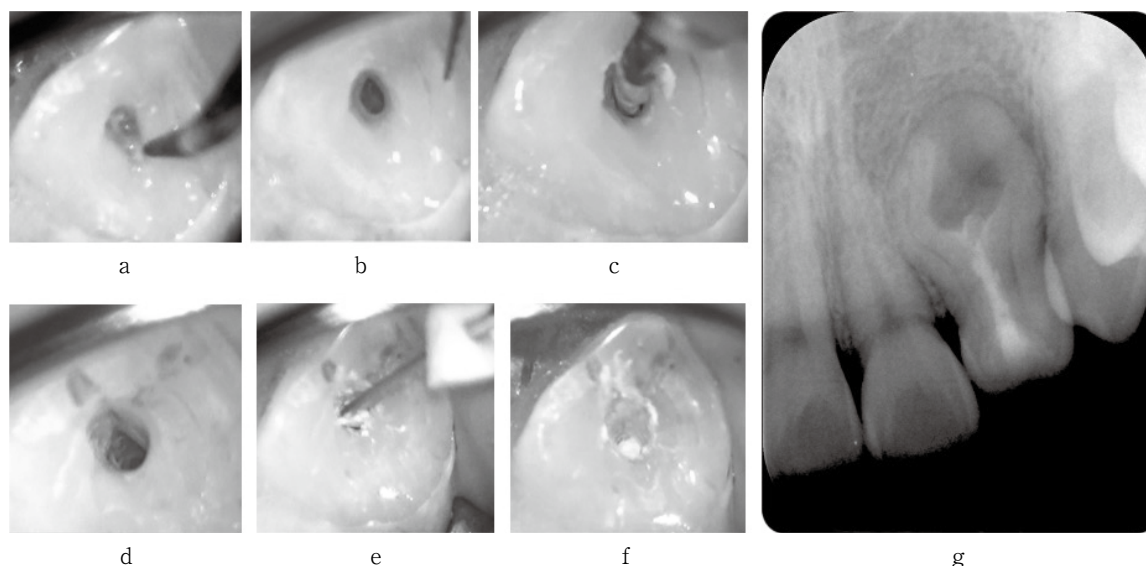
Fig. 5   Intraoperative images of maxillary left lateral incisor

(a) Before enlargement of the dens invaginatus opening. (b) After enlargement of the dens invaginatus opening with ultrasonic instruments. (c) Enlargement of the pseudo-root canal. (d) After cleaning the pseudo-root canal. (e),(f) Filling the pseudo-root canal with MTA cement. (g) After filling the pseudo-root canal.

Whaledent, Cuyahoga Falls, OH, USA). However, because there were some hard parts of the inner surface of the pseudo-root canal, it was thought that it might not have been sufficiently enlarged, and chemical cleaning was therefore performed more thoroughly than during normal root canal treatment. Passive ultrasonic irrigation (PUI) was performed using 2.5% NaOCl and an ultrasonic tip. A final cleaning of the inside of the pseudo-root canal was conducted using 2.5% NaOCl and 17% ethylenediaminetetraacetic acid (EDTA), after which it was dried with a root canal vacuum. The pseudo-root canal was filled with mineral trioxide aggregate (MTA) cement. A rubber stopper was fitted to a root canal filling plugger, and incremental filling was performed while taking care that nothing escaped from the pseudo-apex into the periapical tissue. The use of MTA as a root filling material was approved by the Ethics Committee of Tokyo Dental College Suidobashi Hospital (approval no. SH-41). After pseudo-root canal filling, the entrance to the invagination was closed with composite resin, and dental X-rays were then taken (Figure 5).

Clinical Course

Three months after non-surgical root canal treatment, the clinical symptoms had disappeared, and dental X-rays showed that the radiolucency had decreased in size. One year after filling, there was no change in symptoms, but on dental X-rays, a radiolucency was still present on the inner curve (Figure 6). CBCT scanning was performed to evaluate whether the buccal-side bone had healed. On CBCT images, a radiolucency was still evident on the inner curve of the invagination, but since regeneration of the buccal-side cortical bone was observed, it was considered to be healing (Figure 7).

Discussion

In the treatment of type III dens invaginatus with an apical lesion, if the tooth pulp exhibits a vital reaction, it is reportedly possible to conserve the pulp by treating the pseudo-root canal[10-12]. However, issues of concern in the treatment of pseudo-root canals include: (1) the inner surface of the invagination is covered with enamel and irregular in shape; (2) in parts of the inner surface, dentin is exposed, and the pulp is closely adjacent; and (3) the pseudo-apical foramen is wide open[10]. In the present case, the following two issues were also considered for the three risk factors. The first issue was the appropriate instrument to use for cleaning out the pseudo-root canal. The instruments reported in studies can be broadly divided into three types: manual
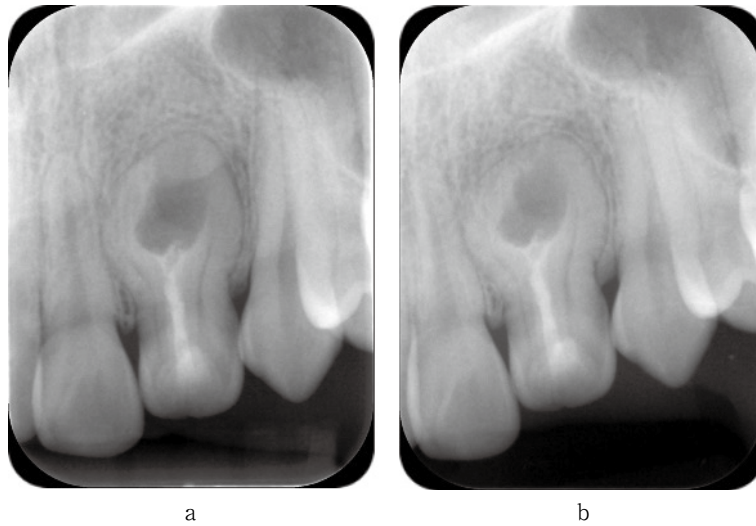
Fig. 6 Post-treatment X-rays of the maxillary left lateral incisors
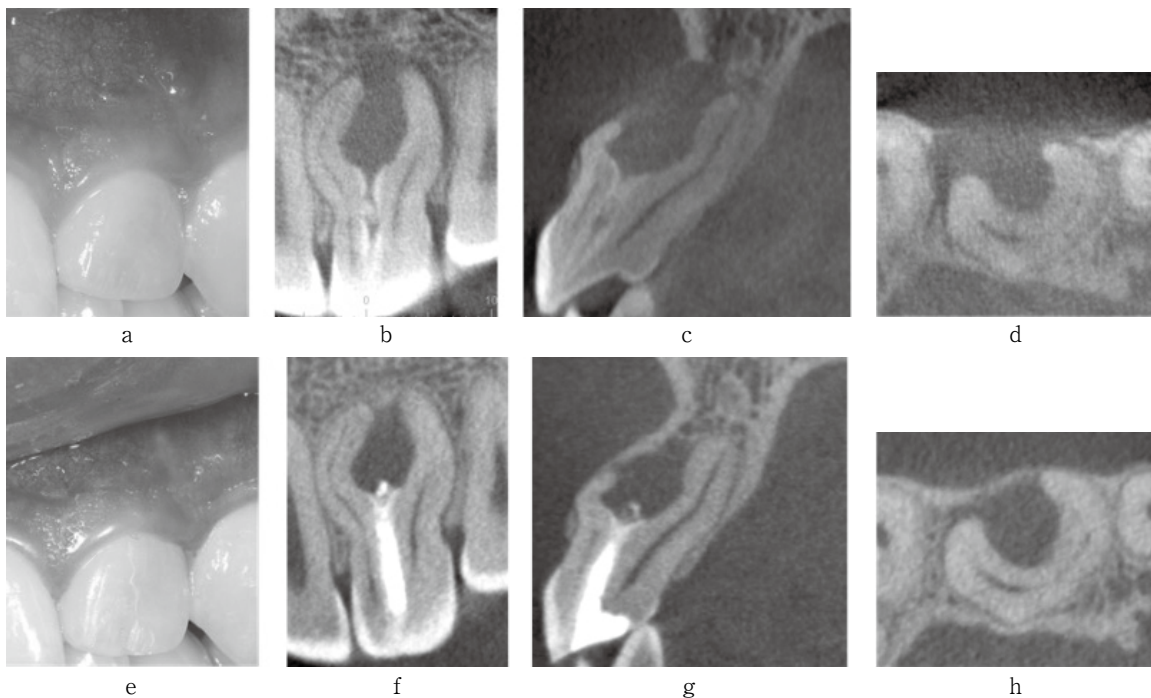(a) Three months after root canal filling. (b) Twelve months after
root canal filling.

Fig. 7 Pre-treatment and post-treatment images
(a) Pre-treatment intraoral photographs. (b)‒(d) Pre-treatment CBCT images. (e) Post-treatment intra-
oral photographs. Loss of sinus tract was observed. (f)‒(h)Post-treatment CBCT images. Bone regeneration
was observed at the root apex and buccal side.

drilling instruments, rotary drilling instruments, and ultrasound drilling instruments. Manual drilling instruments enable the torque during enlargement to be controlled by the operator, preventing instrument fracture and enabling safe treatment, and their use has been widely reported[9,11]. In the present case, the enamel at the invagination entrance was hard, and the inner surface of the pseudo-root canal was irregular. Hard areas were therefore encountered at various points on the inner surface, and a manual instrument could not be

used because the drilling sensation was difficult to distinguish. With respect to rotary drilling instruments, there have been some reports on the use of Gates-Glidden drills in combination with manual drilling instruments[9,13], but if the enamel of the inner surface of the invagination is hard, then drilling with them is also difficult. The use of a Ni-Ti rotary file has also been reported in a few cases[14]. In the present patient, because most of the inner surface of the pseudo-root canal was covered with enamel, the areas of advanced caries had softened and could be drilled away, but the other parts could not be sufficiently drilled. Rotary drilling instruments may be captured by the enamel inside the pseudo-root canal, and if torsion stress is generated, they may break[10]. Their use thus requires caution and care. Ultrasound instruments are reportedly capable of efficiently enlarging and removing the invagination[15], and they can enable sufficient debridement when used in conjunction with cleaning[16]; in the present case, one was useful for drilling out the invagination entrance and debridement during the PUI of the inside of the pseudo-root canal. Ultrasound instruments can also be used under surgical microscopic observation, which enables safe, minimally invasive treatment. We therefore consider ultrasound instruments to be ideal for use in cleaning dens invaginatus. The second issue was which material and method to use for filling the pseudo-root canal. In this case, the pseudo-root canal was closely adjacent to the pulp based on the diagnosis using a 3D model, and pulp irritation and infection during enlargement and filling were both concerns. It is well known that MTA cement causes little damage to pulp, and it is recommended as a pulp capping agent[17], reportedly providing good long-term closure and therapeutic outcomes[18]. We therefore considered that the use of MTA cement was appropriate to prevent pulp irritation and infection. Because the pseudo-apex was wide open, we had to consider the possibility that the filling agent might escape into the periapical tissue. In the conventional root canal filling method using gutta-percha, lateral and vertical condensation filling techniques have been reported[11], but in both techniques, the filling agent may escape, and caution is therefore required. Good results have been reported from the use of MTA cement even when the apical foramen is wide open[18,19], and it may therefore be suitable for filling pseudo-root canals. In addition, the success of the treatment was

due to the fact that we were able to select the appropriate filling method based on the diagnosis using the 3D model in advance[20]. Another report has also noted that, after root canal treatment of a type III dens invaginatus with similar morphology, a radiolucency on the inner curve of the root persisted for a long time despite the absence of clinical symptoms[21]. In that report by Sübay et al., the radiolucency on the inner curve of the root persisted for 3 years after pseudo-root canal treatment with no evident clinical symptoms. They therefore performed surgical curettage, which showed regeneration of the bone. In the present case as well, a persistent bone defect at the same site was still present after 18 months. However, it is possible that healing may have been delayed because of the large size of the bone defect, or that it may never have been filled with bone at all because of the persistence of soft tissue from the time of eruption. We will continue to monitor this case carefully, including the possibility of future surgical intervention.

Conclusion

This case demonstrated the usefulness of an operating microscope for the non-surgical, pulp-conserving treatment of type III-b dens invaginatus.

The authors state that there are no conflcts of interest related to this study.

References

1) Hallett GEM. Incidence, nature and clinical significance of palatal invagination in the maxillary incisor teeth. Proc R Soc Med 1953; 46: 491–499.
2) Hamasha AA, Alomari QD. Prevalence of dens invaginatus in Jordanian adults. Int Endod J 2004; 37: 307–310.
3) Cho SY, Ki Y, Chu V, Chan J. Concomitant developmental dental anomalies in Chinese children with dens evaginatus. Int J Paediatr Dent 2006; 16: 247–251.
4) Shi S, Duan X, Shao J, Duan Q, Peng S. Dens invaginatus in ancient Chinese teeth of 2,000 years ago. Anat Rec (Hoboken) 2013; 296: 1628–1633.
5) Oehlers FA. Dens invaginatus. I. Variations of the invagination process and associated anterior crown forms. Oral Surg Oral Med Oral Pathol 1957; 10: 1204–1218.
6) Ridell K, Mejàre I, Matsson L. Dens invaginatus: a retrospective study of prophylactic invagination treatment.

Int J Paediatr Dent 2001; 11: 92-97.

7) Capar ID, Ertas H, Arslan H, Tarim Ertas E. A retrospective comparative study of cone-beam computed tomography versus rendered panoramic images in identifying the presence, types, and characteristics of dens invaginatus in a Turkish population. J Endod 2015; 41: 473-478.

8) Gotoh T, Kawahara K, Imai K, Kishi K, Fujiki Y. Clinical and radiographic study of dens invaginatus. Oral Surg Oral Med Oral Pathol 1979; 48: 88-91.

9) Schwartz SA, Schindler WG. Management of a maxillary canine with dens invaginatus and a vital pulp. J Endod 1996; 22: 493-496.

10) Bishop K, Alani A. Dens invaginatus. Part 2: clinical, radiographic features and management options. Int Endod J 2008; 41: 1137-1154.

11) Fristad I, Molven O. Root resorption and apical breakdown during orthodontic treatment of a maxillary lateral incisor with dens invaginatus. Endod Dent Traumatol 1998; 14: 241-244.

12) Tsurumachi T. Endodontic treatment of an invaginated maxillary lateral incisor with a periradicular lesion and a healthy pulp. Int Endod J 2004; 37: 717-723.

13) Pitt Ford HE. Peri-radicular inflammation related to dens invaginatus treated without damaging the dental pulp: a case report. Int J Paediatr Dent 1998; 8: 283-286.

14) Zoya A, Ali S, Alam S, Tewari RK, Mishra SK, Kumar A, Andrabi SM. Double dens invaginatus with multiple canals in a maxillary central incisor: Retreatment and managing complications. J Endod 2015; 41: 1927-1932.

15) De Smit A, Demaut L. Nonsurgical endodontic treatment of invaginated teeth. J Endod 1982; 8: 506-511.

16) Girsch WJ, McClammy TV. Microscopic removal of dens invaginatus. J Endod 2002; 28: 336-339.

17) Mente J, Geletneky B, Ohle M, Koch MJ, Friedrich Ding PG, Wolff D, Dreyhaupt J, Martin N, Staehle HJ, Pfefferle T. Mineral trioxide aggregate or calcium hydroxide direct pulp capping: an analysis of the clinical treatment outcome. J Endod 2010; 36: 806-813.

18) Pace R, Giuliani V, Nieri M, Di Nasso L, Pagavino G. Mineral trioxide aggregate as apical plug in teeth with necrotic pulp and immature apices: a 10-year case series. J Endod 2014; 40: 1250-1254.

19) Torabinejad M, Chivian N. Clinical applications of mineral trioxide aggregate. J Endod 1999; 25: 197-205.

20) Kfir A, Telishevsky-Strauss Y, Leitner A, Metzger Z. The diagnosis and conservative treatment of a complex type 3 dens invaginatus using cone beam computed tomography (CBCT) and 3D plastic models. Int Endod J 2013; 46: 275-288.

21) Sübay RK, Kayataş M. Dens invaginatus in an immature maxillary lateral incisor: a case report of complex endodontic treatment. Oral Surg Oral Med Oral Pathol Oral Radiol Endod 2006; 102: e37-41.

Submission Guidelines for *ODEP*

1. *ODEP* aims to develop conservative dentistry (operative dentistry, endodontology, and periodontology) through the publication of research and reviews on the following topics: (1) General dental medicine, clinical practice, and education on conservative dentistry; and (2) Conservative dentistry.

2. Papers are categorized into the following four types: (1) Original articles (reports on unique research discoveries); (2) Reviews (discussions on research questions and objectives to indicate future directions, or summaries of the contents of existing papers to propose new ideas); (3) Mini reviews (concise summaries of recent topics; mini reviews include papers awarded with prizes); and (4) Case and clinical reports (analysis of clinical records useful for dental care practice and development of the field of conservative dentistry). Reviews and mini reviews are categorized into the following: (1) Papers requested by the editorial board; and (2) Submitted papers.

3. Original articles and case and clinical reports are limited to the following: (1) Papers that have not been published in other journals; (2) Papers that are not presently submitted to another journal; and (3) Papers that are not presently scheduled for publication.

4. Acceptance or rejection of papers is determined through peer review (except for papers requested by the editorial board).

5. Submitted papers should be concisely written in English.

6. In principle, original articles should be organized as follows: (1) Abstract; (2) Introduction; (3) Materials and Methods; (4) Results; (5) Discussion; (6) Conclusion; (7) References; (8) Figure legend; (9) Figures and Tables. In principle, papers other than original articles should conform to the style format of original articles.

7. In principle, *ODEP* is published once a year in December. In addition, special issues are published when appropriate.

8. The Japanese Society of Conservative Dentistry provides a certain amount of support for the listing fees of papers. For cases in which the lead author is not a member of the Japanese Society of Conservative Dentistry, such support is not provided. For cases in which the lead author is a member, but the co-authors include a non-member, partial support is provided. The cost to be borne by the authors is determined based on the number of non-members. The costs for figures, tables and photographs, for dispatching and offprints, and for creating the J‑STAGE registration data are borne by the authors. In the case of papers requested by the editorial board, such costs are exempted.

9. Date of submission is the date when the submitted manuscript arrives at the secretariat of the Japanese Society of Conservative Dentistry. Date of acceptance is the date when the reviewers determine that the submitted manuscript can be published.

10. The listing order is the order of acceptance. A certification of publication will be issued upon request.

11. Manuscripts are to be submitted via the Japanese Society of Conservative Dentistry's website, e-mail, or postal mail. Manuscripts submitted for publication should be addressed to the secretariat of the Japanese Society of Conservative Dentistry.

12. In principle, authors can proofread their manuscript a maximum of two times. Extensive changes, additions, or deletions made to the contents of the manuscript cannot be accepted. Proofs should be returned by the designated date. If the authors do not need to proofread their manuscript, they should mention this on the left side of the cover page.

13. The copyrights for articles published in *ODEP* belong to the Japanese Society of Conservative Dentistry.

14. Matters not mentioned in these guidelines will be independently determined by the editorial board.

Submission of your manuscript for publication must conform to the following "Submission Guidance" as well as "Submission Guidelines."

The publishing charge is 10,000 yen for a Journal page including tables and figures. Extra charges for such as figures and tables preparation, color printing of photographs will also be paid by the authors. If authors do not pay publishing charge, the article may be retracted.

Submission Guidance (applied as of the Issue 1 of Vol. 2)

Manuscript organization

1. In principle, original articles should be organized into the following sections: (1) cover page; (2) abstract; (3) Main text (Introduction, Materials and Methods, Results, Discussion, and Conclusion); (4) References; and (5) Figure and table captions. Page numbering should start with the cover page. In principle, manuscripts, such as reviews or case reports, other than original articles should be organized in the same format as that of original articles.

2. Manuscript sections
   1) Title: The title should concisely describe the contents of the manuscript. The subtitle should also clearly describe the contents, and should not consist of only numbers.
   2) Introduction: The introduction should clearly describe the background, novelty, purpose, and significance of the study.
   3) Materials and Methods: This section should provide detailed information on the materials, equipment, or methods used along with clear instructions so that the experiments can be reproduced by others. Parameter settings, number of specimens, extraction methods, statistics processing, and others should comply with the purpose of the study.
   4) Results: This section should simply present the findings without bias or interpretation. Measurement results should show characteristic values including mean values and standard deviations.
   5) Discussion: This section should carefully consider the materials and methods, results, and others referring to relevant literature. Please note that it should not be overly assertive and should avoid off-topic points. The discussion should stay focused on the study purpose and not digress into a general discussion.
   6) Conclusion: The section should precisely summarize the results obtained and relate them to the purpose of the study and hypothesis as presented in the Introduction.

3. Manuscripts should be prepared using A4-size paper. The suggested length of each typed page is 80 alphanumeric characters per line × 25 lines per page using a 12-point font. Top/bottom/left/right margins should be approximately 25 mm.   Non-Japanese names and places should be in their original names..

4. For the manuscript style, refer to the latest issue of the journal.

Ethics Code

1. Each report on the result of clinical research (clinical trial or observational research) or research involving any specimen collected from a human body must include a clear statement that it was approved by the head of the affiliated institution or by the research ethics review board assigned by the institution's head, in order to expressly indicate that the research was conducted in compliance with all applicable guidelines and laws, including the Declaration of Helsinki and the medical research guidelines, etc. issued by the Ministry of Health, Labour and Welfare including the following:
   1) Ethical Guidelines for Life Science and Medical Research Involving Human Subjects;
   2) Guidelines for Gene Therapy and Other Clinical Research; and
   3) Clinical Trials Act.

2. Each report on the result of research on, or a case concerning, regenerative medicine technology, etc. as defined

in the Act on the Safety of Regenerative Medicine must include a clear statement that the technology was provided to the patients in compliance with the aforementioned Act.

3. Each report on a case of a therapeutic method involving any off-label drug or device, or any pharmaceutical, medical device, regenerative medicine, or other related product not domestically approved must include a clear statement that the use was approved by the committee concerned（research ethics review board, review board for unapproved new drugs, etc.）at the affiliated institution.

4. In each instance of publication of an academic paper, all personal information must be thoroughly protected so that none of the research subjects（patients）can be identified from it.

5. In each instance where a patient's clinical photo or X-ray image is included in an academic paper for publication, a clear statement must be provided that the consent of each such patient（or a parent, guardian, or proxy if the patient is a minor or in case it is otherwise difficult to obtain consent from the patient）was duly obtained.

6. Each report on the result of research involving animal subjects must include a clear statement that the research was approved by the animal experiment committee, etc. at the affiliated institution.

Cover page

1. The title, authors' names, institutional affiliations, and corresponding author's contact address should be centered, with a new line for each item, on the cover page.

2. The title should be in upper and lowercase letters, where the first letter of each word is uppercased and the remaining letters are lowercased. Articles, prepositions, conjunctions, and commonly used technical terms are lowercased. For hyphenated compound words, the letters following the hyphen should be lowercased.

3. The corresponding author's contact details should include the following information: one author's name, institutional affiliation, postal address, telephone and fax numbers, and e-mail address.

Abstract

1. The abstract should be a maximum of 400 words organized into four sections with the following headings: Purpose, Methods, Results, and Conclusion. Approximately three keywords should be placed at the end of the abstract.

2. Contributors should put considerable effort into preparing the abstract as it may determine whether or not the reader continues with the manuscript. When necessary, abstracts should be checked by a native English reviewer（preferably with expertise in dental medicine）.

Main text

1. Introduction, Materials and Methods, Results, Discussion, and Conclusion are the main headings and are not numbered.

2. Subparagraphs should be numbered in the following order: 1. 2. 3. …; 1）2）3）…; (1) (2) (3) …; ① ② ③ …; and a. b. c. …

3. English characters should be written in the following manner:
    1) Generally, only the last name should be used to indicate a person.
    2) When the name of a product or manufacturer must be in the original language, the first letter of each word should be uppercased and the remaining letters lowercased.
       In principle, "generic name（product name, company name, city［state in the case of U.S.］, country）"should be used in English manuscripts. Trademark and registration symbols ® and ™ are not required.
    3) Regarding common nouns in German or Latin, the first letter should be uppercased and the remaining letters lowercased. For common nouns in English and French, all letters should be lowercased.
    4) Regarding binominal nomenclature, the first letter of the genus should be uppercased and the remaining letters lowercased. The names of all genera and species should be italicized. When the same genus appears frequently, it is acceptable to replace the name with the initial after the first use.

Example: *Streptococcus mutans* → *S. mutans*

    5) For nouns that must be in their original language, other than German, Latin, English or French, all letters should be lowercased, except for commonly used technical terms.

4. In principle, SI units are used for measurements.

5. Any conflicts of interests (COI) must be declared after the conclusions. When there is no COI, the statement "The authors declare no conflict of interest related to this paper" should be included.

6. Acknowledgments for all sources supporting this study including grant funds should be added after of COI.

References

1. References must be listed at the end of the main text, and numbered in the same order as they appear in the text.

2. In the main text, a cited reference should appear with a superscript numeral and closing parenthesis. When two references are cited, a comma should be used to separate them; more than two references should be connected by an en dash between the first and last numeral.

    Examples: "by authors[3]", "···is reported[7,8]", "previous studies[10-15]show"

3. Examples of Reference

  a. Journal articles

    Number) Last name and first name of all authors with a comma separating each author. Title of paper. Name of journal and publishing year in the Christian era; Volume number: Inclusive page numbers of paper.

    Example:

    1) Clark AB, Erickson D, Hamilton FG. Tensile bond strength and modulus of elasticity of several composite resins. J Dent Res 1992; 37: 618-621.

  b. Book

    Number) Author (co-authors). Title of book. First/last volume. Edition. Publisher's name: Publisher's location (City); Publishing year in the Christian era. Cited pages.

    Example:

    2) Phillips RW. Skinner's science of dental materials. 9th ed. WB Saunders: Philadelphia; 1991. 219-221.

  c. Book with co-authors

    Number) Contributor's name. Title of contributed article. Name of editor (editor-in-chief). Book title. First/last volume. Edition. Publisher's name: Publisher's location (City); Publishing year in the Christian era. Cited pages.

    Example:

    3) Torneck CD. Dentin-pulp complex. Ten Cate AR. Oral histology. 5th ed. Mosby: St. Louis; 1998. 150-196.

    For cases in which each author's contribution is not separately indicated, the author's name and the title of the contributed article should not be listed.

    Number) Name of editor (editor-in-chief). Title of book. First/last volume. Edition. Publisher's name: Publisher's location (City); Publishing year in the Christian era. Cited pages.

  d. Other writing styles

    ・Abstracts of scientific meeting

    Number) Presenter (all presenters should be cited. A comma should be used to separate the authors in the case of co-presentations.). Title of abstract. Name of journal and publishing year in the Christian era; Volume number: Inclusive page numbers, abstract number.

    Example:

    4) Marais JT. Cleaning efficacy of a new root canal irrigation material. J Dent Res 1998; 77: 669, Abst. No. 300.

    ・Journal articles in press

    In principle, the same style as that of a regular journal article should be used; however, when the inclusive page numbers are not known, they can be omitted. The statement "in press" should be shown at the end.

Example:

5) Sato K. Effect of toothbrushes on gingival abrasion. J Periodont Res 1994; 29: in press.

・Electronic journal

In principle, the same style as that of a regular journal article should be used; however, when the inclusive page numbers are not known, the DOI and other indicators should be shown. When papers are published in electronic journals before printing, the statement [Epub ahead of print] should be shown after the publishing year and month.

Example:

6) Sunada N, Ishii R, Shiratsuchi K, Shimizu Y, Tsubota K, Kurokawa H, Miyazaki M. Ultrasonic measurement of the effects of adhesive application and power density on the polymerization behavior of core build-up resins. Acta Odontol Scand; doi: 10.3109/00016357.2011.654252

・Internet website

Page publisher. Title of page. URL address.（Access date）

Example:

7) World Health Organization. Continuous improvement of oral health in the 21st century. http://www.who.int/oral_health/en/（cited 2005. 10. 1）

4. In principle, journal names should be abbreviated in accordance with the format used by the journal.

Figures and Tables

1. Figures, photographs, and tables are categorized into figures and tables, and then numbered. Paper size should be A4, and each figure and table should be printed on a separate page. The numbers allocated for the figures and tables should be consistent with those referred to in the text.

2. Figures and tables should be accompanied by explanations that are easily understandable. Explanations of figures/tables are presented as captions and explanations for tables/tables should be presented as footnotes.

3. If authors wish to have the figures color-printed, color data should be attached; if authors wish to have the figures printed in black and white, black-and-white data should be attached.

   Notes on creating imaging data:

   ・The jpg data format should be used if possible.

   ・Image size should correspond to the layout; image resolution should be at least 300 dpi for photographs and at least 1,200 dpi for line drawings.

4. Figures printed in black and white can be uploaded as color pictures on J-STAGE; authors should request this at the time of submission. The cost to create color data for J-STAGE uploading is to be borne by the authors. In a case where color figures are uploaded only on J-STAGE, new captions cannot be added since it would make the J-STAGE content different from the original content published in the journal. When selecting color/black-and-white figures, the authors themselves should carefully check that the original figure captions are sufficient.

Sending manuscript intended for publication

1. The manuscript（cover page, abstract, main text, references, and figure and table captions are created as one file）should be formatted as a Microsoft Office Word (hereafter "Word") document.

2. Figures should be provided in jpg or pdf format.

3. Tables should be provided in Microsoft Office Excel, jpg, pdf, or Word format.

4. File titles should be as follows: "author name"_"university name (name after department is not needed)"_ "manuscript/figure/table/submission form"_".filename extension (indicating file type)".

   Example）Nihon Tarou_Nihon University/manuscript.docx; Nihon Taro_Nihon University_Figure.jpg; Nihon Taro_Nihon Univesity_Table.xlsx; Nihon Taro_Nihon University_submission form.pdf

   Also, pdf files with embedded fonts for all contents are acceptable for submission. In such cases, file names

should be as follows: Nihon Taro_Nihon University_comprehensive manuscript.pdf

5． E-mail title（subject）should be "Submitted papers for ODEP".

6． Submitted papers should be sent to the e-mail address of Oral Health Association of Japan: hensyu6@kokuhoken. or.jp. For safety, also send as a CC to hensyu5@kokuhoken.or.jp.

7． When e-mail submission is difficult for such reasons as the file size is too large, submission via an FTP server and other methods are acceptable. In such cases, the intent of submission should be informed by e-mail. In the e-mail, information regarding the site and other methods for downloading the file should be provided.

8． The submission form of *ODEP* provided on the Japanese Society of Conservative Dentistry's home page（http: //www.kokuhoken.or.jp/exterior/ jscd/fileform/）can be used for submission.

Simplicity, aesthetics and performance in your hands

ナノハイブリッド充塡用コンポジットレジン

ジーニアル アコード™

シンプルシェードのユニバーサルコンポジットレジン

歯科充塡用コンポジットレジン　ジーシー　ジーニアル　アコード
管理医療機器　302AKBZX00096000

ペースト + パウダー
=Bioceramic Evolution

マルチな性状

パウダーを混ぜる量により
性状を変えられます。

シーラー状　クリーム状　パテ状

マルチな適応

根充から覆髄まで使用できます。

覆髄

根充

ペースト　＋　パウダー　＝
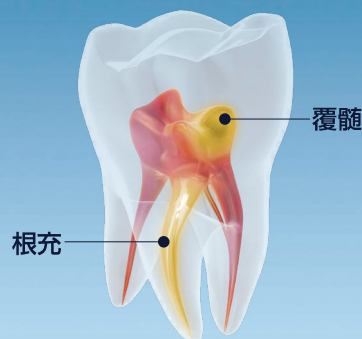
歯科用覆髄材料・歯科用根管充填シーラ

ニシカ キャナルシーラー® BG multi

管理医療機器　一般的名称：歯科用覆髄材料・歯科用根管充填シーラ　医療機器認証番号：302ADBZX00055000

【包装】ペースト（ダブルシリンジ）1本［A材 4.5g（2.5mL）、B材 4.5g（2.5mL）］、パウダー 1個［2g］

【標準価格】19,000 円

室温保管（1〜30℃）※凍結を避けること

＊単品販売もございます。

詳しい製品情報をご覧いただけます →

NISHIKA　日本歯科薬品株式会社　本社　山口県下関市西入江町2-5 〒750-0015　営業所　大阪・東京・福岡
お問合せ・資料請求《お客様窓口》☎ 0120-8020-96
NISHIKAホームページ https://www.nishika.co.jp/

N-2

Thinking ahead. Focused on life.

MORITA

Spaceline EX

スペースライン EXが iFデザイン賞の金賞を受賞

ドイツのiFデザイン賞は、50年以上の歴史を有し、各国から選ばれた審査員によって厳正に選考される世界的に権威のあるデザイン賞です。世界中から6,400以上のエントリーが有った中、最優秀デザインとして75件に授与される金賞（ iF GOLD AWARD ）をスペースライン EXが受賞しました。人間工学に基づき緻密に計算されたデザインは、患者さんだけでなく術者にも理想的で洗練されたデザインであると評価されました。

iF GOLD AWARD 2018